

**Unraveling the Contribution and Molecular Phenotypes of Bone Marrow-Dependent and Bone Marrow-Independent Macrophages in Diaphragm Muscle Homeostasis and Disease**

by Qian Li

Division of Experimental Medicine

McGill University

Montréal, Québec, Canada

August 2023

A thesis submitted to McGill University in partial fulfillment of the requirements for the degree of Doctor of Philosophy.

©Qian Li, 2023

First published on December 1, 2024

## TABLE OF CONTENTS

### Contents

TABLE OF CONTENTS .....	ii
LIST OF TABLES AND FIGURES .....	vii
English abstract .....	ix
French abstract.....	xi
Preface .....	xiv
Contribution of authors to each chapter .....	xv
Contribution to knowledge and elements of original scholarship .....	xvi
Acknowledgements .....	xviii
List of abbreviations .....	xix
Chapter 1: Introduction and Literature Review .....	25
1.1. Introduction to skeletal muscle structure, function, and injury.....	26
1.1.1. Brief overview of skeletal muscle tissue composition and organization .....	26
Figure 1.1 Hierarchical organization of skeletal muscles.....	28
1.1.2 Brief overview of acute skeletal muscle injury with successful muscle regeneration ..	29
1.1.3 Brief overview of Duchenne muscular dystrophy (DMD) – a disease of chronic skeletal muscle injury with unsuccessful muscle regeneration .....	34
1.2. General overview of macrophage biology .....	40
1.2.1 Macrophage function in infection and tissue development/regeneration.....	40
1.2.2 Macrophage ontogeny .....	43
Table 1.1 Fate-mapping models .....	45
Table 1.2 Ontogeny of adult tissue-resident macrophages in different organs .....	46
1.2.3 Phenotypic heterogeneity of macrophages .....	48
Table 1.3 Characteristics of Macrophages in Different Organs/Tissues: Niche Signals, Transcription Factors, Functions, and Phenotypic Markers .....	49
1.3. Heterogeneity and roles of macrophages in skeletal muscle repair .....	51
1.3.1. Macrophage ontogeny in skeletal muscle.....	51
1.3.2. Role of different macrophage functions and subsets leading to successful muscle	

regeneration after acute injury .....	51
Figure 1.2 Impacts of inflammation and macrophage polarization on skeletal muscle injury and repair.....	56
1.3.3. Role of dysregulated macrophage function in the unsuccessful muscle regeneration associated with chronic skeletal muscle injury in DMD.....	58
1.4 Hypotheses and Objectives of the Current Thesis .....	67
Chapter 2:           Dynamic Alterations of Macrophage Ontogeny in the Diaphragm Following Acute Injury and Recovery.....	68
2.1. Abstract .....	69
2.2 Introduction .....	71
2.3. Methods.....	73
2.3.1. Experimental animals.....	73
2.3.2. Bone marrow transplantation .....	73
2.3.3. Diaphragm injury .....	74
2.3.4. Satellite cell isolation and culture .....	74
2.3.5. Satellite cell proliferation and differentiation .....	75
2.3.6. RNA isolation and quantitative real-time PCR (qRT-PCR) .....	76
2.3.7. Identification of monocytes and macrophages by flow cytometry .....	77
2.3.8. Statistics .....	78
2.4 Results .....	79
2.4.1. Preservation of satellite cells and macrophages by diaphragm shielding.....	79
Figure 2.1. Diaphragm shielding during irradiation preserves satellite cell number and proliferative capacity.....	81
Figure 2.2. Diaphragm shielding during irradiation preserves satellite cell differentiation capacity .....	83
Figure 2.3. Diaphragm shielding model preserves the resident macrophage population after irradiation.....	85
2.4.2. Diaphragm shielding reveals a major population of resident macrophages that are bone marrow (monocyte)-independent.....	87
Figure 2.4. Diaphragm shielding reveals a bone marrow (monocyte)-independent macrophage population .....	89
2.4.3. Bone marrow origin macrophages are responsible for the increase in diaphragm macrophages after acute injury .....	90

Figure 2.5. Comparison of bone marrow-dependent versus bone marrow-independent macrophages in acutely injured diaphragms .....	91
2.4.4. The pre-injury pattern of macrophage ontogeny is restored in healed diaphragm muscle	93
Figure 2.6. Comparison of bone marrow-dependent versus bone marrow-independent macrophages following recovery from diaphragm injury.....	94
2.5. Discussion .....	95
References for Chapter 2 .....	99
2.6 Bridging text.....	102
Chapter 3: Macrophage Ontogeny and Phenotypic Alterations in Healthy and Dystrophic Muscle Environments .....	103
3.1. Abstract .....	104
3.2. Introduction.....	106
3.3. Methods.....	108
3.3.1. Experimental animals .....	108
3.3.2. Bone marrow transplantation .....	108
3.3.3. Parabiosis.....	109
3.3.4. Fate mapping .....	110
3.3.5. BrdU incorporation.....	111
3.3.6. Whole mount immunofluorescence microscopy .....	111
3.3.7. Cell preparation and flow cytometry .....	111
3.3.8. RNA sequencing.....	112
3.4. Results .....	114
3.4.1. Bone Marrow-Dependent and Bone Marrow-Independent Macrophages Contribute to the Steady-State Macrophage Pool in Healthy Adult Skeletal Muscle.....	114
Figure 3.1. Fate mapping to assess the ontogeny of bone marrow-independent macrophages which arise during fetal development .....	117
Figure 3.2. Fate mapping reveals the persistence of prenatal origin macrophages in healthy adult muscle .....	120
Figure 3.3. Parabiosis confirms the presence of a major population of bone marrow-independent macrophages in healthy adult muscles .....	123
Figure 3.4. Phenotypic markers and proliferation rates of bone marrow-dependent versus bone marrow-independent macrophages in healthy adult muscles.....	125

3.4.2 Skeletal Muscle Macrophages in DMD (mdx) Mice Are Almost Entirely Bone Marrow (Monocyte)-Dependent .....	127
Figure 3.5. Postnatal monocytes originating from the bone marrow account for almost the entire skeletal muscle macrophage population in adult dystrophic (mdx) mice.....	130
3.4.3. Transcriptional Phenotype of Bone Marrow-Dependent Macrophages in Skeletal Muscle Is Dictated by the Host Environment .....	132
Figure 3.6. Impact of the host muscle environment on the inflammatory phenotype and gene expression profile of bone marrow (monocyte)-dependent macrophages .....	136
3.4.4. Potential Biological Pathways and Transcription Factors Driving Macrophage Responses to the Dystrophic Host Environment.....	137
Figure 3.7. Biological pathway enrichment and transcription factor motif analysis.....	138
3.5. Discussion .....	140
References for Chapter 3 .....	147
Chapter 4: General Discussion .....	151
4.1. Summary of the Major Findings of the Thesis .....	152
4.2. Contributions of the Thesis to Addressing Knowledge Gaps in the Field.....	153
4.3. Limitations of the Thesis and Perspectives for Future Studies .....	159
4.4. Potential Therapeutic Implications of Thesis Findings .....	161
Final conclusion and summary .....	164
References .....	167
Copy right.....	185
Supplementary Information (SI) Appendix: Supplementary tables and figures .....	186
Figure S2.1. Related to Figure 2.3, Figure2.4 and Figure 2.5. Flow cytometry gating strategies for blood and diaphragm.....	186
Figure S3.1 Related to Figure 3.3. Proportions of chimeric blood T cells and origins of macrophages in various tissues.....	188
Figure S3.2 Related to Figure 3.1. Gating strategies for fate mapping experiment harvest at E18.5 .....	189
Figure S3.3 Related to Figure 3.2 and Figure 3.4. Gating strategies for fate mapping experiment harvest at 5 and 9 wks.....	190
Figure S3.4 Related to Figure 3.3 and Figure 3.4. Gating strategies for parabiosis.....	191
Figure S3.5 Related to Figure3.5. Gating strategies for WT-CX3CR1-gfp and mdx-CX3CR1-gfp mice at different ages.....	192
Figure S3.6. Related to Figure3.6. Gating strategies for chimeric mice transplanted with gfp+	

bone marrows .....	193
Table S2.1 qPCR primers .....	194
Table S3.1 Complete DEG list .....	195
Table S3.2 Antibodies resources table .....	208

## LIST OF TABLES AND FIGURES

Figure 1.1 Hierarchical organization of skeletal muscles.....	28
Table 1.1 Fate-mapping models .....	45
Table 1.2 Ontogeny of adult tissue-resident macrophages in different organs .....	46
Table 1.3 Characteristics of Macrophages in Different Organs/Tissues: Niche Signals, Transcription Factors, Functions, and Phenotypic Markers .....	49
Figure 1.2 Impacts of inflammation and macrophage polarization on skeletal muscle injury and repair.....	56
Figure 2.1. Diaphragm shielding during irradiation preserves satellite cell number and proliferative capacity.....	81
Figure 2.2. Diaphragm shielding during irradiation preserves satellite cell differentiation capacity .....	83
Figure 2.3. Diaphragm shielding model preserves the resident macrophage population after irradiation .....	85
Figure 2.4. Diaphragm shielding reveals a bone marrow (monocyte)-independent macrophage population .....	89
Figure 2.5. Comparison of bone marrow-dependent versus bone marrow-independent macrophages in acutely injured diaphragms .....	91
Figure 2.6. Comparison of bone marrow-dependent versus bone marrow-independent macrophages following recovery from diaphragm injury.....	94
Figure 3.1. Fate mapping to assess the ontogeny of bone marrow-independent macrophages which arise during fetal development .....	117
Figure 3.2. Fate mapping reveals the persistence of prenatal origin macrophages in healthy adult muscle .....	120
Figure 3.3. Parabiosis confirms the presence of a major population of bone marrow-independent macrophages in healthy adult muscles .....	123
Figure 3.4. Phenotypic markers and proliferation rates of bone marrow-dependent versus bone marrow-independent macrophages in healthy adult muscles.....	125
Figure 3.5. Postnatal monocytes originating from the bone marrow account for almost the entire skeletal muscle macrophage population in adult dystrophic (mdx) mice.....	130
Figure 3.6. Impact of the host muscle environment on the inflammatory phenotype and gene expression profile of bone marrow (monocyte)-dependent macrophages .....	136
Figure 3.7. Biological pathway enrichment and transcription factor motif analysis.....	138
Figure S2.1. Related to Figure 2.3, Figure2.4 and Figure 2.5. Flow cytometry gating	

strategies for blood and diaphragm .....	186
Figure S3.1 Related to Figure 3.3. Proportions of chimeric blood T cells and origins of macrophages in various tissues .....	188
Figure S3.2 Related to Figure 3.1. Gating strategies for fate mapping experiment harvest at E18.5 .....	189
Figure S3.3 Related to Figure 3.2 and Figure 3.4. Gating strategies for fate mapping experiment harvest at 5 and 9 wks .....	190
Figure S3.4 Related to Figure 3.3 and Figure 3.4. Gating strategies for parabiosis.....	191
Figure S3.5 Related to Figure3.5. Gating strategies for WT-CX3CR1-gfp and mdx-CX3CR1-gfp mice at different ages.....	192
Figure S3.6. Related to Figure3.6. Gating strategies for chimeric mice transplanted with gfp+ bone marrows .....	193
Table S2.1 qPCR primers .....	194
Table S3.1 Complete DEG list .....	195
Table S3.2 Antibodies resources table .....	208

## **English abstract**

Macrophages (MPs) are crucial for tissue homeostasis, immune surveillance, inflammation, and tissue repair. MPs maintain tissue integrity through their diverse functions, including phagocytosis, antigen presentation, and immune regulation. In acute muscle injury, MPs orchestrate the intricate process of muscle regeneration by removing necrotic debris, secreting chemokines, cytokines, and growth factors, and fine-tuning the myogenic process. They transition from a pro-inflammatory M1 phase that enhances inflammation and myogenic progenitor cell proliferation, to an anti-inflammatory M2 phase that facilitates myofiber differentiation and fusion. However, recent studies using single-cell RNA sequencing revealed distinct MP subpopulations within the muscle, necessitating further investigation of their roles in different contexts.

Duchenne muscular dystrophy (DMD) is a severe muscle disease characterized by progressive muscle necrosis and fibrosis. In DMD, MPs contribute to muscle regeneration through myogenic support functions while also becoming a leading factor in inflammation and fibrosis due to persistent muscle damage. However, the relative contributions of bone marrow-dependent MP (BMDMs) and BM-independent MPs (BMIDMs), as well as the molecular triggers underlying their pathological remodeling within the dystrophic muscle environment, remain poorly understood. This thesis aims to investigate the contribution and molecular phenotypes of BMDMs and BMIDMs in healthy skeletal muscle, muscle injury and chronic muscle disorders, specifically focusing on the diaphragm (DIA). The DIA is a unique skeletal muscle which is continuously active in order to maintain adequate ventilation and metabolic homeostasis during both wakefulness and sleep.

A DIA shielding approach in a BM chimeric model was used to study the dynamics and roles of BMDMs and BMIDMs. This approach preserved the functionality and viability of cells in the muscle, establishing it as a reliable model for investigating MP origins and phenotypes. Combining BM

chimeric and parabiosis models, we found that the steady-state MP population in healthy adult DIA muscle comprises approximately 70% BMDMs and 30% BMIDMs. Through timed pregnancy and fate-mapping techniques, we traced the prenatal origin of BMIDMs in the DIA to the yolk sac and fetal liver. Moreover, we observed dynamic changes in the phenotype of adult muscle MPs during post-natal development.

In acute DIA injury, BMDMs were served as the primary source, comprising over 90% of intramuscular MPs. However, after recovery, MP percentages and cell numbers reverted to a non-injured state, restoring the pre-injury steady-state composition. To assess the impact of a disease associated with chronic muscle injury on different MP populations, we employed the mdx mouse model of DMD. In mdx DIA (the most severely affected muscle in this model) we observed significant alterations in MP phenotypes at different stages of disease progression compared to the WT condition. Notably, nearly all intramuscular MPs in the DMD DIA originated from the BM. RNA-seq analysis found that the dystrophic muscle environment significantly affects the phenotype and molecular profile of BMDMs. Differential gene expression analysis showed 262 upregulated and 251 downregulated genes in BMDMs from mdx recipients compared to WT recipients. Upregulated genes were involved in MP immune activation and response, tissue remodeling, and phagocytosis. Transcription factor motif enrichment analysis identified several potential key regulators from IRF families.

Taken together, these studies provide novel insights into the cellular origins and molecular phenotypes of BMDM and BMIDMs in muscle injury and disease. Understanding the contributions and functional characteristics of these MP subsets could pave the way for targeted therapeutic interventions and enhance our overall comprehension of the complex role of MPs in muscle regeneration and pathologies.

## **French abstract**

Les macrophages (MP) sont cruciaux pour l'homéostasie tissulaire, la surveillance immunitaire, l'inflammation et la réparation tissulaire. Les MP maintiennent l'intégrité tissulaire grâce à leurs fonctions diverses, notamment la phagocytose, la présentation d'antigènes et la régulation immunitaire. En cas de lésion musculaire aiguë, les MP orchestrent le processus complexe de régénération musculaire en éliminant les débris nécrotiques, en sécrétant des chimiokines, des cytokines et des facteurs de croissance, et en ajustant finement le processus myogénique. Ils passent d'une phase pro-inflammatoire M1 qui favorise l'inflammation et la prolifération des cellules progénitrices myogéniques, à une phase anti-inflammatoire M2 qui facilite la différenciation et la fusion des myofibres. Cependant, des études récentes utilisant la séquençage d'ARN à cellule unique ont révélé des sous-populations distinctes de MP dans le muscle, nécessitant des investigations plus approfondies sur leurs rôles dans différents contextes.

La dystrophie musculaire de Duchenne (DMD) est une maladie musculaire sévère caractérisée par une nécrose musculaire et une fibrose progressives. Dans la DMD, les MP contribuent à la régénération musculaire grâce à des fonctions de soutien myogénique tout en devenant également un facteur majeur d'inflammation et de fibrose en raison des dommages musculaires persistants. Cependant, les contributions relatives des MP dépendant de la moelle osseuse (BMDM) et des MP indépendants de la moelle osseuse (BMIDM), ainsi que les déclencheurs moléculaires sous-jacents à leur remodelage pathologique au sein de l'environnement musculaire dystrophique, restent mal compris. Cette thèse vise à étudier la contribution et les phénotypes moléculaires des BMDM et des BMIDM dans le muscle squelettique sain, les lésions musculaires et les troubles musculaires chroniques, en se concentrant spécifiquement sur le diaphragme (DIA). Le DIA est un muscle squelettique unique qui est continuellement actif pour maintenir une ventilation adéquate et une

homéostasie métabolique à la fois pendant l'éveil et le sommeil.

Une approche de protection du DIA dans un modèle chimérique de moelle osseuse a été utilisée pour étudier la dynamique et les rôles des BMDM et des BMIDM. Cette approche a préservé la fonctionnalité et la viabilité des cellules dans le muscle, en créant un modèle fiable pour étudier les origines et les phénotypes des MP. En combinant les modèles chimériques de moelle osseuse et de parabiose, nous avons découvert que la population de MP à l'état stable dans le muscle sain de l'adulte DIA comprend environ 70 % de BMDM et 30 % de BMIDM. Grâce à des techniques de grossesse chronométrée et de traçage du destin cellulaire, nous avons retracé l'origine prénatale des BMIDM dans le DIA jusqu'au sac vitellin et au foie fœtal. De plus, nous avons observé des changements dynamiques dans le phénotype des MP musculaires adultes au cours du développement postnatal.

En cas de lésion aiguë du DIA, les BMDM ont servi de source principale, représentant plus de 90 % des MP intramusculaires. Cependant, après la récupération, les pourcentages de MP et le nombre de cellules sont revenus à un état non lésé, restaurant la composition à l'état stable d'avant la lésion. Pour évaluer l'impact d'une maladie associée à une lésion musculaire chronique sur différentes populations de MP, nous avons utilisé le modèle de souris mdx de la DMD. Dans le DIA mdx (le muscle le plus gravement touché dans ce modèle), nous avons observé des altérations significatives dans les phénotypes des MP à différentes étapes de la progression de la maladie par rapport à la condition WT. Notamment, presque tous les MP intramusculaires dans le DIA DMD provenaient de la moelle osseuse. L'analyse de séquençage d'ARN a révélé que l'environnement musculaire dystrophique affecte significativement le phénotype et le profil moléculaire des BMDM. L'analyse de l'expression différentielle des gènes a montré 262 gènes surexprimés et 251 gènes sous-exprimés dans les BMDM des receveurs mdx par rapport aux receveurs WT. Les gènes surexprimés étaient impliqués dans l'activation et la réponse immunitaire des MP, le remodelage tissulaire et la phagocytose. L'analyse d'enrichissement des motifs de facteurs de transcription a identifié plusieurs régulateurs potentiels

clés appartenant à la famille des IRF.

Pris ensemble, ces études fournissent de nouvelles perspectives sur les origines cellulaires et les phénotypes moléculaires des BMDM et des BMIDM dans les lésions musculaires et les maladies. Comprendre les contributions et les caractéristiques fonctionnelles de ces sous-populations de MP pourrait ouvrir la voie à des interventions thérapeutiques ciblées et améliorer notre compréhension globale du rôle complexe des MP dans la régénération musculaire et les pathologies.

## **Preface**

The central body of this thesis comprises two manuscripts that are going to be submitted for publication in peer-reviewed journals, with myself as the first author.

Authors of Chapter 2:

Qian Li, Feng Liang, Basil J Petrof

Authors of Chapter 3:

Qian Li, Salyan Bhattarai, Feng Liang, Eva Kaufmann, Jintao Wang, Orsolya Lapohos, Junying Ding, Jun Ding and Basil J Petrof.

## **Contribution of authors to each chapter**

### Chapter 1

Qian Li wrote the content of this chapter and Basil Petrof edited this chapter.

### Chapter 2

In this chapter, Qian Li contributed to the content, while Basil Petrof provided editing. Feng Liang conducted cardiotoxin injury surgeries on the diaphragm for Figure 2.4 and Figure 2.5, as well as qPCR experiments for Figure 2.1 and Figure 2.2. Qian Li conducted the remaining experiments. Data analysis was carried out by Qian Li. The conceptualization of the paper was done collaboratively by Basil Petrof and Qian Li, with Basil Petrof supervise the project.

### Chapter 3

In this chapter, Qian Li contributed to the content, while Basil Petrof provided editing. Feng Liang conducted parabiosis surgery in Figure 3.3. Jun Ding helped with Quality Control, Preprocessing and Trimming, Read Alignment, and Read counting for raw RNA-seq FASTQ files. The remaining experiments and data analysis were performed by Qian Li. Salyan Bhattarai, Eva Kaufmann, Jintao Wang, Orsolya Lapohos, and Junying Ding provided valuable suggestions and technical support. The conceptualization of the paper was a joint effort by Basil Petrof and Qian Li, with Basil Petrof supervising the project.

### Chapter 4

Qian Li wrote the content of this chapter and Basil Petrof edited this chapter.

## **Contribution to knowledge and elements of original scholarship**

Outlined below in the subsequent section are the original findings and distinct contributions made to the field of macrophage ontogeny in muscle homeostasis and diseases. These elements represented pioneering research at the period when the study was undertaken.

1) Under normal homeostatic conditions, resident macrophages in skeletal muscle consist of both bone marrow-dependent and -independent populations, with the latter predominantly derived from fetal liver hematopoiesis and a lesser contribution from the embryonic yolk sac.

2) Under normal homeostatic conditions, bone marrow-independent macrophages derived from the embryo constitute 30-40% of the skeletal muscle resident macrophages that persist into adulthood.

3) In the early phase after acute muscle injury, the massive increase in diaphragm macrophages is due to the recruitment (and to a lesser degree proliferation) of bone marrow-derived macrophages. During this same period there is no apparent change in cell number within the pre-existent tissue-resident macrophage population.

4) After recovery from acute muscle injury, absolute macrophage numbers and the balance between bone marrow-dependent and bone marrow-independent origin macrophages in the diaphragm both return to their normal pre-injury levels.

5) In neonatal dystrophic (mdx) mice, the phenotype of diaphragm macrophages is dramatically altered from the first day of birth, demonstrating a simultaneous increase in putative markers for both bone marrow-derived and embryo-derived macrophages (CCR2 and TIM4, respectively). Remarkably, this occurs several days before any increase in macrophage numbers or histological

evidence of muscle necrosis.

6) In adult mdx mice, bone marrow-dependent macrophages derived from blood monocytes constitute almost the entire macrophage pool within the diaphragm. Furthermore, in addition to increased recruitment from the bone marrow, a decrease in absolute cell number within the pre-existent tissue-resident macrophage population is also observed.

7) The dystrophic environment is the overarching determinant factor in driving the inflammatory phenotype and gene expression pattern of bone marrow-dependent macrophages in the mdx diaphragm, skewing them towards extracellular matrix (ECM) remodeling and innate immune responses. With respect to the latter, the Interferon Regulatory Factor (IRF) family of transcription factors was identified as possibly playing a central role in orchestrating these responses.

## **Acknowledgements**

I extend my heartfelt gratitude to all those who contributed to the completion of this thesis, including the provision of funding where applicable.

Foremost, I am deeply thankful to my supervisor, Dr. Basil Petrof, for his unwavering support, boundless encouragement, and the freedom he granted me throughout my PhD journey. His passion and dedication to science have not only been inspirational but have also left an indelible mark on my life. I also extend my appreciation to my advisory committee members: Dr. Maziar Divangahi, Dr. Carolyn Baglole, Dr. Irah King, Dr. Jun Ding, and Dr. Elizabeth Fixman. Their insightful suggestions, valuable advice, and guidance have played an instrumental role in shaping my scientific approach and mindset.

I am grateful to Salyan Bhattarai, Eva Kaufmann, Erwan Pernet, and Marianna Orlova for their wholehearted assistance and adept troubleshooting that greatly enriched my research journey.

I extend my thanks to Feng Liang and Ekaterina Gusev for their dedicated support that benefits the entire lab community. My appreciation also goes to Severine Audusseau and Victoria Zismanov for their adept management of flow cytometry and other essential instruments. I would like to acknowledge my fellow lab colleagues, Fatemeh Ostadan, Ryann Lang, Tom Podolsky, and Sami Sedraoui, for their collaboration and camaraderie.

In conclusion, I would like to express my deepest gratitude to my parents for their unwavering and unconditional support. Lastly, I wish to extend a special note of appreciation to my husband, Xu Zhang, for his steadfast encouragement and understanding throughout this journey. Their collective contributions have made this endeavor possible and have enriched my academic and personal growth in immeasurable ways.

## **List of abbreviations**

AGM: Aorta-Gonad-Mesonephros

Akt: Protein Kinase B

AMPK: AMP-activated protein kinase

AMPKa1: AMP-activated protein kinase alpha 1

APC: Antigen-Presenting Cell

AREG: Amphiregulin

BMD: Becker Muscular Dystrophy

BMDM: Bone Marrow-dependent Macrophages

BMIDM: Bone-marrow independent macrophage

CCAC: Canadian Council on Animal Care

CCL2: Chemokine (C-C motif) Ligand 2

CCL3: Chemokine (C-C motif) Ligand 3

CCL4: Chemokine (C-C motif) Ligand 4

CCL5: Chemokine (C-C motif) ligand 5

CCL7: Chemokine (C-C motif) ligand 7

CCR2: C-C Chemokine Receptor Type 2

Cebpb: CCAAT/enhancer-binding protein beta

cMoPs: Common Monocyte Progenitors

CMPs: Common Myeloid Progenitors

c-Myc: Cellular Myelocytomatosis Oncogene

CNS: Central Nervous System

CO<sub>2</sub>: Carbon dioxide

CSF-1: Colony-Stimulating Factor 1

CTGF: Connective tissue growth factor

CTX: Cardiotoxin

CXCL10: Chemokine (C-X-C motif) Ligand 10

CXCL11: Chemokine (C-X-C motif) ligand 11

CXCL8: Chemokine (C-X-C motif) Ligand 8

CXCR4: C-X-C Chemokine Receptor Type 4

DAMPs: Damage-Associated Molecular Patterns

DAPC: Dystrophin-Associated Protein Complex

DC: Dendritic Cell

DIA: Diaphragm

DMD: Duchenne Muscular Dystrophy

DNA: Deoxyribonucleic Acid

DTR: Diphtheria toxin receptor

ECM: Extracellular Matrix

EMP: Erythromyeloid Progenitors

ERK: Extracellular Signal-Regulated Kinase

Ets-1/2: E26 Transformation-Specific 1/2

FAP: Fibroadipogenic progenitor

FGF: Fibroblast Growth Factor

GMPs: Granulocyte-Macrophage Progenitors

GRMD: Golden Retriever Muscular Dystrophy

GO: Gene Ontology

H<sub>2</sub>O<sub>2</sub>: Hydrogen Peroxide

HGF/SF: Hepatocyte Growth Factor/Scatter Factor

HLH: Helix-Loop-Helix

HMGB1: High Mobility Group Box 1

HOCl: Hypochlorous Acid

HSCs: Hematopoietic Stem Cells

ICAM-1: Intercellular Adhesion Molecule 1

IFN $\gamma$ : Interferon Gamma

IKK $\beta$ : I $\kappa$ B kinase beta

IL-10: Interleukin 10

IL-12: Interleukin 12

IL-13: Interleukin 13

IL-18: Interleukin 18

IL-1 $\beta$ : Interleukin 1 Beta

IL-23: Interleukin 23

IL-33: Interleukin 33

IL-4: Interleukin 4

IL-4ra: Interleukin 4 Receptor Alpha

IL-6: Interleukin 6

IL-8: Interleukin 8

iNOS: Inducible nitric oxide synthase

IP-10: Interferon-Gamma-Inducible Protein 10

IRF: Interferon Regulatory Factor

ITGAM: Integrin alpha M

KLF4: Krüppel-Like Factor 4

LPS: Lipopolysaccharide

LTBP4: Latent transforming growth factor beta-binding protein 4

LYVE1: Lymphatic Vessel Endothelial Hyaluronan Receptor 1

MAPK: Mitogen-Activated Protein Kinase

Mark2: Microtubule affinity regulating kinase 2

MCK: Muscle creatine kinase

MCP-1: Monocyte Chemoattractant Protein-1

M-CSF: Macrophage Colony-Stimulating Factor

MDPs: Monocyte-Dendritic Cell Progenitors

MHC-II: Major Histocompatibility Complex Class II

MIP-1 $\alpha$ : Macrophage Inflammatory Protein-1 Alpha

MIP-1 $\beta$ : Macrophage Inflammatory Protein-1 Beta

MMP9: Matrix metalloproteinase 9

MMPs: Matrix Metalloproteinases

MP: Macrophage

MRF: Muscle Regulatory Factor

MRF4: Muscle Regulatory Factor 4

mRNA: Messenger RNA

mTOR: Mechanistic Target of Rapamycin

MYHC-emb: Embryonic Myosin Heavy Chain

Myf4: Myogenic Factor 4

Myf5: Myogenic Factor 5

MyoD: Myogenic Differentiation 1

NASH: Nonalcoholic Steatohepatitis

NFAT: Nuclear Factor of Activated T Cells

NF $\kappa$ B: Nuclear Factor Kappa B

NK: Natural Killer

NO: Nitric Oxide

NOS2: Nitric oxide synthase 2

O<sub>2</sub><sup>-</sup>: Superoxide Anion

PAMPs: Pathogen-Associated Molecular Patterns

Pax3: Paired Box Protein 3

Pax7: Paired Box Protein 7

PDGFs: Platelet-Derived Growth Factors

PI3K: Phosphatidylinositol 3-Kinase

PKC: Protein Kinase C

pMAC: Pre-macrophage

PPAR $\gamma$ : Peroxisome Proliferator-Activated Receptor Gamma

PRRs: Pattern Recognition Receptors

RANKL: Receptor activator of nuclear factor kappa-B ligand

RNIs: Reactive Nitrogen Intermediates

ROS: Reactive Oxygen Species

RUNX: Runt-related transcription factor

SMAD2/3: Mothers Against Decapentaplegic Homolog 2/3

SPP1: Secreted phosphoprotein 1

STAT: Signal Transducer and Activator of Transcription

TGF- $\beta$ : Transforming Growth Factor Beta

TIM4: T-cell immunoglobulin and mucin domain-containing protein 4

TLR2: Toll-like receptor 2

TLR4: Toll-like receptor 4

TLRs: Toll-Like Receptors

TNF $\alpha$ : Tumor Necrosis Factor Alpha

Tregs: Regulatory T Cells

VCAM-1: Vascular Cell Adhesion Molecule 1

WISP1: Wnt-Induced Secreted Protein 1

## **Chapter 1: Introduction and Literature Review**

## **1.1. Introduction to skeletal muscle structure, function, and injury**

### **1.1.1. Brief overview of skeletal muscle tissue composition and organization**

Skeletal muscle tissue, comprising 40% of body weight, is the largest tissue component in humans. Skeletal muscle performs multiple crucial roles in the human body based on a highly organized and multifunctional structure<sup>1</sup>. The most important function is to generate the force required for movement as well as the maintenance of posture and stability during various activities. This includes the actions of the respiratory muscles (diaphragm, intercostal muscles, and others), which are required for breathing and hence survival. The respiratory muscles act as a vital pump to draw air into the lungs, analogous to the role of the heart in pumping blood. In the presence of respiratory muscle failure, patients must be placed on a breathing machine (mechanical ventilation) in order to stay alive. In addition, skeletal muscle tissue plays a key role in metabolism, including in energy production and glucose homeostasis, accounting for up to 30% of resting metabolic rate<sup>2</sup>. Furthermore, muscle plays roles in maintaining body temperature, providing a protective barrier for underlying organs, and improving blood flow throughout the body.

The defining cellular unit of skeletal muscle is the muscle fiber (or myofiber), which is an elongated (up to several centimeters in length) and multinucleated cell which is specialized for contraction. Myofibers contain myofibrils composed of repeating sarcomeres, where actin and myosin filaments interact (sliding filament mechanism) to generate muscle fiber contraction<sup>3</sup>. Organelles such as mitochondria, endoplasmic (sarcoplasmic) reticulum, and Golgi apparatus are also present in each myofiber and contribute to various metabolic processes such as energy provision and calcium handling during muscle contraction and relaxation. Myofibrils within each fiber are surrounded by the cellular cytoplasm (sarcoplasm), encompassing multiple organelles, and the entire fiber is enclosed by the muscle cell surface membrane (sarcolemma). Myofibers

within the whole muscle tissue are organized within three interrelated connective tissue structures: the endomysium, perimysium, and epimysium. The endomysium surrounds individual muscle fibers, the perimysium encloses groups of myofibers, and the epimysium wraps the entire muscle tissue. In addition to the contractile elements of muscle fibers, several other cell types are important for skeletal homeostasis. Fibroblasts produce components of the extracellular matrix (ECM) that support the connective tissue structure between fibers. Oxygen and nutrients are supplied to the myofibers through blood vessels and capillaries, which are composed of endothelial cells and related cell types. The motor neurons innervate each myofiber via specialized contacts on the fiber, neuromuscular junctions, which contain ion channels that depolarize the muscle cell membrane and provide the signals to trigger muscle contraction<sup>4</sup>. Muscle stem cells, known as satellite cells, lie between the surface plasma membrane and basal lamina<sup>5</sup>. These cells are generally quiescent but serve as a pool of myogenic precursor cells when needed for the purposes of muscle fiber turnover or regeneration in response to injury. Fibroadipogenic progenitors (FAPs), a type of mesenchymal stem cell, are also important in supporting muscle regeneration by secreting molecules which act upon fibroblasts, immune cells and satellite cells.

Of particular relevance to this thesis, immune cells such as neutrophils, macrophages and T cells play a key role in maintaining tissue homeostasis, particularly in response to injury or infection. This thesis will focus on the role of macrophages in skeletal muscle (principally diaphragm, the primary muscle of respiration) homeostasis and acute or chronic injury. At steady state, the muscle contains a small population of immune cells, usually ranging from less than 1% to a few percent of all the nuclei present in the tissue<sup>6</sup>, with macrophages constituting the majority.

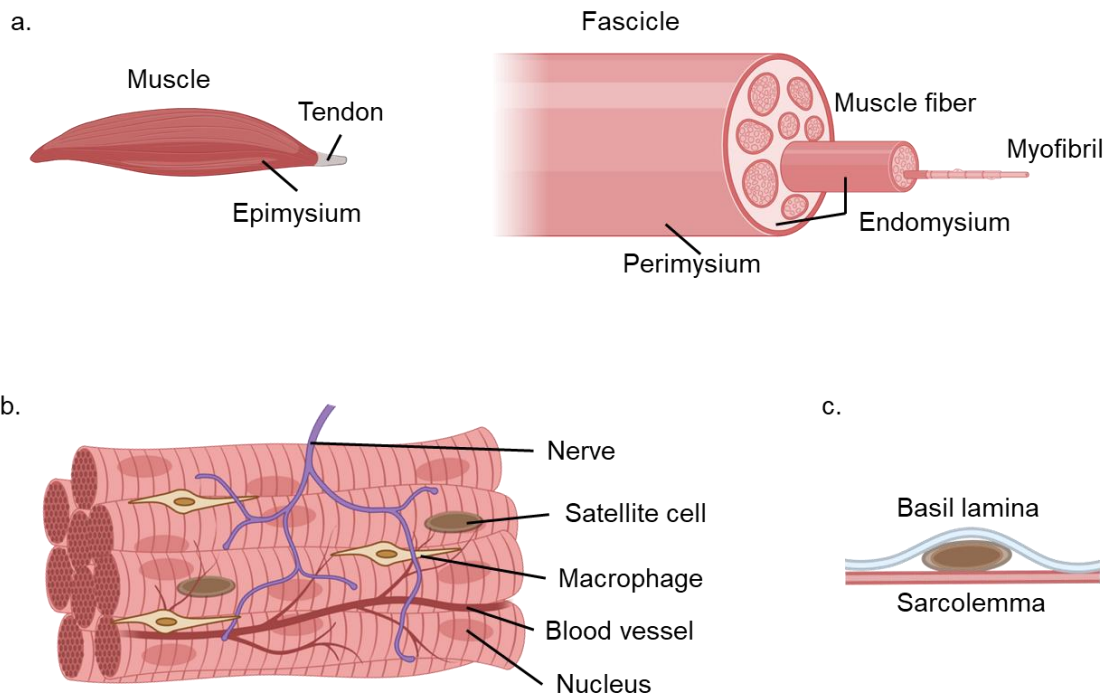


**Figure 1.1 Hierarchical organization of skeletal muscles**

a. At the largest scale, the entire muscle is enveloped by the robust epimysium, providing overall structural support. a&b. Within the muscle, fascicles represent bundles of muscle fibers encased by perimysium, a connective tissue sheath that houses blood vessels and nerves. On a finer scale, individual muscle fibers, or myofibers, are embraced by the delicate endomysium, which contains microvasculature and nerve endings. The skeletal muscle microenvironment hosts additional critical components. c. Satellite cells, residing alongside myofibers beneath the endomysium, play a pivotal role in muscle regeneration and repair. Macrophages, immune cells with distinct phenotypes, dynamically contribute to muscle homeostasis, inflammation, and tissue remodeling. This intricate hierarchy of structural components, satellite cells, and macrophages collaboratively supports and facilitates the multifaceted functions of skeletal muscles.

Other immune cells present in skeletal muscle at steady state include dendritic cells, mast cells, neutrophils, eosinophils, and T cells, albeit in low quantities<sup>7 8</sup>. Residing within the ECM, these cells cooperate to oversee immune surveillance, uphold immune tolerance, and facilitate the initiation of muscle inflammation and repair processes<sup>9</sup>. Macrophages, in particular, perform crucial functions in skeletal muscle health, including the clearance of cell debris, stimulation of muscle formation, promotion of regeneration, and overall tissue stability preservation<sup>10</sup>. In tandem with dendritic cells (DCs), macrophages also serve as antigen-presenting cells (APCs), eliminating potential threats and initiating appropriate immune responses<sup>11 12</sup>. Mast cells, found at densities of 1.8-4.3/mm<sup>2</sup> in mouse muscle tissue under homeostatic conditions<sup>13</sup>, are implicated in immunosurveillance, continuously monitoring the microenvironment for potential pathogens or tissue damage<sup>14</sup>. Although neutrophils, T cells, and eosinophils play a somewhat minor role under normal conditions, they assume more prominent roles in muscle injury and repair, as indicated by variations in their cell numbers and activities<sup>7 9</sup>.

### **1.1.2 Brief overview of acute skeletal muscle injury with successful muscle regeneration**

Various factors can cause acute muscle injury in daily life, including physical trauma, certain forms of exercise, exposure to drugs or chemicals, insufficient blood flow, and infection. Skeletal muscle in adult mammals is typically a relatively stable tissue with a myonuclei turnover rate as low as 1-2% per week for adult rats<sup>15</sup>. In addition, because skeletal muscle fibers are post-mitotic cells lacking the ability to undergo cellular division, a separate muscle stem (satellite) cell population is needed to replenish senescent or damaged fibers. In cases of minor damage such as presumed microtears resulting from everyday wear and tear, local myofiber repair can occur independently of satellite cells and this has been referred to as self-repair<sup>16</sup>. During self-repair, myonuclei are attracted to the site of injury in a calcium-dependent manner and contribute mRNA for the

synthesis of proteins that promote sarcomere repair. In the setting of more severe injury, death of muscle fibers can occur via necrosis, apoptosis, and autophagy<sup>17</sup>. This leads to satellite cell activation, with migration of satellite cells to regions of injury. Upon activation, satellite cells differentiate into myoblasts and fuse with damaged myofibers to repair them, or with other myoblasts to form myotubes and generate entirely new fibers.

Researchers have employed different methods to study acute muscle injury and induce muscle regeneration in experimental settings. These methods include intramuscular injection of chemicals<sup>18 19 20 21</sup>, physical exercise<sup>18 16</sup> (most typically involving eccentric/lengthening contractions), crushing, and freezing<sup>22</sup>. One of the most commonly used approach involves the use of myotoxins, such as cardiotoxin (CTX)<sup>18</sup> and notexin<sup>20</sup>. These agents are derived from snake venoms and cause a loss of plasma membrane integrity leading to calcium influx and muscle fiber death while maintaining satellite cell function. Eccentric contractions, which occur when a muscle lengthens as it contracts, are a prevalent cause of acute muscle injury resulting from certain forms of exercise and have also been used as an experimental model to study muscle injury<sup>23</sup>. During eccentric contractions, the mechanical stress and strain exerted on the muscle fibers causes damage to the muscle cell membrane and other structures within the fibers. Crushing and freezing injury cause more extensive damage with destruction of multiple cell types and disruption of the underlying connective tissue scaffold architecture<sup>24 25 26</sup>. Depending upon the specific scientific question being studied, each of the above models has its own advantages and disadvantages<sup>27 28</sup>. In the current thesis, the CTX model has been used to study the effects on macrophage function of acute skeletal injury, as our laboratory has previously established a reproducible and well characterized model of CTX-induced diaphragm injury<sup>29 30</sup>.

In the event of acute injury, skeletal muscle exhibits a remarkable ability to rapidly and extensively

repair itself through satellite-cell-dependent regeneration. A precisely coordinated series of cellular reactions is triggered, leading to the restoration of a structurally complete and fully functional muscle<sup>9</sup>. Successful regeneration occurs through the activation, migration, proliferation, and differentiation of satellite cells<sup>31 32 33</sup>. The satellite cells are normally quiescent at steady state, expressing Paired box protein Pax-7 (Pax7 and sometimes Pax3) transcription factors and anchored to the ECM through  $\alpha7\beta1$  integrins<sup>34</sup>. Upon muscle damage, satellite cells are activated to exit from quiescence and enter into the cell cycle<sup>35</sup>. Satellite cell proliferation after muscle injury is tightly regulated by a complex interplay of various signaling molecules, growth factors, transcription factors, and microenvironmental cues. Satellite cells can be directly activated by mitogens released from other cell types (immune cells, endothelial cells, etc) as well as ECM components and the damaged muscle fiber itself<sup>36</sup>. This includes the release of muscle damage-associated molecular patterns (DAMPs) from various sources, such as high mobility group box 1 (HMGB1) from the nucleus<sup>37 38</sup>, fibrinogen<sup>39</sup> in the ECM, free DNA<sup>40</sup>, and heat shock proteins<sup>41</sup>. In addition, growth factors present in the ECM, such as platelet-derived growth factors (PDGFs), hepatocyte growth factor/scatter factor (HGF/SF), fibroblast growth factors (FGFs), and insulin-like growth factors (IGFs), all play a role in activating satellite cells and acting as potent mitogens to stimulate their proliferation, thereby resulting in an increase in cell number<sup>42 43 44</sup>. Cytokines are also important modulators of satellite cell proliferation following acute injury. In vitro, IFN $\gamma$  enhances the proliferation of satellite cells while preserving fusion rates<sup>45</sup>. In vivo treatment of mice with anti- IFN $\gamma$  receptor (IFN $\gamma$  R) antibodies in the presence of acute muscle injury resulted in a reduction in the number of proliferating satellite cells and regenerated myofibers<sup>46</sup>. Tumor necrosis factor-alpha (TNF $\alpha$ ) and IL-6, both of which can originate from muscle or immune cells, can also promote the proliferation of satellite cell<sup>47</sup>. In addition, TNF $\alpha$ -induced NF $\kappa$ B activation

can inhibit muscle differentiation by increasing cytolitic enzyme production, promoting cell proliferation through cyclin D1 expression, and suppressing myogenic differentiation 1 (MyoD) protein levels<sup>48 49 50</sup>.

In addition to proliferation, satellite cells migrate to sites of skeletal muscle fiber injury. This migration process is guided by the release of chemotactic molecules secreted by inflammatory cells or chemotactic molecules in the ECM. These include many of the same factors involved in proliferation, including PDGF, HGF, FGF, and laminin<sup>23</sup>. The expression of  $\alpha 7 \beta 1$  integrins, CD34, and CD44 on the satellite cell membrane enables their binding to laminin and promotes cell motility<sup>51 52 53</sup>. Migration of satellite cells to the site of injury is also CXCR4 dependent<sup>54</sup>. Modulation of the cytoskeleton, regulated by signaling pathways such as phosphoinositide 3-kinase (PI3K)/ protein kinase B (Akt) and mitogen-activated protein kinase (MAPK)/ extracellular signal-regulated kinase (ERK), is essential for myoblast migration<sup>55 42</sup>. In addition, matrix metalloproteinases (MMPs) have the capacity to break down components of the extracellular matrix, thereby facilitating the migration of satellite cell and remodeling of the tissue<sup>56</sup>.

The process of myoblast differentiation and fusion involves key regulatory events orchestrated by the myogenic regulatory factors (MRF) myogenic factor 5 (Myf5), MyoD, myogenin, and MRF4/Myf4, which are basic helix-loop-helix (HLH) transcription factors. These MRFs bind to specific DNA motifs and interact with other HLH-containing proteins to initiate myogenic specification and differentiation<sup>57</sup>. During the early stages of satellite cell activation, the cells accumulate transcripts for Myf5 and MyoD, along with cell cycle genes. Myf5, MyoD, and MRF4 collectively promote the commitment of progenitor cells to the myogenic lineage, while myogenin, MyoD, and MRF4 control the differentiation of myoblasts into myotubes<sup>58 59</sup>. In the fusion stage, myoblasts can fuse with one another to form myotubes which eventually become de novo muscle

fibers, or integrate with existing damaged fibers to add myonuclei and thus help to restore their structural and functional integrity. The nuclear factor of activated T cells (NFAT) family of transcription factors plays an important role in regulating the fusion of myoblasts to injured myofibers<sup>60</sup>.

Immune cells play crucial roles in achieving successful muscle regeneration after acute injury. In the chronological sequence, neutrophils rapidly invade the injury site within hours post-injury, and their numbers gradually decrease by 24 hours post-injury<sup>61 62</sup>. Although neutrophils can induce further damage by generating high levels of reactive oxygen species (ROS) and release of proteases, their primary function is to phagocytose and degrade damaged muscle tissue and debris. Macrophages show a significant rise at 24 hours post-injury<sup>63</sup>, and similarly play a key role in phagocytosing damaged myofibers and dead leukocytes. Furthermore, macrophages have a direct impact in promoting myogenesis following acute skeletal muscle injury. Indeed, it is well established that in the setting of acute (as opposed to chronic) skeletal muscle injury, elimination of macrophages (e.g., by treatment with clodronate or genetic abrogation of C-C chemokine receptor type 2 (CCR2)<sup>64 65</sup> has major negative consequences for the efficacy of muscle regeneration. The specific characteristics and contrasting roles of macrophages in acute versus chronic skeletal muscle injury will be discussed in greater detail in a later section of this introduction. In addition to satellite cells and the above innate immune cell types, the following cells have also been reported to play major roles in orchestrating the complex process of muscle regeneration:

1. Regulatory T cells (Tregs). These are a specialized subset of T cells that primarily exert immunosuppressive functions. Tregs target various immune cells, including T helper cells, cytotoxic T cells, B cells, dendritic cells, and macrophages, among others. Accumulation of Tregs

has been observed in skeletal muscle following acute injury, and depletion of Tregs impairs the regenerative process. Notably, Tregs in the injured muscle exhibit unique transcriptomic profiles compared to Tregs found in other tissues such as the spleen, visceral adipose tissue, and kidney<sup>7</sup>. Tregs also possess the capability to secrete the growth factor amphiregulin (AREG), which plays a crucial role in promoting satellite cell expansion and facilitating muscle regeneration<sup>63 7</sup>. Furthermore, Tregs contribute to the phenotypic transition of macrophages from an M1 pro-inflammatory state to an M2 anti-inflammatory state through the production of IL-10<sup>63</sup>.

2. Eosinophils: These innate immune cells are traditionally recognized for their involvement in allergic reactions and responses to parasites. However, studies using the eosinophil-deficient  $\Delta$ dblGATA1 mouse model have revealed impaired muscle regeneration following acute injury, with interleukin-4 (IL-4) signaling likely playing a significant role in these findings<sup>66</sup>. In this regard, mice lacking IL-4 or IL-4 receptor alpha (IL-4ra) have also demonstrated abnormal muscle regeneration<sup>66</sup>. IL-4 exhibits dual functions in muscle regeneration: it regulates myofiber growth and concurrently promotes the proliferation of FAPs<sup>66 67</sup>.

3. FAPs: These are a specific type of mesenchymal stem cell predominantly found in skeletal muscle tissue, which possess the ability to differentiate into both adipocytes and fibroblasts. The presence of FAPs is essential for effective muscle regeneration following acute injury. Molecules secreted by FAPs such as wnt1-inducible signaling pathway protein 1 (WISP1) and IL-6<sup>68 69</sup> directly enhance the proliferation and differentiation of myoblasts. Additionally, FAPs serve as a significant source of IL-33 in muscle tissue, which contributes to the accumulation of Tregs<sup>70</sup>.

### **1.1.3 Brief overview of Duchenne muscular dystrophy (DMD) – a disease of chronic skeletal muscle injury with unsuccessful muscle regeneration**

In addition to acute muscle injury, there are a number of diseases associated with chronic skeletal

muscle injury, often referred to as myopathies, which can be of acquired or genetic origin. These chronic conditions include autoimmune diseases, metabolic disorders, and a large number of genetically-determined muscular dystrophies. With respect to the latter, DMD, the most common X-linked lethal disorder in humans, is a particular focus of this thesis. DMD is caused by mutations in the dystrophin gene, which spans over 2.5 million base pairs of DNA sequence and is the largest known gene in humans<sup>71</sup>. Clinically, DMD is a devastating disease with an incidence of approximately 1 in every 5,000 live male births<sup>72 73</sup>. The occurrence of DMD in females is extremely rare, with less than one affected individual per million<sup>74</sup>. The initial symptoms of DMD typically emerge around 2-3 years of age and include difficulties in climbing stairs, a shuffling gait, and frequent falls. By the age of 10-12 years, most patients become reliant on wheelchairs, and by the time they reach approximately 20-year-old most patients will require a breathing machine (mechanical ventilator) due to the weakness of the diaphragm and other respiratory muscles. Tragically, despite receiving optimal medical care, the majority of individuals with DMD experience fatal cardiac and/or respiratory failure between the ages of 20 and 40. Although a number of different genetic therapies (e.g., exon skipping, viral vector-mediated gene transfer) are under development as a means of restoring dystrophin protein in DMD muscles, thus far these approaches are of uncertain efficacy. The only well established pharmacological treatment is the use of corticosteroids, which are transiently beneficial but also associated with major side effects. The precise mechanisms underlying the benefits of corticosteroid therapy are incompletely understood, but suppression of harmful inflammation is presumed to be the major effect.

Alternative splicing of the dystrophin gene enables the generation of multiple isoforms. The full-length muscle-specific isoform, known as Dp427M, is a large rod-shaped protein with a molecular weight of 427 kDa with its own unique promoter<sup>75</sup>. DMD gene mutations consisting of large

deletions (60-70%), duplications (5-15%), and point mutations/small deletions/insertions (20%) prevent production of a functional dystrophin protein<sup>76 77</sup>. Mutations that maintain the open reading frame (in-frame) can allow for production of abnormal yet partially functional dystrophin and are associated with Becker Muscular Dystrophy (BMD), a milder form of the disease. The dystrophin protein plays a crucial role in preserving the structural integrity of the muscle fiber membrane (sarcolemma), safeguarding it against the mechanical stress and strain induced by muscle contractions<sup>78</sup>. It accomplishes this by establishing a connection between actin filaments in the cytoskeleton and the ECM via the multi-subunit dystrophin-associated protein complex (DAPC), which collectively act as a shock absorber to dissipate the force and prevent damage from mechanical stresses associated with muscle contractions. In addition, dystrophin actively participates in several transmembrane signaling processes and the loss of these functions also contributes to the development of muscle pathology<sup>79</sup>.

The absence of dystrophin results in a weakened sarcolemmal membrane, rendering the muscle fiber more susceptible to being damaged as a result of normal muscle activity<sup>78</sup>. Muscles lacking dystrophin are particularly susceptible to being damaged by muscle activities which involve eccentric contractions, which place a higher level of stress and strain on the sarcolemma. DMD muscle fibers are characterized by persistently elevated intracellular calcium levels due to this sarcolemmal rupture. While short-term elevations in intracellular calcium can stimulate beneficial muscle adaptations through hormesis, chronic overload of intracellular calcium concentrations can trigger cell death<sup>80</sup>. Muscle, being a highly metabolically active tissue, constantly generates reactive oxygen species (ROS) and reactive nitrogen species. The concentration of ROS in muscle is essential for maintaining proper physiological processes, and it varies depending on the site of production, duration of ROS exposure, and the state of the target cell<sup>81</sup>. In the case of DMD, there

is an observed increase in ROS levels, resulting in oxidative injury to the muscle. The influx of calcium, overload of ROS, and recognition of DAMPs by pattern recognition receptors such as Toll-like receptors (TLRs) in the muscle activate NF- $\kappa$ B signaling<sup>82</sup>. This results in an enhanced production of inflammatory mediators, including chemokines and cytokines. Notably, NF- $\kappa$ B activation is one of the earliest histological abnormalities observed in patients affected by DMD, occurring years before the manifestation of symptoms<sup>83</sup>. Suppression of NF- $\kappa$ B signaling during the early stages of DMD has been suggested as a potential therapy to reduce disease progression<sup>84</sup><sup>85</sup><sup>86</sup>. In contrast to acute muscle injury, where inflammation is resolved and injured muscle is repaired, the chronic inflammatory signaling triggered by the loss of dystrophin in DMD is sustained and leads to unsuccessful muscle repair. This chronic pro-inflammatory environment activates both innate and adaptive immune responses, and favors the differentiation of FAPs into adipocytes and fibroblasts which interferes with muscle regeneration, exacerbating the loss of functional muscle fibers by promoting fibrosis and fatty infiltration of the muscles<sup>87</sup><sup>88</sup><sup>89</sup><sup>90</sup>. The presence of repetitive injury and inflammation, as well as the lack of dystrophin itself, also has adverse effects on satellite cell function. Intrinsically, the lack of dystrophin in activated satellite cells in DMD muscle leads to a reduced ability to maintain stem cell properties due to decreased asymmetric division and an increase in progenitor cells that contribute to muscle regeneration through symmetric division<sup>91</sup>. Externally, the persistent presence of oxidative and inflammatory stress causes satellite cells to be unable to re-enter the cell cycle, a condition associated with cellular senescence<sup>92</sup>. In vitro and in vivo studies have also shown that satellite cells from dystrophic muscles exhibit a diminished capacity for muscle generation and tend to adopt a profibrotic role, characterized by the increased expression of fibrogenic genes and collagen production<sup>93</sup><sup>94</sup>. These alterations in satellite cells, in turn, further exacerbate the progression of the

disease<sup>95</sup>.

Animal models have been essential tools in researching the pathogenesis and treatment of DMD. These encompass murine, rat, dog, and zebrafish models, among others. Rat models of DMD, such as the Dmd-KO rat and DMDdel52 rat<sup>96 97 98</sup>, offer advantages in terms of size and similarity to human muscle physiology and structure compared to mice<sup>99</sup>. However, rat models are less frequently employed, likely due to low availability and greater costs, as well as the limited genetic tools for manipulating gene expression in rats. The Golden Retriever Muscular Dystrophy (GRMD) dog serves as a naturally occurring DMD model, exhibiting severe clinical symptoms and premature death that closely mimic DMD in humans<sup>100</sup>. The GRMD model is utilized in preclinical research for promising treatments, including gene and stem cell therapies<sup>101 102 103</sup>. However, in addition to concerns related to ethics and cost, the GRMD model requires a high level of veterinary expertise. Murine models and in particular the mdx mouse currently serve as the predominant animal species for studying DMD.

In the original mdx mouse model, dystrophin deficiency arose spontaneously in C57BL/10 mice from a premature stop codon in exon 23<sup>104</sup>. Chemical mutagens were later employed to induce other point mutations in the dystrophin gene on C57BL/6 background mice, resulting in the generation of Mdx2cv-5cv mice<sup>105</sup>. In comparison to the original model, both mdx4cv (harboring a premature stop codon in exon 53) and mdx5cv (with a point mutation on exon 10), exhibit fewer spontaneous dystrophin gene reversion events (dystrophin protein restoration due to somatic cell mutations) in individual fibers<sup>106</sup>. One critique of the mdx mouse as a model for human DMD is that the very active and successful muscle regeneration observed in the limb muscles of mdx mice mitigates muscle loss, resulting in a better preservation of muscle strength and lifespan than observed in humans. Interestingly, the diaphragm of mdx mice is more severely affected by the

disease than other skeletal muscles, presumably due to the very high respiratory rate of mice (approximately 200 per minute) and consequent increased frequency of contraction-induced muscle injury in this muscle. The mdx diaphragm most closely resembles human affected by DMD in terms of the progression of muscle necrosis, inflammation and fibrosis<sup>107</sup>. Therefore, in the current thesis we have employed the mdx mouse diaphragm model to determine how macrophage properties are affected in chronic muscle injury caused by one of the most common and prototypical of the genetically-based muscular dystrophies, namely DMD.

## **1.2. General overview of macrophage biology**

### **1.2.1 Macrophage function in infection and tissue development/regeneration**

Before discussing what is known specifically about the role of macrophages in skeletal muscle, a more general background of macrophage biology will first be provided. Elie Metchnikof's pioneering research in the 1880s led to the discovery and characterization of macrophages. His observations of macrophages engulfing foreign materials in starfish larvae provided the first insights into their crucial functions in host defense, cell turnover, inflammation, and repair. Macrophages are distributed throughout all tissues, constituting approximately 1-5% of the cellular population<sup>108 109</sup>. They exhibit a high degree of plasticity, adjusting their size and shape based on the local tissue environment, and possess an impressive array of functional capabilities that extend far beyond their initially discovered role as phagocytes.

Macrophages play a critical role in the innate immune system as part of the body's initial defense against infections. Monocytes are recruited from the bone marrow to sites of infection and then differentiate into macrophages responsible for pathogen clearance and initiation of inflammation in the tissue. Macrophages express various pattern recognition receptors (PRRs) on their cell surface and within endosomes, allowing them to recognize specific pathogen-associated molecular patterns (PAMPs) associated with bacteria, viruses, and fungi. These receptors include TLRs, NOD-like receptors, RIG-I-like receptors, C-type lectin receptors, and scavenger receptors, among others<sup>110</sup>. Activation of these PRRs triggers pathways such as the Rho GTPase pathway, PI3K-Akt pathway, protein kinase C (PKC) pathway, and mechanistic target of rapamycin (mTOR) pathway, which are associated with phagocytosis<sup>111 112 113</sup>. After phagocytosis, macrophages employ a process known as phagosome maturation to eliminate engulfed pathogens. An essential aspect of this process is the acidification of the phagosomal lumen, facilitated by proton pumps, which

creates an acidic environment necessary for optimal enzymatic activity <sup>114</sup>.

Multiple mechanisms contribute to the killing of pathogens within macrophages. Fusion events occur between phagosomes and other cellular compartments, including endosomes, lysosomes, and autophagosomes<sup>115 116</sup>. Macrophage autophagy contributes to pathogen clearance by aiding in the elimination of intracellular pathogens. Reactive oxygen species such as superoxide anion (O<sub>2</sub><sup>-</sup>), hydrogen peroxide (H<sub>2</sub>O<sub>2</sub>), and hypochlorous acid (HOCl) are produced <sup>117 118</sup>. Similarly, reactive nitrogen intermediates (RNIs) including nitric oxide (NO) and its reactive derivatives are generated. Additionally, macrophages secrete antimicrobial peptides <sup>119</sup> as well as lytic enzymes that can directly harm parasites. Macrophages also have the capability to actively accumulate metals, such as iron, zinc, copper, and manganese, within the phagolysosome. This sequestration process restricts the availability of essential metals to invading pathogens, depriving them of the necessary nutrients for survival and replication <sup>120</sup>.

Activation of PRRs also induces the production of cytokines. Among the genes regulated by NF- $\kappa$ B are various pro-inflammatory cytokines, including TNF- $\alpha$ , interleukin-1 beta (IL-1 $\beta$ ), interleukin-6 (IL-6), interleukin-12 (IL-12), interleukin-23 (IL-23), IL-18, interferon- $\gamma$  (IFN- $\gamma$ ) and various chemokines that play a crucial role in recruiting immune cells to sites of infection <sup>121</sup> <sup>122</sup>. These chemokines include C-C motif chemokine ligand 2 (CCL2)/ monocyte chemoattractant protein-1 (MCP-1), C-C motif chemokine ligand 3 (CCL3)/ macrophage inflammatory protein-1 alpha (MIP-1 $\alpha$ ), C-C motif chemokine ligand 4 (CCL4)/ macrophage inflammatory protein-1 beta (MIP-1 $\beta$ ), C-X-C motif chemokine ligand 8 (CXCL8)/interleukin-8 (IL-8), and C-X-C motif chemokine ligand 10 (CXCL10)/ interferon-gamma-induced protein 10 (IP-10)<sup>123</sup>. Additionally, NF- $\kappa$ B regulates the expression of adhesion molecules involved in leukocyte recruitment and migration, such as intercellular adhesion molecule-1 (ICAM-1), vascular cell adhesion molecule-

1 (VCAM-1), and E-Selectin<sup>121</sup>. The interferon regulatory factor (IRF) pathway, particularly IRF3 and IRF7<sup>124 125</sup>, serves as key regulators of type I interferon (IFN) and other antiviral genes. Type I interferons are potent antiviral cytokines with autocrine and paracrine effects<sup>126</sup>. They enhance the activation of other immune cells, including natural killer (NK) cells and T cells, to promote viral clearance<sup>127 128</sup>. Macrophages act a bridge to the adaptive immune system by internalizing antigens, which then undergo processing within endosomes or phagosomes. The resulting antigenic peptides are loaded onto major histocompatibility complex class II (MHC-II) molecules at the macrophage cell surface where they are presented to CD4+ T cells<sup>129</sup>. Co-stimulatory molecules on the macrophage surface, such as CD80 and CD86, engage with co-stimulatory receptors on T cells, providing additional signals for T cell activation and proliferation<sup>130</sup>. This antigen presentation process by macrophages is critical for activating adaptive immune responses, enabling the identification and elimination of pathogens or abnormal cells.

In addition to their role in fighting infections, macrophages are heavily involved in responses to sterile injury and tissue regeneration, as well as in organogenesis during embryonic development. Macrophages appear in most organs before birth and are the first type of immune cell to develop in the embryo<sup>131</sup>. Large numbers of macrophages are present in virtually all developing organs, with the maximum numbers correlating with key periods of organogenesis<sup>132</sup>. Their presence during this time, when the embryo is in the uterus and not exposed to external threats, is primarily to promote organ development. For example, macrophages play a key in angiogenesis, which encompasses various morphogenetic processes such as migration, proliferation, polarization, lumen formation, and membrane deposition of endothelial and vascular smooth muscle cells. Alveolar macrophages contribute to lung genesis by surrounding emerging lung buds and elongating bronchi, correlating with alveolar development phases<sup>133 134 131</sup>. In mice lacking

macrophages due to genetic removal of colony-stimulating factor 1 (CSF-1)/ macrophage colony-stimulating factor (M-CSF), abnormal lung morphogenesis with emphysema occurs<sup>135</sup>. Inflammatory activation of macrophages through the NF-κB pathway also inhibits airway branching, emphasizing their role in lung morphogenesis<sup>134</sup>. Additionally, macrophages contribute to lymphatic vessel promotion and tissue remodeling during embryonic development<sup>136</sup>. Microglia, a type of brain macrophage, facilitate postnatal neurogenesis and enhance neuronal survival through growth factor release, neuron death regulation, and synaptogenesis control<sup>137 138 139</sup>.

### **1.2.2 Macrophage ontogeny**

*Prenatal origin macrophages* start to develop during primitive hematopoiesis which occurs in the yolk sac from E7.0 to E11.0<sup>140 141</sup>. Macrophages differentiate directly from hemangioblasts that emerge in the yolk sac at approximately E8.5<sup>142</sup>. The aorta-gonad mesonephros (AGM) also contributes to hematopoiesis during embryonic development from E8.5 to E12.0, giving rise to so-called "definitive hematopoiesis". HSCs in the AGM may arise from migrating cells originating in the yolk sac or develop from specific hemogenic endothelial cells. HSCs undergo proliferation in the fetal liver give rise to the macrophage from E11.5 to E16.5<sup>143 144 145</sup>, and subsequently migrate to the bone marrow before birth<sup>146</sup>. While embryonically derived macrophages were initially thought to be short-lived, recent findings indicate that these cells are long-lived and possess self-renewal capabilities<sup>109</sup>.

*Postnatal origin macrophages* are derived from monocytes released from the adult bone marrow. These cells differentiate from HSCs through a sequential process involving common myeloid progenitors (CMPs), granulocyte-monocyte progenitors (GMPs), monocyte-dendritic cell progenitors (MDPs), and common monocyte progenitors (cMoPs)<sup>147</sup>. Postnatal origin macrophages were traditionally believed to be a relatively uniform group of cells dependent on

monocytes from the adult bone marrow<sup>148</sup>. All tissue-resident macrophages were once considered to be derived from these cells and to be entirely dependent on circulating monocytes for their replenishment<sup>149 150 151</sup>. However, studies utilizing bone marrow and parabiosis (in which the circulations of two animals are joined) experiments have shown that many adult tissues also harbor populations of self-renewing macrophages of prenatal origin, which are not reliant on circulating monocytes<sup>152 153 154 155</sup>. Recent advances in other research tools, such as fate-mapping animal models and single-cell RNA sequencing techniques, have also allowed for the tracking of macrophage development from their precursors to their fully mature state within different organs (Tables 1.1 and 1.2). Taken together, these studies have revealed that most adult organs have tissue-resident macrophage populations which are derived from a combination of prenatal (i.e., embryonic yolk sac and fetal liver) and postnatal (i.e., monocytes released from the adult bone marrow) sources<sup>156 141 157</sup>. However, the relative proportions of these two sources of tissue-resident macrophages in the adult varies according to organ. For example, microglia in the adult brain are almost entirely of prenatal origin, whereas macrophages in the adult intestine are predominantly derived from circulating monocytes<sup>141 158 159</sup>.

**Table 1.1 Fate-mapping models**

Fate-mapping model	target cell	Reference
Runx1CreERT	yolk sac	Florent Ginhoux, 2010
Cx3cr1Cre/ Cx3cr1CreERT/ Cx3CR1gfp/+	MDP, pMac	Simon Yona, 2013; Christian Schulz, 2020; Elvira Mass, 2016; Sarah A. Dick, 2022
Myb-/-	HSC	Christian Schulz, 2020
Csf1rMeriCreMer/ Csf1riCre YFP+	yolk sac, EMP	Christian Schulz, 2020; Elvira Mass, 2016; Elisa Gomez Perdiguero, 2015
Tie2MeriCreMe	yolk sac	Elisa Gomez Perdiguero, 2015
Flt3Cre	pluripotent hemato- poietic progenitors	Christian Schulz, 2020; Elisa Gomez Perdiguero, 2015
Tnfrsf11aCre	pMac	Elvira Mass, 2016
Ms4a3Cre	GMS	Zhaoyuan Liu, 2019
Cxcr4CreERT	hematopoietic stem cells	Yves Werner, 2020
KitMerCreMer	early hematopoietic progenitors	Si Min Lai, 2018
Ccr2CreER	monocyte	Sarah A. Dick, 2022

A summary of fate-mapping models used to track the origin or fate of macrophage. Each model is associated with a target cell type and references.

MDP: Monocyte-dendritic cell progenitor, pMac: Pre-macrophage, HSC: Hematopoietic stem Cell, EMP: Erythro-myeloid progenitor, GMS: Granulocyte-monocyte stem cell/progenitor

**Table 1.2 Ontogeny of adult tissue-resident macrophages in different organs**

Organ/Tissue	Origin	Reference
Brain	microglia: yolk sac EMP	Gomez Perdiguero, 2015; Zhaoyuan Liu, 2019; Guillaume Hoeffel, 2015
Lung	alveolar MP: fetal liver EMP, adult monocyte replacement with aging;	Elisa Gomez Perdiguero, 2015; Zhaoyuan Liu, 2019; Guillaume Hoeffel, 2015
	Interstitial MP: fetal liver, adult monocyte replacement with aging	Chakarov et al., 2019
Liver	Kupffer cell: fetal liver EMP	Elisa Gomez Perdiguero, 2015; Zhaoyuan Liu, 2019; Guillaume Hoeffel, 2015
Intestine	Embryonic origin; adult monocyte replacement with aging	Marcello Delfini, 2022; Calum C Bain, 2014; Zhaoyuan Liu, 2019; Ehud Zigmond, 2012
Spleen	adult monocyte replacement with aging and injury	Zhaoyuan Liu, 2019; Malay Haldar, 2014
Epidermis	Langerhans cells: fetal liver EMP	Elisa Gomez Perdiguero, 2015; Zhaoyuan Liu, 2019; Guillaume Hoeffel, 2015

Overview of the origin of immune cells in various organs and tissues, along with their corresponding references.

Based on these observations, macrophage ontogeny and self-renewal have become an area of intensive research in the field of immunology. Studies indicate that the developmental origin of macrophages could impact their reactions to signals from the surrounding microenvironment<sup>160 161</sup>. Furthermore, macrophages derived from erythro-myeloid progenitors (EMP) and HSCs exhibit distinct patterns of gene expression, distinguishable at the molecular and functional level<sup>160</sup>. In vitro culture experiments using macrophages deficient in the transcription factors MafB and c-Maf, crucial for macrophage differentiation, revealed their unexpected self-renewal capacity<sup>163</sup>. It was found that the inhibition of MafB and c-Maf led to the upregulation of transcription factors E26 transformation-specific-1/2 (Ets-1/2) and PU-box binding protein 1 (PU.1), resulting in enhanced expression of myelocytomatosis oncogene (c-Myc) and kruppel-like factor 4 (KLF4). Additionally, studies investigating steady-state macrophage proliferation using 5-bromo-2'-deoxyuridine (BrdU) incorporation in the lung demonstrated that a significant proportion of lung macrophages actively undergo proliferation<sup>164</sup>. Moreover, the replacement of depleted tissue macrophages in the lung was found to occur through local self-renewal in the absence of CCR2+ monocyte<sup>164</sup>. Similar observations of self-renewal capacity have been made in the liver, where both embryonic and bone marrow-derived macrophages are capable of generating self-renewing liver macrophages<sup>165</sup>. Inflammatory responses can also trigger local proliferation of mature macrophages<sup>166</sup>. For example, in the context of heart injury, both embryonic and bone marrow-derived macrophages were found to proliferate<sup>167</sup>. The proliferation of macrophages is regulated by factors such as CSF1/M-CSF and IL-4. Blocking the CSF1/M-CSF receptor (CD115/CSF1R) with antibodies in an allograft model markedly reduced macrophage proliferation rates<sup>168</sup>. IL-4 has also been implicated in the local self-renewal of macrophages within tissues<sup>169 170 169</sup>. A summary of transcription factors and microenvironmental cues involved in the regulation of

macrophage differentiation is shown in Table 1.3.

### **1.2.3 Phenotypic heterogeneity of macrophages**

Despite macrophages in different organs being identified by similar phenotype markers such as CD11b, F480, and CD64, their gene expression profiles differ depending on the specific organ<sup>171</sup>. The distinct transcriptional programs of macrophages are influenced by the unique microenvironments within different organ niches<sup>172 173</sup>. Within a single tissue, macrophage subsets exhibit phenotypic, transcriptional, and spatial uniqueness that changes over time, reflecting distinct commitment states influenced by cellular and anatomical niches<sup>174</sup>. The brain is one of the most extensively studied organs in terms of macrophage heterogeneity, with more than six subsets identified<sup>175 174</sup>. Macrophage morphology in different brain regions such as the cortex, subconical organ, white matter, ventral pallidum, meninges, and choroid plexus varies based on their location and interactions with neighboring cells<sup>175</sup>. Moreover, genetic signatures differ between macrophages residing in the central nervous system (CNS) parenchyma and non-parenchymal macrophages<sup>176</sup>. Similar to the brain, diverse macrophage subsets are found in other organs such as the lung, liver, and spleen<sup>177 178 179 180</sup>.

**Table 1.3 Characteristics of Macrophages in Different Organs/Tissues: Niche Signals, Transcription Factors, Functions, and Phenotypic Markers**

Organ/tissue	Macrophage	Niche signals	Transcription factors	Functions	Phenotypic markers
Embryo	Premacrophage	CSF1	PU.1, ZEB2, cMAF, BATF3, PPAPY, IRF8	Source of embryonic macrophage	CSF1R, CX3CR1, F480
Brain	Microglia	TGF- $\beta$ , IL-34, SCFAs	SALL1, SALL3, MEIS3, SMAD2/3, MEF2C	Synaptic pruning, learning dependent synapse formation	F480+, CD11b+, CD45low
Lung	Alveolar macrophage	CSF2, TGF- $\beta$	PPAPY, BACH2, CEBP $\beta$ , KLF4, ATF5	Surfactant metabolism, particle clearance, immunosuppression	F480low, CD11b <sup>low</sup> , CD11c high, CD68+, SiglecF+, MACRO+, CD206+, Dectin-
Liver	Kupffer cell	Desmosterol, DLL4	ID1, ID3, LXR $\alpha$ , SPI-C, NR1H3, IRF7	Erythrocyte clearance, portal circulation clearance, interactions with hepatocytes, iron, lipids and micronutrients metabolism	F480 high, CD11b low, CD169+
Intestine	Intestinal macropahge	TGF- $\beta$ , NOTCH	RUNX3, HES1, DTX4	Gut tolerance and immunity	CX3CR1 high, F480+, CD11b+, CD11c+, CD64+
Blood	Ly6C+ Mo	CSF1	IRF8, KLF4	pathogen defense, tissue damage resolution	CD11b+, CCR2, CD115
	Ly6C- Mo	CSF1	KLF2, NR4A1, C/EBP $\beta$	patrolling and surveillance, vasular integrity	CD11b+, CX3CR1+, CD115

Overview of macrophage populations in various organs/tissues, along with their specific niche signals, key transcription factors, functions, and characteristic phenotypic markers.

\*Adapted from References<sup>181, 182, 109</sup>.

Phenotypic heterogeneity of macrophages can be induced by immunological changes or activation from the surrounding environment, including interactions with T cells. In vitro, researchers have attempted to mimic and simplify the microenvironmental cues received by macrophages in vivo by using T cell cytokines. In vitro stimulation with cytokines produced by Th1 cells (e.g., IFN- $\gamma$  and TNF) or TLR agonists like lipopolysaccharide (LPS) polarizes macrophages to a so-called M1 or classical activation state. In vitro stimulation by Th2 cytokines such as IL-4 and interleukin-13 (IL-13) polarizes macrophages to a so-called M2 or alternative activation state. M1-polarized macrophages express pro-inflammatory cytokines and exhibit an increased capacity for phagocytosis and pathogen elimination through the production of ROS and other mechanisms as described at the beginning of this section. M2-polarized macrophages produce anti-inflammatory cytokines, contribute to inflammation resolution through production of cytokines such as interleukin -10 (IL-10) and transforming growth factor-beta (TGF- $\beta$ ), and possess an increased capacity for scavenging receptors and clearance of cell debris. M2-polarized macrophages can be further subdivided into subsets referred to as M2a, M2b, M2c, and M2d, depending on the specific stimuli they encounter, each with distinct functions and characteristics in vitro<sup>183 184</sup>. However, it is important to recognize that although macrophage polarization as described above can be achieved in vitro, the in vivo situation is considerably more complex, both in terms of stimuli and the range of phenotypes encountered<sup>185</sup>. Hence the heterogeneity of macrophage phenotype should not be considered as being simply a spectrum between M1 and M2, but rather as a multi-dimensional concept with myriad combinatorial possibilities.

### **1.3. Heterogeneity and roles of macrophages in skeletal muscle repair**

#### **1.3.1. Macrophage ontogeny in skeletal muscle**

In comparison to other organs, there has been relatively little study of the ontogeny of skeletal muscle macrophages. The only published study which has attempted to directly address this question employed Flt3Cre-Rosa26LSL-YFP mice to trace the lineage of macrophages that had arisen from definitive HSCs<sup>186</sup>. Using this approach these authors reported that approximately 60% of skeletal muscle macrophages were of bone marrow origin by the time the mice were 26 weeks old. They also conducted a bone marrow transplantation experiment (chimeric mice) as a complementary technique to determine the contribution of bone marrow-derived macrophages to the adult skeletal muscle macrophage pool. However, in the chimeric mouse model they found that up to 90% of muscle macrophages originated from the donor adult bone marrow-derived monocytes. To account for the discrepancy between these two models, it was speculated that the greater percentage of bone marrow-derived macrophages observed in chimeric mice could be due the use of whole body irradiation, which might eliminate the prenatal source resident muscle macrophages that are derived from the embryo.

#### **1.3.2. Role of different macrophage functions and subsets leading to successful muscle regeneration after acute injury**

Upon acute skeletal muscle injury, tissue-resident macrophages become activated and secrete chemokines, such as cytokine-induced neutrophil chemoattractant (KC) and CCL2/MCP-1<sup>187</sup>. These chemokines play a crucial role in recruiting much larger numbers of immune cells from the bone marrow to the site of injury. Neutrophils are typically the first immune cells to arrive at the site of injury, where they act as highly efficient phagocytes to remove cellular debris and pathogens. Macrophages are more abundant and have a longer lifespan than neutrophils, allowing them to

participate in different aspects of the muscle repair process. Among the chemokines involved, CCL2 holds particular significance. It is produced by multiple cell types including monocytes, macrophages, endothelial cells<sup>188</sup>, fibroblasts<sup>189</sup>, and muscle cells<sup>65</sup>. CCL2 acts as a chemotactic factor, attracting immune cells, especially monocytes and macrophages, to the site of muscle injury. This recruitment is mediated through the CCR2 receptor, which also binds other members of the monocyte chemoattractant protein (MCP) family that are involved in monocyte/macrophage recruitment<sup>190</sup>. In the setting of acute infectious or sterile injury, release of Ly6C<sup>high</sup> (often referred to as “inflammatory”) monocytes from the bone marrow is critically dependent on monocyte expression of CCR2<sup>191</sup>.

Previous studies have shown that genetic ablation of either CCL2 or CCR2 results in delayed muscle regeneration and impaired muscle strength recovery<sup>29 192 188</sup>. Although myoblasts and their precursors (satellite cells) can express CCR2 and respond to CCL2 stimulation *in vitro*<sup>193</sup><sup>30</sup> bone marrow chimera models have indicated that CCR2 signaling in the myeloid lineage rather than myogenic cells is the main prerequisite for successful regeneration of normal muscles following acute injury<sup>194</sup>. In mice lacking CCL2, there is a significant decrease in macrophage recruitment, delayed clearance of injured fibers, and impaired muscle regeneration. Without CCL2, the release of monocytes from the bone marrow into the bloodstream and their subsequent recruitment from the blood to the injured muscles are both reduced. Therefore, successful recruitment of monocytes to the injured muscle requires the production of CCL2 by both tissue-resident macrophages and bone marrow-derived monocytes. Similarly impaired muscle regeneration has been observed in CCR2-deficient mice, again highlighting the importance of monocyte recruitment<sup>187 65 195</sup>.

In the context of acute skeletal muscle injury, there is a dynamic interplay between M1 and M2

macrophages. Immediately following injury, monocytes differentiate into M1 macrophages and the presence of M1 macrophages significantly increases, reaching peak levels at 48 hours post-injury<sup>9</sup>. In general, M1 macrophages, associated with pro-inflammatory responses, exhibit a high phagocytic capacity and are efficient in engulfing pathogens and debris. They produce pro-inflammatory cytokines and reactive oxygen species to eliminate pathogens but may also contribute to tissue damage. Subsequently, there is a rapid decline in the M1 macrophage population until day 4 post-injury. The number of M2 macrophages starts to rise from 24 hours post-injury onward, reaching its highest point at day 4-7 post-injury, followed by a gradual decrease<sup>9</sup>. M2 macrophages are involved in tissue repair and resolution of inflammation. They are responsible for clearing apoptotic cells and promoting tissue healing through the secretion of anti-inflammatory cytokines and growth factors. As a general rule, pro-inflammatory M1 macrophages play a key role in promoting myoblast proliferation, while anti-inflammatory M2 macrophages support their differentiation.

M1 macrophages exhibit a high migratory ability towards activated satellite cells<sup>196</sup>. This enables the M1 macrophages to move towards the site of muscle injury where the activated satellite cells are located. M1 macrophage-derived cytokines and growth factors are able to stimulate the proliferation of satellite cells and other myogenic precursor cells (eg. satellite cell-derived myoblasts). Studies have demonstrated that M1-conditioned macrophages, compared to untreated macrophages, display a dual role in muscle regeneration. On one hand, they actively facilitate the growth and proliferation of myogenic precursor cells. On the other hand, they hinder the differentiation and fusion of these cells<sup>197</sup>. Once M1 macrophages have been replaced by M2 macrophages this reduces the migration of myogenic cells and increases the probability of cell-to-cell contacts between M2 macrophages and activated satellite cells<sup>196</sup>. This promotes muscle repair

because M2 macrophages release various cytokines, growth factors, and extracellular matrix components that facilitate the differentiation and fusion of myoblasts into myotubes/myofibers<sup>197</sup>. It is important to note that the transition from M1 to M2 macrophages during muscle regeneration is not attributed to the recruitment of two distinct macrophage populations from the blood, but rather represents a phenotypic shift within the existing macrophage population. This transition is accompanied by a reduction in the expression of peroxisome proliferator-activated receptor gamma (PPAR $\gamma$ ), a regulator that inhibits the production of pro-inflammatory cytokines and chemokines such as TNF- $\alpha$  and IL-1 $\beta$ , while promoting the production of anti-inflammatory cytokines like IL-10. Phagocytosis of cellular debris plays a crucial role in facilitating the M1 to M2 transition, as it leads to reduced TNF secretion and increased TGF- $\beta$  production<sup>197</sup>. In this regard, blocking phagocytosis impedes the production of M2 cytokines. AMP-activated protein kinase alpha 1 (AMPK $\alpha$ 1), an energy sensor in macrophages, is also essential for this transition. AMPK $\alpha$ 1 deficiency disrupts the macrophage's ability to differentiate into M2 phenotypes and impairs phagocytosis, highlighting its significance in orchestrating the transition from M1 to M2 macrophages during regeneration<sup>198</sup>.

Timely resolution of the M1 phase and a smooth transition to M2 macrophages is crucial for successful skeletal muscle regeneration following acute injury. Dysregulation of this process may contribute to more complex muscle diseases and pathological conditions, while also impeding the repair and regeneration of the affected tissue. For example, the use of  $\beta\Delta$ Cre mice, which harbor a mutation in the *Cebpb* promoter, disrupts the induction of M2-specific genes while leaving the M1 inflammatory genes unaffected. This disruption of M2-specific macrophage gene expression hampers the later phases of muscle regeneration and the replacement of muscle fibers, while the initial removal of necrotic tissue remains intact<sup>199</sup>. The interplay between macrophage phenotype

(M1-M2 polarization) and the different steps of myogenesis highlights the fact that the activation, proliferation, and differentiation of satellite cells are all regulated by a complex combination of pro- and anti-inflammatory mediators expressed at different points in time. Below is a brief description of some of the main mediators produced by macrophages (as well as skeletal muscle cells in many cases), and their potential effects on myogenesis in the setting of acute skeletal muscle injury.

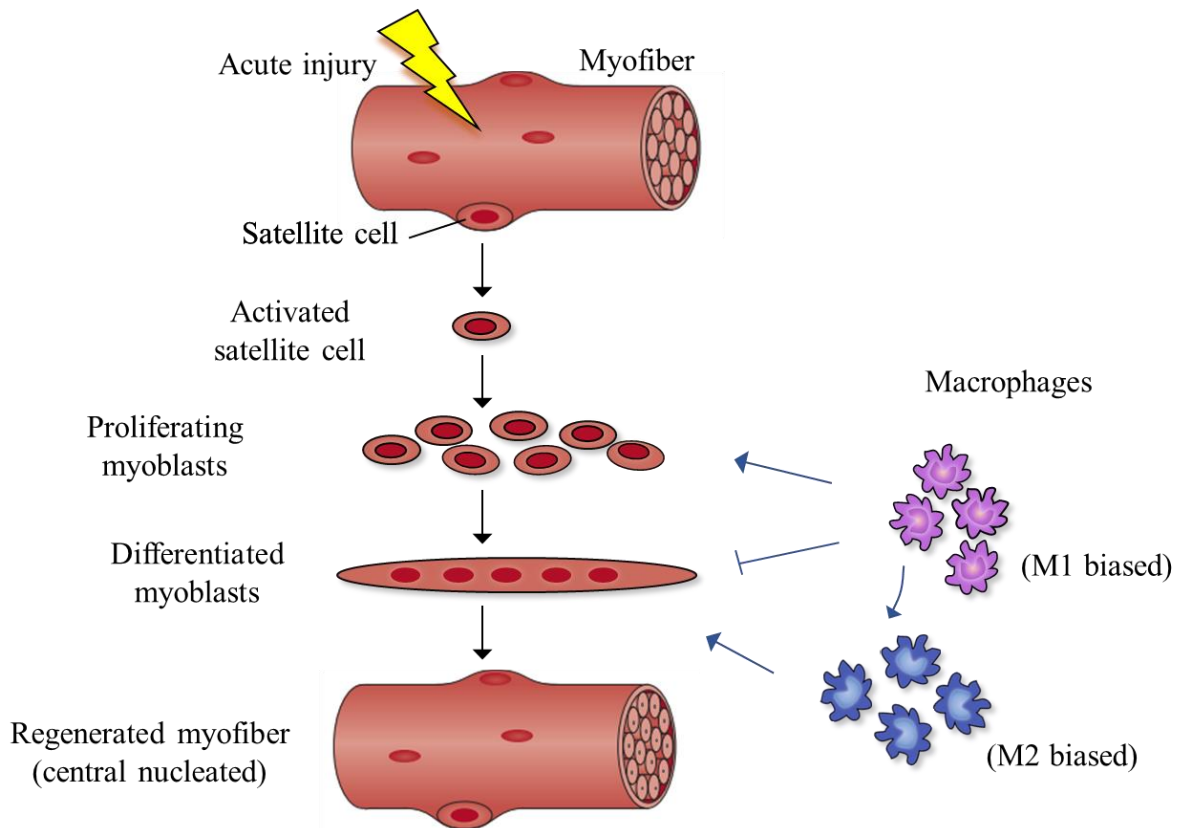


**Figure 1.2 Impacts of inflammation and macrophage polarization on skeletal muscle injury and repair**

In response to muscle injury, satellite cells become activated, initiating proliferation as myoblasts. Subsequently, they fuse and undergo differentiation into myotubes, contributing to the regeneration process and replacing damaged muscle tissue. Several cell types play critical roles in influencing the outcome of regeneration, with macrophages entering the injured areas shortly after damage. Initially, these invading macrophages differentiate into proinflammatory macrophages, exhibiting phenotypic similarities to M1 macrophages. These proinflammatory macrophages are involved in clearing damaged tissue and releasing various cytokines that stimulate myoblast proliferation. As the injury progresses into later stages, there is a phenotypic shift among macrophages from the M1 to the M2-biased state. M2-like macrophages take on the role of promoting myoblast differentiation and fusion, contributing to the regenerative process.

1. TNF- $\alpha$ . TNF is produced by M1 macrophages, and its effects on myogenesis can vary depending on the specific time point, dose, and concentration, as well as the interplay with pathways such as p38<sup>200 201</sup>. TNF has been reported to stimulate myoblast proliferation<sup>202</sup>. In addition, TNF-mediated NF- $\kappa$ B activation has been shown to post transcriptionally suppress MyoD mRNA, thus hindering the differentiation process<sup>203</sup>. Blocking TNF has been shown to reduce the activation of p38  $\alpha$  and  $\beta$  kinases, which in turn leads to a reduction in the expression of Pax7, a key regulatory gene of satellite cells<sup>204</sup>. TNF receptor deficient mice exhibit impaired or delayed myogenic differentiation following muscle injury caused by cardiotoxin<sup>202</sup>. Additionally, in wild-type mice treated with anti-TNF antibodies prior to freeze-induced injury, there is a reduction in the number of fibers expressing MyoD mRNA and decreased recovery of muscle strength<sup>205</sup>.

2. Nitric oxide synthase 2 (NOS2)/ inducible nitric oxide synthase (iNOS). This enzyme is a classical marker of pro-inflammatory M1 macrophages<sup>206</sup>. Mice lacking NOS2 exhibit impaired proliferation and differentiation of myogenic precursor cells following muscle injury<sup>207</sup>. Moreover, NOS2 exerts an influence on the recruitment of inflammatory cells, as evidenced by elevated levels of chemokines and increased infiltration of neutrophils and macrophages observed in the injured muscles of NOS2-deficient mice<sup>207</sup>.

3. IFN- $\gamma$ . This cytokine is expressed by M1 macrophages, and is upregulated at both the mRNA and protein levels in muscle following injury<sup>46</sup>. Mice lacking IFN- $\gamma$  display compromised muscle regeneration and fibrosis. Blocking the IFN- $\gamma$  receptor on myoblasts with an antibody leads to decreased proliferation and fusion<sup>46</sup>.

4. IL-6 and IL-1 $\beta$ . These cytokines are primarily secreted by M1 macrophages. IL-6 elicits a proliferative response in myogenic progenitor cells but this effect is dependent upon dosage<sup>208</sup>. Furthermore, myoblasts themselves can produce IL-6 upon activation. When myotubes are

exposed to IL-1b, there is a significant increase in IL-6 production. This effect is partially mediated through the activation of the MAP kinase pathway and NF- $\kappa$ B<sup>209</sup>. Additionally, studies have indicated that IL-1b can effectively suppress myogenic differentiation<sup>210</sup>.

5. IGF-1. IGF-1 is a growth factor produced by M2 macrophages. Depending on its dose, it can promote myoblast proliferation or differentiation<sup>211</sup>. It enhances protein synthesis, can prevent cell death, and modulates the transition of macrophage phenotypes<sup>212</sup>. During the transition from the inflammatory phase to the repair phase following muscle injury, there is a notable increase in IGF-1 production by M2 macrophages<sup>212</sup>. Moreover, when IGF-1 is lacking in macrophages, there is a decrease in myoblast numbers and reduced cross-sectional area of myofibers<sup>212</sup>. Interestingly, the replacement of IGF-1 significantly enhances muscle regeneration in CCR2-deficient mice, where macrophage migration is impaired<sup>213</sup>.

6. TGF- $\beta$ . TGF- $\beta$  is a marker of M2 macrophages, and exerts complex effects on myogenic transcription<sup>214</sup>. For example, TGF- $\beta$  promotes C2C12 proliferation by the phosphorylation of smad2<sup>215</sup>. It inhibits myoblast fusion in low mitogen differentiation medium<sup>216</sup>. This could be partially due to the degradation of MyoD, which hinders the commitment of myoblasts<sup>217</sup>. However, when TGF- $\beta$  was added to mitogen-rich medium, it facilitated fusion and triggered expression of the myogenic differentiation marker muscle creatine kinase (MCK)<sup>218</sup>.

### **1.3.3. Role of dysregulated macrophage function in the unsuccessful muscle regeneration associated with chronic skeletal muscle injury in DMD**

Muscle regeneration after acute injury is efficient and reliable due to the evolutionary adaptation for rapid recovery following trauma. However, there is less evolutionary pressure for mechanisms to regenerate chronically damaged muscle since chronic muscle damage is rare. As a result, without an adapted system for chronic injuries, immune cell modulation of muscle regeneration

can malfunction, leading to muscle fibrosis and impaired regeneration. In DMD, the lack of dystrophin protein causes ongoing muscle damage. The continuous release of signals indicating damage in the muscle hampers the body's ability to effectively resolve the associated inflammation in a timely manner. As a result, this prolonged immune response leads to pathological inflammation and hinders the process of muscle regeneration. The persistent inflammation in the muscle is significantly contributed to by macrophages, and to a lesser extent by other immune cells such as eosinophils, mast cells, and T cells<sup>8 9</sup>. In young patients affected by DMD aged 2-8 years old, macrophages constitute approximately 37% of the muscle immune cells present in the muscle<sup>219</sup>. In mdx mice, peak macrophage infiltration occurs at 4-8 weeks of age, reaching a count of over 80,000 cells/mm<sup>3</sup><sup>220 221 222</sup>. Importantly, an increased prevalence of macrophages in mdx muscle tissue is found even until the end of the animal's lifespan, indicating a sustained presence throughout the disease course.

Several studies have highlighted that depleting different immune cell populations at early stages of the disease in mdx mice reduces the severity of muscle pathology<sup>223 224 225 226</sup>. The Petrof lab has shown that genetic ablation of CCR2 in mdx mice leads to a decrease in the recruitment of monocyte-derived macrophages to dystrophic muscle. This reduction in monocyte recruitment is associated with a phenotypic shift in macrophages (towards a less inflammatory state) as well as improved histopathological outcomes and greater force generation by the dystrophic diaphragm, which is the muscle showing the greatest physiologic impairment in the mdx model<sup>223</sup>. However, it is noteworthy that the protective effect of macrophage depletion is not permanent. While a decrease in muscle damage and endomysial fibrosis can be observed in both the diaphragm and quadriceps muscles at 14 weeks, these improvements are not sustained at 6 months<sup>224</sup>. These findings highlight the complex and time-dependent nature of macrophage-mediated effects on

muscle regeneration and disease progression of DMD. In addition, the Toll-like receptor 4 (TLR4) pathway has been identified as a contributor to DMD pathology. In studies involving the ablation of TLR4 in mdx mice, several positive effects have been observed. These include increased muscle force generation in the diaphragm, improved histopathology characterized by reduced fibrosis, decreased expression of pro-inflammatory genes, and reduced recruitment of macrophages. Notably, the ablation of TLR4 also induces a shift in muscle macrophages towards anti-inflammatory phenotypes<sup>227</sup>. Similar observations have been made in mdx mice lacking Toll-like receptor 2 (TLR2)<sup>228</sup>.

In mdx mice, the dystrophic muscle pathology can be broadly categorized into 3 different stages<sup>229</sup>. The pre-necrotic stage, occurring prior to 2-3 weeks of age, shows few signs of muscle fiber degeneration or immune cell infiltration. Subsequently the necrotic stage, typically observed from 3-8 weeks of age, shows a substantial level of muscle fiber necrosis and inflammatory cell infiltration, principally by macrophages. The level of necrosis and inflammatory cell infiltration then subsides with the gradual development of fibrosis due to defective muscle regeneration. The severity of this final fibrotic stage differs greatly among different mdx muscles, being relatively mild in most limb muscles until late in life. However, the mdx mouse diaphragm exhibits early and progressive fibrosis that more closely resembles what is observed in patients affected with DMD, suggesting that the mdx diaphragm can serve as a particularly useful model of the human disease<sup>107</sup>.

Macrophages in DMD exhibit a complex and diverse phenotype, with an increased prevalence of hybrid phenotypes including both M1 and M2 characteristics. For example, during the early necrotic stage at 4 weeks of age, macrophages isolated from muscles of mdx mice express proteins associated with both M1 (IFN $\gamma$ , NOS2) and M2 (arginase-1, dectin, IL-1Ra) markers<sup>230</sup>. In a 13-

week mdx diaphragm, single-cell PCR analysis of macrophages revealed that 43% simultaneously expressed both TNF (M1 marker) and TGF- $\beta$ 1 (M2 marker), 23% expressed only TNF, and 33% expressed only TGF- $\beta$ 1<sup>231</sup>. These results provide valuable insights into the heterogeneity of macrophages within the dystrophic muscles which could arise from multiple factors, including the ontogeny of macrophages, various stimuli present within the muscle microenvironment, and the temporal and spatial characteristics of these events.

DMD muscles demonstrate increased expression of chemokines that are typically not found in healthy muscle. These chemokines can attract neutrophils (CXCL1-3 and CXCL8), as well as monocytes/macrophages (CCL2, CCL5, CCL7), and T cells (CXCL11). Notably, activated macrophages serve as a significant source of these chemokines. The expression of CCL2, CCL5, and CCL7 is primarily observed in CD68+ M1 macrophages, rather than in muscle fibers, T cells, or dendritic cells<sup>232</sup>. The increased expression of these chemokines has also been reported in mdx mouse muscles<sup>233</sup>. NF- $\kappa$ B activity is elevated in both muscle cells and immune cells, and heterozygous p65-null mdx mice showed improved muscle pathology with reduced macrophage infiltration<sup>82</sup>. Targeted depletion of I $\kappa$ B kinase beta (IKK $\beta$ ) specifically in cells expressing lysozyme, mainly myeloid cells, reduced the expression of pro-inflammatory cytokines such as TNF and IL-1 $\beta$ , as well as CCL2, with improved muscle pathology<sup>82</sup>. Pharmacological blockade of the receptor activator of nuclear factor NF- $\kappa$ B ligand (RANKL) inhibited the NF- $\kappa$ B pathway, increased the proportion of M2 macrophages, and mitigated muscle pathology in utrophin haploinsufficient mdx mice<sup>234</sup>.

Both IFN $\gamma$  and inducible NOS2 (iNOS) are recognized as potent inducers of Th1 cytokines, promoting inflammation and myofiber damage. Additionally, both IFN $\gamma$  and iNOS play mitogenic roles in acute muscle injury. Studies have investigated the involvement of IFN $\gamma$  and iNOS in the

pathogenesis of DMD in mdx mice. At 4 weeks old, IFN $\gamma$ <sup>-/-</sup> mdx mice did not differ significantly from the mdx control mice<sup>235</sup>. However, at 12 weeks the IFN $\gamma$ -deleted mdx mice showed reduced muscle damage and all examined M2-biased cytokines showed an increase at that time point. Furthermore, an increased size of CD206-expressing macrophages was observed in the 12-week-old IFN $\gamma$ -deleted mdx mice<sup>235</sup>. In vitro experiments have provided evidence that macrophages derived from mdx muscle can induce muscle cell lysis through the production of NO<sup>221 230</sup>. Furthermore, when the iNOS gene (responsible for the production of NO) is completely absent in mdx mice, there is a reduction in fiber damage<sup>230</sup>. Conversely, mdx mice deficient in the anti-inflammatory cytokine IL-10 displayed higher levels of macrophage infiltration, increased iNOS and cytokine levels, elevated muscle damage, greater fibrosis, reduced muscle strength, and a shortened lifespan<sup>236 237</sup>.

One of the hallmark features of DMD is the presence of muscle fibrosis, and there is a positive correlation between fibrosis and macrophage numbers<sup>238 239</sup>. Fibrosis is characterized by the excessive accumulation of ECM proteins, particularly collagen, leading to a disruption of normal muscle structure and a loss of muscle fibers. In the case of DMD, fibrosis hinders muscle regeneration by impairing satellite cell function<sup>240</sup>. Additionally, fibrosis stiffens the muscle tissue, limiting its ability to contract. Notably, the presence of endomysial fibrosis in limb muscles has been shown to be associated with poorer motor outcomes in individuals with DMD<sup>238</sup>. Fibroblasts, the primary cell type responsible for collagen production, can undergo a phenotypic transformation and acquire myofibroblast characteristics in response to tissue injury or fibrotic stimuli. Upon activation, fibroblasts generate type I collagen, fibronectin, and connective tissue growth factor (CTGF), while suppressing matrix metalloproteinases (MMPs) involved in ECM degradation. In the context of acute muscle injury, fibroblast and myofibroblast presence is transient, but in DMD,

myofibroblast activation becomes persistent due to continuous myofiber injury. This sustained activation of myofibroblasts in DMD differs from the transient response observed in acute muscle injury. FAPs, resident mesenchymal progenitor cells, serve as another source of myofibroblasts<sup>241</sup><sup>242</sup>. Although they are quiescent in undamaged muscle, FAPs exhibit robust proliferation in response to injury. Activation of FAPs occurs in both acute muscle injury and chronic degenerative conditions<sup>69 243 88</sup>.

TGF- $\beta$  has been identified as an inducer of fibrotic gene expression in FAPs, leading to the production of collagens and CTGF associated with fibrosis<sup>69 88</sup>. TGF- $\beta$ , known for its role in normal muscle regeneration, also plays a crucial part in the development of fibrosis in DMD<sup>83</sup>. Increased levels of TGF- $\beta$  have been observed in muscles from patients affected with DMD<sup>244</sup>, as well as in mdx mice where the expression of TGF- $\beta$ 1, - $\beta$ 2, and - $\beta$ 3 and their receptors is elevated<sup>245</sup>. In cases of repetitive muscle injury, persistent TGF- $\beta$  signaling perpetuates ECM production, leading to fibrosis. Blocking TGF- $\beta$ 1 has been shown to have protective effects on skeletal muscles in mdx mice<sup>246</sup>. Furthermore, a study examining mRNA profiling data from patients with various muscle diseases, including DMD and other dystrophy diseases, revealed a strong correlation between the severity of muscle pathology and the TGF- $\beta$ -centered network. This network comprises genes and signaling pathways associated with TGF- $\beta$  signaling and showed a close relationship to the extent of muscle damage or dysfunction observed in the patients' biopsies<sup>247</sup>.

In patients affected by DMD, single nucleotide polymorphisms in the osteopontin/secreted phosphoprotein 1 (SPP1) and latent TGF- $\beta$  binding protein 4 (LTBP4) genes have been identified as significant modifiers of disease severity<sup>248 249</sup>. Osteopontin is highly expressed by macrophages and elevated in the muscles of mdx mice and patients affected with DMD<sup>250 251</sup>. This matricellular protein and cytokine has chemotactic properties and influences TGF- $\beta$  signaling by promoting the

expression of MMP9<sup>252</sup>. Depleting osteopontin in mdx mice results in reduced tissue collagen and fibrosis<sup>250</sup>. LTBP4 acts as a binding protein for latent TGF- $\beta$  complexes, preventing active TGF- $\beta$  from freely interacting with cell surface receptors and anchoring it to the ECM. In mdx mice, the introduction of a 12-amino acid insertion into the protease target region of LTBP4 impairs cleavage and leads to reduced TGF- $\beta$  signaling and fibrosis<sup>253</sup>. Conversely, depletion of the 12-amino acid region in LTBP4 results in increased TGF- $\beta$  signaling, as indicated by increased phosphorylation of decapentaplegic homolog 2/3 (SMAD2/3), highlighting the regulatory role of LTBP4 in TGF- $\beta$  signaling and fibrosis in mdx<sup>253</sup>.

In the biopsies from human affected by DMD, CD68+ macrophages (M1 marker) are predominantly found in necrotic areas, while CD206+ macrophages (M2 marker) exhibit a strong association with fibrosis<sup>238</sup>. These results are consistent with the notion that M2 macrophages are more involved in fibrosis due to their TGF- $\beta$  production, but this concept is evolving and it is now known that M1-biased macrophages can also contribute to fibrosis<sup>254</sup>. In DMD muscle sections, iNOS+ or TNF+ macrophages positively correlated with collagen I staining. Ly6C+ macrophages, which exhibit a bias towards the M1 phenotype compared to Ly6C- macrophages, also exhibit profibrotic features<sup>254</sup>. When co-cultured with fibroblasts, Ly6C+ macrophages isolated from microneedle-induced highly fibrotic mdx muscle demonstrate increased collagen 1 expression and a higher activation of fibroblasts compared to Ly6C- macrophages. Furthermore, Ly6C+ macrophages from these fibrotic muscles produce 6.3 times more TGFb-1 than Ly6C- macrophages. Although both macrophage types produced mainly latent TGFb-1, the expression of LTBP4, a protein regulating TGFb activation, was significantly elevated in Ly6C+ macrophages. Both the inhibition of LTBP4 expression and activation of the AMPK pathway in Ly6C+ macrophages significantly reduced TGFb1 levels in the dystrophic muscles<sup>254</sup>. These findings

highlight the complex involvement of macrophages in fibrosis, with both M1 and M2 macrophages playing a role in the fibrotic process.

As discussed earlier, FAPs play an important role in supporting successful skeletal muscle regeneration after acute injury. In the setting of acute injury the FAPs undergo transient proliferation and expansion but rapidly return to their baseline levels, primarily through apoptosis induced by TNF signaling<sup>231</sup>. However, in dystrophic muscle the ratio of TGF- $\beta$  to TNF production by macrophages is increased, which diminishes FAP apoptosis and leads to their abnormal persistence thus favoring the development of fibrosis<sup>231</sup>. This may also help to explain the apparently contradictory effects of blocking TNF in mdx mice. In this regard, TNF blockade by antibodies has been reported to have protective effects in mdx muscles<sup>255 225 256</sup>. However, in genetically TNF-ablated mdx mice, the effects on pathology differed between the less fibrotic quadriceps (improved by TNF ablation) and the more fibrotic diaphragm (worsened by TNF ablation) muscles<sup>257</sup>.

In addition to FAPs, muscle stem cells undergo distinct changes within the chronic inflammatory environment of DMD. There is a gradual transition of satellite cells into a state of senescence, wherein they cease to divide and proliferate due to persistent stress, inflammatory signals, and excessive proliferation<sup>92 258</sup>. Senescent satellite cells not only exhibit a decreased capability for muscle regeneration but also contribute to muscle inflammation. These senescent cells maintain high metabolic activity and secrete inflammatory cytokines<sup>259</sup>, thereby further contributing to chronic inflammation. The interactions between macrophages and satellite cells in DMD play a pivotal role in muscle repair and regeneration. A study using mdx Integrin Alpha M (ITGAM)-diphtheria toxin receptor (DTR) mice have demonstrated that transient elimination of macrophages leads to a notable decrease in satellite cell numbers and impairs their ex vivo proliferation and

differentiation capacity<sup>260</sup>. However, this phenomenon can be rescued through the injection of IL-10. Satellite cells employ an asymmetric division mechanism, resulting in two distinct cell types: MYF5<sup>-</sup> (stem cell) and MYF5<sup>+</sup> (progenitor) satellite cells, which contribute to maintaining the satellite cell pool and facilitating muscle repair respectively<sup>261 262</sup>. It should be noted that the DMD gene dystrophin is also a key regulator that remains dormant in quiescent satellite cells but becomes activated upon their activation, plays a critical role in this asymmetric division process<sup>91</sup>. A deficiency of dystrophin leads to reduced satellite cell asymmetric division due to the decreased expression of the microtubule affinity regulating kinase 2 (Mark2) protein, which subsequently hinders its interaction with Pard3, resulting in failed polarization. Consequently, this deficiency leads to an insufficient pool of myogenic progenitors available to participate in muscle repair. Additionally, Stat3 signaling has been identified as a crucial regulator governing the behavior of satellite cells, influencing their progression towards the myogenic lineage through the regulation of Myod1. Inhibition of Stat3 in mdx/mTR mice has been shown to enhance satellite cell proliferation *ex vivo* and promote muscle repair *in vivo*<sup>263</sup>.

Taken together, all of the above findings illustrate the complex interplay between the multiple functions of macrophages (phagocytosis, production of mediators, interactions with FAPs and satellite cells, etc.) and their roles in the muscle regeneration process under different pathological states, including in DMD where there is a lack of dystrophin.

## **1.4 Hypotheses and Objectives of the Current Thesis**

My project sought to further our understanding of the interplay between postnatal origin macrophages derived from monocytes released from the adult bone marrow, and the prenatal origin macrophages that arise from the embryo. I explored this issue under conditions of both skeletal muscle health (homeostasis) and in the presence of disease (acute and chronic skeletal muscle injury). I hypothesized that the equilibrium between adult bone marrow (monocyte)-derived macrophages and embryo-derived macrophages would be disrupted in the setting of muscle disease, and that this would have implications for how the skeletal muscle microenvironment modulates macrophage phenotype. In addition, I focused most of my work on the diaphragm, which is the main respiratory muscle and relatively understudied compared to the limb musculature.

The major objectives of my thesis were as follows:

**Objective 1: To develop a chimeric mouse model that preserves the muscle microenvironment and permits the identification of bone marrow-dependent (monocyte-derived) versus bone marrow-independent (embryo-derived) macrophage populations in the diaphragm**

**Objective 2: To describe the normal ontogeny of diaphragm macrophages during embryonic development and adulthood**

**Objective 3: To determine how macrophage ontogeny is dynamically altered by acute and chronic (mdx mouse model of muscular dystrophy) skeletal muscle injury**

**Objective 4: To explore how interactions between macrophage ontogeny and the skeletal muscle microenvironment determine macrophage phenotype in healthy versus dystrophic diaphragm muscle**

**Chapter 2: Dynamic Alterations of Macrophage Ontogeny in the Diaphragm  
Following Acute Injury and Recovery**

## **2.1. Abstract**

*Background:* The diaphragm is the chief muscle of respiration with distinct characteristics. Unlike limb muscles, the diaphragm's continuous activation and position as an anatomical barrier contribute to its unique vulnerability to both acute and chronic conditions. Many studies have demonstrated the role of acutely recruited bone marrow (monocyte)-derived macrophages in limb muscle regeneration, but the role of tissue resident macrophages in this process is unclear. Studies employing chimeric mice to study bone marrow-derived macrophages generally employ whole-body irradiation, which damages both tissue resident macrophages and satellite cells in the muscle. To address this limitation, we have developed a novel chimeric mouse model that uses radioprotective shielding of the diaphragm to mitigate the confounding effects of irradiation by preserving the local skeletal muscle microenvironment. Using this model, we sought to determine the dynamic responses of diaphragm macrophages of different origins (bone marrow recruitment versus tissue resident): 1) at steady-state, 2) shortly after acute injury, and 3) upon complete recovery from injury.

*Results:* We found that diaphragm shielding effectively preserves satellite cells' functionality and prevents depletion of the resident macrophage pool after irradiation. This allowed us to determine that under baseline steady-state conditions, there is a major population of diaphragmatic macrophages which appears to be independent of blood monocyte replenishment. In contrast, bone marrow-derived macrophages overwhelmingly dominate the regenerative response in the early period following acute injury. However, this dominance is transient and the situation reverts to the pre-injury equilibrium between bone marrow-dependent and bone marrow-independent macrophages once recovery from injury has occurred.

*Conclusions:* This new model provides unique insights into skeletal muscle macrophage dynamics

by permitting the identification and analysis of macrophages of different origins under various conditions. The diaphragm shielding model will be a useful tool for better understanding the role of macrophage ontogeny in muscle regeneration, including in fatal pathologies which affect the diaphragm such as Duchenne muscular dystrophy.

## 2.2 Introduction

Macrophages play several critical roles in the process of skeletal muscle regeneration after acute injury. This includes the clearance of dead cells, mediation of cytokine responses, secretion of growth factors, and cross-talk with various other cell types in the muscle, all of which are necessary to achieve effective muscle repair. To date almost all studies of the role of macrophages in skeletal muscle repair have focused on the limb musculature. In contrast, very little is known about the role of macrophages in the diaphragm, which is the primary muscle of respiration. The diaphragm differs from limb skeletal muscles not only in terms of its key role in respiration, but also with respect to its evolutionary origin, continuous pattern of rhythmic activation 24 hours per day, and unique function as an anatomical barrier between the thoracic and abdominal cavities<sup>264 265</sup>. The diaphragm can undergo acute injury in the setting of severe pulmonary diseases<sup>266</sup> as well as in several chronic myopathic conditions which lead to respiratory failure and death such as Duchenne muscular dystrophy (DMD).

Acute skeletal muscle injury leads to a rapid accumulation of macrophages in the tissue. It is well established that interference with the recruitment and/or the normal functioning of bone marrow-derived macrophages leads to impairment of the muscle repair process, which is delayed and associated with abnormal fibrosis or adipose tissue accumulation<sup>267 268 269 270 271</sup>. In previous investigations of the role of bone marrow-derived macrophages in limb muscle regeneration, many studies have employed chimeric mice generated through whole body irradiation and bone marrow transplantation<sup>272 194 273 198</sup>. The use of such chimeric mice with different genotypes in the bone marrow and the host recipient, has provided new insights into the roles of genes such as CCL2, CCR2, CD13, AMPK $\alpha$ 1, as well as other genes involved in macrophage-mediated muscle repair<sup>272 194 273 198</sup>. However, it is important to recognize that whole body irradiation also has significant

local effects on the skeletal muscle tissue environment. In particular, this includes the myogenic precursor cells known as satellite cells<sup>274 275</sup> as well as the local resident macrophage pool which is normally present in the muscle<sup>187</sup>. Therefore, while chimeric mice are a powerful tool to study skeletal muscle regeneration, the effects of irradiation on the muscle tissue itself introduce confounding effects and potential experimental artifacts by fundamentally altering the cellular microenvironment.

Here we report the development of a new chimeric mouse model that preserves the diaphragm muscle microenvironment and thus permits delineation of the dynamic changes in macrophage ontogeny which occur at different stages of muscle injury and repair. By protecting the local diaphragmatic niche from the adverse effects of irradiation, it was possible to determine how bone marrow-dependent and bone marrow-independent macrophages differentially respond to acute muscle injury, as well as their relative contributions to the overall steady-state macrophage pool prior to injury and once the muscle is fully recovered. Accordingly, this model can serve as a tool to study the role of macrophage ontogeny in different disease states in which the diaphragm undergoes acute or chronic injury conditions.

## **2.3. Methods**

### **2.3.1. Experimental animals**

All experimental procedures involving mice were conducted in compliance with the guidelines and regulations set forth by the Canadian Council on Animal Care (CCAC) and were approved by the animal ethics committee of the McGill University Health Centre. C57BL/6J CD45.2 and CD45.1 allele breeding pairs were obtained from The Jackson Laboratories. Mice were housed under germ-free conditions in a controlled environment. Trained personnel provided appropriate care and maintenance, including regular monitoring, feeding, and handling, to ensure the well-being of the animals throughout the study.

### **2.3.2. Bone marrow transplantation**

To establish chimeric mice, whole-body irradiation was performed on CD45.1 mice using the X-RAD SmART irradiator (Precision X-ray, USA) either with or without diaphragm shielding with a protective lead bar (see Fig 2.1a). The irradiation was carried out using two 6 Gy doses, administered 4 hours apart with parameters set at 225kV, 13mA, and 1.0265Gy/min<sup>276</sup>. Twenty-four hours after the second irradiation, CD45.1 mice received intravenous injections of bone marrow cells from CD45.2 mice ( $4 \times 10^6$  cells for unshielded mice with complete bone marrow ablation,  $2 \times 10^7$  bone marrow cells for shielded mice with partial radioprotection of the underlying bones) suspended in 200  $\mu$ l of RPMI (Wisent). CD45.2 bone marrow cells were collected by flushing the bones with ice-cold RPMI, followed by filtration through a 70 $\mu$ m cell strainer (Fisherbrand). The cell suspension was then centrifuged at 500g for 5 minutes at 4 degrees Celsius, and the pellet was resuspended in RPMI at the desired concentrations. To prevent infections, recipient mice were treated with 1% enrofloxacin (Baytril, 50mg/ml; Bayer, USA) in their drinking water for 7 days after irradiation. Subsequently, the mice were allowed to recover for 8 weeks to

allow for bone marrow reconstitution.

### **2.3.3. Diaphragm injury**

Mice were anesthetized using isoflurane for the procedure. To induce acute diaphragm injury, the mice first underwent laparotomy to expose the abdominal surface of the diaphragm as previously described<sup>228</sup>. The fascial layer of the diaphragm was gently abraded, followed by application of a cotton swab immersed in a solution of the myonecrotic agent cardiotoxin (10 $\mu$ M), which was applied to the entire muscle (30 s for each hemidiaphragm). The diaphragmatic surface was then generously rinsed with saline and the abdominal incision was closed. The animals continued to breathe spontaneously throughout the procedure and recovered well post-operatively.

### **2.3.4. Satellite cell isolation and culture**

The diaphragm was dissected into small pieces and digested in F12 medium (Gibco) containing 1% Trypsin (Gibco) and 1% Collagenase D (Roche) at 37°C with gentle rotation. After every 1 hour of digestion, the supernatant was collected and transferred to a 50 ml Falcon tube on ice, containing 10 ml of FBS. Fresh digestion medium was added, and the digestion and collection steps were repeated until all muscle pieces were processed. The collected cell suspensions were filtered through a 70  $\mu$ m strainer to remove any debris, and then centrifuged at 1800 rpm for 18 minutes at 4°C. The resulting cell pellet was resuspended in 80  $\mu$ l of buffer, which consisted of PBS supplemented with 0.5% FBS. To isolate satellite cells, the resuspended cell suspension was mixed with 20  $\mu$ l of microbeads from the Satellite Cell Isolation Kit (Miltenyi Biotec) and incubated on ice for 15 minutes. Subsequently, the cell suspension was applied to a rinsed LS column (Miltenyi Biotec) placed within a magnetic field. After applying the suspension, the column was washed twice with 1 ml of buffer to remove unbound cells. The cells passing through the column, which contained the desired satellite cells, were collected by centrifugation at 300g

for 10 minutes. The resulting cell pellet was then resuspended in 80  $\mu$ l of buffer and mixed thoroughly with 20  $\mu$ l of Anti-Integrin  $\alpha$ 7 microbeads (Miltenyi Biotec). The suspension was again incubated on ice for 15 minutes and subsequently transferred to a new rinsed column placed in the magnetic field. To further purify the satellite cells, the column was washed three times with 0.5 ml of buffer, ensuring the removal of any non-specifically bound cells. Finally, the column was removed from the magnetic field, and the satellite cells were collected by washing with 1 ml of full culture medium. The full culture medium used consisted of 20% FBS, 39% DMEM, 39% F12, and 2% Ultrosero G, providing the necessary nutrients and growth factors for subsequent cell culture experiments.

### **2.3.5. Satellite cell proliferation and differentiation**

To evaluate satellite cell proliferation, the isolated satellite cells were plated onto Matrigel-coated 48-well plates at a density of 10,000 cells per well in full culture medium. The culture medium was replaced on day 3 post-seeding. On day 3 of culturing, a concentration of 0.03 mg/ml of BrdU (Sigma) was added to the full culture medium. At 24 hours after BrdU exposure the cells were washed with PBS, then fixed with cold 70% ethanol for 5 minutes at room temperature, followed by rinsing in 1X PBS. Subsequently, to denature the DNA and expose the incorporated BrdU, the cells were treated with 1.5M HCl for 30 minutes and washed again with PBS. To block non-specific binding, the cells were incubated with Protein Block Serum-Free (DAKO) for 60 minutes. Primary mouse anti-BrdU antibody (Cell signaling) staining was performed overnight at 4°C using a 1:1000 dilution in Antibody Diluent (DAKO), followed by rinsing with PBS. The cells were then incubated with rabbit anti-mouse secondary antibody Alexa Flour 488 (Invitrogen) at a 1:500 dilution in Antibody Diluent for 60 minutes in the dark. After further PBS rinsing, the cellular DNA was stained with Hoechst to visualize nuclei using 1:5000 dilution in PBS for 5 minutes,

followed by additional PBS rinses. The satellite cells were visualized by fluorescence microscopy, and BrdU incorporation was expressed as the percentage of BrdU-positive nuclei divided by total (Hoechst-positive) nuclei<sup>277</sup>.

To induce satellite cell differentiation into myotubes, the cells were cultured in medium lacking FBS for 4 days. The cells were then fixed by 4% PFA for 10 mins and permeabilized by 0.1 Triton X for 10 mins. After blocking, the chamber slides were incubated with F1.652 embryonic myosin MIgG1 antibody (DSHB) in a 1:50 dilution overnight. On the second day, the chamber slides were incubated with Alex Fluor 488-conjugated anti-mouse secondary antibody 1:500 for 60mins, followed by Hoechst nuclear staining. The differentiated myotubes were visualized by fluorescence microscopy and individual myotubes were randomly selected for analysis using stereology software ImageJ<sup>278</sup>. The average myotube diameter was determined by measuring the diameter of the myotubes at the randomly selected sites. The myotube fusion index was calculated by dividing the number of nuclei within myotubes (containing more than 2 nuclei) by the total number of nuclei as previously described<sup>279</sup>.

### **2.3.6. RNA isolation and quantitative real-time PCR (qRT-PCR)**

RNA was extracted using TRIzol Reagent (ThermoFisher, USA) according to the manufacturer's recommendations. RNA purity and integrity were assessed according to the absorbance ratios (A260/280) using a spectrophotometer (BioTek Co., Ltd., Canada), aiming for values between 1.8 and 2.0. The first strand cDNA was synthesized employing the iScript Supermix (Biorad, Canada) according to the manufacturer's instructions. The resulting cDNA was stored at -20 °C. qRT-PCR was performed in a 10- $\mu$ L reaction system consisting of 5  $\mu$ L 2x SYBR<sup>TM</sup> Green PCR Master Mix (ThermoFisher, USA), 0.5  $\mu$ L primer mix (10 mM), and 2.5  $\mu$ L ddH<sub>2</sub>O on a StepOne plus thermal cycler (Applied Biosystems, USA). Briefly, after an initial denaturation step at 95 °C for 10

minutes, the amplifications were carried out with 40 cycles at a melting temperature of 95 °C for 30 seconds and an annealing temperature of 60 °C for 1 minute, followed by a melting curve analysis at 42 °C. Primers for the following genes were used: MyoD, Myogenin, and the embryonic isoform of Myosin Heavy Chain (MYHC-emb). The relative expression levels of the target genes were determined using the  $2^{-\Delta\Delta C_t}$  method<sup>280</sup>. HPRT1 and  $\beta$ -actin were employed as the housekeeping genes.

### **2.3.7. Identification of monocytes and macrophages by flow cytometry**

Prior to euthanasia, the mice were anesthetized with isoflurane and blood was drawn by cardiac puncture using a tube containing sodium citrate (0.48% citrate acid, 1.32% sodium citrate, 1.47% glucose) as an anticoagulant. The heart was perfused with 20 ml of phosphate-buffered saline (PBS) (Wisent), followed by an additional 20 ml of PBS after severing the dorsal aorta. For the blood samples, red blood cells were lysed using a red blood cell lysis buffer (0.78% NH<sub>4</sub>Cl, 0.01% KHCO<sub>3</sub>, 0.003% EDTA). The diaphragm, tibialis anterior (TA), and soleus muscles were dissected into small pieces and digested in PBS supplemented with 0.2% collagenase B (Roche) for 1.5 hours to obtain a cell suspension.

Cell populations obtained from the blood and muscles were stained with a viability dye (Violet, Invitrogen) to discriminate live and dead cells. To prevent non-specific binding, the cells were blocked with Fc blocking solution (BD). Macrophages in the skeletal muscles were defined as CD45<sup>+</sup> (either CD45.1 or CD45.2), SiglecF-negative, CD11c-negative, CD11b<sup>+</sup>, and F480<sup>+</sup>. Monocytes in the blood were defined as CD45<sup>+</sup> (either CD45.1 or CD45.2), CD11b<sup>+</sup>, and Ly6C<sup>high</sup>. For Ki67 staining to assess cellular proliferation, permeabilization buffer (eBioscience) was used before adding the Ki67 antibody. Cell phenotypes identified by flow cytometry were analyzed using Flowjo software.

### **2.3.8. Statistics**

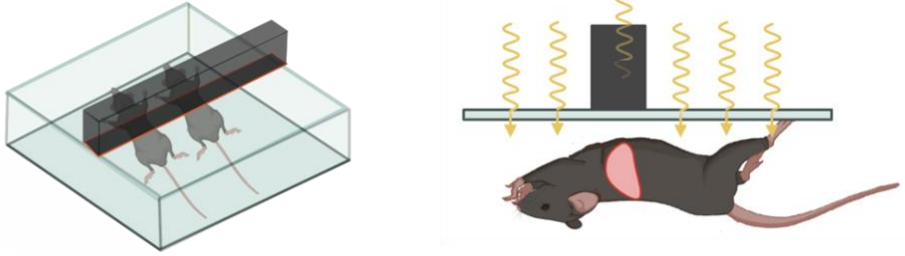
Data analysis for significance was performed using Prism GraphPad version 9. Comparison between two groups were made using Students unpaired t-test. Comparisons between more than two groups were made with one- or two-way ANOVA followed by post-hoc correction for multiple comparisons. A significance level of  $p < 0.05$  was considered statistically significant. All graphs show group mean data with each dot on the graph representing an individual animal unless specified otherwise. The error bars indicate the standard deviation (SD).

## **2.4 Results**

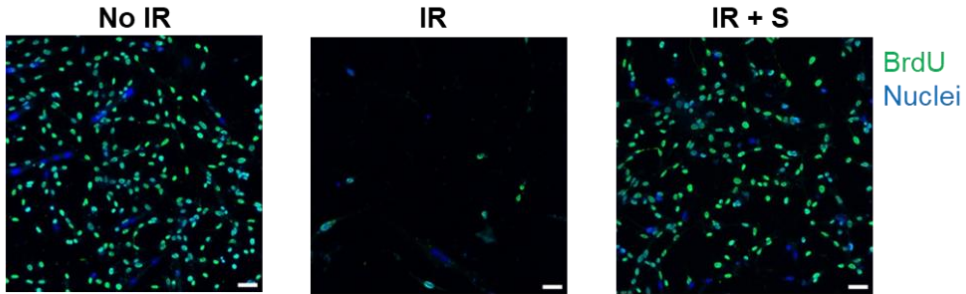
### **2.4.1. Preservation of satellite cells and macrophages by diaphragm shielding**

The experimental set-up employed for lead shielding of the diaphragm during whole body irradiation is depicted in Fig 2.1a. Anesthetized mice were placed in a Plexiglas box with their forelimbs raised and a lead bar (2cm height and 1.5cm width) positioned over the lower ribcage with 70% of the bar width caudal to the xyphoid process. To assess the ability of lead shielding to provide radioprotection to diaphragm satellite cells, the latter were isolated 24 hours after irradiation and then studied on the fourth day in culture. In comparison to the group that was non-irradiated, the number of viable satellite cells isolated from the diaphragms of mice irradiated without shielding was greatly reduced (Fig 2.1b-c). However, when diaphragm shielding was used during irradiation the number of diaphragm satellite cells in the culture was not significantly different from the non-irradiated control group. In addition, the percentage of satellite cells demonstrating BrdU staining was similar for the shielded and non-irradiated groups, while it was greatly reduced in the very small number of satellite cells obtained from the group without shielding (Fig 2.1d). We also examined the mRNA expression levels of several genes involved in myogenesis (MyoD, Myogenin, and MYHC-emb) and found no significant differences in satellite cells obtained from the non-irradiated and diaphragm-shielded groups (Fig 2.1e).

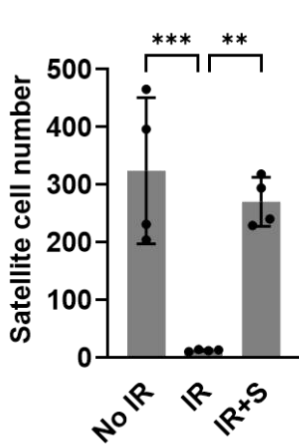
a



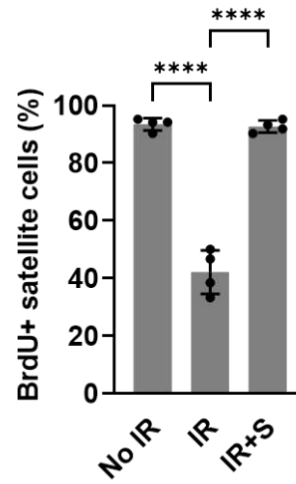
b



c



d



e

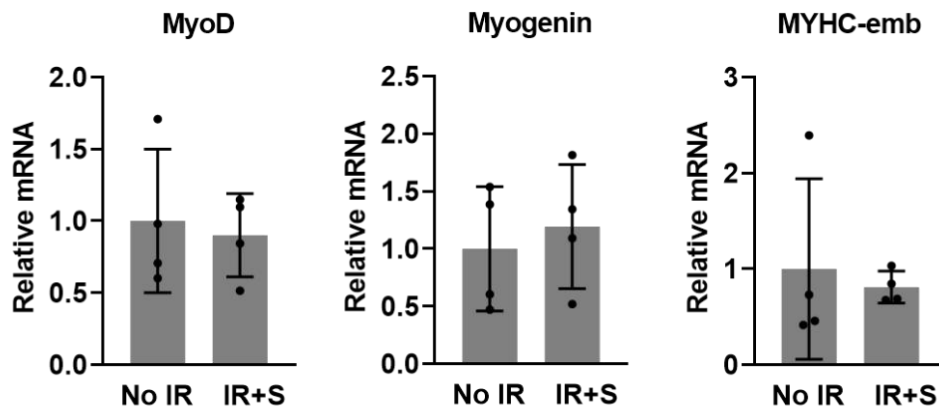


**Figure 2.1. Diaphragm shielding during irradiation preserves satellite cell number and proliferative capacity**

(a) Schematic illustration of the lead bar shielding procedure used to protect the diaphragm during total body irradiation.

(b) Satellite cells were isolated from the diaphragms of mice that were not irradiated (no IR), irradiated (IR), or irradiated with concurrent diaphragm shielding (IR+S). Representative staining of the cells is shown for BrdU (green) and Hoechst (blue nuclei). Scale bars = 50  $\mu$ m.

(c) Quantification of the mean cell number per field of view (n=4 diaphragms/group, 3 wells/diaphragm, 5-8 photos/well) in diaphragm satellite cell cultures from the 3 groups of mice. \*\* p<0.01, \*\*\* p<0.001.

(d) Percentage of BrdU-positive among satellite cells with Hoechst-positive nuclear staining. \*\*\*\* p<0.0001.

(e) Transcript levels for myogenesis genes in cultured satellite cells obtained from the non-irradiated and diaphragm-shielded groups ( n=4 diaphragms/group). All data are expressed as fold-change relative to the non-irradiated (No IR) group mean value.

The capacity of diaphragm satellite cells to differentiate into myotubes was evaluated after switching the satellite cells to low serum medium for 4 days. Myotubes with positive immunostaining for MYHC-emb were widely present in both the non-irradiated and diaphragm-shielded groups, whereas the group irradiated without shielding yielded very few myotubes (Fig 2.2a). The average myotube diameter (Fig 2.2b) and myotube fusion index (Fig 2.2c) did not differ between the non-irradiated and diaphragm-shielded groups, but could not be determined in the group irradiated without shielding due to the very sparse number of myotubes. The mRNA transcript levels of myogenesis genes were similar in myotubes obtained from the non-irradiated and diaphragm-shielded groups (Fig 2.2d).

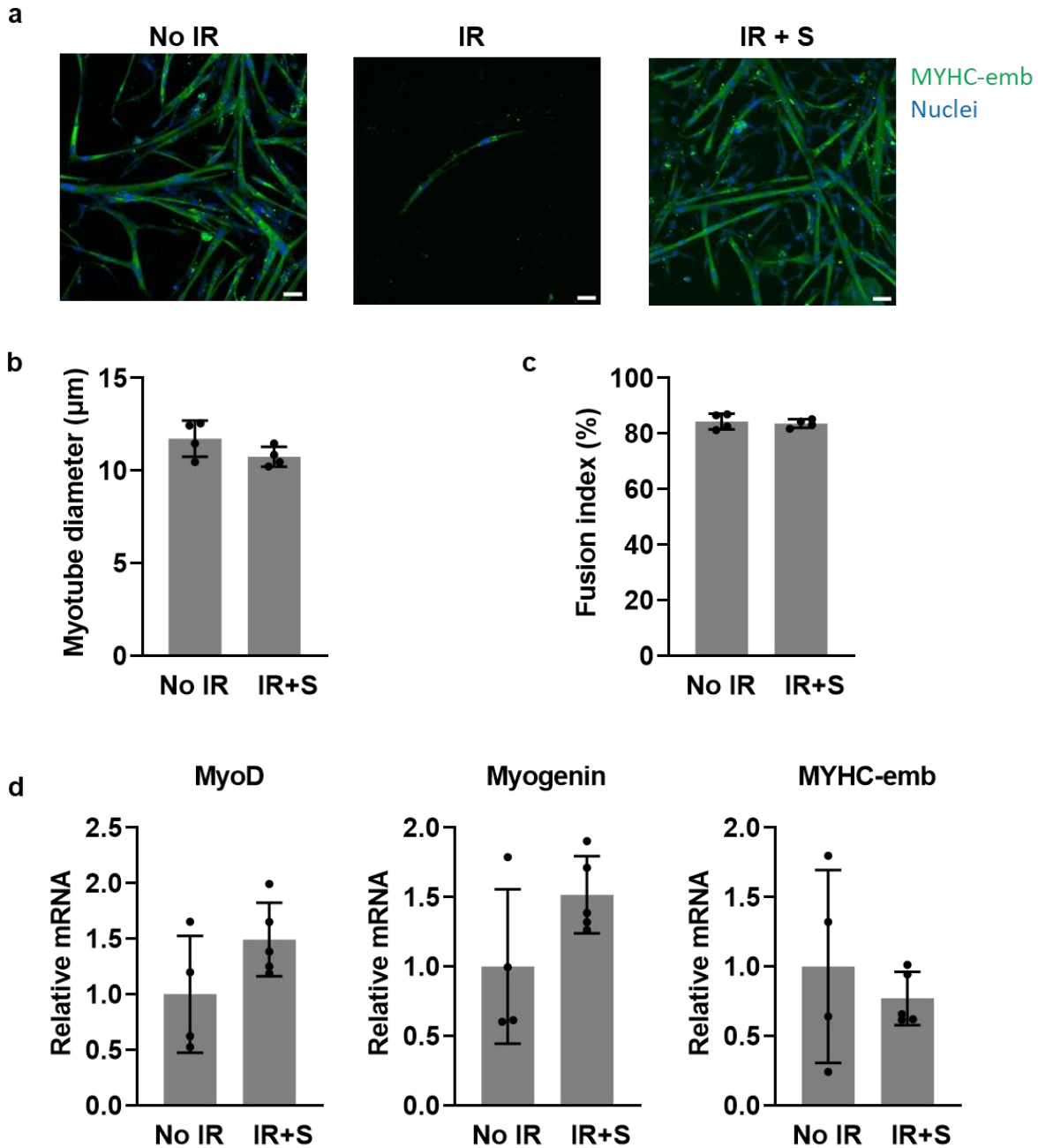


**Figure 2.2. Diaphragm shielding during irradiation preserves satellite cell differentiation capacity**

(a) Representative images of differentiated myotubes stained for the embryonic isoform of Myosin Heavy Chain (MYHC-emb) and nuclear DNA (Hoechst). Scale bars = 50 µm.

(b) Quantification of mean myotube diameter (n=4 diaphragms/group, 3 wells/diaphragm, 3 photos/well).

(c) Quantification of the myotube fusion index (n=4 diaphragms/group, 3 wells/diaphragm, 3 photos/well).

(d) Transcript levels for myogenesis genes in cultured myotubes obtained from the non-irradiated and diaphragm-shielded groups (n=2 diaphragms/group). All data are expressed as fold-change relative to the

non-irradiated (No IR) group mean value.

We next generated chimeric mice by transplanting CD45.2 donor bone marrow into CD45.1 host recipient mice that received whole body irradiation, either with or without the presence of diaphragm shielding (Fig 2.3a). The mice were studied after 8 weeks of bone marrow reconstitution, at which time we observed a decrease in diaphragm weight in the mice that did not receive diaphragm shielding (Fig 2.3b). Flow cytometry to quantify intramuscular macrophages revealed that in the chimeric mice without diaphragm shielding, the percentage of host-origin (CD45.1) macrophages remaining in the diaphragm at 8 weeks after bone marrow transplantation was negligible. In contrast, approximately half of the macrophages retained their host origin in the shielded diaphragm after 8 weeks (Fig 2.3c). Consistent with this finding, the absolute number of host (CD45.1) macrophages was significantly higher in the shielded diaphragm compared to the unshielded group (Fig 2.3d).

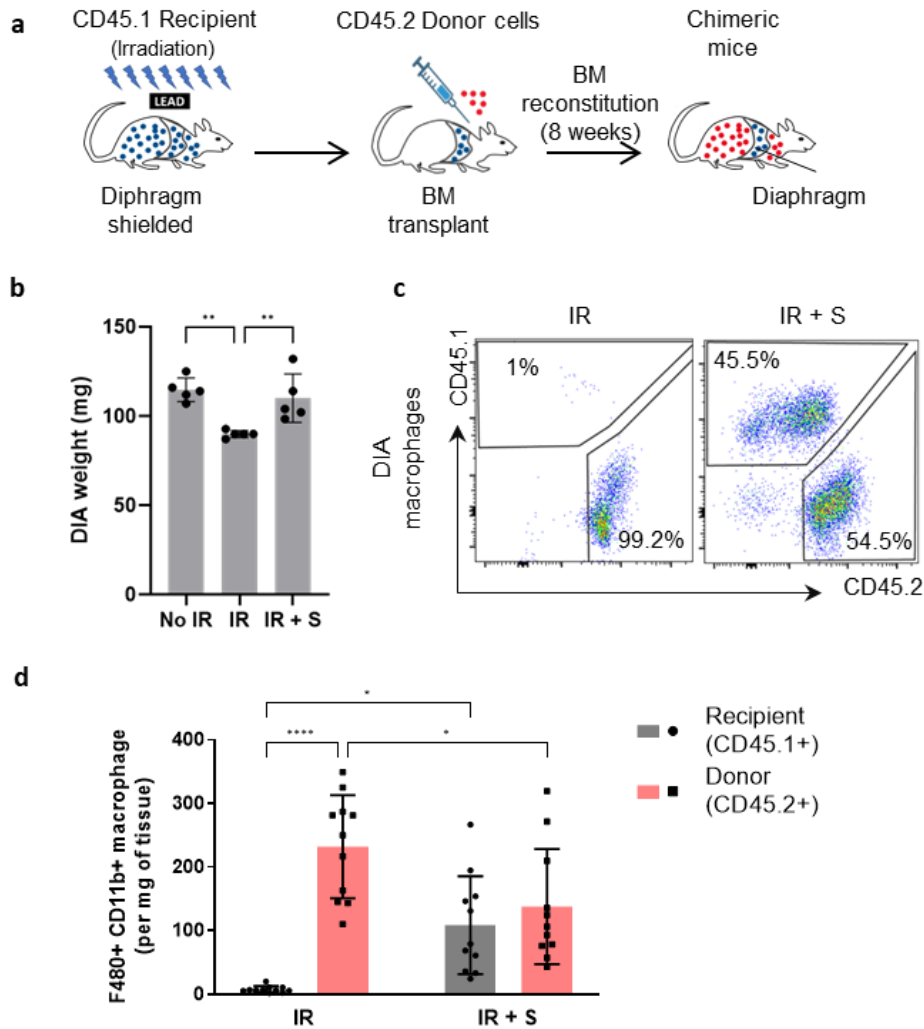


**Figure 2.3. Diaphragm shielding model preserves the resident macrophage population after irradiation**

- (a) Chimeric mouse model combined with diaphragm shielding used to study dynamic responses of the bone marrow (monocyte)-derived and local resident macrophage populations in the diaphragm. Irradiated host recipient mice (CD45.1) were transplanted with bone marrow from donor mice (CD45.2) and allowed to undergo bone marrow reconstitution for 8 weeks.
- (b) Weight of diaphragm from the 3 groups of recipient mice, analyzed 8 weeks post bone marrow reconstitution. (n=5/group) \*\* P<0.01.
- (c) Representative FACS plots are shown for macrophages of either host recipient or donor origin in diaphragms that were either unshielded (IR) or shielded (IR + S) during irradiation, and analyzed 8 weeks later.
- (d) Absolute quantification of macrophages derived from either host recipient or donor in diaphragms that were either unshielded (IR) or shielded (IR + S) during irradiation, and analyzed 8 weeks later. (n=11/group) \* P<0.05, \*\*\*\* p<0.0001.

Taken together, the above findings suggest that the diaphragm shielding model preserves a more physiologically relevant microenvironment after whole body irradiation by maintaining satellite cell functionality and preventing the depletion of resident macrophages observed in the diaphragms of unshielded mice.

#### **2.4.2. Diaphragm shielding reveals a major population of resident macrophages that are bone marrow (monocyte)-independent**

To better understand the relationship between bone marrow (monocyte)-derived macrophages and the resident macrophage population in skeletal muscles, we directly compared the relative percentages of circulating blood monocytes and muscle macrophages of either donor (CD45.2) or host (CD45.1) origin. In both the diaphragm-shielded and unshielded models, this analysis was performed for the diaphragm as well as two hindlimb muscles, the fast-twitch TA and slow-twitch soleus (note that the hindlimb muscles are fully exposed to irradiation in both the shielded and unshielded mice). In the group without diaphragm shielding, the percentages of host-origin macrophages in both the diaphragm and hindlimb muscles were minimal and closely mirrored the percentage of host-origin monocytes in the blood (Fig. 2.4a). In keeping with their lack of radioprotection, the hindlimb muscles of diaphragm-shielded mice also exhibited low percentages of host-origin macrophages which did not differ from the corresponding percentage of host-origin monocytes. In contrast, the diaphragms of shielded mice contained a markedly higher percentage of host-origin macrophages compared to the percentage of host-origin monocytes in the blood (Fig 2.4b). Note that diaphragm-shielded mice had a higher background percentage of host-origin monocytes, presumably due to partial radioprotection of the underlying ribcage and spine by the lead shield. To investigate the stability of macrophage origin in the diaphragm over time, we followed the levels of macrophage and monocyte chimerism in the diaphragm-shielded mice out to 16 weeks post-transplantation. There were no significant differences in the levels of macrophage donor chimerism between 8 and 16 weeks post-transplantation (Fig. 2.4c-d). The above findings suggest that a significant proportion of macrophages (approximately 40% based on the blood monocyte-normalized chimerism level) in the diaphragm do not originate from blood monocytes

under stable homeostatic conditions and are thus independent from the bone marrow as a source of replenishment.

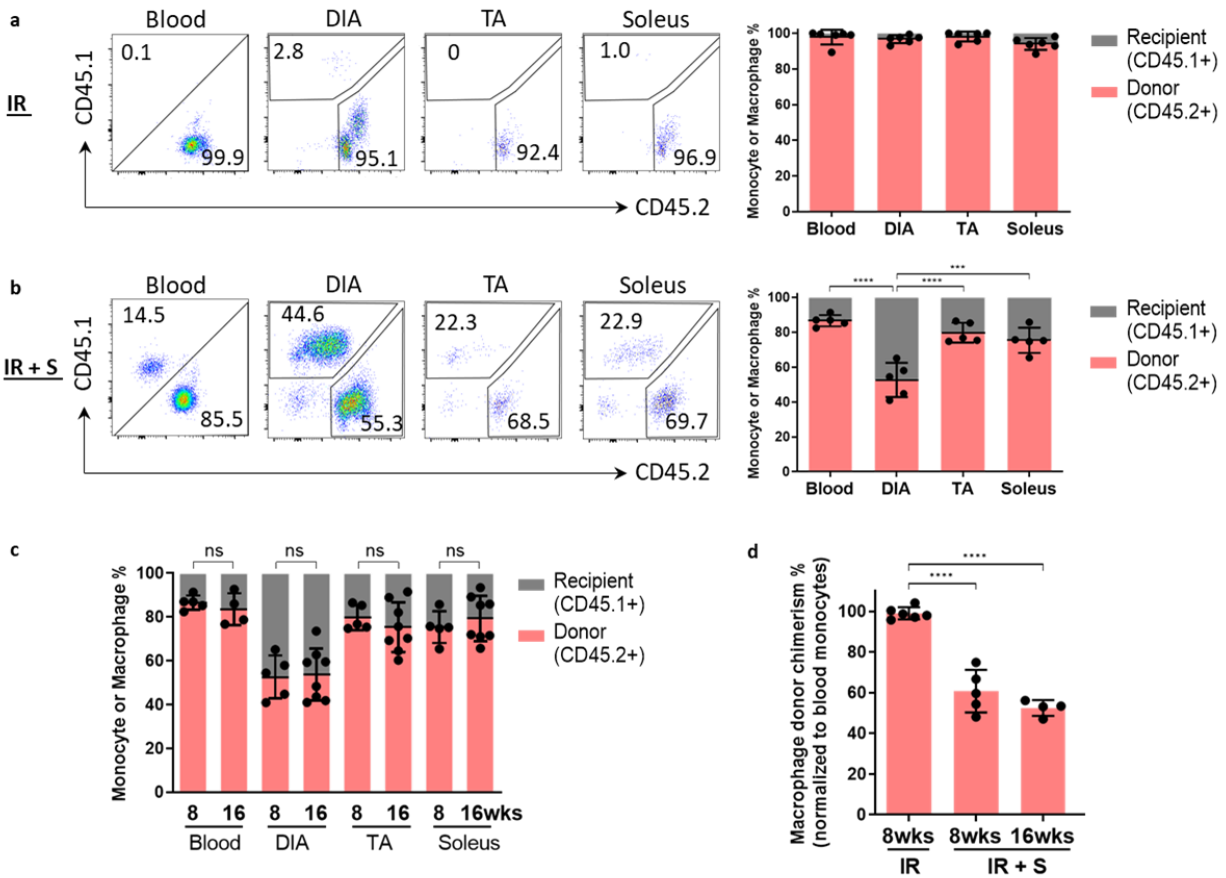


**Figure 2.4. Diaphragm shielding reveals a bone marrow (monocyte)-independent macrophage population**

- (a) Representative FACS plots (left) and group mean data (right) show the relative proportions of CD45.1+ versus CD45.2+ monocytes (Blood) and macrophages in the diaphragm (DIA), tibialis anterior (TA), and soleus muscles at 8 weeks after bone marrow transplantation without diaphragm shielding (IR). (n=6 mice/group).
- (b) Same analysis as in panel (a) performed with diaphragm shielding (IR+S). (n=5 mice/group) \*\*\* P<0.001, \*\*\*\* P<0.0001.
- (c) In diaphragm-shielded mice, the relative percentages of CD45.1+ versus CD45.2+ monocytes (Blood) or macrophages (DIA, TA, and soleus muscles) are shown at 8 weeks and 16 weeks post-transplantation. (n=4-8 mice/group) ns= not statistically significant.
- (d) Diaphragm macrophage donor chimerism was determined by normalizing the percentage of donor macrophages in the muscle to the percentage of donor blood monocytes. The analysis were performed in unshielded mice (IR) and diaphragm-shielded mice (IR+S) at different time points after bone marrow transplantation. (n=4-6 mice/group). \*\*\*\* P<0.0001

### **2.4.3. Bone marrow origin macrophages are responsible for the increase in diaphragm macrophages after acute injury**

Acute necrotic injury of skeletal muscle causes a massive increase in intramuscular macrophages, but the precise contribution of bone marrow-dependent versus bone marrow-independent macrophages under these conditions has not been determined. Therefore, we compared the proportions of bone marrow-dependent versus bone marrow-independent macrophages at 4 days after inducing acute necrotic injury with cardiotoxin in the shielded diaphragm. The blood monocyte-normalized donor chimerism level in uninjured control mice indicated that approximately 65% of diaphragm macrophages were of bone marrow origin, whereas this level rose to nearly 100% in the acutely injured muscle (Fig 2.5a). Along the same lines, the number of bone marrow origin (CD45.2) macrophages per mg of diaphragm tissue increased by approximately 15-fold, whereas CD45.1 macrophages were not significantly increased under the same conditions (Fig 2.5b). In addition to recruitment of monocyte-derived macrophages from the bone marrow, it is possible that augmented cellular proliferation could also contribute to the increased numbers of macrophages observed in the acutely injured diaphragm. Therefore, we assessed Ki67 expression in diaphragm macrophages using flow cytometry at day 4 post-injury. Both macrophage populations exhibited an increased percentage of Ki67-positive cells, with the CD45.2 macrophages increasing from 12% to 32% and the CD45.1 macrophages increasing from 7% to 24% (Fig 2.5c). Taken together, these findings indicate that bone marrow-derived macrophages are overwhelmingly the main source of the increased macrophage population in the acutely injured diaphragm, and that this occurs through a combination of macrophage recruitment and proliferation.

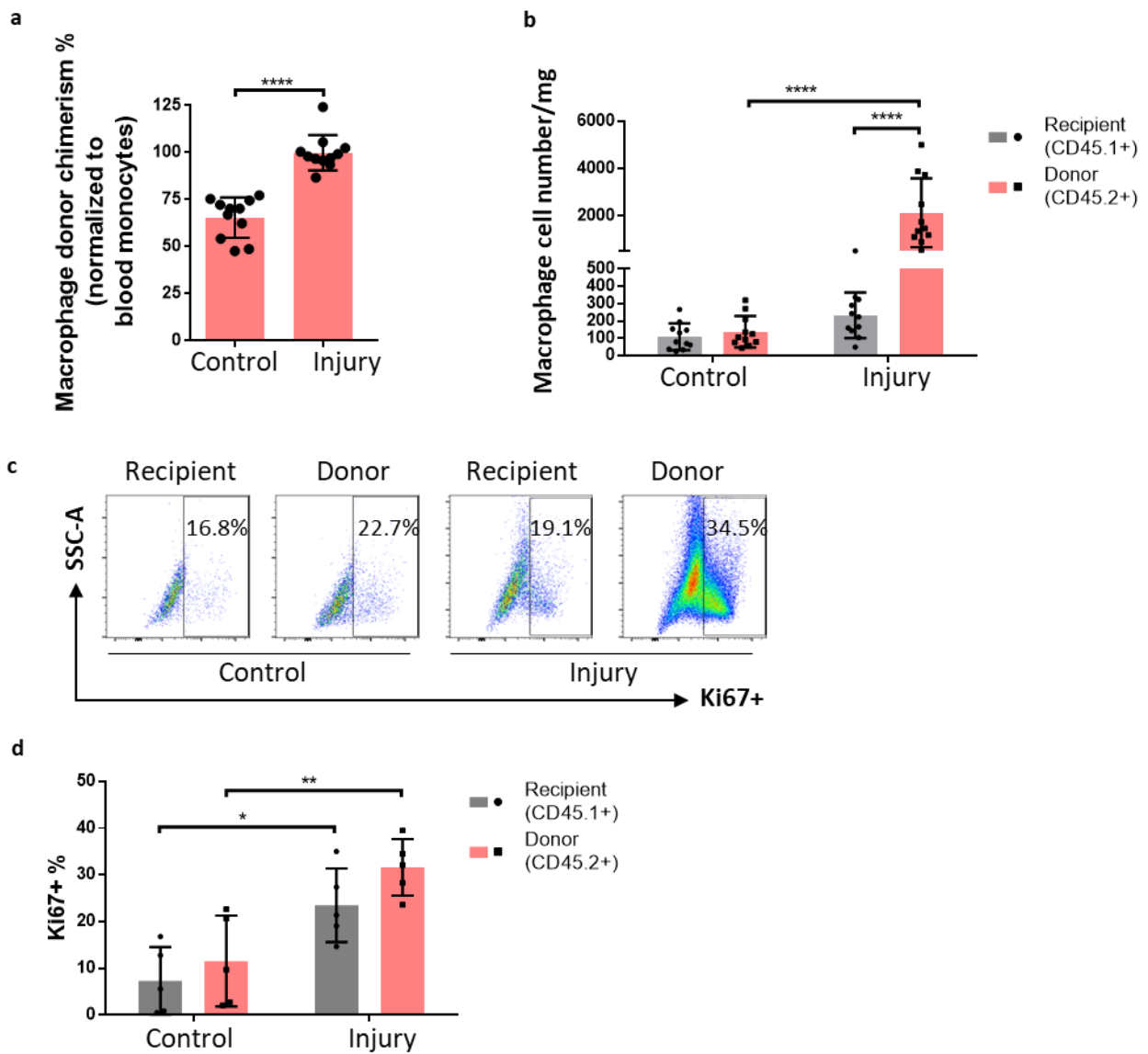


**Figure 2.5. Comparison of bone marrow-dependent versus bone marrow-independent macrophages in acutely injured diaphragms**

(a) Diaphragm macrophage donor chimerism (normalized to the percentage of donor blood monocytes) is shown for uninjured control mice versus cardiotoxin-injured mice; both groups were diaphragm-shielded and the experiments were performed 8 weeks after bone marrow transplantation. (n=11 mice/group). \*\*\*\* P<0.0001.

- (b) Absolute cell number (per mg of tissue) for diaphragm macrophages of donor (CD45.2) versus host recipient (CD45.1) origin for the same mice depicted in (a). \*\*\*\* P<0.0001.
- (c) Ki67 positivity in diaphragm macrophages of donor versus host recipient origin under the same experimental conditions described in (a).
- (d) Ki67 expression in diaphragm macrophages of donor versus host recipient origin as described in (a) and (c) (n=5 mice/group). \*\*\*\* P<0.0001.

#### **2.4.4. The pre-injury pattern of macrophage ontogeny is restored in healed diaphragm muscle**

Finally, given the overwhelming predominance of bone marrow-derived macrophages after acute diaphragm injury, we wished to ascertain whether this dominance is maintained once the muscle has recovered from injury and returned to homeostatic conditions. To address this question, we analyzed diaphragm-shielded chimeric mice that had undergone acute diaphragm injury 60 days earlier (Fig 2.6a-b). The percentage and absolute number of host recipient origin macrophages remained unaltered across all conditions. In addition, the percentage and absolute number of donor bone marrow-derived macrophages, while greatly increased at 4 days post-injury, had declined to approach the non-injured control levels by 60 days of recovery. These data indicate that the dramatic alterations of macrophage ontogeny in the setting of acute diaphragm injury are transient, with a return to the normal balance between bone marrow-dependent versus bone marrow-independent macrophages once the muscle has recovered from injury.

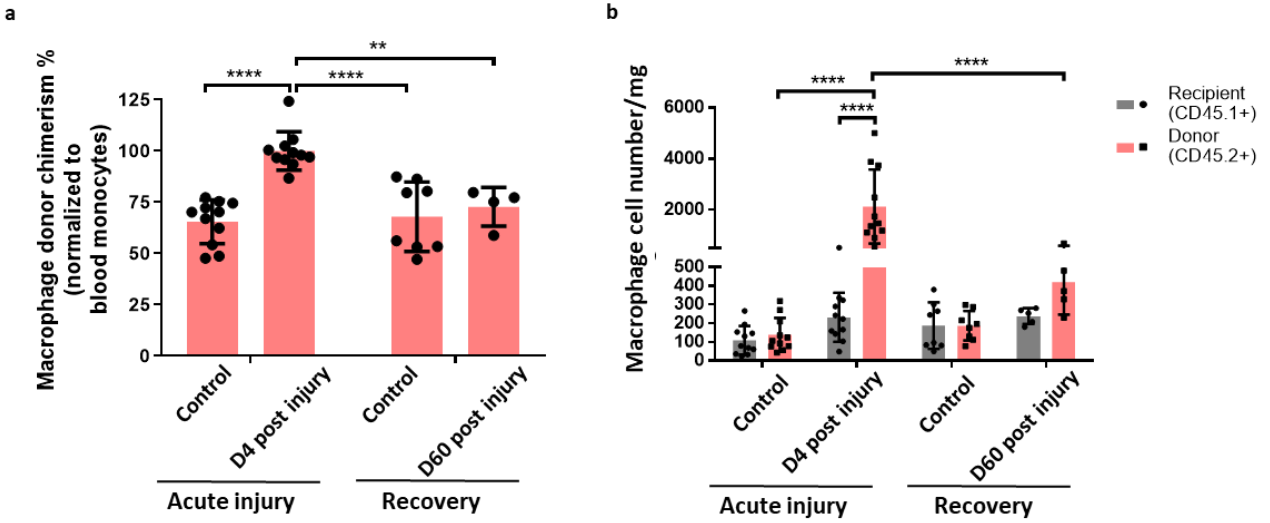


**Figure 2.6. Comparison of bone marrow-dependent versus bone marrow-independent macrophages following recovery from diaphragm injury**

- (a) Diaphragm macrophage donor chimerism (normalized to the percentage of donor blood monocytes) is shown for uninjured control mice versus cardiotoxin-injured mice at either 4 days or 60 days post-injury; both groups were diaphragm-shielded and the injury was performed 8 weeks after bone marrow transplantation. (n=4-11 mice/group). \*\*P<0.01, \*\*\*\* P<0.0001.
- (b) Absolute cell number (per mg of tissue) for diaphragm macrophages of donor (CD45.2) versus host recipient (CD45.1) origin for the same mice depicted in (a). \*\*\*\* P<0.0001.

## 2.5. Discussion

In the present study, we developed a new experimental model to study the dynamics of macrophage ontogeny in the diaphragm under different conditions while simultaneously protecting the local muscle tissue from irradiation to preserve a physiologically relevant microenvironment. The main findings of our study can be summarized as follows. First, we observed that irradiation impaired satellite cell proliferation and differentiation capacity whereas lead shielding of the diaphragm effectively preserved the viability and function of satellite cells. Second, diaphragm shielding also allowed for preservation of the resident macrophage population, and approximately 40% of the macrophage pool at steady-state appeared to be bone marrow-independent. Third, in the early period following acute diaphragm injury there was a dramatic increase in macrophage cell number which was comprised almost entirely of bone marrow-dependent macrophages, whereas the absolute number of bone marrow-independent macrophages remained unchanged. Finally, once the diaphragm had undergone regeneration and recovered from acute injury, the macrophage balance in the muscle returned to the original pre-injury proportions of bone marrow-derived and bone marrow-independent resident macrophages.

Previous studies have made extensive use of whole-body irradiation followed by bone marrow transplantation to study gene functions and muscle regeneration roles of monocyte-derived macrophages recruited from the bone marrow<sup>194 198 281 282</sup>. However, irradiation itself is well established as having profound inhibitory effects on muscle regeneration through its effects on satellite cells<sup>283</sup>. The ability of satellite cells to proliferate and differentiate effectively is crucial, with any deficiency in these functions leading to compromised muscle regeneration<sup>284</sup>. In a previous study it was shown that irradiation of limb muscle leads to fewer satellite cells with increased necrotic fibers and a longer recovery time from injury; lead shielding of the limb muscle

mitigated these effects<sup>285</sup>. In our ex vivo culture experiments, we noted a decline in the survival and proliferation of diaphragm satellite cells in the irradiated group. Satellite cells appeared to survive within 24 hours following irradiation consistent with a previous report based on in vivo staining at Day 0 and Day 3 post-irradiation<sup>286</sup>. However, in our study the number of satellite cells was significantly decreased during the proliferation stage in vitro. A similar phenomenon is found after irradiation in a mouse satellite cell line, C2C12 cells<sup>287</sup>. This decrease could be due to DNA damage and oxidative-induced apoptosis<sup>288 287</sup>. Interestingly, some studies have indicated that a subset of satellite cells exhibits radio-tolerance and retains its potential to proliferate<sup>289 290</sup>. Radiation also impairs myoblast differentiation<sup>291</sup>. Importantly, in our study the use of diaphragm shielding preserved both the proliferation and differentiation capacities of satellite cells to the same levels observed in the non-irradiated diaphragm, as reflected by cell number, BrdU incorporation, myotube size, fusion index and the expression of several prototypical genes involved in myogenesis.

Although the effects of radiation on satellite cell function have been studied in detail as noted above, the impact of skeletal muscle irradiation on the resident macrophage population is much less recognized. In most organs, the resident macrophage pool that is present in the tissue under normal homeostatic conditions consists of a mixture of adult bone marrow-dependent (monocyte-derived) and bone marrow-independent (embryo-derived) cells. The relative proportions of these two macrophage origins in the resident macrophage pool varies according to the specific organ and in some cases the age of the animal<sup>292</sup>. Previous studies have shown that macrophage populations in different tissues can exhibit varying levels of radio-resistance, and it has been suggested that resident macrophages are more radio-resistant than acutely recruited macrophages in some tissues<sup>293 294 295</sup>. Macrophages are critical in providing key mediators that support satellite

cell proliferation and differentiation during muscle regeneration<sup>9</sup>. It has been reported that irradiation of limb muscles without shielding delays the normal macrophage phenotypic transition from Ly6C<sup>high</sup>F480<sup>low</sup> to Ly6C<sup>low</sup>F480<sup>high</sup> following induced injury<sup>285</sup>. In our study, we observed that in the absence of shielding almost no macrophages which were of recipient host origin could be found in the diaphragm at 8 weeks post-irradiation. Instead, there was an influx of donor bone marrow origin macrophages to compensate for the loss of host resident macrophages. To our knowledge this is the first demonstration that total body irradiation (at least with the current radiation protocol) effectively depletes the skeletal muscle resident macrophage pool. In contrast, under conditions of diaphragm shielding approximately 40% of muscle resident macrophages were of recipient host origin.

One limitation of the diaphragm shielding model is that a portion of the rib cage and spine are also protected from irradiation, such that these bone marrow sources of host macrophages are not ablated. Despite this, the donor bone marrow contribution (chimerism) to blood monocytes is approximately 85%, and normalization of the donor macrophages in the muscle to donor monocytes in the blood is able to adjust for the incomplete (i.e., less than 100%) donor bone marrow engraftment. However, we cannot exclude the possibility that this minor population of bone marrow-dependent macrophages from the host somehow influences the behavior of the host resident macrophage population which is bone marrow-independent.

In addition to establishing a model for studying muscle regeneration in the diaphragm, our investigation has yielded new insights into the dynamic behaviors of macrophages from different origins in the setting acute diaphragmatic injury and subsequent recovery. Although it was previously known that acute skeletal muscle injury causes a large influx of monocyte-derived macrophages recruited from the bone marrow, little is known about the response of bone marrow-

independent macrophages in this setting. Our data suggest that the number of bone marrow-independent macrophages, which are presumed to be of embryonic origin, does not change in the immediate aftermath of acute injury. This remarkable dichotomy in the numerical contributions of bone marrow-dependent and -independent macrophages suggests that they have fundamentally different roles in the immediate response to muscle injury.

Furthermore, beyond documenting that the number of macrophages in the muscle returns to normal following successful regeneration<sup>42</sup>, there has been little exploration of how acute injury affects the newly established resident macrophage pool after recovery. A fundamental question is whether the massive influx of bone marrow-dependent macrophages causes a larger percentage of these cells to remain within the recovered tissue as part of the newly reconstituted resident population, as has been previously reported in the heart and lung<sup>296 297</sup>. This was not the case in the diaphragm, and we observed that the relative proportions as well as the absolute numbers of bone marrow-dependent and bone marrow-independent macrophages returned to their pre-injury levels.

In summary, our study has revealed a complex, dynamic shift in macrophage populations throughout diaphragm muscle injury and recovery. We believe the diaphragm shielding model we have developed will be a useful tool for exploring the impact of macrophage ontogeny on the multifaceted and indispensable roles played by these cells in muscle health and disease. In particular, further investigation is warranted to better comprehend the function of bone marrow-dependent versus -independent macrophages, such as to discern how their numbers are controlled and to define the specific roles they fulfill along the spectrum between skeletal muscle injury and either successful or unsuccessful repair.

## References for Chapter 2

9. Tidball JG. Regulation of muscle growth and regeneration by the immune system. *Nat Rev Immunol*. 2017;17(3):165-178. doi:10.1038/nri.2016.150
187. Brigitte M, Schilte C, Plonquet A, et al. Muscle resident macrophages control the immune cell reaction in a mouse model of notexin-induced myoinjury. *Arthritis Rheum*. 2010;62(1):268-279. doi:10.1002/art.27183
194. Sun D, Martinez CO, Ochoa O, et al. Bone marrow-derived cell regulation of skeletal muscle regeneration. *FASEB J*. 2009;23(2):382-395. doi:10.1096/fj.07-095901
198. Mounier R, Théret M, Arnold L, et al. AMPK $\alpha$ 1 regulates macrophage skewing at the time of resolution of inflammation during skeletal muscle regeneration. *Cell Metab*. 2013;18(2):251-264. doi:10.1016/j.cmet.2013.06.017
228. Mojumdar K, Giordano C, Lemaire C, et al. Divergent impact of Toll-like receptor 2 deficiency on repair mechanisms in healthy muscle versus Duchenne muscular dystrophy. *J Pathol*. 2016;239(1):10-22. doi:10.1002/path.4689
264. Pickering M, Jones JFX. The diaphragm: Two physiological muscles in one. *J Anat*. 2002;201(4):305-312. doi:10.1046/j.1469-7580.2002.00095.x
265. Perry SF, Similowski T, Klein W, Codd JR. The evolutionary origin of the mammalian diaphragm. *Respir Physiol Neurobiol*. 2010;171(1):1-16. doi:10.1016/j.resp.2010.01.004
266. Orozco-Levi M, Lloreta J, Minguella J, Serrano S, Broquetas JM, Gea J. Injury of the human diaphragm associated with exertion and chronic obstructive pulmonary disease. *Am J Respir Crit Care Med*. 2001;164(9):1734-1739. doi:10.1164/ajrccm.164.9.2011150
267. Tidball JG, Wehling-Henricks M. Macrophages promote muscle membrane repair and muscle fibre growth and regeneration during modified muscle loading in mice in vivo. *J Physiol*. 2007;578(1):327-336. doi:10.1113/JPHYSIOL.2006.118265
268. Wang H, Melton DW, Porter L, Sarwar ZU, McManus LM, Shireman PK. Altered macrophage phenotype transition impairs skeletal muscle regeneration. *Am J Pathol*. 2014;184(4):1167-1184. doi:10.1016/J.AJPATH.2013.12.020
269. Mirza R, DiPietro LA, Koh TJ. Selective and Specific Macrophage Ablation Is Detrimental to Wound Healing in Mice. *Am J Pathol*. 2009;175(6):2454-2462. doi:10.2353/AJPATH.2009.090248
270. Liu X, Liu Y, Zhao L, Zeng Z, Xiao W, Chen P. Macrophage depletion impairs skeletal muscle regeneration: The roles of regulatory factors for muscle regeneration. *Cell Biol Int*. 2017;41(3):228-238. doi:10.1002/CBIN.10705
271. Summan M, Warren GL, Mercer RR, et al. Macrophages and skeletal muscle regeneration: a clodronate-containing liposome depletion study. *Am J Physiol Regul Integr Comp Physiol*. 2006;290(6):R1488-95. doi:10.1152/ajpregu.00465.2005
272. Tidball JG, Flores I, Wehling-henricks M, Ramos J, Wang Y, Bertoni C. Targeting a therapeutic LIF transgene to muscle via the immune system ameliorates muscular dystrophy. *Nat Commun*. Published online 2019:1-17. doi:10.1038/s41467-019-10614-1
273. Rahman MM, Ghosh M, Subramani J, Fong GH, Carlson ME, Shapiro LH. CD13 regulates anchorage and differentiation of the skeletal muscle satellite stem cell population in ischemic injury. *Stem Cells*. 2014;32(6):1564-1577. doi:10.1002/stem.1610
274. Caiozzo VJ, Giedzinski E, Baker M, et al. The Radiosensitivity of Satellite Cells: Cell Cycle Regulation, Apoptosis and Oxidative Stress. <https://doi.org/10.1667/RR2190.1> 2010;174(5):582-589. doi:10.1667/RR2190.1

275. McDonald AA, Kunz MD, McLoon LK. Dystrophic changes in extraocular muscles after gamma irradiation in mdx:utrophin+/- mice. *PLoS One*. 2014;9(1). doi:10.1371/journal.pone.0086424
276. Cui YZ, Hisha H, Yang GX, et al. Optimal protocol for total body irradiation for allogeneic bone marrow transplantation in mice. *Bone Marrow Transplant*. 2002;30(12):843-849. doi:10.1038/sj.bmt.1703766
277. McCroskery S, Thomas M, Maxwell L, Sharma M, Kambadur R. Myostatin negatively regulates satellite cell activation and self-renewal. *J Cell Biol*. 2003;162(6):1135-1147. doi:10.1083/jcb.200207056
278. Schneider CA, Rasband WS, Eliceiri KW. NIH Image to ImageJ: 25 years of image analysis. *Nat Methods*. 2012;9(7):671-675. doi:10.1038/nmeth.2089
279. Malerba A, Pasut A, Frigo M, De Coppi P, Baroni MD, Vitiello L. Macrophage-secreted factors enhance the in vitro expansion of DMD muscle precursor cells while preserving their myogenic potential. *Neurol Res*. 2010;32(1):55-62. doi:10.1179/174313209X380865
280. Rao X, Lai D, Huang X. A new method for quantitative real-time polymerase chain reaction data analysis. *J Comput Biol*. 2013;20(9):703-711. doi:10.1089/cmb.2012.0279
281. Wehling-Henricks M, Welc SS, Samengo G, et al. Macrophages escape Klotho gene silencing in the mdx mouse model of Duchenne muscular dystrophy and promote muscle growth and increase satellite cell numbers through a Klotho-mediated pathway. *Hum Mol Genet*. 2018;27(1):14-29. doi:10.1093/HMG/DDX380
282. Perdiguero E, Sousa-Victor P, Ruiz-Bonilla V, et al. p38/MKP-1-regulated AKT coordinates macrophage transitions and resolution of inflammation during tissue repair. *J Cell Biol*. 2011;195(2):307-322. doi:10.1083/JCB.201104053
283. Granata AL, Vecchi C, Graciotti L, Fulgenzi G, Maggi S, Corsi A. Gamma irradiation can reduce muscle damage in mdx dystrophic mice. *Acta Neuropathol*. 1998;96(6):564-568. doi:10.1007/s004010050936
284. Von Maltzahn J, Jones AE, Parks RJ, Rudnicki MA. Pax7 is critical for the normal function of satellite cells in adult skeletal muscle. *Proc Natl Acad Sci U S A*. 2013;110(41):16474-16479. doi:10.1073/pnas.1307680110
285. Patsalos A, Pap A, Varga T, et al. In situ macrophage phenotypic transition is affected by altered cellular composition prior to acute sterile muscle injury. *J Physiol*. 2017;595(17):5815-5842. doi:10.1113/JP274361
286. Boldrin L, Neal A, Zammit PS, Muntoni F, Morgan JE. Donor Satellite Cell Engraftment Is Significantly Augmented When the Host Niche Is Preserved and Endogenous Satellite Cells Are Incapacitated. *Stem Cells*. 2012;30(9):1971-1984. doi:10.1002/STEM.1158
287. Zhou T, Lu L, Wu S, Zuo L. Effects of Ionizing Irradiation on Mouse Diaphragmatic Skeletal Muscle. *Front Physiol*. 2017;0(JUL):506. doi:10.3389/FPHYS.2017.00506
288. Hsieh CH, Lin YC, Chen YJ, Wu HD, Wang LY. Diaphragm contractile dysfunction causes by off-target low-dose irradiation. *Am J Transl Res*. 2016;8(3):1510. Accessed December 8, 2022. /pmc/articles/PMC4859636/
289. Heslop L, Morgan JE, Partridge TA. Evidence for a myogenic stem cell that is exhausted in dystrophic muscle. *J Cell Sci*. 2000;113(12):2299-2308. doi:10.1242/jcs.113.12.2299
290. Scaramozza A, Park D, Kollu S, et al. Lineage Tracing Reveals a Subset of Reserve Muscle Stem Cells Capable of Clonal Expansion under Stress. *Cell Stem Cell*. 2019;24(6):944-957.e5. doi:10.1016/J.STEM.2019.03.020
291. Rota Graziosi E, François S, Pateux J, et al. Muscle regeneration after high-dose radiation

- exposure: therapeutic potential of Hedgehog pathway modulation? *Int J Radiat Biol.* 2022;98(5):968-979. doi:10.1080/09553002.2021.2013574
292. Park MD, Silvin A, Ginhoux F, Merad M, Lipschultz J. Macrophages in health and disease. doi:10.1016/j.cell.2022.10.007
293. Nishiyama K, Nakashima H, Ikarashi M, et al. Mouse CD11b+Kupffer Cells Recruited from Bone Marrow Accelerate Liver Regeneration after Partial Hepatectomy. *PLoS One.* 2015;10(9):e0136774. doi:10.1371/JOURNAL.PONE.0136774
294. Barreiro O, Cibrian D, Clemente C, et al. Pivotal role for skin transendothelial radio-resistant anti-inflammatory macrophages in tissue repair. *Elife.* 2016;5(JUN2016). doi:10.7554/ELIFE.15251
295. Shemer A, Grozovski J, Tay TL, et al. Engrafted parenchymal brain macrophages differ from microglia in transcriptome, chromatin landscape and response to challenge. *Nat Commun.* 2018;9(1). doi:10.1038/S41467-018-07548-5
296. Bajpai G, Bredemeyer A, Li W, et al. Tissue Resident CCR2- and CCR2+ Cardiac Macrophages Differentially Orchestrate Monocyte Recruitment and Fate Specification Following Myocardial Injury. *Circ Res.* 2019;124(2):263-278. doi:10.1161/CIRCRESAHA.118.314028
297. Misharin A V, Nebreda LM, Reyfman PA, et al. Monocyte-derived alveolar macrophages drive lung fibrosis and persist in the lung over the life span. *JEM.* Published online 2017;2387-2404. doi:10.1084/jem.20162152

## 2.6 Bridging text

In CHAPTER 1, we introduced the diaphragm shielding model and presented evidence supporting its efficacy as an enhanced model to differentiate between transplanted and local cells during muscle regeneration. This model effectively reduces the irradiation impact on the survival and functionality of myogenic precursor cells and resident macrophages essential for tissue repair. Using this approach, we explored macrophage heterogeneity concerning their origin under homeostatic conditions. Our findings revealed a significant portion of diaphragm macrophages originating independently of bone marrow. However, the precise embryonic lineage of these independent macrophages remains unclear. Additionally, while we detailed the dynamic roles of both bone marrow-dependent and independent macrophages during acute injury, the contributions of these macrophage subsets in chronically inflamed dystrophic muscles remain uncharted. Furthermore, the distinct environmental influences—whether in a healthy or dystrophic setting—on their transcriptional activities are yet to be comprehensively addressed.

Transitioning from CHAPTER 1's foundational insights, CHAPTER 2 delves deeper into the embryonic origins of these tissue-resident macrophages. Employing a comprehensive strategy, encompassing fate mapping and parabiosis experiments, our aim is to elucidate the contributions from both embryonic progenitor cells and adult bone marrow. As we shift our focus to the chronic dystrophic condition, we thoroughly examine the macrophage subsets' role in the DMD mdx model, aiming to uncover how the dystrophic muscle environment influences the phenotypic and transcriptional identity of diaphragm macrophages.

**Chapter 3: Macrophage Ontogeny and Phenotypic Alterations in Healthy and Dystrophic Muscle Environments**

### **3.1. Abstract**

*Background:* Macrophages are crucial innate immune cells which play pivotal roles in tissue homeostasis, development, inflammation, and repair. Although macrophages are the most abundant inflammatory cell type in Duchenne Muscular Dystrophy (DMD), the ontogeny and associated phenotypic characteristics of these macrophages remain poorly defined. Here we sought to dissect the contributions of prenatal embryonic progenitor-derived versus postnatal bone marrow-derived macrophages in the diaphragms of both healthy and dystrophic (mdx) mice along with their phenotypic characteristics.

*Results:* Using a combination of tamoxifen-inducible pulse-chase lineage tracing, parabiosis experiments, and chimeric mouse models, we elucidated the origins, dynamics and phenotypic characteristics of these cells in both healthy and dystrophic (mdx) mouse muscles.

In healthy adult skeletal muscles we found that 30-40% of the tissue resident macrophage pool originates from prenatal embryonic progenitors (predominantly from the fetal liver with a minor contribution from the yolk sac), whereas the remaining resident macrophages originate postnatally from bone marrow-derived monocytes. Our studies showed comparable macrophage numbers in wild-type (WT) and mdx diaphragms at birth, but a significant surge occurs in mdx mice from 3 weeks of age onward, attributed to bone marrow-derived macrophages which eventually make up almost the entire macrophage population in mdx mice. In contrast, there is a depletion of the prenatal origin tissue resident population in mdx muscle. Additionally, through flow cytometry, RNA-seq, GO and Homer motif analysis, we observed that the phenotype and gene expression of bone marrow-derived macrophages are heavily dictated by the host environment. Specifically, a dystrophic environment leads to augmented inflammatory phenotypes associated with increased genes enriched in immune activation, tissue remodeling, and extracellular matrix interactions. Key

transcriptional drivers of this phenomenon appear to include members of the Interferon Regulatory Factor family of transcription factors.

*Conclusions:* These findings underscore the ability of the dystrophic microenvironment to profoundly alter macrophage ontogeny, phenotype and function in DMD.

### **3.2. Introduction**

Macrophages are multi-functional immune cells that play a key role in muscle homeostasis, development, immune surveillance, inflammation, and tissue repair. Skeletal muscle macrophages can have heterogeneous origins, and the steady-state tissue-resident macrophage pool in adult skeletal muscles is believed to arise from two primary sources<sup>186</sup>. The first originates from embryonic progenitor cells established during in utero development, contributing to a macrophage population in muscle present at birth. The second source encompasses a postnatal population of macrophages, derived from definitive monocytes that have been recruited from the adult bone marrow. These heterogeneous origins might influence their functions, phenotypes, and responses to various stimuli. While recent studies have elucidated the roles of various macrophage subsets in tissues like the brain and lungs<sup>298 299</sup>, their precise origins, contributions, and functions in skeletal muscles are less well understood. For instance, what percentage of muscle macrophages are derived from embryonic progenitors versus those from the adult bone marrow under different conditions? How stable are these populations over time, especially in the setting of disease? Moreover, phenotypic markers such as CCR2 and T-cell immunoglobulin and mucin domain containing 4 (TIM4) have been implicated in distinguishing between monocyte-dependent and monocyte-independent macrophages, respectively<sup>300 301</sup>. Yet, the exact relationship between these markers, macrophage origin, and macrophage function in skeletal muscle remains to be fully elucidated.

DMD is a severe genetic disorder characterized by progressive muscle wasting and fibrosis<sup>9</sup>. One of the hallmarks of this condition is the chronic injury to skeletal muscles. Macrophages are recognized as key mediators of both muscle repair and disease progression in DMD. Understanding the dynamics and origins of macrophages in DMD becomes crucial, especially

since these cells are implicated in both successful repair and injury progression leading to pathological fibrosis. A pertinent question in the field of macrophage biology is how much of the macrophage phenotype is intrinsic and determined by the lineage, and how much is malleable and shaped by the environment. This delineation is particularly important in the context of chronic diseases such as DMD, as it provides insights into whether altering the tissue environment or directly targeting macrophage precursors can be a viable therapeutic strategy.

This purpose of this study was to begin to unravel the intricate relationships between macrophage ontogeny, phenotypic markers, and macrophage functionality in adult skeletal muscles. Using a combination of fate mapping, parabiosis, and chimeric mice, we examined the origins, persistence, and characteristics of skeletal muscle macrophages with a particular focus on the diaphragm given its essential role in respiration. In addition to determining the situation in healthy skeletal muscle under homeostatic conditions, we sought to delineate the predominant source and phenotypic characteristics of macrophages in mdx mice, which share the same genetic defect (mutations in the dystrophin gene) as patients affected with DMD.

### **3.3. Methods**

#### **3.3.1. Experimental animals**

CD45.1, C57BL6, B6.129P2(Cg)-CX3CR1<sup>tm2.1(cre/ERT2)Litt/WganJ</sup> (referred to as CX3CR1<sup>CreER-YFP</sup>), B6.Cg-Gt(ROSA)26Sor<sup>tm14(CAGtdTomato)Hze/J</sup> (referred to as R26Td), and mdx.4cv mice were obtained from The Jackson Laboratory (Bar Harbor, ME). CX3CR1<sup>gfp/gfp</sup> mice were generously provided by Dr. Irah King's lab while CCR2<sup>-/-</sup> mice were generously provided by Dr. Maziar Divangahi's lab. To obtain CX3CR1<sup>CreER-YFP</sup> -R26Td mice, a crossbreeding was performed between CX3CR1<sup>CreER-YFP</sup> and R26Td mice. Mdx- CX3CR1(GFP)+ mice were obtained by mating male CX3CR1<sup>gfp/gfp</sup> with female mdx mice, and control WT-CX3CR1(GFP)+ mice were similarly obtained by crossing CX3CR1<sup>gfp/gfp</sup> with wild-type C57BL6 mice. All mice were bred and housed in a sterile environment in the animal facility. The mice were subjected to a light and dark cycle consisting of 12 hours each. The habitat temperature was maintained at 21 ± 1 °C, and the humidity ranged from 40-60%. The experimental procedures involving the mice were ethically approved by the Animal Care and Use Committee of the McGill University Health Centre (RI-MUHC). The research was conducted in accordance with the guidelines set forth by the Canadian Council on Animal Care.

#### **3.3.2. Bone marrow transplantation**

To generate chimeric mice, bone marrow transplantations were performed after total body irradiation. In order to protect the diaphragm muscle from the effects of irradiation, in recipient mice a lead bar, measuring 2 cm in thickness and 1.5 cm in width, was placed over the lower section of the chest overlying the diaphragm as described in the preceding chapter of this thesis. The mice received two doses of irradiation 4 hours apart, each dose being 6 Gy. The radiation was administered at a voltage of 225kV, a current of 13mA, and a rate of 1.0265Gy/min (X-RAD

SmART, Precision X-ray, USA). At 24 hours following the second irradiation, the mice were intravenously injected with  $2 \times 10^7$  bone marrow cells in 200ul of RPMI. Bone marrow cells were collected by flushing both femurs and tibiae with ice-cold RPMI, followed by filtration through a  $70\mu\text{m}$  cell strainer. The cell suspension was then centrifuged at 500g for 5 minutes at 4 degrees Celsius, and the pellet was resuspended in RPMI. A subset of recipient mice received a single dose of busulfan (30mg/kg IP) 18 hours (half-life = approx. 3 hours) before delivering the donor bone marrow, in order to eliminate any residual host bone marrow protected from irradiation by the diaphragm shielding procedure. Busulfan (Sigma, USA) was first dissolved in dimethyl sulfoxide (DMSO) and then further diluted in 5 volumes of sterile H<sub>2</sub>O. To prevent infections, recipient mice were treated with 1% enrofloxacin (Baytril, 50mg/ml; Bayer, USA) in their drinking water for 7 days after irradiation. Subsequently, the mice were allowed to recover for 8 weeks to allow for bone marrow reconstitution.

### **3.3.3. Parabiosis**

Parabiosis surgeries were performed between CD45.1 wild-type and CD45.2 CCR2<sup>-/-</sup> strains (n=4, 2 female pairs and 2 male pairs). Male pairs were housed together in the same cage for 3 weeks prior to the surgery, while female pairs were cohabitated for 1 week. To prepare for the surgery, the hair on the side of the mouse to be incised was removed by applying Nair from the neck to the tail. Slow-release buprenorphine (0.1mg/kg) was administered to the mice before the surgery, and the mice received isoflurane (0.5-2 unit/min) during the surgical procedure. A longitudinal incision was made from the scapula to the femur location. Careful scissor dissection was used to cut the fascia along the incision within a 0.5 cm area. The olecranon of two mice was tied together under the skin using sutures. The incision points, including the starting and ending points, abdominal muscles, and several locations along the incision, were sutured. The remaining part of the incision

was closed using staples. The tibia of two mice were tightened by a suture passing through the muscles. Finally, saline (0.5ml) was injected into each mouse for hydration. The mice were allowed to recover from the surgery and maintained for 5 months prior to sacrifice.

#### **3.3.4. Fate mapping**

CX3CR1<sup>CreER-YFP</sup> mice were used as a tool to selectively label macrophage and their precursors. R26Td mice carry a genetic modification that results in the expression of the red fluorescent protein Td-Tomato. This fluorescent marker can be used to track and visualize cells in which the Td-Tomato gene is active. Female R26Td mice were mated with male CX3CR1<sup>CreER-YFP</sup> mice. The resulting offspring inherit both genetic traits: the CX3CR1 expression specific to macrophages and the Td-Tomato marker gene. This genetic combination allows for specific red fluorescence labeling of macrophages at the desired embryonic development stage through tamoxifen treatment, which can be subsequently detected by flow cytometry. The presence of a vaginal plug was checked the following morning, and mice showing a vaginal plug were considered pregnant at embryonic development day 0.5 (E0.5). To determine the embryonic origin of diaphragm macrophages, the pregnant R26Td mice were intraperitoneally administered tamoxifen (2.5mg/mouse) and progesterone (1.75mg/mouse, Sigma) dissolved in corn oil (Sigma–Aldrich, USA) at one of 3 time points corresponding to different phases of embryonic development: E7.5, E10.5, and E13.5. At E7.5, primitive hematopoiesis predominantly takes place in the yolk sac. By E10.5, a transition occurs as definitive hematopoiesis initiates, relocating from the yolk sac to various sites, with a notable emphasis on the fetal liver. By E13.5, definitive hematopoiesis is firmly established within the fetal liver, which remains the principal hub for macrophage production. The tissues (diaphragm, lung, and brain) from these embryos were then harvested at E18.5 and analyzed by flow cytometry. Tissues from two embryos were pooled into one sample

for analysis. Embryos that did not receive tamoxifen injection were used as controls. In a separate experiment designed to track the persistence of embryo-derived macrophages into adulthood, tamoxifen and progesterone were injected at E18.5 (shortly before normal birth) and a caesarean section was performed at E19.5 with transfer of the pups to foster cages and maintenance of the mice until either 5 or 9 weeks of age. Some studies use corn oil treated mice as control, here we use untreated mice as control. Although the omission of corn oil-treated mice may restrict our capacity to evaluate potential effects of the vehicle (corn oil), it does not undermine the validity of our primary focus, which centers on the labeling and effects of tamoxifen.

### **3.3.5. BrdU incorporation**

Four-week-old mice were injected daily with 100  $\mu$ l of a 10 mg/ml BrdU solution dissolved in PBS for a duration of 28 days. The mice were sacrificed at 24 hours after the last injection, and the percentage of macrophages demonstrating BrdU incorporation was determined by flow cytometry following the instructions of the APC BrdU Flow Kit (BD Biosciences).

### **3.3.6. Whole mount immunofluorescence microscopy**

The diaphragm was dissected and placed on a 6 cm culture plate directly on ice. Whole mount immunofluorescence microscopy was performed by capturing images of the diaphragm using a confocal microscope immediately after dissection.

### **3.3.7. Cell preparation and flow cytometry**

Prior to euthanasia, the mice were anesthetized with isoflurane and blood was drawn by cardiac puncture using a tube containing sodium citrate (0.48% citrate acid, 1.32% sodium citrate, 1.47% glucose) as an anticoagulant. The heart was perfused with 20 ml of phosphate-buffered saline (PBS) (Wisent), followed by an additional 20 ml of PBS after severing the dorsal aorta. For the blood samples, red blood cells were lysed using a red blood cell lysis buffer (0.78%  $\text{NH}_4\text{Cl}$ , 0.01%

KHCO<sub>3</sub>, 0.003% EDTA). Muscles (diaphragm, tibialis anterior, and soleus), lung, and embryonic brain (E18.5) were dissected into small pieces and digested in PBS containing 0.2mg/ml collagenase B (Roche) for 1.5 hours. The digested tissue was loosened into a cell suspension by pipetting up and down. The cell suspensions from all tissues were passed through a cell strainer. Cells were stained with a viability dye (Violet, Invitrogen) and blocked with Fc blocking antibody (anti-CD16/CD32, BD Biosciences). Flow surface antibody was stained for 30 mins at 4 degree and washed with 0.5% bovine serum albumin (BioShop, CA) in PBS. Antibodies used for flow cytometry are listed in the Supplementary Material section. Stained cells were fixed with 1% PFA and stored at 4 degrees C until analysis. Cell phenotype analysis was performed using Flowjo software, with adult skeletal muscle macrophages defined as live cells that were CD45+ / Siglec F- / CD11c- / CD11b+ / F480+.

### **3.3.8. RNA sequencing**

Macrophages defined according to the same cellular markers indicated above were sorted from the diaphragm using a BD FACSAria™ Fusion cell sorter and placed directly into lysis buffer. Diaphragm samples were pooled as required to obtain sufficient macrophage numbers (>30,000 cells) for bulk RNA sequencing. RNA extraction was carried out using the RNeasy® Micro Kit according to the manufacturer's protocol. The integrity of the extracted RNA was evaluated using the Agilent 2100 Bioanalyzer (Agilent Technologies, Santa Clara, CA, USA). Samples with an RNA Integrity Number (RIN) greater than 7 were selected for subsequent analysis.

Sequencing was performed on the Illumina Nextseq500 platform using 1 Flowcell High Output and 75 cycles for single-end reads. The quality of the sequencing reads generated from the Illumina platform was assessed using FastQC. Genes with zero reads (rowsum > 10) and unknown 'Rik' genes were filtered out. Analysis was performed using the Deseq2 package in the statistical

software R to identify genes that showed significant differential expression. Genes were filtered based on a base mean over 100, log fold change (FC) over 1, and adjusted p-value (padj) less than 0.05. These differentially expressed genes (DEGs) were then subjected to further bioinformatic analysis.

Gene function analysis was conducted using the Gene Ontology website<sup>302 303</sup>. The biological pathways involved in the identified DEGs were explored using the Gene Ontology (GO) Enrichment Analysis and Reactome Pathway databases. Motif enrichment analysis was carried out using the Hypergeometric Optimization of Motif Enrichment (HOMER) software by using the findMotifs.pl program according to the website instructions using the default Mus musculus Promoter Set<sup>304</sup>. The analysis spanned regions from -300 to 50, focusing on motifs of lengths 8bp, 10bp, and 12bp.

### **3.3.9. Statistics**

Statistical analysis was performed using GraphPad Prism version 9. For comparisons between two groups, a Student's t-test was used to assess differences in a single parameter. When comparing a single parameter among more than two groups, ANOVA followed by Tukey's multiple comparisons test was employed. Dunnett's multiple comparisons test was utilized to compare data from each group to a specific reference group. A p-value of less than 0.05 was considered statistically significant. All graphs show group mean data with each dot on the graph representing an individual animal unless specified otherwise. The error bars indicate the standard deviation (SD).

### 3.4. Results

#### 3.4.1. Bone Marrow-Dependent and Bone Marrow-Independent Macrophages Contribute to the Steady-State Macrophage Pool in Healthy Adult Skeletal Muscle

In principle the steady-state tissue-resident macrophage pool in adult skeletal muscle can originate from two primary sources: 1) a macrophage population that is established in the muscle prenatally from embryonic progenitor cells during in utero development; and 2) a population of macrophages that is derived postnatally from definitive monocytes recruited from the adult bone marrow. To determine the relative contributions of these two populations, we first used a tamoxifen-inducible pulse-chase lineage tracing strategy to identify bone marrow-independent macrophages arising in the fetus and present in healthy skeletal muscles at birth. Male mice carrying tamoxifen-inducible Cre recombinase and constitutive YFP under the control of the CX3CR1 promoter (CX3CR1<sup>CreERT2-YFP</sup>) were bred with female Rosa26-TdTomato (R26Td) Cre reporter mice (Fig. 3.1a). Tamoxifen was administered to the timed-pregnancy R26Td reporter mice as a pulse dose at one of 3 distinct stages of embryonic development (E7.5, E10.5, or E13.5). The fetal diaphragm was then harvested at E18.5 to quantify the percentage of prenatal macrophages (CX3CR1-YFP+) exhibiting TdTomato expression immediately prior to birth (Fig. 3.1b). The brain and lung were used as reference tissues since they are both known to harbor significant populations of bone marrow-independent resident macrophages derived from embryonic precursor cells<sup>141 144 164</sup>.

Pulse-labeling with tamoxifen at E7.5 resulted in approximately 80% of brain microglia being TdTomato+ at E18.5 (Fig. 3.1b-c), which is consistent with their known embryonic yolk sac origin. TdTomato+ labeling was also observed in the diaphragm and lungs of mice that received tamoxifen at E7.5 but at a substantially lower level (20-25%) than the brain. Tamoxifen administration at E13.5, when monocytes from the fetal liver are in circulation, was associated

with approximately 75% of diaphragm macrophages being TdTomato+ immediately prior to birth. The majority of TdTomato+ brain microglia were CD11b<sup>low</sup> F480<sup>high</sup> across all time points, whereas both the diaphragm and lungs exhibited a rise in the percentage of CD11b<sup>high</sup> F480<sup>low</sup> macrophages from E10.5 to E13.5 (Fig. 3.1d-e). The above findings collectively suggest that the majority of resident macrophages present in the diaphragm at birth originate from fetal liver hematopoiesis, with a lesser contribution from the embryonic yolk sac.

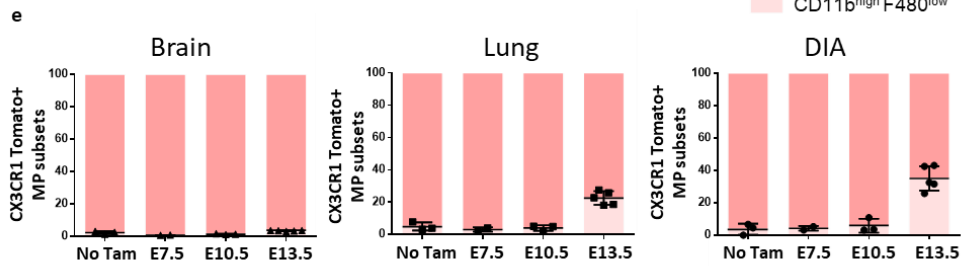
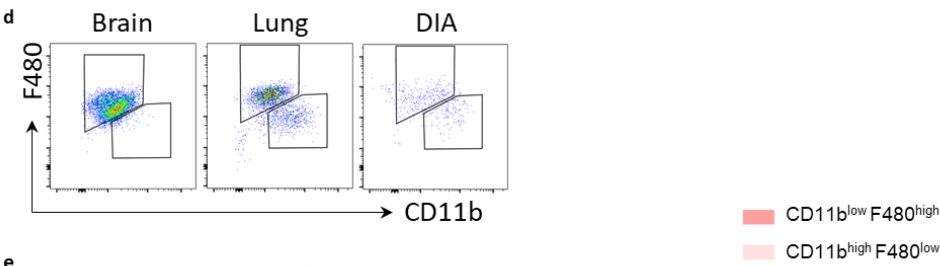
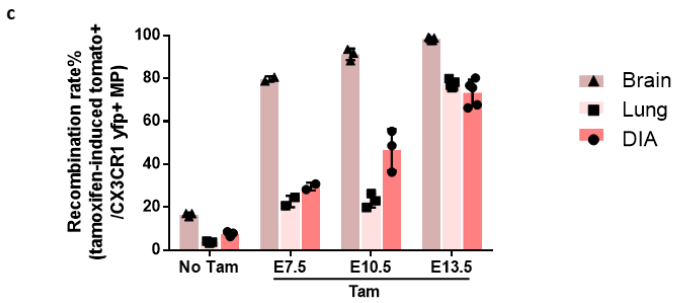
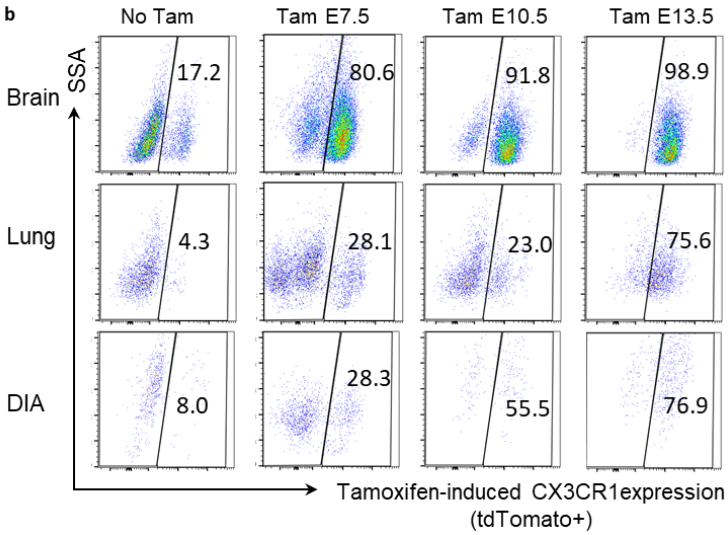
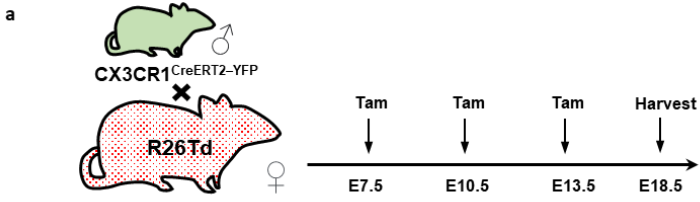


**Figure 3.1. Fate mapping to assess the ontogeny of bone marrow-independent macrophages which arise during fetal development**

- a. Schematic illustration of the tamoxifen administration protocol in timed pregnancy mice. A single dose of tamoxifen was injected into pregnant R26Td mice at the indicated time points, and the tissues from all embryos were harvested at E18.5. To ensure adequate sample volume, tissues from two individual embryos were combined for analysis.
- b. Representative FACS plots show tamoxifen-induced recombination (TdTomato+) in prenatal macrophages (CD45+, CX3CR1-YFP+) of the brain, lung, and diaphragm (DIA) after pulse administration of tamoxifen at different stages of fetal development. Tissues from non-tamoxifen-treated embryos (no Tam) were used as controls.
- c. Group mean data are shown for recombination rates (TdTomato+) of macrophages in the brain, lung, and diaphragm (DIA) from embryos which were either untreated (no Tam) or treated with tamoxifen at the indicated time points (n=3, 2, 3, or 5 pooled embryos for each group, respectively).
- d. Representative FACS plots show F480 and CD11b expression in TdTomato+ macrophages (CD45+, CX3CR1-YFP+) from the different fetal organs after treatment with tamoxifen at E13.5. Distinct populations of CD11b<sup>low</sup> F480<sup>high</sup> and CD11b<sup>high</sup> F480<sup>low</sup> macrophages were identified.
- e. The proportion of CD11b<sup>high</sup> F480<sup>low</sup> macrophages in the lung and diaphragm (DIA) increased at the later stage (E13.5) of fetal development, whereas it remained stable in the brain.

In order to assess the persistence of fetal-origin resident macrophages in skeletal muscles during the postnatal period, we next administered tamoxifen at E18.5 to label the entire prenatal macrophage population immediately prior to birth (Fig 3.2a). The CX3CR1<sup>CreER-YFP</sup> / R26Td offspring were delivered via cesarian section 24 hours later and subsequently analyzed at 5 and 9 weeks of age. In control mice that were not exposed to tamoxifen, a higher level of background “leaky” TdTomato expression was found in adult muscles (eg., approximately 20% of macrophages in the diaphragm) as compared to the fetal period shown in Fig. 3.1c. However, the tamoxifen-treated mice had significantly higher percentages of TdTomato<sup>+</sup> macrophages (approximately 50-60%) in the both the diaphragm and soleus muscles (Fig 3.2b-c). Furthermore, this level of TdTomato<sup>+</sup> macrophage labeling was stably maintained between 5 and 9 weeks of age (Fig 3.2c-d).

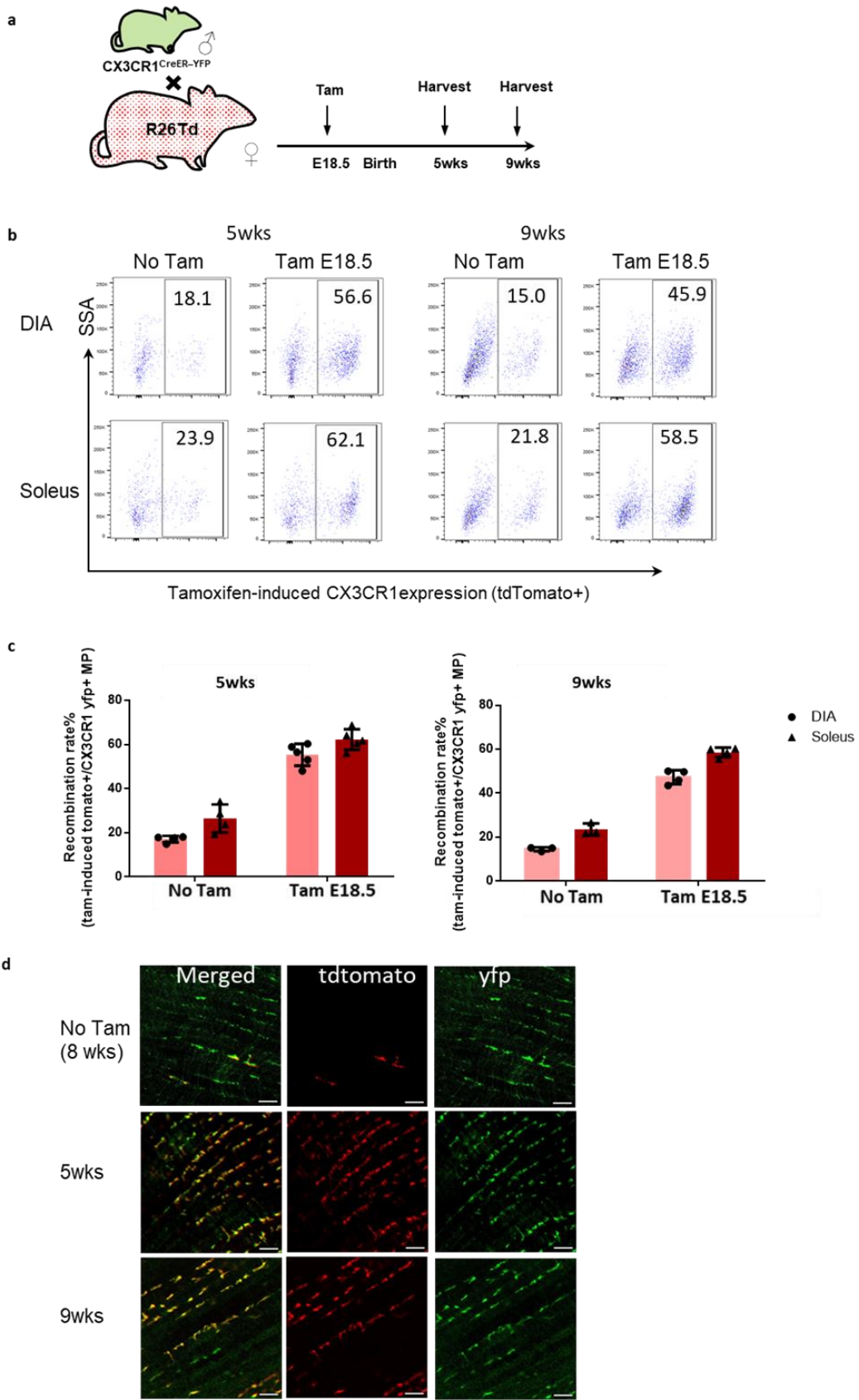


**Figure 3.2. Fate mapping reveals the persistence of prenatal origin macrophages in healthy adult muscle**

- a. Schematic illustration of the tamoxifen administration protocol in mice studied post-natally. A single dose of tamoxifen was injected into pregnant R26Td mice at E18.5 and the skeletal muscles of their offspring were collected at 5 or 9 weeks of age.
- b. Representative FACS plots show TdTomato+ macrophages (CD45+, SiglecF-, CD11c-, CD11b+, F480+, YFP+) in the post-natal adult diaphragm (DIA) and soleus muscles after pulse administration of tamoxifen shortly before birth at E18.5. Note that although TdTomato+ macrophages were also present in the muscles of non-tamoxifen-treated embryos (no Tam), the level was substantially lower than in the tamoxifen-treated groups.
- c. Group mean data are shown for recombination rates (TdTomato+) of macrophages in the diaphragm (DIA) and soleus muscles from embryos which were either untreated (no Tam) or treated with tamoxifen at E18.5 and harvested at 5 weeks and 9 weeks of age (n=3-5/group).
- d. Representative confocal images of the diaphragm showing TdTomato and YFP fluorescence in post-natal mice at the two adult ages after having received tamoxifen at E18.5. Scale bar equals 50µm.

To further confirm the important contribution of macrophages which are independent of the adult bone marrow to the steady-state postnatal macrophage population, we conducted parabiosis experiments in which the blood circulations of CD45.1 allele wild-type (WT) mice and CD45.2 allele CCR2-deficient (CCR2<sup>-/-</sup>) mice were surgically joined (Fig 3.3a). Since CCR2<sup>-/-</sup> mice have impaired monocyte release from the bone marrow<sup>305 306</sup>, in this model the WT mice effectively act as monocyte donors to the paired CCR2<sup>-/-</sup> mice. After 5 months of parabiosis under steady-state conditions, successful blood chimerism was confirmed and macrophages in various organs (lung, liver, spleen) of CCR2<sup>-/-</sup> mice displayed the expected levels of either dependence or independence from blood monocytes as previously reported in the literature<sup>164</sup> (Supplemental Fig 3.1a-b).

If prenatal macrophages are all eventually replaced by postnatal macrophages derived from blood monocytes, one expects that the relative percentages of CD45.1 monocytes in the blood and CD45.1 macrophages in the tissues of CCR2<sup>-/-</sup> mice will closely correspond to one another. However, the percentage of WT “donor” origin (CD45.1) macrophages in the skeletal muscles of CCR2<sup>-/-</sup> mice was significantly lower than the corresponding percentage of WT-origin monocytes in the blood after 5 months of parabiosis (Fig 3.3b-c). For example, the average percentage of CD45.1+ macrophages in the diaphragm was only 37% compared to 68% of CD45.1+ monocytes in the blood. We normalized the degree of skeletal muscle macrophage donor chimerism to the blood monocyte donor chimerism level. If this normalized macrophage chimerism level reaches 100% it suggests that all of the skeletal muscle macrophages are derived from blood monocytes<sup>160</sup>. This was not the case and the analysis of several muscles (diaphragm, tibialis anterior, soleus) suggested that only about 55-60% of the intramuscular macrophage pool could be accounted for by blood monocytes originating from the adult bone marrow (Fig 3.3d). Therefore, the findings from the parabiosis and fate mapping models both point to the existence of a population of

monocyte-independent resident macrophages, which appear to comprise approximately 30-40% of the overall steady-state macrophage pool and be stably maintained in healthy skeletal muscle during adulthood.

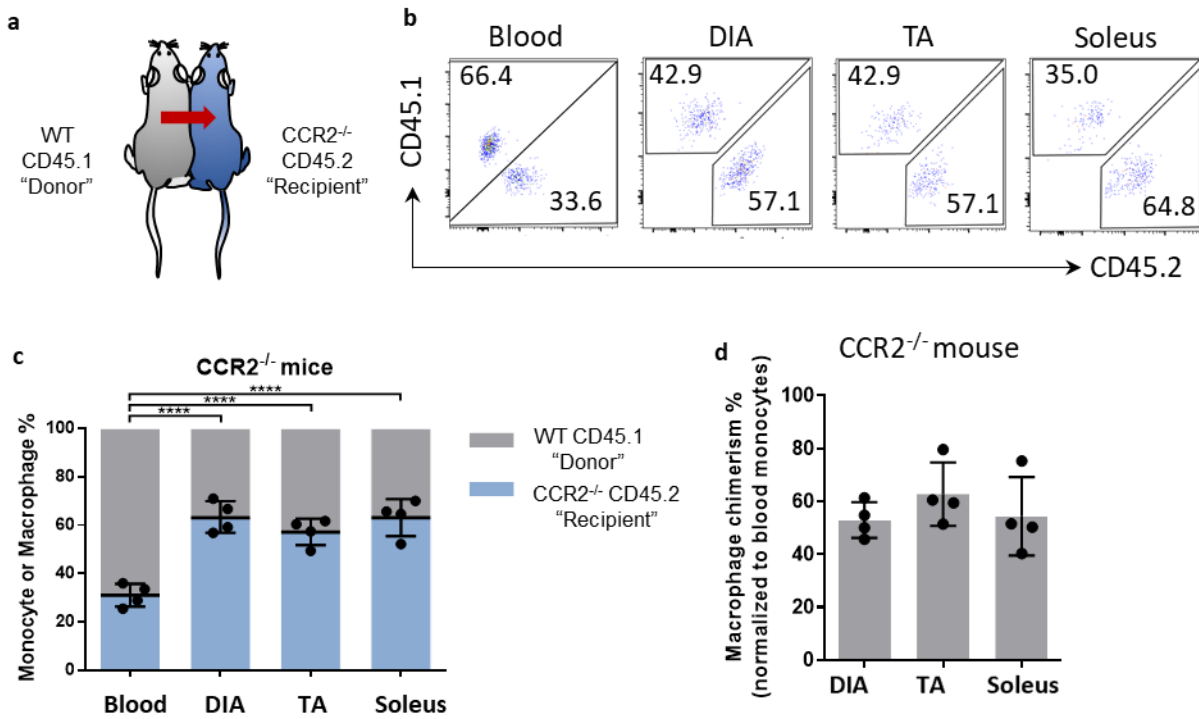


**Figure 3.3. Parabiosis confirms the presence of a major population of bone marrow-independent macrophages in healthy adult muscles**

- Illustration of parabiosis model. The wild-type (WT) CD45.1 mouse acts as a de facto monocyte donor (represented by the arrow) to the CCR2<sup>-/-</sup> CD45.2 mouse.
- Representative FACS plots after 5 months of parabiosis showing the relative percentages of CD45.1+ "donor" and CD45.2+ "recipient" monocytes or macrophages in the blood, diaphragm (DIA), tibialis anterior (TA), and soleus muscles of CCR2<sup>-/-</sup> mice.
- Group mean data are shown for the relative percentages of CD45.1+ and CD45.2+ monocytes or macrophages in the blood, diaphragm (DIA), tibialis anterior (TA), and soleus muscles in CCR2<sup>-/-</sup> mice after 5 months of parabiosis (n=4 parabioc pairing).
- The normalized macrophage chimerism level in CCR2<sup>-/-</sup> mice was calculated by dividing the percentage of WT CD45.1+ macrophages by the percentage of WT CD45.1+ blood monocytes.

It has been suggested that CCR2 is primarily expressed in adult bone marrow-dependent macrophages, whereas TIM4 expression may be more prominent in the bone marrow-independent macrophage population. In postnatal muscles of CX3CR1<sup>CreER-YFP</sup> / R26Td mice, flow cytometry detected significantly more TIM4<sup>+</sup> and fewer CCR2<sup>+</sup> macrophages among the TdTomato<sup>+</sup> population at both 5 weeks (Fig 3.4a) and 9 weeks (Fig 3.4b) of age. Furthermore, in the parabiosis experiments approximately 80% of CD45.2 macrophages in the diaphragms of CCR2<sup>-/-</sup> mice were TIM4<sup>+</sup>, as compared to only 20% of the CD45.1 macrophages originating from the WT parabiont monocytes (Fig 3.4c). To determine the relative proliferation rates of CCR2<sup>+</sup> and TIM4<sup>+</sup> macrophages in the postnatal diaphragm, we conducted daily injections of BrdU for 28 days starting at 4 weeks of age. At 24 hours after BrdU cessation, significantly lower BrdU incorporation was observed among TIM4<sup>+</sup> / CCR2-negative macrophages in comparison to other groups (Fig 3.4d). These findings support the idea that in healthy adult skeletal muscle, CCR2 and TIM4 show a general tendency to be preferentially expressed in monocyte-dependent and monocyte-independent macrophages, respectively. In addition, the data suggest that the putative monocyte-independent macrophage population (TIM4<sup>+</sup>, CCR2-negative) has a lower proliferation rate than the monocyte-derived macrophages.

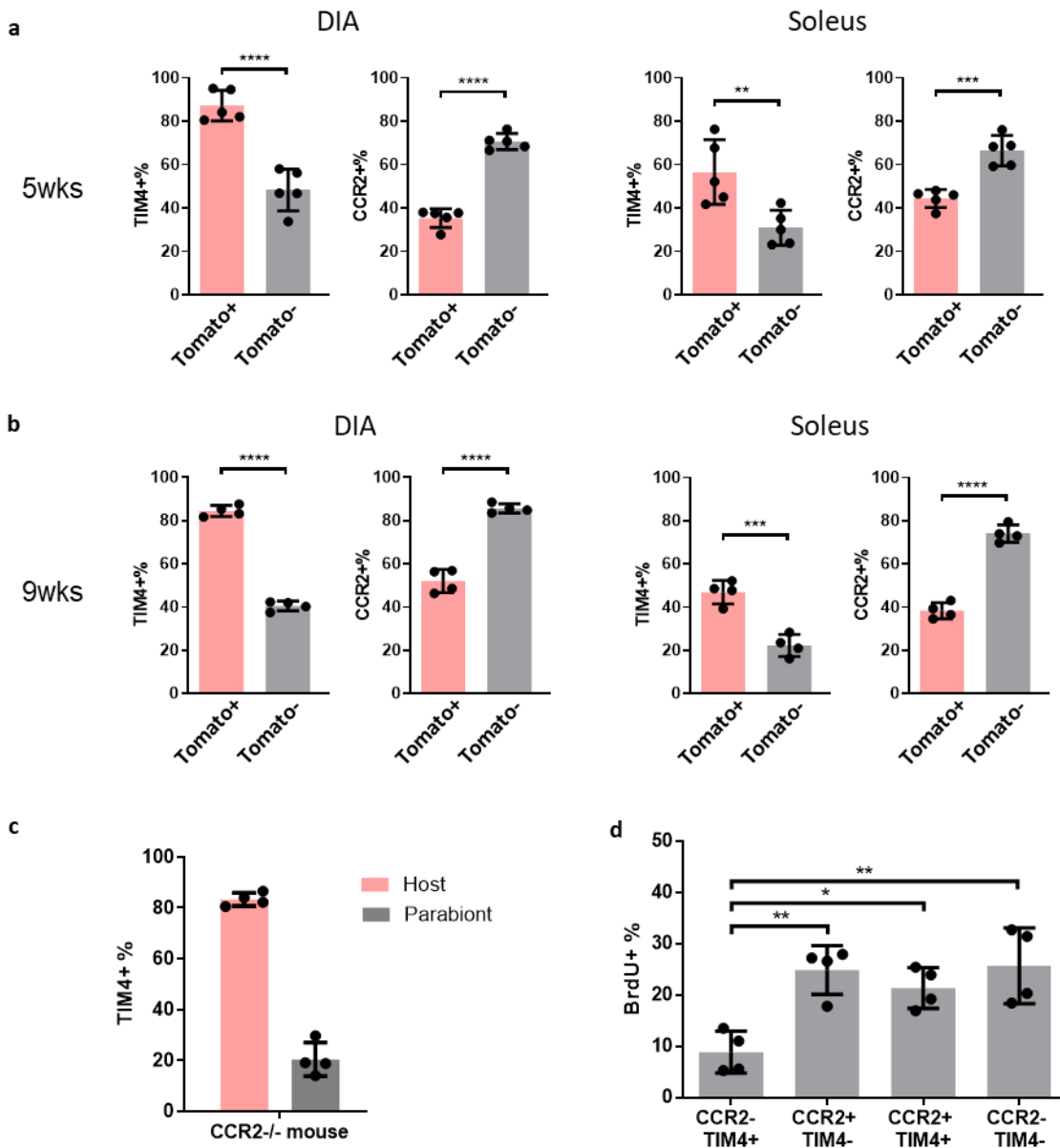


**Figure 3.4. Phenotypic markers and proliferation rates of bone marrow-dependent versus bone marrow-independent macrophages in healthy adult muscles**

- In postnatal CX3CR1<sup>CreER-YFP</sup> / R26Td mice exposed prenatally to tamoxifen at E18.5, flow cytometry was used to quantify the percentages of TIM4<sup>+</sup> and CCR2<sup>+</sup> cells within the TdTomato<sup>+</sup> and TdTomato<sup>-</sup> macrophage populations of the diaphragm (DIA) and soleus at 5 weeks of age (n=5).
- Using the same approach as (a), the percentages of TIM4<sup>+</sup> and CCR2<sup>+</sup> cells within the TdTomato<sup>+</sup> and TdTomato<sup>-</sup> macrophage populations of adult mice are shown at 9 weeks of age (n=4).
- Comparison of the percentage of TIM4<sup>+</sup> macrophages in the diaphragm originating from either the “host” CD45.2 CCR2<sup>-/-</sup> mouse or the “donor” CD45.1 WT parabiont in the CCR2<sup>-/-</sup> mouse after 5 months of parabiosis (n=4 parabiotic pairings).

- d. At 8 weeks of age, cellular proliferation rates (% BrdU incorporation) are shown for diaphragm macrophages having different patterns of TIM4 and CCR2 expression as determined by flow cytometry (n=4/group).

### **3.4.2 Skeletal Muscle Macrophages in DMD (mdx) Mice Are Almost Entirely Bone Marrow (Monocyte)-Dependent**

We next sought to determine the predominant source and phenotypic features of macrophages in a chronic skeletal muscle disease that is characterized by repetitive skeletal muscle injury. Mdx mice share the same genetic defect as patients affected by DMD, and the mdx diaphragm closely resembles the human disease in demonstrating early muscle fiber necrosis which evolves into extensive fibrosis. Therefore, we conducted a comparative analysis of macrophage numbers in the diaphragms of dystrophic mdx-CX3CR1(GFP)+ versus healthy control WT-CX3CR1(GFP)+ mice, starting shortly after birth and continuing up until about 6 months of age (Fig 3.5a-b). At birth, the absolute number of macrophages in the diaphragm did not differ between WT and mdx mice. However, starting from the onset of necrosis at approximately 3 weeks old, the number of macrophages increased dramatically in the mdx group and remained greatly elevated out to at least 23 weeks of age. We next compared the time course of expression for the putative markers of macrophage origin (CCR2, TIM4) as well as other commonly employed phenotypic markers (Ly6C, MHC2, LYVE1) of monocytes and macrophages (Fig 3.5c-g). There were pronounced differences in CCR2 positivity on the first day after birth, with nearly 100% CCR2+ macrophages in the mdx diaphragm compared to less than 20% in the WT group. The percentage of CCR2+ macrophages in WT and mdx muscles gradually converged at a level of approximately 65% in both groups by 13-16 weeks of age. A significantly higher percentage of TIM4+ macrophages was found in the mdx diaphragm from postnatal day 1 until 4-6 weeks of age, but this pattern was then reversed by 13-16 weeks of age with greater TIM4 positivity in the WT group. Ly6C and MHC2 showed very similar patterns in the WT and mdx groups, both being expressed at low levels shortly after birth and then rising rapidly during the first 4-6 weeks of age. LYVE1+ macrophages did not

differ during the first 6 weeks but were more prevalent in the WT group by 13-16 weeks.

To definitively establish whether bone marrow-dependent or bone marrow-independent macrophages are primarily responsible for the increased macrophage numbers found in dystrophic muscles, we employed a chimeric mdx mouse model in which donor bone marrow from WT (CD45.1) mice was transplanted into irradiated 6-week-old mdx or WT host recipient mice (CD45.2). The diaphragm was shielded with a lead bar during the irradiation procedure in order to preserve and protect the local intramuscular macrophage microenvironment from radiation effects, and a subset of mice also received a single dose of busulfan (given the day prior to bone marrow transplantation) to eliminate any residual host bone marrow protected by the shielding (Fig 3.5h). At 14 weeks of age, we compared the donor chimerism levels of blood monocytes and diaphragm macrophages (Fig 3.5i). In WT recipients, the percentage of donor monocytes in the blood was significantly higher than the corresponding percentage of donor macrophages in the diaphragm. This is consistent with the presence of a monocyte-independent macrophage population in healthy adult skeletal muscle as indicated by our earlier fate mapping and parabiosis experiments. Normalizing the donor chimerism of macrophages in the WT diaphragm to the level of blood monocyte chimerism indicated that on average approximately 69% of the intramuscular macrophages could be attributed to a bone marrow-dependent source (Fig 3.5j). In contrast, for the mdx recipient mice the percentage of donor macrophages in the diseased diaphragm closely matched that of donor monocytes in the blood. Accordingly, the normalized macrophage chimerism level in the mdx diaphragm approached nearly 100%, and this was true either with or without the use of busulfan (Fig 3.5i-j). Furthermore, in the mdx group there was a significant reduction in the absolute number of host origin macrophages in the diaphragm (Fig 3.5k).

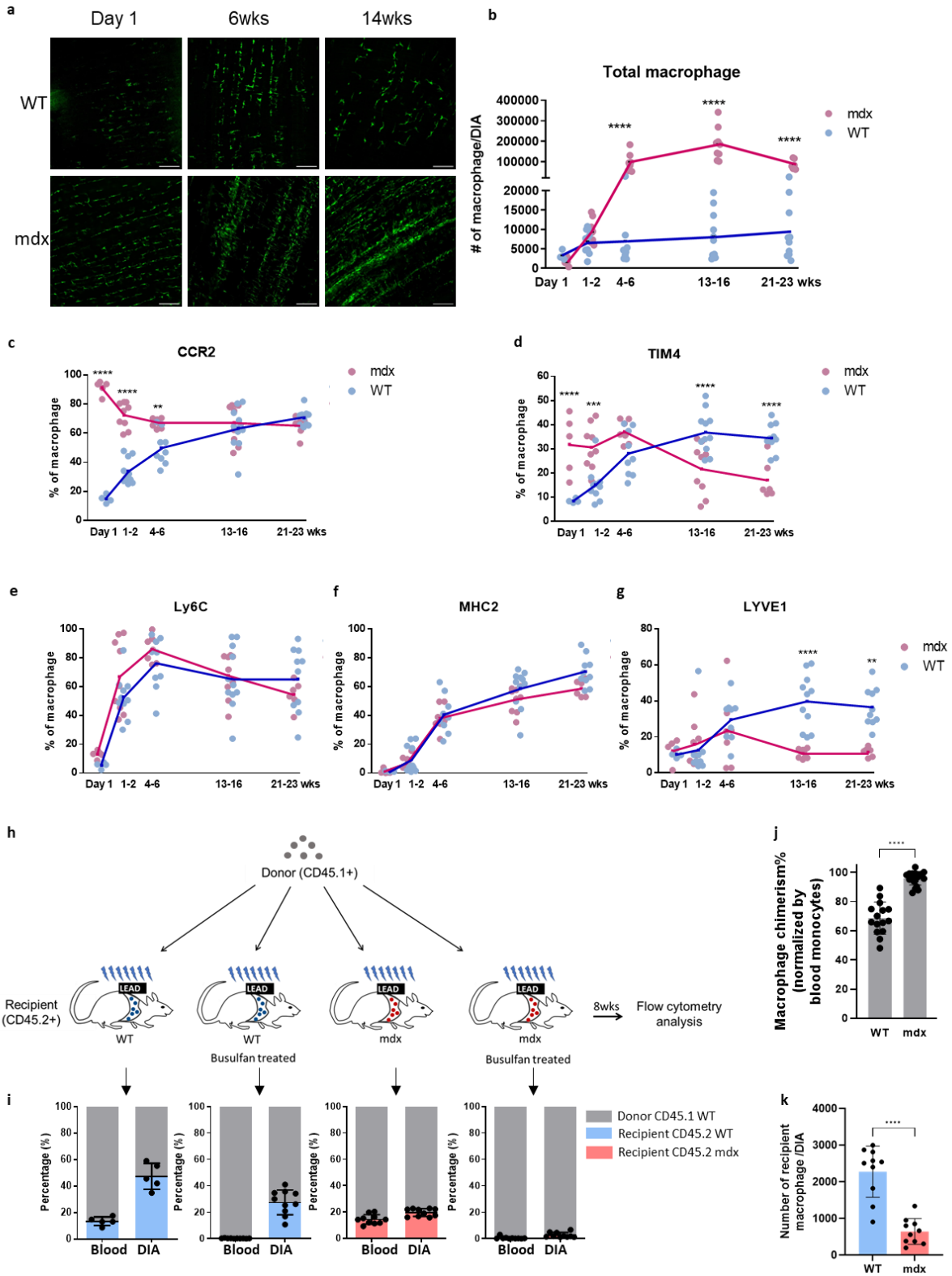


**Figure 3.5. Postnatal monocytes originating from the bone marrow account for almost the entire skeletal muscle macrophage population in adult dystrophic (mdx) mice**

- a. Representative confocal fluorescence images of WT-CX3CR1 (GFP+) and mdx-CX3CR1 (GFP+) diaphragms at the indicated ages are shown (n=4-11/group). The scale bar is 100µm.
- b. Total macrophage cell numbers in the entire diaphragm of WT-CX3CR1 (GFP+) and mdx-CX3CR1 (GFP+) mice at the indicated ages are shown (n=4-11/group).
- c. - g. Post-natal time course for the expression of CCR2, TIM4, Ly6C, MHC2, and LYVE1 in WT versus mdx diaphragm macrophages as determined by flow cytometry.
- h. Schematic illustration of the chimeric mouse model with diaphragm shielding, in which donor bone marrow from 6-week old CD45.1 WT mice was transplanted into 6-week old recipient CD45.2 WT or mdx mice, either with or without pre-treatment with busulfan. The mice were analyzed at 8 weeks after bone marrow transplantation.
- i. Group mean data showing the relative percentages of blood monocytes versus diaphragm (DIA) macrophages that are either of bone marrow donor (CD45.1+) or bone marrow recipient (CD45.2+) origin (n=4-10/group).
- j. The normalized macrophage chimerism level was calculated by dividing the percentage of WT CD45.1+ macrophages in the diaphragm by the percentage of WT CD45.1+ blood monocytes.
- k. Absolute numbers of host origin resident macrophages found in the diaphragms of WT versus mdx mice.

Overall, the above data demonstrate that although the absolute numbers of macrophages in the diaphragm are similar in WT and mdx mice at birth, dystrophic muscle macrophages exhibit complex phenotypic alterations from the first day of birth onward. In particular, there are simultaneous and pronounced elevations of both CCR2 and TIM4 expression in mdx macrophages well before the onset of muscle necrosis and the associated massive influx of macrophages. In addition, these findings indicate that the macrophages in adult dystrophic muscle are almost entirely derived postnatally from the bone marrow due to a combination of increased monocyte recruitment and concomitant loss of the steady-state resident population found in healthy muscle.

### **3.4.3. Transcriptional Phenotype of Bone Marrow-Dependent Macrophages in Skeletal Muscle Is Dictated by the Host Environment**

Given that the vast majority of macrophages in the dystrophic muscle are monocyte-derived, we next sought to determine how the dystrophic disease environment influences monocyte-dependent macrophages. Specifically, we wished to ascertain whether monocyte-derived macrophages from healthy mice would adopt a phenotype resembling mdx mice when recruited into the dystrophic muscle environment. Conversely, we also assessed the influence of the WT microenvironment on the phenotype of monocyte-dependent macrophages derived from mdx mice. Bone marrow from WT-CX3CR1(GFP)<sup>+</sup> or mdx-CX3CR1(GFP)<sup>+</sup> mice was transplanted into either WT or mdx recipient mice (Fig 3.6a). Flow cytometry was used to determine the percentage of bone marrow-derived donor macrophages (GFP<sup>+</sup>) which expressed prototypical pro-inflammatory (IL-1 $\beta$ , iNOS) or anti-inflammatory (IL-10, CD206) markers (Fig 3.6b). The percentages of IL-1 $\beta$ <sup>+</sup>, iNOS<sup>+</sup> and IL-10<sup>+</sup> bone marrow-derived macrophages were all similarly increased in mdx recipient mice, irrespective of whether the donor bone marrow source was WT or mdx. In addition, the percentage of CD206<sup>+</sup> macrophages was significantly reduced in the mdx recipients of WT donor bone marrow. Overall, when different sources of bone marrow were compared in the same recipient mouse strain (either WT or mdx), no significant differences were detected. These results suggest that the inflammatory phenotype of bone marrow-derived macrophages in skeletal muscle is primarily shaped by the host environment rather than being intrinsic to the bone marrow donor source of these cells.

To further delineate the specific impact of the dystrophic environment on bone marrow-dependent macrophages, we next transplanted bone marrow from healthy WT (CD45.1) mice into either WT (CD45.2) or mdx (CD45.2) recipients (Fig 3.6c). At 8 weeks after transplantation, we employed

FACS to collect CD45.1 macrophages from the diaphragm and performed bulk RNA-seq analysis on these cells. Despite having been transplanted with the same bone marrow obtained from healthy mice, UMAP analysis of differentially expressed genes (DEGs) revealed a clear separation between the diaphragm macrophages in WT and mdx recipients (Fig 3.6d). We identified 513 DEGs (for complete list see Supplemental Table 2.1) as illustrated on the heatmap (Fig 3.6e) and volcano plots (Fig 3.6f-g). The upregulated genes in the mdx group which were among the top 50 hits with respect to both log<sub>2</sub> Fold Change (FC) and P values were (from highest to lowest fold-change): Cd300lf, Lhfp12, Fabp5, Vegfa, Olfml3, Basp1, Parvg, Fam46c, Slfn4, Ms4a4c, Havcr2, LOC108167440, Clec4n, Ncapg2, Ctsd, Lgals3. The downregulated genes in the mdx group which met these criteria were (from highest to lowest fold-change): Aldh1a2, Retnla, Cd226, Hr, Gfra2, Mmp9, Fgfr1, Fcna, Lyve1, Gprc5b, Cd163, Mrvi1, Lyz1, Cd209a, Cd2, Ccl24, Tmod1, Cxcl12, Tppp, Ednrb, Aqp1, Myh11, Dpysl3, Jup, Rcn3, Ltc4s, Adgrf5, Gypc, Ptk2, Cdr2.

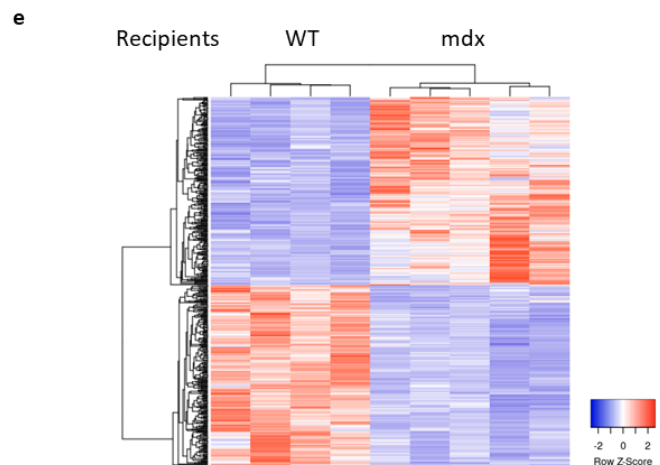
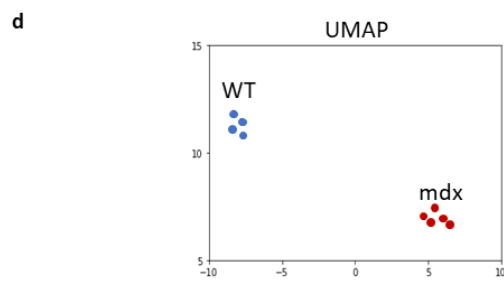
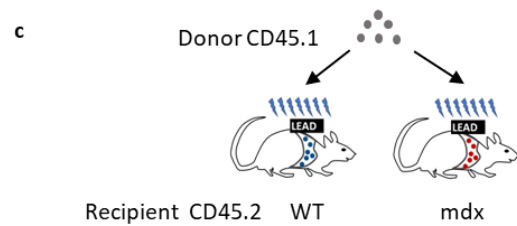
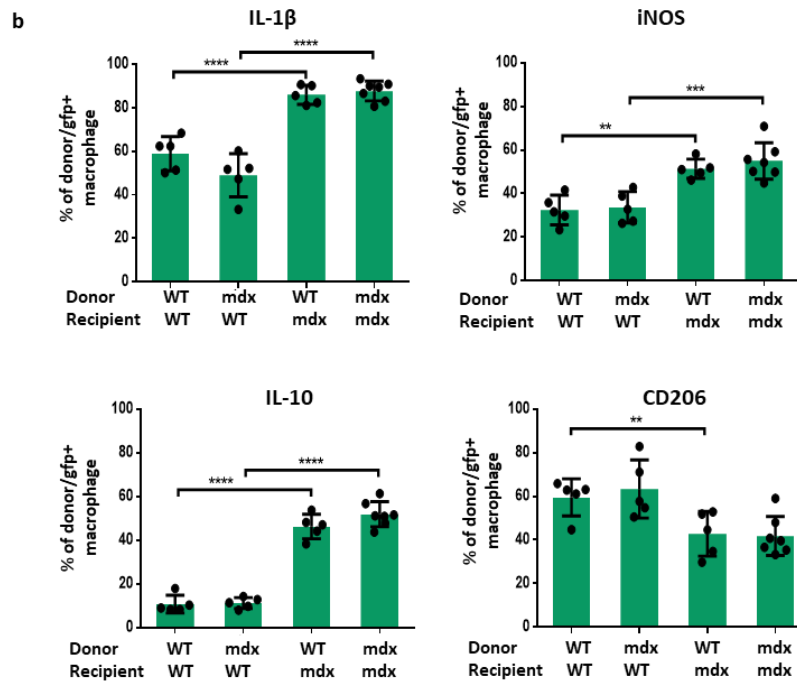
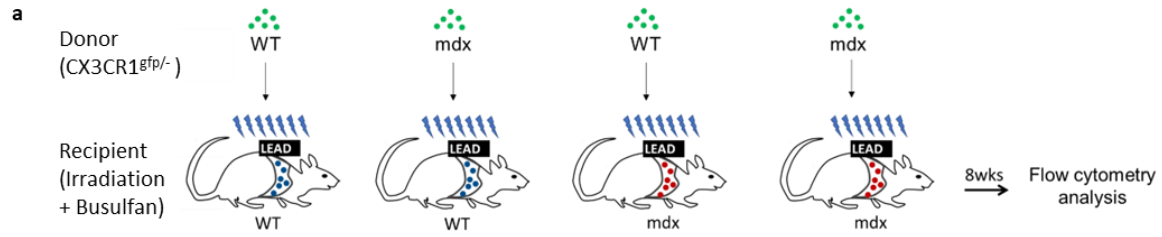




**Figure 3.6. Impact of the host muscle environment on the inflammatory phenotype and gene expression profile of bone marrow (monocyte)-dependent macrophages**

- a. Schematic illustration of the chimeric mouse model in which donor bone marrow from 6 week old WT-CX3CR1 (GFP+) or mdx-CX3CR1 (GFP+) mice was transplanted into 6 week old recipient non-transgenic WT or mdx mice. All mice were analyzed at 8 weeks after bone marrow transplantation.
- b. In the different chimeric mice groups depicted in (a), the percentages of GFP+ monocyte-derived diaphragm macrophages expressing IL-1b, NOS2 (iNOS), IL-10, and CD206 were determined by flow cytometry. (n=5-7/group)
- c. Schematic illustration of the chimeric mouse model in which donor bone marrow from 6-week old CD45.1 WT mice was transplanted into 6-week old recipient CD45.2 WT or mdx mice. Diaphragm macrophages were harvested for RNA-seq analysis at 8 weeks after bone marrow transplantation.
- d. UMAP plot analysis of RNA-seq data from (c) indicates distinct clustering patterns for the WT bone marrow-derived macrophages which were placed into either the WT or mdx host recipient environment.
- e. Heatmap (Z-score) depicting the clusters of differentially expressed genes (DEGs) in WT and mdx macrophages. The heatmap includes 262 up-regulated genes and 251 down-regulated genes based on  $\log_2$  Fold Change (FC) > 1 and adjusted P-value (padj) < 0.05. (WT n=4, mdx n=5)
- f. Volcano plot depicting the hierarchical distribution of  $\log_2$ FC (x-axis) and P values (y-axis) for the same DEGs. The top 15 genes are labeled based on the highest  $\log_2$ FC values.
- g. Identical volcano plot to (f) labeled with the top 15 genes based on the lowest P values.

#### **3.4.4. Potential Biological Pathways and Transcription Factors Driving Macrophage Responses to the Dystrophic Host Environment**

To gain additional insights into the functional impact of DEGs in the mdx group, biological pathway analysis was performed using the Gene Ontology (GO) enrichment and Reactome informatics databases. Among the 262 genes that were upregulated in the mdx group, there was a notable enrichment of pathways associated with macrophage function (migration, phagocytosis), innate immune system activation, extracellular matrix biology (including integrin interactions and collagen metabolism), and the defense response to viruses including interferon signaling (Fig 3.7a). Among the 251 genes that were downregulated in the mdx group, the most prominent enrichment was for biological pathways linked to cell migration, angiogenesis, hemostatic functions, and smooth muscle contraction (Fig 3.7b).

We next sought to explore the underlying regulatory mechanisms which drive the differential gene expression observed in bone marrow-derived macrophages recruited to the dystrophic muscle environment. To this end we performed HOMER motif analysis of DNA regulatory elements within gene promoter regions to identify candidate transcription factors which could potentially govern these changes. We first assessed known transcription factor binding sites and found 8 motifs that were significantly enriched (Fig 3.7c). It is noteworthy that 7 of these 8 motifs are associated with transcription factors of the interferon regulatory factor (IRF) family. In addition, 3 de novo motifs were identified which are also potential targets for different transcription factors of the IRF, RUNX, STAT, and SMAD families (Fig 3.7d). The same analysis applied to the downregulated genes revealed only one de novo motif which best matched with the OSR2 transcription factor (Fig 3.7e).

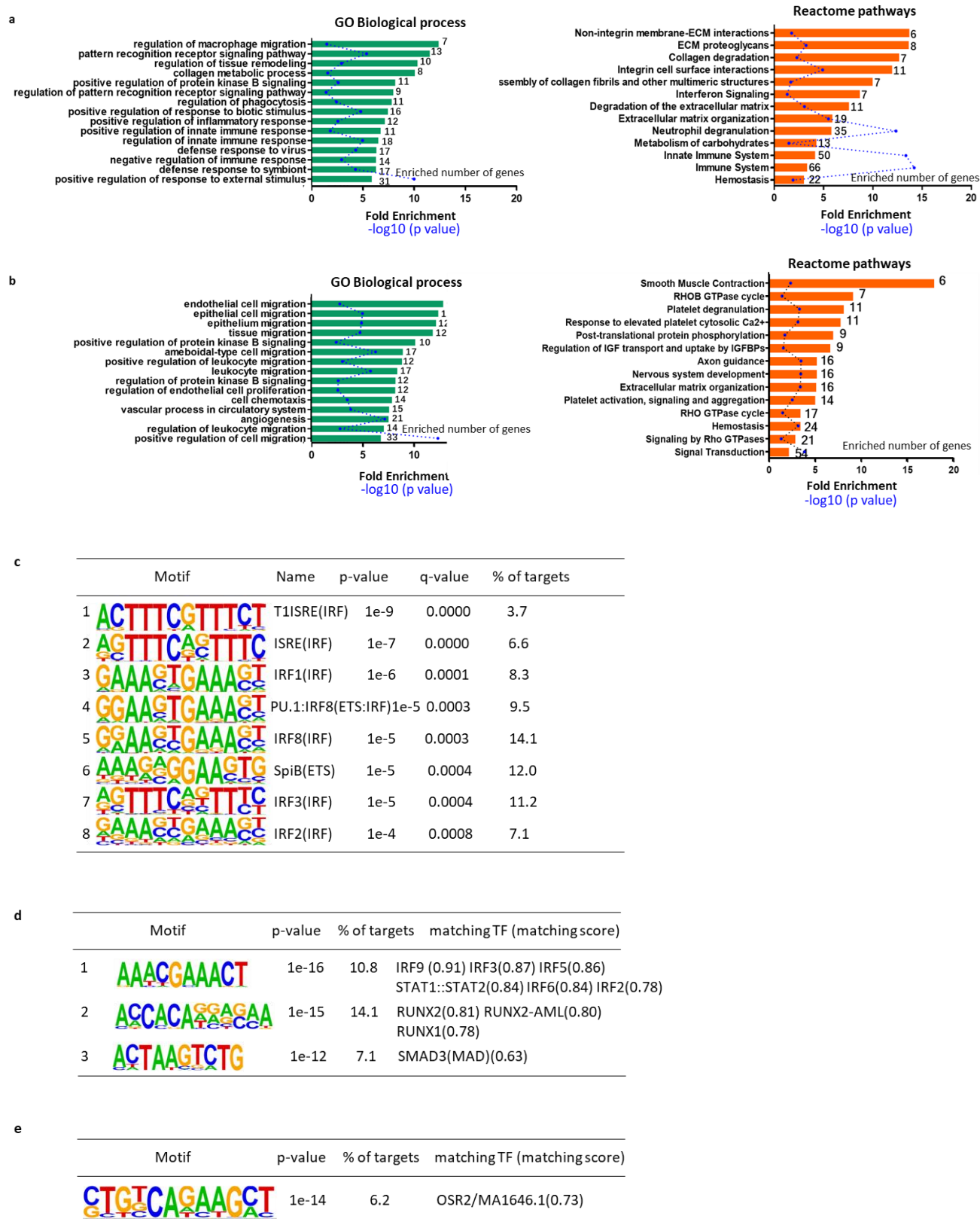


**Figure 3.7. Biological pathway enrichment and transcription factor motif analysis**

- a. Biological pathway enrichment analysis was performed for the upregulated DEGs found in bone marrow-derived macrophages of WT origin placed into mdx host recipients. The top 15 enrichment categories are shown based upon both the Gene Ontology (left panel) and Reactome (right panel) databases. For each enrichment category listed in the figure: the bar graph represents the magnitude of enrichment, the adjacent number indicates how many DEGs fell into this category, and the dotted blue line depicts the P value.
- b. An identical biological pathway enrichment analysis as described in (a) was performed for the downregulated DEGs.
- c. HOMER motif analysis was conducted on the promoter regions of genes that were upregulated in bone marrow-derived macrophages of WT origin placed into mdx host recipients. Eight known motifs were identified as being enriched (Q-value <0.001) as shown in the figure. The table shows the sequence logo, name and family of the motif, p-value, q-value (Benjamini correction for multiple testing) and % of target sequences with the motif.
- d. HOMER motif analysis of upregulated genes suggested 3 de novo motifs (p-value <1e-12) as putative targets for the transcription factors listed in the figure. The sequence logo, p-value, percentage of target sequences with motif and matching transcription factor with a matching score (range 0-1) > 0.6 is shown in the table.
- e. HOMER motif analysis conducted on the promoter regions of downregulated genes suggested a single de novo motif as a putative transcription factor target.

### 3.5. Discussion

In the present study we used a combination of fate mapping, parabiosis and chimeric mouse models to discern the ontogeny of skeletal muscle macrophages and the factors driving their phenotype in the mdx mouse model of DMD. We focused our study on the diaphragm due to its essential role in survival and the fact that the severity of its involvement in mdx mice closely resembles the pathology found in human DMD<sup>107</sup>. Specifically, we sought to determine if the balance between embryonically-derived macrophages and monocyte-derived macrophages in the diaphragm differs between healthy and dystrophic mice. We also wondered whether macrophages derived from healthy mice would adopt a phenotype akin to that seen in mdx mice when recruited into the dystrophic environment. Furthermore, by comparing differential gene expression patterns and their associated biological pathways under these conditions, we hoped to identify the very early alterations in macrophage phenotype which are induced by exposure to the dystrophic milieu. The elucidation of these early changes, as well as the dominant transcriptional regulators which are responsible for pathological reprogramming of macrophages, could help to identify promising targets for the future treatment of patients affected with DMD.

The main findings of our study can be summarized as follows. First, our fate mapping, parabiosis, and chimeric mouse studies all suggest that 30-40% of the resident macrophage pool in the normal diaphragm is independent of the adult bone marrow and instead derived prenatally from the embryo. Second, the prenatal origin resident macrophages found in normal adult diaphragm arise primarily from the fetal liver with a lesser contribution from the embryonic yolk sac; these prenatal origin macrophages preferentially express TIM4 whereas the postnatal bone marrow-derived macrophages demonstrate more prevalent expression of CCR2. Third, in mdx mice the macrophage phenotype in the diaphragm is profoundly altered from the first day of postnatal life

with more prevalent expression of both TIM4 and CCR2; remarkably, this occurs many days prior to the appearance of either muscle necrosis or increased macrophage infiltration. Fourth, once the process of muscle necrosis has begun almost all macrophages in the mdx diaphragm are derived from the adult bone marrow, which is due not only to increased monocyte recruitment but also to depletion of the prenatal origin resident macrophage population. Finally, the dystrophic disease environment plays an overwhelmingly dominant role in dictating the phenotype of these bone marrow origin macrophages, which demonstrate an exaggerated signature for the interferon pathway amongst many other innate immune genes.

We employed the CX3CR1<sup>CreER-YFP</sup>:R26-TdTomato model to track the embryonic origin of muscle macrophages. This model has been employed to fate map the origin of macrophages in the brain<sup>141</sup>, liver, lung, spleen, and peritoneal<sup>144 307 167</sup> due to the high expression of CX3CR1 on macrophages and macrophage precursor MDPs during prenatal development<sup>308</sup>. We successfully labelled a small fraction (20-25%) of diaphragmatic macrophages at E7.5 (indicating their yolk sac origin) and approximately 75% at E13.5 (indicating the fetal liver origin). To determine whether prenatal muscle macrophages persist into adulthood, we also labelled the majority of these macrophages just before birth (at E18.5) and confirmed their persistence at a stable level between 5 and 9 weeks of age. One limitation of this model in adult mice is the presence of leaky TdTomato expression in mice that were not exposed to tamoxifen prenatally, which has also been reported in cardiac muscle macrophages<sup>167</sup>. However, even if one assumes that all of these “false positive” macrophages were of postnatal bone marrow origin, the remaining “true positive” macrophages of prenatal origin still amounted to 30-40% of the resident macrophage population of adult muscles (diaphragm and soleus). The parabiosis and diaphragm-shielded chimeric mouse studies also indicated that 30-40% of the resident macrophage pool in adult skeletal muscle is bone marrow-

independent. To our knowledge, only one previous study has performed a detailed examination of macrophage ontogeny in skeletal muscle using a different fate mapping model (*Flt3<sup>Cre</sup> R26<sup>LSL-YFP</sup>* mice) and came to a similar conclusion<sup>186</sup>.

TIM4 functions as a phosphatidylserine receptor expressed on macrophages, facilitating the binding and phagocytosis of apoptotic cells<sup>309 310</sup>. TIM4 has been proposed as a marker for identifying embryo-derived macrophages in adipose tissue<sup>300</sup>, the heart<sup>311 167</sup>, and in skeletal muscle<sup>301</sup>. In keeping with this notion, we found that over 80% of TdTomato+ macrophages in the adult diaphragm at 9 weeks of age expressed TIM4. However, the percentage of TIM4+ macrophages found in normal diaphragm on the first day after birth was less than 10%, which is consistent with a relatively low gene expression level in the limb muscle at a similar age<sup>312</sup>. Accordingly, there appears to be a major increase in TIM4 expression from the newborn period to adulthood. In addition, while almost 90% of TdTomato-negative (presumed to be bone marrow-derived) macrophages expressed CCR2 in the diaphragm at 9 weeks of age, a substantial proportion of these macrophages also exhibited TIM4 expression. Therefore, the ability of TIM4 and CCR2 to reliably distinguish between embryo-derived and adult bone marrow-derived macrophages, respectively, is called into question by our findings. The situation is even more complex in the mdx diaphragm, where on the first postnatal day both CCR2+ (approximately 95%) and TIM4+ (approximately 30%) macrophages are significantly more prevalent than in healthy diaphragm muscle. This very high percentage of CCR2+ macrophages at such an early time point, which precedes the onset of histologically detectable muscle damage, suggests that an immunological response to the disease may have been initiated in utero or triggered by the sudden transition to breathing air. It is also possible that these CCR2+ macrophages in neonatal mdx mice, which are almost certainly embryo-derived at this very early age, play a role in signaling the bone

marrow to deliver monocytes to the dystrophic muscle. A similar mechanism was previously described in non-dystrophic skeletal muscle subjected to acute injury<sup>187</sup>.

In the previous chapter we described the development of a diaphragm shielding model to study the dynamics of bone marrow-dependent versus bone marrow-independent macrophages in the diaphragm following acute muscle injury. In the current study, we modified this model by administering busulfan to eliminate the residual host bone marrow protected by the shielding, thus allowing us to unambiguously distinguish between the bone marrow-dependent and bone marrow-independent macrophage populations. It should be noted that the half-life of busulfan is 2-3 hours and the drug was administered 18 hours before the donor bone marrow transplantation. In the present study we demonstrate for the first time that the macrophage population within adult mdx muscle is almost exclusively composed of bone marrow origin macrophages derived from blood monocytes. This finding was robustly observed irrespective of whether or not the mice had received busulfan as part of the bone marrow transplant pre-conditioning regimen. In addition, the overwhelmingly increased proportion of bone marrow-derived macrophages was not only due to their increased recruitment, since the absolute number of bone marrow-independent macrophages was also decreased in the mdx diaphragm. This decrease of embryo-derived macrophages could help to explain the decreased percentages of TIM4<sup>+</sup> and LYVE1<sup>+</sup> macrophages in the mdx diaphragm over time. A similar observation has been made in a model of chronic liver inflammation (NASH), in which a marked decline in TIM4<sup>+</sup> Kupffer cells occurs and is followed by their replacement with monocyte-derived CCR2<sup>+</sup> macrophages<sup>313</sup>. The diminished presence of bone marrow-independent macrophages might be due to decreased local proliferation leading to an impairment of self-renewal, or a heightened level of cell death<sup>154</sup>. The mdx milieu is characterized by elevated levels of reactive oxygen species and inflammatory cytokines, both of

which can potentially result in cell senescence or cell cycle arrest.

The results of this study clearly indicate the profound impact of the dystrophic environment on the molecular profile of bone marrow-dependent macrophages. Our group has previously reported that the mdx environment can alter the transcriptional responsiveness, metabolic profile and epigenetic programming of bone marrow-derived macrophages even prior to their entry into the dystrophic muscle<sup>314</sup>. In the above study, we provided evidence that DAMPs which are systemically released from damaged dystrophic muscles can signal through TLR4 to induce such changes at the level of the bone marrow, which has been referred to as trained immunity<sup>315</sup>. In the current study, it is likely that the altered macrophage phenotype observed in mdx diaphragm macrophages is due to the continuous abnormal signals received at both the systemic (bone marrow) and local (dystrophic muscle) levels.

When previously healthy (WT) bone marrow was transplanted into a dystrophic (mdx) host in the current study, the bone marrow-derived macrophages in the mdx diaphragm rapidly developed a gene expression pattern indicative of innate immune system activation and extracellular matrix (ECM) remodelling. Notably, *Spp1* was at the forefront of differentially expressed genes (DEGs) and is recognized as a genetic modifier of DMD<sup>248</sup>. The protein encoded by this gene, osteopontin, is produced by both myoblasts and macrophages<sup>316</sup>. In the mdx model, osteopontin has been found to enhance the TGF- $\beta$  pathways in fibroblasts, leading to increased collagen deposition and fibrosis<sup>252</sup>. Interestingly, interventions aimed at blocking or depleting osteopontin have shown promise in alleviating mdx pathology<sup>316</sup>. Several other upregulated DEGs connected to the ECM were identified, including *Coll1a1*, *Itgav*, *Vegfa*, *Coll1a2*, *Mmp19*, *Thbs4*, *Postn*, *Can*, *Col6a3*, *Col3a1*, *Mmp14*, *Emilin1*, and *Thbs1*. An upsurge in the expression of ECM-associated genes could signify the body's endeavour to mend damaged muscle tissue. However, excessive or

misdirected ECM deposition could lead to fibrosis, a characteristic trait of DMD pathology.

Fabp5 is another DEG which demonstrated a combination of being among the largest fold-change difference and lowest P value. This protein is primarily involved in transporting long-chain fatty acids within cells, and can be induced by stimuli such as LPS<sup>317</sup>. Notably, Fabp5 expression varies across different macrophage subsets<sup>318</sup>. For instance, its levels rise in macrophages present in inflammatory tissues, which has been associated with promoting inflammatory signaling<sup>317 319 320</sup>. Furthermore, Fabp5 has a role in governing macrophage metabolic pathways. This includes its involvement in PPAR $\gamma$  activation, managing oxidative stress, eicosanoid production, and cholesterol metabolism<sup>321 322 323 324</sup>. However, precisely how Fabp5 influences DMD progression is unknown. Apart from Fabp5, other DEGs linked to lipid metabolism included Plin2, Soat1, Slc27a1, Abcg1, Lpcat2, Pparg, and Ldlrap1. These changes imply altered lipid metabolism which could directly contribute to the distinct metabolic and inflammatory conditions in dystrophic muscles<sup>325 326 327 328 329 330 331 332 333</sup>. The heightened expression of PPAR $\gamma$  hints at a shift of macrophages towards an anti-inflammatory (M2-like) phenotype<sup>334</sup>. Additionally, the amplified expression of lipid metabolism genes may indicate that macrophages are actively involved in clearing lipid debris.

The Homer motif analysis revealed that the IRF family of transcription factors may play an important role in orchestrating the inflammatory response in DMD. IRFs undergo homo- or heterodimerization upon phosphorylation, facilitating their nuclear translocation and subsequent promotion of target gene transcription<sup>335</sup>, and are critical for host defence against viruses and bacteria. However, aberrant IRF activation has also been implicated in autoimmune diseases outside of infectious contexts. In conditions like psoriasis, a subset of IRF-regulated genes remains perpetually active, propelling skin inflammation<sup>336 337</sup>. Systemic Lupus Erythematosus (SLE)

presents another example where heightened signalling, especially from IRF5 and IRF7, leads to a pronounced surge in type I interferons and their downstream genes. This pattern, known as the "interferon signature" aligns with disease severity<sup>338</sup>. In the realm of dystrophic muscle research, the study of IRFs and type I interferon remains scant. Notably, one investigation highlighted the enrichment of IRF1 in upregulated DEGs from muscle biopsies of young patients affected with DMD<sup>339</sup>. In addition, IFN- $\gamma$  impedes the macrophage M1 to M2 transition and serves as a myogenic inhibitor in mdx mice<sup>235</sup>. This cytokine indirectly modulates the expression and/or activity of specific IRFs, with IRF1, IRF7, and IRF8 notably inducible by IFN- $\gamma$ <sup>335</sup>.

In situations of sterile inflammation, IRFs can be triggered by cellular sensors, including cyclic GMP-AMP synthase (cGAS), RIG-I, and TLRs, activated by DAMPs<sup>340 341 342</sup>. Activation of these sensors propels signaling cascades, culminating in the activation of select IRFs, particularly IRF3 and IRF7<sup>343</sup>. Furthermore, type I interferon-driven signaling can activate IRF1, IRF7, IRF8, and IRF9<sup>344 345</sup>. This intricate signaling network, starting with the engagement of specific receptors to adaptor proteins, orchestrates the recruitment and activation of kinases like TBK1 and IKK $\epsilon$ , which in turn phosphorylate specific IRFs. Beyond this, signaling through MyD88 activates IRF5, and pathways involving TRAF6 can prompt IRF8 activation.

Targeting IRF pathways offers the potential to mitigate the macrophage-induced inflammatory responses observed in DMD. One strategy is inhibiting upstream activators like kinases TBK1 and IKK $\epsilon$ , attenuating IRF activation. Another avenue is inhibiting receptors like TLRs and RIG-I. Compounds like resveratrol can thwart IRF phosphorylation by targeting these kinases. Further research is needed to determine whether more specific inhibitors can be designed to interfere with IRF function in DMD.

### References for Chapter 3

9. Tidball JG. Regulation of muscle growth and regeneration by the immune system. *Nat Rev Immunol*. 2017;17(3):165-178. doi:10.1038/nri.2016.150
107. Stedman HH, Sweeney HL, Shrager JB, et al. The mdx mouse diaphragm reproduces the degenerative changes of Duchenne muscular dystrophy. *Nature*. 1991;352(6335):536-539. doi:10.1038/352536a0
141. Ginhoux F, Greter M, Leboeuf M, et al. Fate Mapping Analysis Reveals That Adult Microglia Derive from Primitive Macrophages. *Science (80- )*. 2010;330(6005):841-845. doi:10.1126/science.1194637
144. Yona S, Kim KW, Wolf Y, et al. Fate mapping reveals origins and dynamics of monocytes and tissue macrophages under homeostasis. *Immunity*. 2013;38(1):79-91. doi:10.1016/J.IMMUNI.2012.12.001
154. Heidt T, Courties G, Dutta P, et al. Differential contribution of monocytes to heart macrophages in steady-state and after myocardial infarction. *Circ Res*. 2014;115(2):284-295. doi:10.1161/CIRCRESAHA.115.303567
164. Hashimoto D, Chow A, Noizat C, et al. Tissue-resident macrophages self-maintain locally throughout adult life with minimal contribution from circulating monocytes. *Immunity*. 2013;38(4):792-804. doi:10.1016/j.immuni.2013.04.004
167. Dick SA, Macklin JA, Nejat S, et al. Self-renewing resident cardiac macrophages limit adverse remodeling following myocardial infarction. *Nat Immunol* /. 2019;20:29-39. doi:10.1038/s41590-018-0272-2
186. Wang X, Sathe AA, Smith GR, et al. Heterogeneous origins and functions of mouse skeletal muscle-resident macrophages. *Proc Natl Acad Sci U S A*. 2020;117(34):20729-20740. doi:10.1073/PNAS.1915950117
187. Brigitte M, Schilte C, Plonquet A, et al. Muscle resident macrophages control the immune cell reaction in a mouse model of notexin-induced myoinjury. *Arthritis Rheum*. 2010;62(1):268-279. doi:10.1002/art.27183
235. Villalta SA, Deng B, Rinaldi C, Wehling-Henricks M, Tidball JG. IFN- $\gamma$  Promotes Muscle Damage in the mdx Mouse Model of Duchenne Muscular Dystrophy by Suppressing M2 Macrophage Activation and Inhibiting Muscle Cell Proliferation . *J Immunol*. 2011;187(10):5419-5428. doi:10.4049/jimmunol.1101267
248. Pegoraro E, Hoffman EP, Piva L, et al. SPP1 genotype is a determinant of disease severity in Duchenne muscular dystrophy. *Neurology*. 2011;76(3):219-226. doi:10.1212/WNL.0B013E318207AFEB
252. Kramerova I, Kumagai-Cress C, Ermolova N, et al. Spp1 (osteopontin) promotes TGF $\beta$  processing in fibroblasts of dystrophin-deficient muscles through matrix metalloproteinases. *Hum Mol Genet*. 2019;28(20):3431-3442. doi:10.1093/HMG/DDZ181
298. Gomez Perdiguero E, Klapproth K, Schulz C, et al. Tissue-resident macrophages originate from yolk-sac-derived erythro-myeloid progenitors. *Nature*. 2015;518(7540):547-551. doi:10.1038/nature13989
299. Schulz C, Perdiguero EG, Chorro L, et al. A Lineage of Myeloid Cells Independent of Myb and Hematopoietic Stem Cells Christian. *Science (80- )*. 2012;336(6077):86-89. doi:10.1126/science.1213307
300. Félix I, Jokela H, Karhula J, et al. Single-Cell Proteomics Reveals the Defined Heterogeneity of Resident Macrophages in White Adipose Tissue. *Front Immunol*.

- 2021;12(July):1-17. doi:10.3389/fimmu.2021.719979
301. Babaeijandaghi F, Cheng R, Kajabadi N, et al. Metabolic reprogramming of skeletal muscle by resident macrophages points to CSF1R inhibitors as muscular dystrophy therapeutics. *Sci Transl Med.* 2022;14(651). doi:10.1126/scitranslmed.abg7504
  302. Ashburner M, Ball CA, Blake JA, et al. Gene Ontology: tool for the unification of biology. *Nat Genet.* 2000;25(1):25. doi:10.1038/75556
  303. Carbon S, Douglass E, Good BM, et al. The Gene Ontology resource: enriching a Gold mine. *Nucleic Acids Res.* 2021;49(D1):D325. doi:10.1093/NAR/GKAA1113
  304. Heinz S, Benner C, Spann N, et al. Simple Combinations of Lineage-Determining Transcription Factors Prime cis-Regulatory Elements Required for Macrophage and B Cell Identities. *Mol Cell.* 2010;38(4):576-589. doi:10.1016/J.MOLCEL.2010.05.004
  305. Shi C, Pamer EG. Monocyte recruitment during infection and inflammation. *Nat Rev Immunol* 2011 1111. 2011;11(11):762-774. doi:10.1038/nri3070
  306. Serbina N V., Pamer EG. Monocyte emigration from bone marrow during bacterial infection requires signals mediated by chemokine receptor CCR2. *Nat Immunol* 2006 73. 2006;7(3):311-317. doi:10.1038/ni1309
  307. Culemann S, Grüneboom A, Nicolás-Ávila JÁ, et al. Locally renewing resident synovial macrophages provide a protective barrier for the joint. *Nature.* 2019;572(7771):670-675. doi:10.1038/s41586-019-1471-1
  308. Fogg DK, Sibon C, Miled C, et al. A clonogenic bone marrow progenitor specific for macrophages and dendritic cells. *Science (80- ).* 2006;311(5757):83-87. doi:10.1126/SCIENCE.1117729/SUPPL\_FILE/FOGG.SOM.PDF
  309. Miyanishi M, Tada K, Koike M, Uchiyama Y, Kitamura T, Nagata S. Identification of Tim4 as a phosphatidylserine receptor. *Nature.* 2007;450(7168):435-439. doi:10.1038/nature06307
  310. Kobayashi N, Karisola P, Peña-Cruz V, et al. TIM-1 and TIM-4 Glycoproteins Bind Phosphatidylserine and Mediate Uptake of Apoptotic Cells. *Immunity.* 2007;27(6):927-940. doi:10.1016/J.IMMUNI.2007.11.011
  311. Thornley TB, Fang Z, Balasubramanian S, et al. Fragile TIM-4-expressing tissue resident macrophages are migratory and immunoregulatory. *J Clin Invest.* 2014;124(8):3443-3454. doi:10.1172/JCI73527
  312. Mass E, Ballesteros I, Farlik M, et al. Specification of tissue-resident macrophages during organogenesis. *Science (80- ).* 2016;353(6304). doi:10.1126/science.aaf4238
  313. Daemen S, Gainullina A, Kalugotla G, et al. Dynamic Shifts in the Composition of Resident and Recruited Macrophages Influence Tissue Remodeling in NASH. *Cell Rep.* 2021;34(2). doi:10.1016/j.celrep.2020.108626
  314. Bhattarai S, Li Q, Ding J, et al. TLR4 is a regulator of trained immunity in a murine model of Duchenne muscular dystrophy. *Nat Commun.* 2022;13(1). doi:10.1038/S41467-022-28531-1
  315. Petrof BJ, Podolsky T, Bhattarai S, Tan J, Ding J. Trained immunity as a potential target for therapeutic immunomodulation in Duchenne muscular dystrophy. *Front Immunol.* 2023;14(June):1-10. doi:10.3389/fimmu.2023.1183066
  316. Capote J, Kramerova I, Martinez L, et al. Osteopontin ablation ameliorates muscular dystrophy by shifting macrophages to a proregenerative phenotype. *J Cell Biol.* 2016;213(2):275-288. doi:10.1083/jcb.201510086
  317. Moore SM, Holt V V., Malpass LR, Hines IN, Wheeler MD. Fatty acid-binding protein 5

- limits the anti-inflammatory response in murine macrophages. *Mol Immunol*. 2015;67(2):265-275. doi:10.1016/j.molimm.2015.06.001
318. Jin R, Hao J, Yi Y, Sauter E, Li B. Regulation of macrophage functions by FABP-mediated inflammatory and metabolic pathways. *Biochim Biophys Acta - Mol Cell Biol Lipids*. 2021;1866(8):158964. doi:10.1016/J.BBALIP.2021.158964
  319. Zeng J, Zhang Y, Hao J, et al. Stearic Acid Induces CD11c Expression in Proinflammatory Macrophages via Epidermal Fatty Acid Binding Protein. *J Immunol*. 2018;200(10):3407-3419. doi:10.4049/jimmunol.1701416
  320. Zhang Y, Li Q, Rao E, et al. Epidermal Fatty Acid Binding Protein Promotes Skin Inflammation Induced by High-Fat Diet. *Immunity*. 2015;42(5):953-964. doi:10.1016/j.immuni.2015.04.016
  321. El Kharbili M, Aviszus K, Sasse SK, et al. Macrophage programming is regulated by a cooperative interaction between fatty acid binding protein 5 and peroxisome proliferator-activated receptor  $\gamma$ . *FASEB J*. 2022;36(5):1-13. doi:10.1096/fj.202200128R
  322. Furuhashi M, Hotamisligil GS. Fatty acid-binding proteins: Role in metabolic diseases and potential as drug targets. *Nat Rev Drug Discov*. 2008;7(6):489-503. doi:10.1038/nrd2589
  323. Furuhashi M, Ogura M, Matsumoto M, et al. Serum FABP5 concentration is a potential biomarker for residual risk of atherosclerosis in relation to cholesterol efflux from macrophages. *Sci Rep*. 2017;7(1):1-10. doi:10.1038/s41598-017-00177-w
  324. Furuhashi M, Ishimura S, Ota H, Miura T. Lipid Chaperones and Metabolic Inflammation. *Int J Inflamm*. 2011;2011:1-12. doi:10.4061/2011/642612
  325. Robichaud S, Fairman G, Vijithakumar V, et al. Identification of novel lipid droplet factors that regulate lipophagy and cholesterol efflux in macrophage foam cells. *Autophagy*. 2021;17(11):3671-3689. doi:10.1080/15548627.2021.1886839
  326. Luo M, Opoku E, Traugher CA, et al. Soat1 mediates the mouse strain effects on cholesterol loading-induced endoplasmic reticulum stress and CHOP expression in macrophages. *Biochim Biophys Acta - Mol Cell Biol Lipids*. 2021;1866(1):158825. doi:10.1016/j.bbalip.2020.158825
  327. Zhao C, Yang Q, Tang R, et al. DNA methyltransferase 1 deficiency improves macrophage motility and wound healing by ameliorating cholesterol accumulation. *npj Regen Med*. 2023;8(1):1-17. doi:10.1038/s41536-023-00306-2
  328. Nishiyama K, Fujita T, Fujimoto Y, Nakajima H, Takeuchi T, Azuma YT. Fatty acid transport protein 1 enhances the macrophage inflammatory response by coupling with ceramide and c-Jun N-terminal kinase signaling. *Int Immunopharmacol*. 2018;55(June 2017):205-215. doi:10.1016/j.intimp.2017.12.003
  329. Graham A. Mitochondrial function and regulation of macrophage sterol metabolism and inflammatory responses. *World J Cardiol*. 2015;7(5):277. doi:10.4330/wjc.v7.i5.277
  330. Abate W, Alrammah H, Kiernan M, Tonks AJ, Jackson SK. Lysophosphatidylcholine acyltransferase 2 (LPCAT2) co-localises with TLR4 and regulates macrophage inflammatory gene expression in response to LPS. *Sci Rep*. 2020;10(1):1-13. doi:10.1038/s41598-020-67000-x
  331. Lee CH, Evans RM. Peroxisome proliferator-activated receptor- $\gamma$  in macrophage lipid homeostasis. *Trends Endocrinol Metab*. 2002;13(8):331-335. doi:10.1016/S1043-2760(02)00668-9
  332. Leopold Wager CM, Arnett E, Schlesinger LS. Mycobacterium tuberculosis and

- macrophage nuclear receptors: What we do and don't know. *Tuberculosis*. 2019;116(October 2018):S98-S106. doi:10.1016/j.tube.2019.04.016
333. Rodríguez-Jiménez C, de la Peña G, Sanguino J, et al. Identification and Functional Analysis of APOB Variants in a Cohort of Hypercholesterolemic Patients. *Int J Mol Sci*. 2023;24(8):86-88. doi:10.3390/ijms24087635
334. Odegaard JI, Ricardo-Gonzalez RR, Goforth MH, et al. Macrophage-specific PPAR $\gamma$  controls alternative activation and improves insulin resistance. *Nature*. 2007;447(7148):1116-1120. doi:10.1038/nature05894
335. Honda K, Taniguchi T. IRFs: Master regulators of signalling by Toll-like receptors and cytosolic pattern-recognition receptors. *Nat Rev Immunol*. 2006;6(9):644-658. doi:10.1038/nri1900
336. Lande R, Gregorio J, Facchinetti V, et al. Plasmacytoid dendritic cells sense self-DNA coupled with antimicrobial peptide. *Nature*. 2007;449(7162):564-569. doi:10.1038/nature06116
337. Arakura F, Hida S, Ichikawa E, et al. Genetic Control Directed toward Spontaneous IFN- $\alpha$ /IFN- $\beta$  Responses and Downstream IFN- $\gamma$  Expression Influences the Pathogenesis of a Murine Psoriasis-Like Skin Disease. *J Immunol*. 2007;(16).
338. Crow MK. Type I Interferon in the Pathogenesis of Lupus. *J Immunol*. 2014;192(12):5459-5468. doi:10.4049/jimmunol.1002795
339. Baron D, Magot A, Ramstein G, et al. Immune response and mitochondrial metabolism are commonly deregulated in DMD and Aging skeletal muscle. *PLoS One*. 2011;6(11). doi:10.1371/journal.pone.0026952
340. Zhang X, Bai X chen, Chen ZJ. Structures and Mechanisms in the cGAS-STING Innate Immunity Pathway. *Immunity*. 2020;53(1):43-53. doi:10.1016/j.immuni.2020.05.013
341. Stok JE, Vega Quiroz ME, van der Veen AG. Self RNA Sensing by RIG-I-like Receptors in Viral Infection and Sterile Inflammation. *J Immunol*. 2020;205(4):883-891. doi:10.4049/jimmunol.2000488
342. Colonna M. TLR pathways and IFN-regulatory factors: To each its own. *Eur J Immunol*. 2007;37(2):306-309.
343. Decout A, Katz JD, Venkatraman S, Ablasser A. The cGAS-STING pathway as a therapeutic target in inflammatory diseases. *Nat Rev Immunol*. 2021;21(9):548-569. doi:10.1038/s41577-021-00524-z
344. Sato M, Hata N, Asagiri M, Nakaya T, Taniguchi T, Tanaka N. Positive feedback regulation of type I IFN genes by the IFN-inducible transcription factor IRF-7. *FEBS Lett*. 1998;441(1):106-110. doi:10.1016/S0014-5793(98)01514-2
345. Gong T, Liu L, Jiang W, Zhou R. DAMP-sensing receptors in sterile inflammation and inflammatory diseases. *Nat Rev Immunol* 2019 202. 2019;20(2):95-112. doi:10.1038/s41577-019-0215-7

## **Chapter 4: General Discussion**

#### **4.1. Summary of the Major Findings of the Thesis**

The overall goal of this thesis was to explore the role of macrophages and particularly macrophage ontogeny in acute and chronic skeletal muscle injury by employing several complementary approaches including fate mapping, parabiosis, chimeric mice and RNA sequencing. In doing so, we developed a diaphragm shielding model which is able to maintain the muscle microenvironment, including satellite cell proliferative and differentiation abilities as well as preservation of the tissue resident macrophage population. In combining this new model with other techniques, the main findings of this thesis are as follows:

- 1) Under normal homeostatic conditions, resident macrophages in skeletal muscle consist of both bone marrow-dependent and -independent populations, with the latter predominantly derived from fetal liver hematopoiesis and a lesser contribution from the embryonic yolk sac.
- 2) Under normal homeostatic conditions, bone marrow-independent macrophages derived from the embryo constitute 30-40% of the skeletal muscle resident macrophages that persist into adulthood.
- 3) In the early phase after acute muscle injury, the massive increase in diaphragm macrophages is due to the recruitment (and to a lesser degree proliferation) of bone marrow-derived macrophages. During this same period there is no apparent change in cell number within the pre-existent tissue-resident macrophage population.
- 4) After recovery from acute muscle injury, absolute macrophage numbers and the balance between bone marrow-dependent and bone marrow-independent origin macrophages in the diaphragm both return to their normal pre-injury levels.
- 5) In neonatal dystrophic (mdx) mice, the phenotype of diaphragm macrophages is dramatically altered from the first day of birth, demonstrating a simultaneous increase in putative markers for

both bone marrow-derived and embryo-derived macrophages (CCR2 and TIM4, respectively). Remarkably, this occurs several days before any increase in macrophage numbers or histological evidence of muscle necrosis.

6) In adult mdx mice, bone marrow-dependent macrophages derived from blood monocytes constitute almost the entire macrophage pool within the diaphragm. Furthermore, in addition to increased recruitment from the bone marrow, a decrease in absolute cell number within the pre-existent tissue-resident macrophage population is also observed.

7) The dystrophic environment is the overarching determinant factor in driving the inflammatory phenotype and gene expression pattern of bone marrow-dependent macrophages in the mdx diaphragm, skewing them towards extracellular matrix (ECM) remodeling and innate immune responses. With respect to the latter, the Interferon Regulatory Factor (IRF) family of transcription factors was identified as possibly playing a central role in orchestrating these responses.

#### **4.2. Contributions of the Thesis to Addressing Knowledge Gaps in the Field**

Macrophages are well known to be critical components in muscle regeneration and repair in previously healthy muscle, but their role in chronic inflammatory muscle diseases is more nuanced as these cells are also implicated in disease progression. Rather than being a single, homogeneous population within muscle tissue, macrophages are highly heterogeneous. Their origin, which could be from either embryonic or adult bone marrow sources, may significantly influence their function. To fully grasp how these specific attributes affect muscle repair and regeneration, it is essential to start by identifying the precise origins of macrophages in different tissues. Although organs such as the brain, heart, lung, and many others have been extensively studied, there has been very little research into the normal contributions of embryo-derived

versus adult bone marrow-derived macrophages in healthy skeletal muscle, and even less study of how this is altered by pathological states such as acute injury or muscular dystrophy.

The role of macrophages in acute muscle injury involves coordinating various responses such as clearing debris, facilitating phenotypic switching, promoting regeneration, aiding in ECM remodeling, and managing the resolution of inflammation. Researchers have extensively investigated the significance of macrophages derived from the adult bone marrow in cases of acute muscle injury. However, there remains a significant gap in understanding the contribution of macrophages originating from sources other than the bone marrow. One of the challenges in studying this aspect is the absence of a suitable model to accurately distinguish and track macrophages from these two different origins. The conventional bone marrow chimeric model, while informative, inadvertently disrupts the resident macrophage population (as well as satellite cells) within the muscle, thereby introducing an important confounding artifact within much of the existing literature.

To address these knowledge gaps and technical problems, I developed a new chimeric mouse model with radioprotective shielding of the diaphragm, which can be used to study the relationships between macrophage ontogeny and function in both healthy and injured (acute or chronic) diaphragm muscle. The novel diaphragm shielding model presented in this thesis effectively preserves satellite cell function and macrophage viability. This model offers a versatile platform for investigating both bone marrow-dependent and bone marrow-independent macrophage contributions. By combining various transgenic modifications in bone marrow and recipient cells, it can enable a comprehensive exploration of these macrophage subsets' roles in diverse aspects of muscle repair, including myogenesis, angiogenesis, and fibrosis. Furthermore, the model's utility extends beyond macrophages, allowing tracking of other immune cell

types like neutrophils, T cells, NK cells, as well as other cell types.

As noted above, there has been very little study of how macrophage ontogeny is affected by different pathological conditions, or whether macrophage ontogeny has an impact on the skeletal muscle repair process. On the other hand, there has been a substantial amount of work done in this area for cardiac muscle. Because skeletal and cardiac muscles share many features<sup>346 1</sup>, it is of interest to compare the existing literature on cardiac muscle macrophages to the findings we obtained for skeletal muscle in this thesis. Whereas skeletal muscle macrophages predominantly originate from bone marrow under normal homeostatic conditions, the majority of resident macrophages found in the healthy adult heart stem from the yolk sac or fetal liver<sup>347</sup>, and are characteristically TIM4+ and CCR2-negative<sup>347 167</sup>. These embryonically derived macrophages persist into adulthood, maintaining themselves locally<sup>164 347 167</sup>. Based on our findings, a similar process appears to occur in the smaller population of skeletal muscle macrophages which originate from the embryo. However, we show that although there is preferential TIM4 and CCR2 expression in embryo-derived macrophages and adult bone marrow-derived macrophages, respectively, these markers cannot be used to reliably distinguish between these two populations in skeletal muscle as has been suggested by others<sup>301</sup> because there is considerable overlap. During acute injury to the heart, there is a major increase in the total number of cardiac macrophages<sup>347 348</sup>, mirroring the response we noted in acutely injured skeletal muscle. The escalation in cardiac macrophages can be attributed to both recruitment of monocytes and local proliferation<sup>347</sup> – again paralleling the response observed in skeletal muscle. However, cardiac muscle responds differently in terms of embryonically-derived macrophages: their population dramatically contracts due to localized cell death, before gradually rebounding<sup>167 154</sup>. This is in contrast to acute skeletal muscle injury, where we did not observe a decrease in the population of

embryonically-derived macrophages following acute injury (although this was observed in the mdx mouse scenario of chronic injury). Interestingly, once recruited to the heart some of the blood monocyte-derived macrophages begin to express embryonic molecular and phenotypic features<sup>347,167</sup>, which is consistent with our data in skeletal muscle indicating that a substantial percentage of bone marrow-derived macrophages express TIM4.

In models involving chronic cardiac inflammation, such as the pressure-overload transverse aortic constriction model, both CCR2-negative embryo-derived macrophages and CCR2+ bone marrow-derived macrophages are increased in numbers<sup>349</sup>. This finding is also replicated in *Tnnt2*<sup>ΔK210/ΔK210</sup> mice, a model of hypertrophic cardiomyopathy, where macrophages from both origins show a significant increase in concert with the development of cardiomyopathy<sup>350</sup>. This behavior differs from what we observed in the chronically inflamed diaphragm muscle of mdx mice, where the large increase in macrophage numbers was almost entirely due to monocyte recruitment from the bone marrow along with a simultaneous decrease in the absolute number (and not just the percentage) of embryonically-derived macrophages. The heart relies on embryonically-derived macrophages for its reparative processes, and despite their reduced presence during acute injury, their absence significantly hampers recovery<sup>167</sup>. The dramatic alteration of the normal steady-state macrophage ontogeny equilibrium in dystrophic muscle is an important new finding of this thesis. A similar situation has been observed in other chronic inflammatory diseases, where it has been speculated that disruption of the normal steady-state cues and cellular niche required to maintain the embryonically-derived macrophage pool is responsible<sup>292</sup>. Although the mechanism underlying the elimination of embryo-derived macrophages in the mdx diaphragm remains to be determined, this loss could potentially play an important role in the lack of successful regeneration.

This notion is supported by a recent study in which the function of embryonically-derived macrophages in skeletal muscle was explored using a CSF1 receptor inhibition and withdrawal approach in both acutely injured normal muscle and in mdx mice<sup>301</sup>. The authors reported that TIM4+ macrophages (presumed to be of embryonic origin) were essential for removing apoptotic cells in acute muscle injury. In mdx mice the long-term inhibition of the CSF1 receptor depleted both the presumed embryonic source macrophages and the bone marrow-derived population, and this was associated with a change in muscle fiber type toward more oxidative fibers. The muscles of the CSF1 receptor-inhibited mdx mice were also smaller and showed an increased ability to resist the force loss associated with eccentric contractions. This outcome is difficult to interpret given the fact that CSF1 receptor inhibition had effects on both embryonically-derived and bone marrow-derived macrophages, as well as the fact that CSF1 could have direct effects on the muscle fibers themselves. Furthermore, as mentioned earlier our data suggest that putative markers of macrophage origin such as TIM4 do not reliably distinguish between the embryonically-derived and bone marrow-derived macrophage populations, particularly in the complex dystrophic muscle environment.

In DMD, a significant knowledge gap exists in our understanding of the temporal dynamics of macrophage phenotypic and functional changes during different stages of disease progression. Moreover, the precise mechanisms underlying inflammation dysregulation in DMD and the role of macrophages from different origin in this process remain inadequately understood. Extensive research has been dedicated to understanding the role of macrophages and other inflammatory cell types in mdx mice, but the focus has mainly revolved around limb muscles which are less severely affected than the diaphragm. Indeed, the mdx mouse has been criticized as not being a faithful model of human DMD due to the comparatively mild muscle disease found in the limb

musculature. In contrast, the mdx diaphragm presents more severe pathology, particularly with respect to the early development of fibrosis, which is much more similar to the human DMD situation<sup>351 352 353 354 355</sup>. However, there remains a notable gap in studies that delve into the specific role of macrophages in driving this more severe pathology in the mdx diaphragm, which could offer valuable clues to pathogenesis of the human disease. Therefore, this thesis was particularly focused on the early changes which take place in the mdx diaphragm.

Our studies show for the first time the extent to which the dystrophic environment rapidly modifies previously normal bone marrow-derived macrophages to adopt a pathological phenotype. When previously healthy bone marrow was placed into mdx mice, the bone marrow-derived macrophages in the mdx diaphragm developed a gene expression pattern indicative of innate immune system activation and extracellular matrix (ECM) remodelling. Genes which have been previously implicated in the progression of DMD pathology, such as *Spp1* (osteopontin) and *Lgals3* (galectin-3), were prominently upregulated in our bulk RNA-seq analysis of bone marrow-derived macrophages, which constituted approximately 99% of the macrophage population in the adult mdx diaphragm. Many other genes, such as *Fabp5* and other metabolic genes, were also identified which will serve as candidates for future investigations of the early initiators of DMD pathology.

We also identified members of the Interferon Regulatory Factor (IRF) family of transcription factors as potential master regulators of this process. IRFs are not only critical for host defence against infectious agents (particularly viruses) but have also been implicated in sterile inflammation associated with autoimmune diseases. The IRF family members dimerize not only with each other but also with other transcription factors involved in inflammation such as NF- $\kappa$ B, STATs, and PU.1<sup>356</sup>. They play an important role in orchestrating the TLR and interferon

signaling pathways which are involved in both infectious and non-infectious inflammatory responses. Therefore, our transcription factor motif analysis has revealed a new potential target for modulating the innate immune response in DMD.

#### **4.3. Limitations of the Thesis and Perspectives for Future Studies**

In this thesis, the reasons we chose the CX3CR1<sup>CreERT2-YFP</sup> model for our fate mapping experiments were as follows: 1) CX3CR1 is expressed on macrophages and pre-macrophages during embryonic development; 2) the CreER fusion allows for temporally controlled activation of Cre activity in CX3CR1-expressing cells, upon tamoxifen administration; 3) cross-breeding with mice harboring a fluorescent gene downstream of a LoxP-flanked "stop" sequence at the Rosa26 locus, enabled us to visually track CX3CR1-expressing cells following tamoxifen treatment; and 4) the CreERT2 is an improved variant of CreER with reduced sensitivity to endogenous estrogens, thereby minimizing unwanted activation in the absence of tamoxifen, and has been adopted in many recent studies<sup>357 358 159 167</sup>. Nevertheless, we still observed the problem of "leaky" expression of Cre-recombinase, particularly pronounced with aging, leading to false detection of non-tamoxifen treated cells as has been previously described in some tissues<sup>359 167 360</sup>. In our experiment, we found the non-targeted rate in the diaphragm and soleus at both 5 weeks (17.1% and 26.5%, respectively) and 9 weeks (14.6% and 23.6%, respectively) of age to be comparable to that previously reported in the heart. After normalizing the results by subtracting the mean percentage of leaky expression in non-tamoxifen treated mice, we still identified a considerable percentage of tamoxifen-labeled cells at E18.5, indicating a substantial presence of embryonically derived macrophages. Furthermore, we used parabiosis and chimeric mice with diaphragm shielding to demonstrate that all of these methods were collectively consistent in showing that about one third of the skeletal muscle macrophages do not come from

the adult bone marrow.

Single-cell RNA sequencing (scRNA-seq) is a technique which empowers researchers to delve deeper into gene expression at the level of individual cells, and is thus a good tool to dissect the heterogeneity of macrophage in skeletal muscle. Several recent studies have employed scRNA-seq on muscle macrophages in both healthy and mdx muscles. In healthy diaphragm muscle it was reported that macrophages segregate into four distinct clusters: "proliferating cluster", "CCR2 cluster", "KLF2 cluster", and a low variable "cluster 0"<sup>186</sup>. Each of these clusters presents a unique gene expression profile, hinting at specialized roles. In a scRNA-seq investigation directed at the gastrocnemius muscles of 8-week-old WT-NSG and mdx-NSG mice, a categorization into 8 macrophage subsets was made<sup>8</sup>. A salient finding was the sharp decrease of "Lyve1 M2-like macrophages" in mdx muscles from 88% to a mere 35%, while "M1" and "M2c-like macrophages" showed significant increases. Delving further into 4-week-old WT and mdx hindlimb muscles, another study identified a prominent cluster in normal muscle accounting for about 70% of the macrophages<sup>361</sup>. This cluster, denoted as skeletal muscle-resident macrophages, exhibited hallmark genes *Fcrl2*, *Fcgrt*, *Mt2*, *Mt1*, *Lyve1*, *Cbr2*, *Gas6*, *Ltc4s*, *Fxyd2* and *Sepp1*. Notably, in mdx muscles, this cluster dwindled to less than 5%. Interestingly, 7 of these genes intersected with our dataset of down-regulated genes in bone marrow-derived macrophages from mdx recipients. Furthermore, in the mdx dataset, a dominant cluster emerged, exhibiting fibrotic characteristics with genes including *Spp1*, *Ctsl*, *Fabp5*, *Trem2*, *Gpnmb*, *Syng1*, *Lgals3*, *Cxcl1*, *Ctsd* and *Ctss*. Eight of these genes are also upregulated in our list of differentially expressed genes.

In the current thesis, we employed bulk RNA sequencing to determine how the dystrophic environment is able to rapidly alter the intramuscular macrophage phenotype. Our results, while

generally complementary to the above scRNA-seq studies, prompt other questions such as to determine the origins of these clusters and whether the shifts we have observed at the bulk RNA level represent genotypic transitions of individual cells or cellular subset size variations? In addition, a major challenge remains in associating these macrophage clusters with their ontogeny since they rely solely on the assigned annotations of mRNA data rather than actual proof of cellular origin. Future studies should combine scRNA-seq with the approaches used in this thesis which are able to more definitively identify macrophage origin, and we have already initiated studies in this direction.

Finally, the gene expression alterations in the mdx recipient mice can potentially result from both the influence of systemic inflammation at the level of the bone marrow, and the direct effects of the local dystrophic muscle environment. A prior study from our lab has shown that bone marrow-derived macrophages from mdx mice undergo TLR4-mediated alterations consisting of heightened cytokine responses to DAMP stimulation, metabolic shifts, and epigenetic modifications<sup>314</sup>. These changes occur at the level of the bone marrow before the future monocytes/macrophages have entered the circulation, and are consistent with the phenomenon known as trained immunity. In this thesis, we are uncertain whether the duration of 8 weeks post-transplantation was sufficient time to induce trained immunity in WT bone marrow that was transferred into recipient mdx mice. This will be an important question for future study and help to ascertain the relative influences of systemic factors signaling to the bone marrow (DAMPs, cytokines, etc) versus the local dystrophic muscle environment in modulating macrophage phenotype in DMD.

#### **4.4. Potential Therapeutic Implications of Thesis Findings**

This thesis made the novel observation that macrophages in the mdx diaphragm, which phenotypically resembles human DMD, are almost entirely derived from circulating blood monocytes. These macrophages are consistently recruited and typically distributed around myofibers, particularly necrotic ones. Given that monocytes, the precursors of macrophages in mdx muscle, circulate in the bloodstream, our findings suggest that systemic therapies that target these cells might be considered. Proof-of-principle for this approach is provided by the amelioration of dystrophic pathology in mdx mice that are either CCR2-deficient<sup>223</sup> or treated with a dual CCR2/CCR5 inhibitor, cenicriviroc<sup>362</sup>.

Alternatively, in certain scenarios macrophages can actually serve as carriers for delivering drugs, beneficial molecules for muscle repair, or even DNA/RNA sequences for gene therapy. This is particularly valuable for molecules that struggle to access muscle fibers due to challenges such as immune-related barriers or limited penetration. For example, previous research has exploited macrophages to deliver drugs to tumor sites<sup>363 364</sup>, and as carriers for nanoparticles, thereby enhancing efficiency<sup>365</sup>. Notably, a study has suggested that endogenous macrophages can act as a reservoir for morpholino antisense oligonucleotides which then facilitates their more efficient delivery to the muscle fibers of mdx mice<sup>366</sup>.

Finally, this thesis has demonstrated a very early postnatal change in macrophage phenotype, suggesting that DMD treatments should ideally commence as soon as possible, and potentially even prior to birth. This early intervention could potentially delay disease progression and improve patient outcomes. In later stages of DMD, potential therapeutic interventions may include reprogramming macrophages to a less fibrotic state. For example, strategies such as the use of folate-targeted TLR7 agonist (FA-TLR7-54) have been proven effective in inhibiting fibrosis-causing cytokines<sup>367</sup>. This method has been successfully deployed for conditions like

rheumatoid arthritis and idiopathic pulmonary fibrosis. In addition, a particularly interesting approach would be to attempt to shift the balance between embryonically-derived and bone marrow-derived macrophages back towards the normal homeostatic state found in healthy muscle. Future studies should explore whether different drugs are capable of achieving this goal.

## **Final conclusion and summary**

The main objectives of the thesis are

Objective 1: To develop a chimeric mouse model that preserves the muscle microenvironment and permits the identification of bone marrow-dependent (monocyte-derived) versus bone marrow-independent (embryo-derived) macrophage populations in the diaphragm

Objective 2: To describe the normal ontogeny of diaphragm macrophages during embryonic development and adulthood

Objective 3: To determine how macrophage ontogeny is dynamically altered by acute and chronic (mdx mouse model of muscular dystrophy) skeletal muscle injury

Objective 4: To explore how interactions between macrophage ontogeny and the skeletal muscle microenvironment determine macrophage phenotype in healthy versus dystrophic diaphragm muscle

We achieved Objective 1 in Chapter 2 by utilizing lead shielding during whole-body irradiation. This approach preserved diaphragm satellite cell functionality and prevented the depletion of resident macrophages, which occurred in unshielded mice. By maintaining this microenvironment, we identified bone marrow-dependent and bone marrow-independent macrophage populations in the diaphragm. The chimeric mouse model developed in this thesis is valuable for studying interactions between bone marrow-derived and embryo-derived macrophages in the diaphragm. This model holds promise for investigating muscle regeneration, immune responses, and tissue repair following acute and chronic muscle injuries.

Objective 2 was accomplished through experiments in both Chapter 2 and Chapter 3. The diaphragm shielding model revealed bone marrow-independent macrophages in healthy adult

skeletal muscles. Parabiosis experiments and fate mapping models provided additional evidence for monocyte-independent resident macrophages, constituting around 30-40% of steady-state macrophages in healthy adult muscles. Using tamoxifen-inducible lineage tracing, it was established that a notable portion of diaphragm resident macrophages originate from fetal liver hematopoiesis, with a minor contribution from the embryonic yolk sac. These findings shed light on the origins and dynamics of skeletal muscle macrophage populations, emphasizing both prenatal and postnatal sources in muscle development and maintenance. Understanding this interplay has implications for skeletal muscle health, repair, and disease.

Objective 3 was met from experiments in both Chapter 2 and Chapter 3. In Chapter 2, we showed that bone marrow-derived macrophages are primarily responsible for the substantial increase in intramuscular macrophages. The absolute number of embryonic-derived macrophages was not changed. This increase of bone marrow-derived macrophages occurs through macrophage recruitment and proliferation. However, these alterations in macrophage ontogeny are not permanent, as we demonstrated that the pre-injury pattern of macrophage populations is restored once the muscle has healed and returned to homeostasis. In the dystrophic mdx muscle studied in Chapter 3, bone marrow-derived macrophages are primarily responsible for the substantial increase in intramuscular macrophages. This increase lasts for the entire necrotic stage. The absolute number of embryonic-derived macrophages was dramatically decreased. Through analysis of macrophage markers and phenotypic features, we demonstrated that the macrophage population in dystrophic muscle exhibits complex alterations from birth, characterized by simultaneous elevations of CCR2 and TIM4 expressing macrophages. The findings from Objective 3 of the study shed light on the complex interplay between different macrophage populations in response to muscle injury and dystrophic conditions. These insights contribute to understanding

tissue repair mechanisms, immune responses, and potential therapeutic strategies for muscle-related disorders.

Objective 4 was achieved in Chapter 3 using transplantation models and RNA-sequencing. These models demonstrate that healthy mouse bone marrow-derived macrophages adopt inflammatory phenotypes when entering dystrophic muscle, highlighting the dystrophic environment's profound impact. Transcriptomic analysis identifies genes and pathways affected in dystrophic muscle-recruited macrophages, unveiling molecular mechanisms behind their responses. These insights emphasize environmental influence on macrophage phenotype and reveal crucial pathways in dystrophic muscles. Understanding this interplay aids therapeutic strategies for muscular dystrophy and muscle-related disorders, addressing both healthy and pathological states.

## References

1. Frontera WR, Ochala J. Skeletal Muscle: A Brief Review of Structure and Function. *Behav Genet.* 2015;45(2):183-195. doi:10.1007/s00223-014-9915-y
2. Zurlo F, Larson K, Bogardus C, Ravussin E. Skeletal Muscle Metabolism Is a Major Determinant of Resting Energy Expenditure.
3. Mukund K, Subramaniam S. Skeletal muscle: A review of molecular structure and function, in health and disease. *Wiley Interdiscip Rev Syst Biol Med.* 2020;12(1). doi:10.1002/WSBM.1462
4. Gillies AR, Lieber RL. Structure and function of the skeletal muscle extracellular matrix. *Muscle Nerve.* 2011;44(3):318-331. doi:10.1002/MUS.22094
5. Hawke TJ, Garry DJ. Myogenic satellite cells: Physiology to molecular biology. *J Appl Physiol.* 2001;91(2):534-551. doi:10.1152/JAPPL.2001.91.2.534/ASSET/IMAGES/LARGE/DG0810890005.JPEG
6. Petrany MJ, Swoboda CO, Sun C, et al. Single-nucleus RNA-seq identifies transcriptional heterogeneity in multinucleated skeletal myofibers. *Nat Commun.* 2020;11(1). doi:10.1038/S41467-020-20063-W
7. Burzyn D, Kuswanto W, Kolodin D, et al. A Special Population of Regulatory T Cells Potentiates Muscle Repair. *Cell.* 2013;155(6):1282-1295. doi:10.1016/J.CELL.2013.10.054
8. Saleh KK, Xi H, Switzler C, et al. Single cell sequencing maps skeletal muscle cellular diversity as disease severity increases in dystrophic mouse models. *iScience.* 2022;25(11). doi:10.1016/J.ISCI.2022.105415
9. Tidball JG. Regulation of muscle growth and regeneration by the immune system. *Nat Rev Immunol.* 2017;17(3):165-178. doi:10.1038/nri.2016.150
10. Bonomo AC, Pinto-Mariz F, Riederer I, et al. Crosstalk Between Innate and T Cell Adaptive Immunity With(in) the Muscle. *Front Physiol.* 2020;11(September):1-11. doi:10.3389/fphys.2020.573347
11. PIMORADY-ESFAHANI A, GROUNDS MD, MCMENAMIN PG. Cells in Normal and Regenerating Murine Skeletal Muscle. *Muscle and Nerve.* 1997;(February):158-166.
12. Wiendl H, Hohlfeld R, Kieseier BC. Immunobiology of muscle: Advances in understanding an immunological microenvironment. *Trends Immunol.* 2005;26(7):373-380. doi:10.1016/j.it.2005.05.003
13. Lefaucheur JP, Gjata B, Sebille A. Factors inducing mast cell accumulation in skeletal muscle. *Neuropathol Appl Neurobiol.* 1996;22(3):248-255. doi:10.1111/j.1365-2990.1996.tb00901.x
14. Galli SJ, Nakae S, Tsai M. Mast cells in the development of adaptive immune responses. *Nat Immunol.* 2005;6(2):135-142. doi:10.1038/ni1158
15. Schmalbruch H, Lewis DM. Dynamics of nuclei of muscle fibers and connective tissue cells in normal and denervated rat muscles. *Muscle and Nerve.* 2000;23(4):617-626. doi:10.1002/(SICI)1097-4598(200004)23:4<617::AID-MUS22>3.0.CO;2-Y
16. Roman W, Pinheiro H, Pimentel MR, et al. Muscle repair after physiological damage relies on nuclear migration for cellular reconstruction.
17. Sciorati C, Rigamonti E, Manfredi AA, Rovere-Querini P. Cell death, clearance and immunity in the skeletal muscle. *Cell Death Differ.* 2016;23(6):927-937. doi:10.1038/CDD.2015.171

18. Bian Z, Wang Q, Zhou X, et al. Sustained elevation of MG53 in the bloodstream increases tissue regenerative capacity without compromising metabolic function. *Nat Commun* 2019 10(1):1-16. doi:10.1038/s41467-019-12483-0
19. Okubo K, Kurosawa M, Kamiya M, et al. Macrophage extracellular trap formation promoted by platelet activation is a key mediator of rhabdomyolysis-induced acute kidney injury. *Nat Med* 2018 24(2):232-238. doi:10.1038/nm.4462
20. Reza M, Subramaniyam N, Sim CM, et al. Irisin is a pro-myogenic factor that induces skeletal muscle hypertrophy and rescues denervation-induced atrophy. doi:10.1038/s41467-017-01131-0
21. Jung HW, Choi JH, Jo T, Shin H, Suh JM. Systemic and local phenotypes of barium chloride induced skeletal muscle injury in mice. *Ann Geriatr Med Res.* 2019;23(2):83-89. doi:10.4235/agmr.19.0012
22. Bondesen BA, Mills ST, Kegley KM, Pavlath GK. The COX-2 pathway is essential during early stages of skeletal muscle regeneration. *Am J Physiol - Cell Physiol.* 2004;287(2 56-2):475-483. doi:10.1152/AJPCELL.00088.2004/ASSET/IMAGES/LARGE/ZH00080420600006.JPG
23. Tidball JG. Mechanisms of muscle injury, repair, and regeneration. *Compr Physiol.* 2011;1(4):2029-2062. doi:10.1002/cphy.c100092
24. Malinoski DJ, Slater MS, Mullins RJ. Crush injury and rhabdomyolysis. *Crit Care Clin.* 2004;20(1):171-192. doi:10.1016/S0749-0704(03)00091-5
25. Long B, Liang SY, Gottlieb M. Crush injury and syndrome: A review for emergency clinicians. *Am J Emerg Med.* 2023;69:180-187. doi:10.1016/j.ajem.2023.04.029
26. Warren GL, Summan M, Gao X, Chapman R, Hulderman T, Simeonova PP. Mechanisms of skeletal muscle injury and repair revealed by gene expression studies in mouse models. *J Physiol.* 2007;582(2):825-841. doi:10.1113/jphysiol.2007.132373
27. Hardy D, Besnard A, Latil M, et al. Comparative Study of Injury Models for Studying Muscle Regeneration in Mice. *PLoS One.* 2016;11(1):e0147198. doi:10.1371/JOURNAL.PONE.0147198
28. Souza J de, Gottfried C. Muscle injury: Review of experimental models. *J Electromyogr Kinesiol.* 2013;23(6):1253-1260. doi:10.1016/j.jelekin.2013.07.009
29. Martinez CO, McHale MJ, Wells JT, et al. Regulation of skeletal muscle regeneration by CCR2-activating chemokines is directly related to macrophage recruitment. *Am J Physiol - Regul Integr Comp Physiol.* 2010;299(3):832-842. doi:10.1152/ajpregu.00797.2009
30. Yahiaoui L, Gvozdic D, Danialou G, Mack M, Petrof BJ. CC family chemokines directly regulate myoblast responses to skeletal muscle injury. *J Physiol.* 2008;586(Pt 16):3991. doi:10.1113/JPHYSIOL.2008.152090
31. Sambasivan R, Yao R, Kissenpfennig A, et al. Pax7-expressing satellite cells are indispensable for adult skeletal muscle regeneration. *Development.* 2011;138(17):3647-3656. doi:10.1242/DEV.067587
32. Malea M, Murphy J, JALSJMDAH and GK. \_Satellite cells, connective tissue fibroblasts and their interactions are crucial for muscle regeneration. Published online 2011. doi:10.1242/dev.064162
33. Lepper C, Partridge TA, Fan CM. An absolute requirement for Pax7-positive satellite cells in acute injury-induced skeletal muscle regeneration. *Development.* 2011;138(17):3639-3646. doi:10.1242/DEV.067595

34. Rozo M, Li L, Fan CM. Targeting  $\beta$ 1-integrin signaling enhances regeneration in aged and dystrophic muscle in mice. *Nat Med*. 2016;22(8):889-896. doi:10.1038/NM.4116
35. Dumont NA, Bentzinger CF, Sincennes MC, Rudnicki MA. Satellite Cells and Skeletal Muscle Regeneration. *Compr Physiol*. 2015;5(3):1027-1059. doi:10.1002/CPHY.C140068
36. Bischoff R. A Satellite Cell Mitogen from Crushed Adult Muscle. *Dev Biol*. 1986;115:140-147.
37. Ho TL, Tang CH, Chang SLY, Tsai CH, Chen H Te, Su CM. HMGB1 Promotes In Vitro and In Vivo Skeletal Muscle Atrophy through an IL-18-Dependent Mechanism. *Cells*. 2022;11(23):3936. doi:10.3390/CELLS11233936/S1
38. Venereau E, Casalgrandi M, Schiraldi M, et al. Mutually exclusive redox forms of HMGB1 promote cell recruitment or proinflammatory cytokine release. *J Exp Med*. 2012;209(9):1519. doi:10.1084/JEM.20120189
39. Niels M, E. HH. Paternity testing with VNTR DNA systems. *Int J Leg Med*. 1993;105:198-196.
40. Stawski R, Walczak K, Kosielski P, et al. Repeated bouts of exhaustive exercise increase circulating cell free nuclear and mitochondrial DNA without development of tolerance in healthy men. Published online 2017. doi:10.1371/journal.pone.0178216
41. Clarkson PM, Sayers SP. Etiology of exercise-induced muscle damage. *Can J Appl Physiol*. 1999;24(3):234-248. doi:10.1139/H99-020
42. Contreras O, Córdova-Casanova A, Brandan E. PDGF-PDGFR network differentially regulates the fate, migration, proliferation, and cell cycle progression of myogenic cells. *Cell Signal*. 2021;84. doi:10.1016/j.cellsig.2021.110036
43. Tatsumi R, Anderson JE, Nevoret CJ, Halevy O, Allen RE. HGF/SF is present in normal adult skeletal muscle and is capable of activating satellite cells. *Dev Biol*. 1998;194(1):114-128. doi:10.1006/DBIO.1997.8803
44. Zeng L, Akasaki Y, Sato K, Ouchi N, Izumiya Y, Walsh K. Insulin-like 6 is induced by muscle injury and functions as a regenerative factor. *J Biol Chem*. 2010;285(46):36060-36069. doi:10.1074/JBC.M110.160879
45. Kelić S, Olsson T, Kristensson K. Interferon-gamma promotes proliferation of rat skeletal muscle cells in vitro and alters their AChR distribution. *J Neurol Sci*. 1993;114(1):62-67. doi:10.1016/0022-510X(93)90050-9
46. Cheng M, Nguyen MH, Fantuzzi G, Koh TJ. Endogenous interferon- $\gamma$  is required for efficient skeletal muscle regeneration. *Am J Physiol - Cell Physiol*. 2008;294(5):1183-1191. doi:10.1152/AJPCELL.00568.2007/ASSET/IMAGES/LARGE/ZH00050855850008.JPG
47. Li Y-P. TNF-is a mitogen in skeletal muscle. Published online 2003. doi:10.1152/ajpccell.00453.2002.-Emerging
48. Bakkar N, Wang J, Ladner KJ, et al. IKK/NF-kappaB regulates skeletal myogenesis via a signaling switch to inhibit differentiation and promote mitochondrial biogenesis. *J Cell Biol*. 2008;180(4):787-802. doi:10.1083/JCB.200707179
49. Hinz M, Krappmann D, Eichten A, Heder A, Scheidereit C, Strauss M. NF-kappaB function in growth control: regulation of cyclin D1 expression and G0/G1-to-S-phase transition. *Mol Cell Biol*. 1999;19(4):2690-2698. doi:10.1128/MCB.19.4.2690
50. Langen RCJ, Velden JLJ, Schols AMWJ, Kelders MCJM, Wouters EFM, Janssen-Heininger YMW. Tumor necrosis factor-alpha inhibits myogenic differentiation through

- MyoD protein destabilization. *FASEB J.* 2004;18(2):227-237. doi:10.1096/FJ.03-0251COM
51. Crawley S, Farrell EM, Wang W, et al. The alpha7beta1 integrin mediates adhesion and migration of skeletal myoblasts on laminin. *Exp Cell Res.* 1997;235(1):274-286. doi:10.1006/EXCR.1997.3671
  52. Alfaro LAS, Dick SA, Siegel AL, et al. CD34 promotes satellite cell motility and entry into proliferation to facilitate efficient skeletal muscle regeneration. *Stem Cells.* 2011;29(12):2030-2041. doi:10.1002/STEM.759
  53. Mylona E, Jones KA, Mills ST, Pavlath GK. CD44 regulates myoblast migration and differentiation. *J Cell Physiol.* 2006;209(2):314-321. doi:10.1002/JCP.20724
  54. Shams AS, Arpke RW, Gearhart MD, et al. The chemokine receptor CXCR4 regulates satellite cell activation, early expansion, and self-renewal, in response to skeletal muscle injury. *Front Cell Dev Biol.* 2022;10(September):1-17. doi:10.3389/fcell.2022.949532
  55. González MN, de Mello W, Butler-Browne GS, et al. HGF potentiates extracellular matrix-driven migration of human myoblasts: involvement of matrix metalloproteinases and MAPK/ERK pathway. *Skelet Muscle.* 2017;7(1). doi:10.1186/S13395-017-0138-6
  56. Nishimura T, Nakamura K, Kishioka Y, Kato-Mori Y, Wakamatsu JI, Hattori A. Inhibition of matrix metalloproteinases suppresses the migration of skeletal muscle cells. *J Muscle Res Cell Motil.* 2008;29(1):37-44. doi:10.1007/S10974-008-9140-2
  57. Lluís F, Perdiguero E, Nebreda AR, Muñoz-Cánoves P. Regulation of skeletal muscle gene expression by p38 MAP kinases. *Trends Cell Biol.* 2006;16(1):36-44. doi:10.1016/J.TCB.2005.11.002
  58. Kassam-Duchossoy L, Gayraud-Morel B, Gomès D, et al. Mrf4 determines skeletal muscle identity in Myf5:MyoD double-mutant mice. *Nature.* 2004;431(7007):466-471. doi:10.1038/NATURE02876
  59. Ishikawa K, Araki M, Nagano Y, et al. Knockdown of optineurin controls C2C12 myoblast differentiation via regulating myogenin and MyoD expressions. *Differentiation.* 2022;123:1-8. doi:10.1016/J.DIFF.2021.11.004
  60. Lehka L, Rędownicz MJ. Mechanisms regulating myoblast fusion: A multilevel interplay. Published online 2020. doi:10.1016/j.semcd.2020.02.004
  61. Fielding RA, Manfredi TJ, Ding W, Fiatarone MA, Evans WJ, Cannon JG. Acute phase response in exercise. III. Neutrophil and IL-1 beta accumulation in skeletal muscle. <https://doi-org.proxy3.library.mcgill.ca/101152/ajpregu19932651R166>. 1993;265(1 34-1). doi:10.1152/AJPREGU.1993.265.1.R166
  62. Dumont N, Bouchard P, Frenette J. Neutrophil-induced skeletal muscle damage: A calculated and controlled response following hindlimb unloading and reloading. *Am J Physiol - Regul Integr Comp Physiol.* 2008;295(6):1831-1838. doi:10.1152/AJPREGU.90318.2008/ASSET/IMAGES/LARGE/ZH60110865510007.JPEG
  63. Castiglioni A, Corna G, Rigamonti E, et al. FOXP3 + T Cells Recruited to Sites of Sterile Skeletal Muscle Injury Regulate the Fate of Satellite Cells and Guide Effective Tissue Regeneration. Published online 2015. doi:10.1371/journal.pone.0128094
  64. M SM. Macrophages and skeletal muscle regeneration: a clodronate-containing liposome depletion study. *Am J Physiol - Regul Integr Comp Physiol.* 290(6):1488-1495.
  65. Lu H, Huang D, Ransohoff RM, Zhou L. Acute skeletal muscle injury: CCL2 expression by both monocytes and injured muscle is required for repair. *FASEB J.* 2011;25(10):3344-

3355. doi:10.1096/fj.10-178939
66. Heredia JE, Mukundan L, Chen FM, et al. Type 2 innate signals stimulate fibro/adipogenic progenitors to facilitate muscle regeneration. *Cell*. 2013;153(2):376-388. doi:10.1016/J.CELL.2013.02.053
  67. Horsley V, Jansen KM, Mills ST, Pavlath GK. IL-4 acts as a myoblast recruitment factor during mammalian muscle growth. *Cell*. 2003;113(4):483-494. doi:10.1016/S0092-8674(03)00319-2
  68. Lukjanenko L, Karaz S, Stuelsatz P, et al. Aging Disrupts Muscle Stem Cell Function by Impairing Matricellular WISP1 Secretion from Fibro-Adipogenic Progenitors. *Cell Stem Cell*. 2019;24(3):433-446.e7. doi:10.1016/J.STEM.2018.12.014
  69. Joe AWB, Yi L, Natarajan A, et al. Muscle injury activates resident fibro/adipogenic progenitors that facilitate myogenesis. *Nat Cell Biol*. 2010;12(2):153-163. doi:10.1038/ncb2015
  70. Kuswanto W, Burzyn D, Panduro M, et al. Poor Repair of Skeletal Muscle in Aging Mice Reflects a Defect in Local, Interleukin-33-Dependent Accumulation of Regulatory T Cells. *Immunity*. 2016;44(2):355-367. doi:10.1016/j.immuni.2016.01.009
  71. Koenig M, Hoffman EP, Bertelson CJ, Monaco AP, Feener C, Kunkel LM. Complete cloning of the duchenne muscular dystrophy (DMD) cDNA and preliminary genomic organization of the DMD gene in normal and affected individuals. *Cell*. 1987;50(3):509-517. doi:10.1016/0092-8674(87)90504-6
  72. Mendell JR, Shilling C, Leslie ND, et al. Evidence-based path to newborn screening for duchenne muscular dystrophy. *Ann Neurol*. 2012;71(3):304-313. doi:10.1002/ANA.23528
  73. Ryder S, Leadley RM, Armstrong N, et al. The burden, epidemiology, costs and treatment for Duchenne muscular dystrophy: an evidence review. doi:10.1186/s13023-017-0631-3
  74. Duan D, Goemans N, Takeda S, Mercuri E, Aartsma-Rus A. Duchenne muscular dystrophy. *Nat Rev Dis Prim* 2021 71. 2021;7(1):1-19. doi:10.1038/S41572-021-00248-3
  75. Muntoni F, Torelli S, Ferlini A. Dystrophin and mutations: One gene, several proteins, multiple phenotypes. *Lancet Neurol*. 2003;2(12):731-740. doi:10.1016/S1474-4422(03)00585-4
  76. Magri F, Govoni A, Grazia D' M, et al. Genotype and phenotype characterization in a large dystrophinopathic cohort with extended follow-up. doi:10.1007/s00415-011-5979-z
  77. Aartsma-Rus A, Van Deutekom JCT, Fokkema IF, Van Ommen GJB, Den Dunnen JT. Entries in the Leiden Duchenne muscular dystrophy mutation database: an overview of mutation types and paradoxical cases that confirm the reading-frame rule. *Muscle Nerve*. 2006;34(2):135-144. doi:10.1002/MUS.20586
  78. Petrof BJ, Shrager JB, Stedman HH, Kelly AM, Sweeney HL. Dystrophin protects the sarcolemma from stresses developed during muscle contraction. *Proc Natl Acad Sci U S A*. 1993;90(8):3710-3714. doi:10.1073/pnas.90.8.3710
  79. Lapidos KA, Kakkar R, McNally EM. The Dystrophin Glycoprotein Complex. *Circ Res*. 2004;94(8):1023-1031. doi:10.1161/01.RES.0000126574.61061.25
  80. Duchen MR. Mitochondria and calcium: from cell signalling to cell death. *J Physiol*. 2000;529(Pt 1):57. doi:10.1111/J.1469-7793.2000.00057.X
  81. Barbieri E, Sestili P. Reactive Oxygen Species in Skeletal Muscle Signaling. *J Signal Transduct*. 2012;2012:17. doi:10.1155/2012/982794
  82. Acharyya S, Villalta SA, Bakkar N, et al. Interplay of IKK/NF- $\kappa$ B signaling in macrophages and myofibers promotes muscle degeneration in Duchenne muscular

- dystrophy. *J Clin Invest*. 2007;117(4):889. doi:10.1172/JCI30556
83. Chen YW, Nagaraju K, Bakay M, et al. Early onset of inflammation and later involvement of TGF $\beta$  in Duchenne muscular dystrophy. *Neurology*. 2005;65(6):826-834. doi:10.1212/01.WNL.0000173836.09176.C4
  84. by Dove Press published. Anti-inflammatory drugs for Duchenne muscular dystrophy: focus on skeletal muscle-releasing factors. Published online 2016:2745-2758. doi:10.2147/DDDT.S110163
  85. Finkel RS, Finanger E, Vandenborne K, et al. Disease-modifying effects of edasalonexent, an NF- $\kappa$ B inhibitor, in young boys with Duchenne muscular dystrophy: Results of the MoveDMD phase 2 and open label extension trial. *Neuromuscul Disord*. 2021;31(5):385-396. doi:10.1016/j.nmd.2021.02.001
  86. Finkel RS, McDonald CM, Lee Sweeney H, et al. A Randomized, Double-Blind, Placebo-Controlled, Global Phase 3 Study of Edasalonexent in Pediatric Patients with Duchenne Muscular Dystrophy: Results of the PolarisDMD Trial. *J Neuromuscul Dis*. 2021;8(5):769-784. doi:10.3233/JND-210689
  87. Reggio A, Rosina M, Kraemer N, et al. Metabolic reprogramming of fibro/adipogenic progenitors facilitates muscle regeneration. *Life Sci Alliance*. 2020;3(3). doi:10.26508/LSA.202000660
  88. Uezumi A, Ito T, Morikawa D, et al. Fibrosis and adipogenesis originate from a common mesenchymal progenitor in skeletal muscle. *J Cell Sci*. 2011;124(21):3654-3664. doi:10.1242/JCS.086629
  89. Marinkovic M, Fuoco C, Sacco F, et al. Fibro-adipogenic progenitors of dystrophic mice are insensitive to NOTCH regulation of adipogenesis. *Life Sci alliance*. 2019;2(3). doi:10.26508/LSA.201900437
  90. Cordani N, Pisa V, Pozzi L, Sciorati C, Clementi E. Nitric Oxide Controls Fat Deposition in Dystrophic Skeletal Muscle by Regulating Fibro-Adipogenic Precursor Differentiation. *Stem Cells*. 2014;32(4):874-885. doi:10.1002/STEM.1587
  91. Dumont NA, Wang YX, Von Maltzahn J, et al. Dystrophin expression in muscle stem cells regulates their polarity and asymmetric division. *Nat Med*. 2015;21(12):1455-1463. doi:10.1038/nm.3990
  92. Sugihara H, Teramoto N, Nakamura K, et al. Cellular senescence-mediated exacerbation of Duchenne muscular dystrophy. *Sci Rep*. 2020;10(1):1-17. doi:10.1038/s41598-020-73315-6
  93. Biressi S, Miyabara EH, Gopinath SD, Carlig PMM, Rando TA. A Wnt-TGF2 axis induces a fibrogenic program in muscle stem cells from dystrophic mice. *Sci Transl Med*. 2014;6(267). doi:10.1126/scitranslmed.3008411
  94. Alexakis C, Partridge T, Bou-Gharios G. Implication of the satellite cell in dystrophic muscle fibrosis: a self-perpetuating mechanism of collagen overproduction. *Am J Physiol Cell Physiol*. 2007;293:661-669. doi:10.1152/ajpcell.00061.2007.-Because
  95. Kodippili K, Rudnicki MA. Satellite cell contribution to disease pathology in Duchenne muscular dystrophy. 2023;(May):1-11. doi:10.3389/fphys.2023.1180980
  96. Iyer SR, Xu S, Shah SB, Lovering RM. Muscle phenotype of a rat model of Duchenne muscular dystrophy. *Muscle Nerve*. 2020;62(6):757-761. doi:10.1002/MUS.27061
  97. Nakamura K, Fujii W, Tsuboi M, et al. Generation of muscular dystrophy model rats with a CRISPR/Cas system. *Sci Rep*. 2014;4. doi:10.1038/SREP05635
  98. Waldmann H, Hall BM, Davies KE, et al. Immunophenotype of a Rat Model of

- Duchenne's Disease and Demonstration of Improved Muscle Strength After Anti-CD45RC Antibody Treatment. *Front Immunol* / [www.frontiersin.org](http://www.frontiersin.org). 2019;10:2131. doi:10.3389/fimmu.2019.02131
99. Larcher T, Lafoux A, Tesson L, et al. Characterization of dystrophin deficient rats: a new model for Duchenne muscular dystrophy. *PLoS One*. 2014;9(10). doi:10.1371/JOURNAL.PONE.0110371
  100. Kornegay JN. The golden retriever model of Duchenne muscular dystrophy. doi:10.1186/s13395-017-0124-z
  101. Birch SM, Lawlor MW, Conlon TJ, et al. Assessment of systemic AAV-microdystrophin gene therapy in the GRMD model of Duchenne muscular dystrophy. *Sci Transl Med*. 2023;15(677):eabo1815. doi:10.1126/SCITRANSLMED.ABO1815
  102. Punzón I, Mauduit D, Holvoet B, et al. In Vivo Myoblasts Tracking Using the Sodium Iodide Symporter Gene Expression in Dogs. *Mol Ther - Methods Clin Dev*. 2020;17:317-327. doi:10.1016/J.OMTM.2019.12.011
  103. Barraza-Flores P, Fontelonga TM, Wuebbles RD, et al. Laminin-111 protein therapy enhances muscle regeneration and repair in the GRMD dog model of Duchenne muscular dystrophy. *Hum Mol Genet*. 2019;28(16):2686-2695. doi:10.1093/HMG/DDZ086
  104. García-Rodríguez R, Hiller M, Jiménez-Gracia L, et al. Premature termination codons in the DMD gene cause reduced local mRNA synthesis. *Proc Natl Acad Sci U S A*. 2020;117(28):15664-16464. doi:10.1073/PNAS.1910456117/SUPPL\_FILE/PNAS.1910456117.SAPP.PDF
  105. Yucel N, Chang AC, Day JW, Rosenthal N, Blau HM. Humanizing the mdx mouse model of DMD: the long and the short of it. *npj Regen Med* 2018 31. 2018;3(1):1-11. doi:10.1038/s41536-018-0045-4
  106. Im W Bin, Phelps SF, Copen EH, Adams EG, Slightom JL, Chamberlain JS. Differential Expression of Dystrophin Isoforms in Strains of mdx Mice with Different Mutations. *Hum Mol Genet*. 1996;5(8):1149-1153. doi:10.1093/HMG/5.8.1149
  107. Stedman HH, Sweeney HL, Shrager JB, et al. The mdx mouse diaphragm reproduces the degenerative changes of Duchenne muscular dystrophy. *Nature*. 1991;352(6335):536-539. doi:10.1038/352536a0
  108. Wynn TA, Chawla A, Pollard JW. Macrophage biology in development, homeostasis and disease. *Nat* 2013 4967446. 2013;496(7446):445-455. doi:10.1038/nature12034
  109. Cox N, Pokrovskii M, Vicario R, Geissmann F. Origins, Biology, and Diseases of Tissue Macrophages. <https://doi-org.proxy3.library.mcgill.ca/101146/annurev-immunol-093019-111748>. 2021;39:313-344. doi:10.1146/ANNUREV-IMMUNOL-093019-111748
  110. Weiss G, Schaible UE. Macrophage defense mechanisms against intracellular bacteria. *Immunol Rev*. 2015;264(1):182-203. doi:10.1111/imr.12266
  111. Mao Y, Finnemann SC. Regulation of phagocytosis by Rho GTPases. <https://doi.org/104161/215412482014989785>. 2015;6(2):89-99. doi:10.4161/21541248.2014.989785
  112. Zhu M, Li D, Wu Y, Huang X, Wu M. TREM-2 Promotes Macrophage-Mediated Eradication of *Pseudomonas aeruginosa* via a PI3K/Akt Pathway. *Scand J Immunol*. 2014;79(3):187-196. doi:10.1111/sji.12148
  113. Wang R, Town T, Gokarn V, Flavell RA, Chandawarkar RY. HSP70 Enhances Macrophage Phagocytosis by Interaction With Lipid Raft-Associated TLR-7 and Upregulating p38 MAPK and PI3K Pathways. Published online 2006.

- doi:10.1016/j.jss.2006.06.003
114. Criscitiello MF, Dickman MB, Samuel JE, de Figueiredo P. Tripping on Acid: Trans-Kingdom Perspectives on Biological Acids in Immunity and Pathogenesis. *PLoS Pathog.* 2013;9(7):e1003402. doi:10.1371/JOURNAL.PPAT.1003402
  115. Claus V, Jahraus A, Tjelle T, et al. Lysosomal enzyme trafficking between phagosomes, endosomes, and lysosomes in J774 macrophages. Enrichment of cathepsin H in early endosomes. *J Biol Chem.* 1998;273(16):9842-9851. doi:10.1074/JBC.273.16.9842
  116. Yu-Kyoung OH, Alpuche-Aranda C, Berthiaume E, Jinks T, Miller SI, Swanson JA. Rapid and complete fusion of macrophage lysosomes with phagosomes containing *Salmonella typhimurium*. *Infect Immun.* 1996;64(9):3877-3883. doi:10.1128/IAI.64.9.3877-3883.1996
  117. Nathan CF, Tsunawaki S. Secretion of toxic oxygen products by macrophages: regulatory cytokines and their effects on the oxidase. *Ciba Found Symp.* 1986;118:211-230. doi:10.1002/9780470720998.CH14
  118. Vatansever F, de Melo WCMA, Avci P, et al. Antimicrobial strategies centered around reactive oxygen species--bactericidal antibiotics, photodynamic therapy, and beyond. *FEMS Microbiol Rev.* 2013;37(6):955-989. doi:10.1111/1574-6976.12026
  119. Fernandez GJ, Ramírez-Mejía JM, Castillo JA, Urcuqui-Inchima S. Vitamin D modulates expression of antimicrobial peptides and proinflammatory cytokines to restrict Zika virus infection in macrophages. *Int Immunopharmacol.* 2023;119:110232. doi:10.1016/J.INTIMP.2023.110232
  120. Michael Niederweis, Frank Wolschendorf, Avishek Mitra ON. Mycobacteria, Metals, and the Macrophage. *Immunol Rev.* 2015;264(1):249-263. doi:10.1111/imr.12265.Mycobacteria
  121. Oeckinghaus A, Ghosh S. The NF- $\kappa$ B Family of Transcription Factors and Its Regulation. *Cold Spring Harb Perspect Biol.* 2009;1(4). doi:10.1101/CSHPERSPECT.A000034
  122. Tsuji-Takayama K, Aizawa Y, Okamoto I, et al. Interleukin-18 induces interferon- $\gamma$  production through NF- $\kappa$ B and NFAT activation in murine T helper type 1 cells. *Cell Immunol.* 1999;196(1):41-50. doi:10.1006/cimm.1999.1542
  123. Richmond A. NF- $\kappa$ B, chemokine gene transcription and tumour growth. *Nat Rev Immunol* 2002 29. 2002;2(9):664-674. doi:10.1038/nri887
  124. Tseng PH, Matsuzawa A, Zhang W, Mino T, Vignali DAA, Karin M. Different modes of TRAF3 ubiquitination selectively activate type I interferon and proinflammatory cytokine expression. *Nat Immunol.* 2010;11(1):70. doi:10.1038/NI.1819
  125. Ning S, Pagano JS, Barber GN. IRF7: activation, regulation, modification and function. *Genes Immun* 2011 126. 2011;12(6):399-414. doi:10.1038/gene.2011.21
  126. Michalska A, Blaszczyk K, Wesoly J, Bluysen HAR. A positive feedback amplifier circuit that regulates interferon (IFN)-stimulated gene expression and controls type I and type II IFN responses. *Front Immunol.* 2018;9(MAY):1135. doi:10.3389/FIMMU.2018.01135/BIBTEX
  127. Littwitz-Salomon E, Dittmer U, Sutter K. Insufficient natural killer cell responses against retroviruses: how to improve NK cell killing of retrovirus-infected cells. *Retrovirology.* 2016;13:77. doi:10.1186/s12977-016-0311-8
  128. Oriol-Tordera BI, Berdasco MI, Llano A, et al. Methylation regulation of Antiviral host factors, Interferon Stimulated Genes (ISGs) and T-cell responses associated with natural HIV control. Published online 2020. doi:10.1371/journal.ppat.1008678

129. Sercarz EE, Maverakis E. MHC-GUIDED PROCESSING: BINDING OF LARGE ANTIGEN FRAGMENTS. Published online 2003. doi:10.1038/nri1149
130. Kawasaki T, Ikegawa M, Yunoki K, et al. Alveolar macrophages instruct CD8+ T cell expansion by antigen cross-presentation in lung. *Cell Rep.* 2022;41(11):111828. doi:10.1016/j.celrep.2022.111828
131. Morris L, Graham CF, Gordon S. Macrophages in haemopoietic and other tissues of the developing mouse detected by the monoclonal antibody F4/80. *Development.* 1991;112(2):517-526. doi:10.1242/dev.112.2.517
132. Cecchini MG, Dominguez MG, Mocci S, et al. Role of colony stimulating factor-1 in the establishment and regulation of tissue macrophages during postnatal development of the mouse. *Development.* 1994;120(6):1357-1372. doi:10.1242/DEV.120.6.1357
133. Jones C V., Williams TM, Walker KA, et al. M2 macrophage polarisation is associated with alveolar formation during postnatal lung development. *Respir Res.* 2013;14(1):41. doi:10.1186/1465-9921-14-41
134. Blackwell TS, Hipps AN, Yamamoto Y, et al. NF- $\kappa$ B Signaling in Fetal Lung Macrophages Disrupts Airway Morphogenesis. *J Immunol.* 2011;187(5):2740-2747. doi:10.4049/JIMMUNOL.1101495
135. Shibata Y, Berclaz PY, Chronos ZC, Yoshida M, Whitsett JA, Trapnell BC. GM-CSF regulates alveolar macrophage differentiation and innate immunity in the lung through PU.1. *Immunity.* 2001;15(4):557-567. doi:10.1016/S1074-7613(01)00218-7
136. Lichanska AM, Hume DA. Origins and functions of phagocytes in the embryo. *Exp Hematol.* 2000;28(6):601-611. doi:10.1016/S0301-472X(00)00157-0
137. Walton NM, Sutter BM, Laywell ED, et al. Microglia Instruct Subventricular Zone Neurogenesis. doi:10.1002/glia.20419
138. Liao H, Bu WY, Wang TH, Ahmed S, Xiao ZC. Tenascin-R plays a role in neuroprotection via its distinct domains that coordinate to modulate the microglia function. *J Biol Chem.* 2005;280(9):8316-8323. doi:10.1074/JBC.M412730200
139. Bessis A, Echade CB, Bernard D, Roumier A. Microglial Control of Neuronal Death and Synaptic Properties. doi:10.1002/glia.20459
140. Orkin SH, Zon LI. Review Hematopoiesis : An Evolving Paradigm for Stem Cell Biology. *Cell.* Published online 2008:631-644. doi:10.1016/j.cell.2008.01.025
141. Ginhoux F, Greter M, Leboeuf M, et al. Fate Mapping Analysis Reveals That Adult Microglia Derive from Primitive Macrophages. *Science (80- ).* 2010;330(6005):841-845. doi:10.1126/science.1194637
142. Stremmel C, Schuchert R, Wagner F, et al. Yolk sac macrophage progenitors traffic to the embryo during defined stages of development. *Nat Commun.* 2018;9(1). doi:10.1038/s41467-017-02492-2
143. Kumaravelu P, Hook L, Morrison AM, et al. Quantitative developmental anatomy of definitive haematopoietic stem cells/long-term repopulating units (HSC/RUs): role of the aorta-gonad-mesonephros (AGM) region and the yolk sac in colonisation of the mouse embryonic liver. *Development.* 2002;129(21):4891-4899. doi:10.1242/DEV.129.21.4891
144. Yona S, Kim KW, Wolf Y, et al. Fate mapping reveals origins and dynamics of monocytes and tissue macrophages under homeostasis. *Immunity.* 2013;38(1):79-91. doi:10.1016/J.IMMUNI.2012.12.001
145. Hoeffel G, Wang Y, Greter M, et al. Adult Langerhans cells derive predominantly from embryonic fetal liver monocytes with a minor contribution of yolk sac-derived

- macrophages. *J Exp Med*. 2012;209(6):1167-1181. doi:10.1084/jem.20120340
146. McGrath KE, Frame JM, Fegan KH, et al. Distinct Sources of Hematopoietic Progenitors Emerge before HSCs and Provide Functional Blood Cells in the Mammalian Embryo. *Cell Rep*. Published online 2015. doi:10.1016/j.celrep.2015.05.036
  147. Kurotaki D, Sasaki H, Tamura T. Transcriptional control of monocyte and macrophage development. *Int Immunol*. 2017;29(3):97-107. doi:10.1093/intimm/dxx016
  148. Geissmann F, Manz MG, Jung S, et al. Development of monocytes, macrophages and dendritic cells. 2010;327(5966):656-661.
  149. Bowden DH. The pulmonary macrophage. *Environ Health Perspect*. 1976;Vol.16(August):55-60. doi:10.1289/ehp.761655
  150. Jordan FL, Eric Thomas W. Brain macrophages: questions of origin and interrelationship. *Brain Res Rev*. 1988;13(2):165-178. doi:10.1016/0165-0173(88)90019-7
  151. Treves AJ. the Origin of Monocyte-Macrophage Heterogeneity : Possible Alternatives. *Med Hypotheses*. 1984;14:335-346.
  152. Ginhoux F, Guilliams M. Tissue-Resident Macrophage Ontogeny and Homeostasis. *Immunity*. 2016;44(3):439-449. doi:10.1016/j.immuni.2016.02.024
  153. Goldmann T, Wieghofer P, Jordão MJC, et al. Origin, fate and dynamics of macrophages at central nervous system interfaces. *Nat Immunol*. 2016;17(7):797-805. doi:10.1038/ni.3423
  154. Heidt T, Courties G, Dutta P, et al. Differential contribution of monocytes to heart macrophages in steady-state and after myocardial infarction. *Circ Res*. 2014;115(2):284-295. doi:10.1161/CIRCRESAHA.115.303567
  155. Kennedy DW, Abkowitz JL. Kinetics of central nervous system microglial and macrophage engraftment: Analysis using a transgenic bone marrow transplantation model. *Blood*. 1997;90(3):986-993. doi:10.1182/blood.v90.3.986.986\_986\_993
  156. Höfer T, Busch K, Klapproth K, Rodewald HR. Fate Mapping and Quantitation of Hematopoiesis in Vivo. *Annu Rev Immunol*. 2016;34:449-478. doi:10.1146/annurev-immunol-032414-112019
  157. Hoeffel G, Ginhoux F. Fetal monocytes and the origins of tissue-resident macrophages. *Cell Immunol*. 2018;330:5-15. doi:10.1016/J.CELLIMM.2018.01.001
  158. Scott CL, Henri S, Malissen B, et al. Constant replenishment from circulating monocytes maintains the macrophage pool in the intestine of adult mice. *Nat Immunol*. 2014;15(10):929-937. doi:10.1038/ni.2967
  159. Liu Z, Gu Y, Chakarov S, et al. Fate Mapping via Ms4a3-Expression History Traces Monocyte-Derived Cells. *Cell*. 2019;178(6):1509-1525.e19. doi:10.1016/J.CELL.2019.08.009
  160. Chakarov S, Lim HY, Tan L, et al. Two distinct interstitial macrophage populations coexist across tissues in specific subtissular niches. *Science (80- )*. 2019;363(6432):eaau0964. doi:10.1126/science.aau0964
  161. Guilliams M, Scott CL. Does niche competition determine the origin of tissue-resident macrophages? *Nat Rev Immunol*. 2017;17(7):451-460. doi:10.1038/nri.2017.42
  162. Mass E, Nimmerjahn F, Kierdorf K, Schlitzer A. Tissue-specific macrophages: how they develop and choreograph tissue biology. *Nat Rev Immunol* 2023. Published online March 15, 2023;1-17. doi:10.1038/s41577-023-00848-y
  163. Aziz A, Soucie E, Sarrazin S, Sieweke MH. MafB/c-Maf deficiency enables self-renewal of differentiated functional macrophages. *Science*. 2009;326(5954):867-871.

- doi:10.1126/SCIENCE.1176056
164. Hashimoto D, Chow A, Noizat C, et al. Tissue-resident macrophages self-maintain locally throughout adult life with minimal contribution from circulating monocytes. *Immunity*. 2013;38(4):792-804. doi:10.1016/j.immuni.2013.04.004
  165. Scott CL, Zheng F, De Baetselier P, et al. Bone marrow-derived monocytes give rise to self-renewing and fully differentiated Kupffer cells. *Nat Commun*. 2016;7:1-10. doi:10.1038/ncomms10321
  166. Davies LC, Rosas M, Smith PJ, Fraser DJ, Jones SA, Taylor PR. A quantifiable proliferative burst of tissue macrophages restores homeostatic macrophage populations after acute inflammation. *Eur J Immunol*. 2011;41(8):2155-2164. doi:10.1002/eji.201141817
  167. Dick SA, Macklin JA, Nejat S, et al. Self-renewing resident cardiac macrophages limit adverse remodeling following myocardial infarction. *Nat Immunol* /. 2019;20:29-39. doi:10.1038/s41590-018-0272-2
  168. Jose MD, Le Meur Y, Atkins RC, Chadban SJ. Blockade of macrophage colony-stimulating factor reduces macrophage proliferation and accumulation in renal allograft rejection. *Am J Transplant*. 2003;3(3):294-300. doi:10.1034/j.1600-6143.2003.00068.x
  169. Jenkins SJ, Ruckerl D, Thomas GD, et al. IL-4 directly signals tissue-resident macrophages to proliferate beyond homeostatic levels controlled by CSF-1. *J Exp Med*. 2013;210(11):2477-2491. doi:10.1084/jem.20121999
  170. Jenkins SJ, Ruckerl D, Cook PC, et al. Local macrophage proliferation, rather than recruitment from the blood, is a signature of T H2 inflammation. *Science (80- )*. 2011;332(6035):1284-1288. doi:10.1126/science.1204351
  171. Varol C, Mildner A, Jung S. Macrophages: Development and Tissue Specialization. Published online 2015. doi:10.1146/annurev-immunol-032414-112220
  172. Blériot C, Chakarov S, Ginhoux F. Determinants of Resident Tissue Macrophage Identity and Function. *Immunity*. 2020;52(6):957-970. doi:10.1016/J.IMMUNI.2020.05.014
  173. Gosselin D, Link VM, Romanoski CE, et al. Environment drives selection and function of enhancers controlling tissue-specific macrophage identities. *Cell*. 2014;159(6):1327-1340. doi:10.1016/j.cell.2014.11.023
  174. Hammond TR, Dufort C, Dissing-Olesen L, et al. Single-Cell RNA Sequencing of Microglia throughout the Mouse Lifespan and in the Injured Brain Reveals Complex Cell-State Changes. *Immunity*. 2019;50(1):253-271.e6. doi:10.1016/j.immuni.2018.11.004
  175. Gordon S, Plüddemann A. Tissue macrophages: heterogeneity and functions. *BMC Biol*. 2017;15(1). doi:10.1186/S12915-017-0392-4
  176. Li Q, Barres BA. Microglia and macrophages in brain homeostasis and disease. *Nat Rev Immunol* 2017 184. 2017;18(4):225-242. doi:10.1038/nri.2017.125
  177. Gibbings SL, Thomas SM, Atif SM, et al. Three Unique Interstitial Macrophages in the Murine Lung at Steady State. 2017;57(1):66-76. doi:10.1165/rcmb.2016-0361OC
  178. MacParland SA, Liu JC, Ma XZ, et al. Single cell RNA sequencing of human liver reveals distinct intrahepatic macrophage populations. *Nat Commun*. 2018;9(1):1-21. doi:10.1038/s41467-018-06318-7
  179. Hettlinger J, Richards DM, Hansson J, et al. Origin of monocytes and macrophages in a committed progenitor. *Nat Immunol*. 2013;14(8):821-830. doi:10.1038/ni.2638
  180. Lai SM, Sheng J, Gupta P, et al. Organ-Specific Fate, Recruitment, and Refilling Dynamics of Tissue-Resident Macrophages during Blood-Stage Malaria. *Cell Rep*.

- 2018;25(11):3099-3109.e3. doi:10.1016/j.celrep.2018.11.059
181. Davies LC, Jenkins SJ, Allen JE, Taylor PR. Tissue-resident macrophages. *Nat Immunol.* 2013;14(10):986-995. doi:10.1038/ni.2705
  182. Yan J, Horng T. Lipid Metabolism in Regulation of Macrophage Functions Trends in Cell Biology. *Trends Cell Biol.* 2020;30(12). doi:10.1016/j.tcb.2020.09.006
  183. Chistiakov DA, Myasoedova VA, Revin V V, Orekhov AN, Bobryshev Y V. The impact of interferon-regulatory factors to macrophage differentiation and polarization into M1 and M2. Published online 2017. doi:10.1016/j.imbio.2017.10.005
  184. Grinberg S, Hasko G, Wu D, Leibovich SJ. Suppression of PLC $\beta$ 2 by Endotoxin Plays a Role in the Adenosine A2A Receptor-Mediated Switch of Macrophages from an Inflammatory to an Angiogenic Phenotype. *Am J Pathol.* 2009;175(6):2439-2453. doi:10.2353/AJPATH.2009.090290
  185. Murray PJ. Macrophage Polarization. <https://doi.org/10.1146/annurev-physiol-022516-034339>. 2017;79:541-566. doi:10.1146/ANNUREV-PHYSIOL-022516-034339
  186. Wang X, Sathe AA, Smith GR, et al. Heterogeneous origins and functions of mouse skeletal muscle-resident macrophages. *Proc Natl Acad Sci U S A.* 2020;117(34):20729-20740. doi:10.1073/PNAS.1915950117
  187. Brigitte M, Schilte C, Plonquet A, et al. Muscle resident macrophages control the immune cell reaction in a mouse model of notexin-induced myoinjury. *Arthritis Rheum.* 2010;62(1):268-279. doi:10.1002/art.27183
  188. Ochoa O, Sun D, Reyes-Reyna SM, et al. Delayed angiogenesis and VEGF production in CCR2 $^{-/-}$  mice during impaired skeletal muscle regeneration. *Am J Physiol - Regul Integr Comp Physiol.* 2007;293(2):651-661. doi:10.1152/ajpregu.00069.2007
  189. D'Alessandro E, Scaf B, Munts C, et al. Coagulation factor xa induces proinflammatory responses in cardiac fibroblasts via activation of protease-activated receptor-1. *Cells.* 2021;10(11):1-12. doi:10.3390/cells10112958
  190. Geissmann F. Blood Monocytes Consist of Two Principal Subsets with Distinct Migratory Properties. *Immunity.* Published online 2003. doi:10.1016/j.watres.2017.11.031
  191. Ingersoll MA, Platt AM, Potteaux S, Randolph GJ. Innate immune cell trafficking Monocyte trafficking in acute and chronic inflammation. doi:10.1016/j.it.2011.05.001
  192. Contreras-Shannon V, Ochoa O, Reyes-Reyna SM, et al. Fat accumulation with altered inflammation and regeneration in skeletal muscle of CCR2 $^{-/-}$  mice following ischemic injury. *Am J Physiol - Cell Physiol.* 2007;292(2):953-967. doi:10.1152/ajpcell.00154.2006
  193. Warren GL, Hulderman T, Mishra D, et al. Chemokine receptor CCR2 involvement in skeletal muscle regeneration. *FASEB J.* 2005;19(3):1-23. doi:10.1096/fj.04-2421fje
  194. Sun D, Martinez CO, Ochoa O, et al. Bone marrow-derived cell regulation of skeletal muscle regeneration. *FASEB J.* 2009;23(2):382-395. doi:10.1096/fj.07-095901
  195. Varga T, Mounier R, Gogolak P, Poliska S, Chazaud B, Nagy L. Tissue LyC6 $^{-}$  Macrophages Are Generated in the Absence of Circulating LyC6 $^{-}$  Monocytes and Nur77 in a Model of Muscle Regeneration. *J Immunol.* 2013;191(11):5695-5701. doi:10.4049/jimmunol.1301445
  196. Saclier M, Yacoub-Youssef H, Mackey AL, et al. Differentially activated macrophages orchestrate myogenic precursor cell fate during human skeletal muscle regeneration. *Stem Cells.* 2013;31(2):384-396. doi:10.1002/stem.1288
  197. Arnold L, Henry A, Poron F, et al. Inflammatory monocytes recruited after skeletal muscle injury switch into antiinflammatory macrophages to support myogenesis. *J Exp*

- Med.* 2007;204(5):1057-1069. doi:10.1084/jem.20070075
198. Mounier R, Théret M, Arnold L, et al. AMPK $\alpha$ 1 regulates macrophage skewing at the time of resolution of inflammation during skeletal muscle regeneration. *Cell Metab.* 2013;18(2):251-264. doi:10.1016/j.cmet.2013.06.017
  199. Ruffell D, Mourkioti F, Gambardella A, et al. A CREB-C/EBP $\beta$  cascade induces M2 macrophage-specific gene expression and promotes muscle injury repair. *Proc Natl Acad Sci U S A.* 2009;106(41):17475-17480. doi:10.1073/pnas.0908641106
  200. Li Y-P, Schwartz RJ. TNF- $\alpha$  regulates early differentiation of C2C12 myoblasts in an autocrine fashion. *FASEB J.* 2001;15(8):1413-1415. doi:10.1096/fj.00-0632fje
  201. Suelves M, Lluís F, Ruiz V, Nebreda AR, Muñoz-Cánoves P. Phosphorylation of MRF4 transactivation domain by p38 mediates repression of specific myogenic genes. *EMBO J.* 2004;23(2):365-375. doi:10.1038/sj.emboj.7600056
  202. Chen SE, Jin B, Li YP. TNF- $\alpha$  regulates myogenesis and muscle regeneration by activating p38 MAPK. *Am J Physiol - Cell Physiol.* 2007;292(5):1660-1671. doi:10.1152/ajpcell.00486.2006
  203. Guttridge DC, Mayo MW, Madrid L V., Wang CY, Baldwin J. NF- $\kappa$ B-induced loss of MyoD messenger RNA: Possible role in muscle decay and cachexia. *Science (80- ).* 2000;289(5488):2363-2365. doi:10.1126/science.289.5488.2363
  204. Palacios D, Mozzetta C, Consalvi S, et al. TNF/p38 $\alpha$ /polycomb signaling to Pax7 locus in satellite cells links inflammation to the epigenetic control of muscle regeneration. *Cell Stem Cell.* 2010;7(4):455-469. doi:10.1016/j.stem.2010.08.013
  205. WARREN GL, HULDERMAN T, JENSEN N, et al. Physiological role of tumor necrosis factor  $\alpha$  in traumatic muscle injury. *FASEB J.* 2002;16(12):1630-1632. doi:10.1096/fj.02-0187fje
  206. Orecchioni M, Ghosheh Y, Pramod AB, Ley K. Macrophage polarization: Different gene signatures in M1(Lps+) vs. Classically and M2(LPS-) vs. Alternatively activated macrophages. *Front Immunol.* 2019;10(MAY):1084. doi:10.3389/FIMMU.2019.01084/FULL
  207. Rigamonti E, Touvier T, Clementi E, Manfredi AA, Brunelli S, Rovere-Querini P. Requirement of Inducible Nitric Oxide Synthase for Skeletal Muscle Regeneration after Acute Damage. *J Immunol.* 2013;190(4):1767-1777. doi:10.4049/jimmunol.1202903
  208. Wang X, Wu H, Zhang Z, et al. Effects of interleukin-6, leukemia inhibitory factor, and ciliary neurotrophic factor on the proliferation and differentiation of adult human myoblasts. *Cell Mol Neurobiol.* 2008;28(1):113-124. doi:10.1007/s10571-007-9247-9
  209. Luo G, Hershko DD, Robb BW, Wray CJ, Hasselgren PO. IL-1 $\beta$  stimulates IL-6 production in cultured skeletal muscle cells through activation of MAP kinase signaling pathway and NF- $\kappa$ B. *Am J Physiol - Regul Integr Comp Physiol.* 2003;284(5 53-5):1249-1254. doi:10.1152/AJPREGU.00490.2002/ASSET/IMAGES/LARGE/H60531678004.JPEG
  210. Broussard SR, Mccusker RH, Novakofski JE, et al. Cytokine-hormone interactions: Tumor necrosis factor  $\alpha$  impairs biologic activity and downstream activation signals of the insulin-like growth factor I receptor in myoblasts. *Endocrinology.* 2003;144(7):2988-2996. doi:10.1210/en.2003-0087
  211. JAMES R. FLORINI, DAINA Z. EWTON SAC. Growth hormone, the insulin-like growth factor system, and the kidney. *Endocr Rev.* 1996;17(5):423-480. doi:10.1210/er.17.5.423

212. Tonkin J, Temmerman L, Sampson RD, et al. Monocyte/macrophage-derived IGF-1 orchestrates murine skeletal muscle regeneration and modulates autocrine polarization. *Mol Ther*. 2015;23(7):1189-1200. doi:10.1038/mt.2015.66
213. Lu H, Huang D, Saederup N, Charo IF, Ransohoff RM, Zhou L. Macrophages recruited via CCR2 produce insulin-like growth factor-1 to repair acute skeletal muscle injury. *FASEB J*. 2011;25(1):358-369. doi:10.1096/fj.10-171579
214. Delaney K, Kasprzycka P, Ciemerych MA, Zimowska M. The role of TGF- $\beta$ 1 during skeletal muscle regeneration. *Cell Biol Int*. 2017;41(7):706-715. doi:10.1002/cbin.10725
215. Rodgers BD, Wiedeback BD, Hoversten KE, Jackson MF, Walker RG, Thompson TB. Myostatin Stimulates, Not Inhibits, C2C12 Myoblast Proliferation. Published online 2014. doi:10.1210/en.2013-2107
216. Olson EN, Sternberg E, Jing Shan Hu, Spizz G, Wilcox C. Regulation of myogenic differentiation by type  $\beta$  transforming growth factor. *J Cell Biol*. 1986;103(5):1799-1805. doi:10.1083/jcb.103.5.1799
217. Schabort EJ, van der Merwe M, Loos B, Moore FP, Niesler CU. TGF- $\beta$ 's delay skeletal muscle progenitor cell differentiation in an isoform-independent manner. *Exp Cell Res*. 2009;315(3):373-384. doi:10.1016/j.yexcr.2008.10.037
218. Zentella A, Massague J. Transforming growth factor  $\beta$  induces myoblast differentiation in the presence of mitogens. *Proc Natl Acad Sci U S A*. 1992;89(11):5176-5180. doi:10.1073/pnas.89.11.5176
219. Arahata K, Engel AG. Monoclonal antibody analysis of mononuclear cells in myopathies. I: Quantitation of subsets according to diagnosis and sites of accumulation and demonstration and counts of muscle fibers invaded by T cells. *Ann Neurol*. 1984;16(2):193-208. doi:10.1002/ana.410160206
220. Carnwath JW, Shotton DM. Muscular dystrophy in the mdx mouse: Histopathology of the soleus and extensor digitorum longus muscles. *J Neurol Sci*. 1987;80(1):39-54. doi:10.1016/0022-510X(87)90219-X
221. Wehling M, Spencer MJ, Tidball JG. A nitric oxide synthase transgene ameliorates muscular dystrophy in mdx mice. *J Cell Biol*. 2001;155(1):123-131. doi:10.1083/jcb.200105110
222. Evans NP, Misyak SA, Robertson JL, Bassaganya-Riera J, Grange RW. Dysregulated intracellular signaling and inflammatory gene expression during initial disease onset in duchenne muscular dystrophy. *Am J Phys Med Rehabil*. 2009;88(6):502-522. doi:10.1097/PHM.0b013e3181a5a24f
223. Mojumdar K, Liang F, Giordano C, et al. Inflammatory monocytes promote progression of Duchenne muscular dystrophy and can be therapeutically targeted via CCR2. *EMBO Mol Med*. 2014;6(11):1476-1492. doi:10.15252/emmm.201403967
224. Zhao W, Wang X, Ransohoff RM, Zhou L. CCR2 deficiency does not provide sustained improvement of muscular dystrophy in mdx5cv mice. *FASEB J*. 2017;31(1):35-46. doi:10.1096/fj.201600619R
225. Hodgetts S, Radley H, Davies M, Grounds MD. Reduced necrosis of dystrophic muscle by depletion of host neutrophils, or blocking TNF $\alpha$  function with Etanercept in mdx mice. doi:10.1016/j.nmd.2006.06.011
226. A Farini, M Meregalli, M Belicchi, M Battistelli, D Parolini, G D'Antona, MGavina LO. T and B lymphocyte depletion has a marked effect on the fibrosis of dystrophic skeletal muscles in the scid/mdx mouse. *J Pathol*. 2007;213(July):229-238. doi:10.1002/path

227. Giordano, C., Mojumdar, K., Liang, F., Lemaire, C., Li, T., Richardson, J., Divangahi, M., Qureshi, S., & Petrof BJ. Toll-like receptor 4 ablation in mdx mice reveals innate immunity as a therapeutic target in Duchenne muscular dystrophy. *Hum Mol Genet.* 2015;24(8):2147-2162. doi:10.1093/HMG/DDU735
228. Mojumdar K, Giordano C, Lemaire C, et al. Divergent impact of Toll-like receptor 2 deficiency on repair mechanisms in healthy muscle versus Duchenne muscular dystrophy. *J Pathol.* 2016;239(1):10-22. doi:10.1002/path.4689
229. Grounds MD, Radley HG, Lynch GS, Nagaraju K, De Luca A. Towards developing standard operating procedures for pre-clinical testing in the mdx mouse model of Duchenne muscular dystrophy. *Neurobiol Dis.* 2008;31(1):1-19. doi:10.1016/j.nbd.2008.03.008
230. Villalta SA, Nguyen HX, Deng B, Gotoh T, Tidball JG. Shifts in macrophage phenotypes and macrophage competition for arginine metabolism affect the severity of muscle pathology in muscular dystrophy. *Hum Mol Genet.* 2009;18(3):482-496. doi:10.1093/hmg/ddn376
231. Lemos DR, Babaeijandaghi F, Low M, et al. Nilotinib reduces muscle fibrosis in chronic muscle injury by promoting TNF-mediated apoptosis of fibro/adipogenic progenitors. *Nat Med* 2015 217. 2015;21(7):786-794. doi:10.1038/NM.3869
232. De Paepe B, Creus KK, Martin JJ, De Bleecker JL. Upregulation of chemokines and their receptors in duchenne muscular dystrophy: Potential for attenuation of myofiber necrosis. *Muscle and Nerve.* 2012;46(6):914-916. doi:10.1002/mus.23481
233. Howard ZM, Lowe J, Blatnik AJ, et al. Early Inflammation in Muscular Dystrophy Differs between Limb and Respiratory Muscles and Increases with Dystrophic Severity. *Am J Pathol.* 2021;191(4):730-747. doi:10.1016/J.AJP.2021.01.008
234. Hamoudi D, Marcadet L, Boulanger AP, et al. An anti-RANKL treatment reduces muscle inflammation and dysfunction and strengthens bone in dystrophic mice. *Hum Mol Genet.* 2019;28(18):3101-3112. doi:10.1093/HMG/DDZ124
235. Villalta SA, Deng B, Rinaldi C, Wehling-Henricks M, Tidball JG. IFN- $\gamma$  Promotes Muscle Damage in the mdx Mouse Model of Duchenne Muscular Dystrophy by Suppressing M2 Macrophage Activation and Inhibiting Muscle Cell Proliferation . *J Immunol.* 2011;187(10):5419-5428. doi:10.4049/jimmunol.1101267
236. Nitahara-Kasahara Y, Hayashita-Kinoh H, Chiyo T, et al. Dystrophic mdx mice develop severe cardiac and respiratory dysfunction following genetic ablation of the anti-inflammatory cytokine IL-10. *Hum Mol Genet.* 2014;23(15):3990-4000. doi:10.1093/HMG/DDU113
237. Villalta SA, Rinaldi C, Deng B, Liu G, Fedor B, Tidball JG. Interleukin-10 reduces the pathology of mdx muscular dystrophy by deactivating M1 macrophages and modulating macrophage phenotype. *Hum Mol Genet.* 2011;20(4):790. doi:10.1093/HMG/DDQ523
238. Desguerre I, Mayer M, Leturcq F, Barbet JP, Gherardi RK, Christov C. Endomysial Fibrosis in Duchenne Muscular Dystrophy: A Marker of Poor Outcome Associated With Macrophage Alternative Activation. *J Neuropathol Exp Neurol.* 2009;68(7):762-773. doi:10.1097/NEN.0B013E3181AA31C2
239. Kharraz Y, Guerra J, Pessina P, Serrano AL, Muñoz-Cánoves P. Understanding the Process of Fibrosis in Duchenne Muscular Dystrophy. Published online 2014. doi:10.1155/2014/965631
240. Serrano AL, Muñoz-Cánoves P. Regulation and dysregulation of fibrosis in skeletal

- muscle. Published online 2010. doi:10.1016/j.yexcr.2010.05.035
241. Loomis T, Hu L-Y, Wohlgemuth RP, Chellakudam RR, Muralidharan PD, Smith LR. Matrix stiffness and architecture drive fibro-adipogenic progenitors' activation into myofibroblasts. *Sci Reports* /. 123AD;12:13582. doi:10.1038/s41598-022-17852-2
  242. Contreras O, Rossi FMV, Theret M. Origins, potency, and heterogeneity of skeletal muscle fibro-adipogenic progenitors—time for new definitions. *Skelet Muscle* 2021 111. 2021;11(1):1-25. doi:10.1186/S13395-021-00265-6
  243. Wosczyzna MN, Konishi CT, Perez Carbajal EE, et al. Mesenchymal Stromal Cells Are Required for Regeneration and Homeostatic Maintenance of Skeletal Muscle. doi:10.1016/j.celrep.2019.04.074
  244. Bernasconi P, Torchiana E, Confalonieri P, et al. Expression of transforming growth factor- $\beta$ 1 in dystrophic patient muscles correlates with fibrosis. Pathogenetic role of a fibrogenic cytokine. *J Clin Invest*. 1995;96(2):1137-1144. doi:10.1172/JCI118101
  245. Zhou L, Lu H. Targeting Fibrosis in Duchenne Muscular Dystrophy. *J Neuropathol Exp Neurol*. 2010;69(8):771-776. doi:10.1097/NEN.0B013E3181E9A34B
  246. Taniguti APT, Pertille A, Matsumura CY, Neto HS, Marques MJ. Prevention of muscle fibrosis and myonecrosis in mdx mice by suramin, a TGF- $\beta$ 1 blocker. *Muscle and Nerve*. 2011;43(1):82-87. doi:10.1002/mus.21869
  247. Dadgar S, Wang Z, Johnston H, et al. Asynchronous remodeling is a driver of failed regeneration in Duchenne muscular dystrophy. *J Cell Biol*. 2014;207(1):139-158. doi:10.1083/jcb.201402079
  248. Pegoraro E, Hoffman EP, Piva L, et al. SPP1 genotype is a determinant of disease severity in Duchenne muscular dystrophy. *Neurology*. 2011;76(3):219-226. doi:10.1212/WNL.0B013E318207AFEB
  249. Flanigan KM, Ceco E, Lamar KM, et al. LTBP4 genotype predicts age of ambulatory loss in duchenne muscular dystrophy. *Ann Neurol*. 2013;73(4):481-488. doi:10.1002/ANA.23819
  250. Vetrone SA, Montecino-Rodriguez E, Kudryashova E, et al. Osteopontin promotes fibrosis in dystrophic mouse muscle by modulating immune cell subsets and intramuscular TGF- $\beta$ . *J Clin Invest*. 2009;119(6):1583-1594. doi:10.1172/JCI37662
  251. Gibertini S, Zanotti S, Savadori P, et al. Fibrosis and inflammation are greater in muscles of beta-sarcoglycan-null mouse than mdx mouse. *Cell Tissue Res*. 2014;356(2):427-443. doi:10.1007/S00441-014-1854-4/FIGURES/11
  252. Kramerova I, Kumagai-Cress C, Ermolova N, et al. Spp1 (osteopontin) promotes TGF $\beta$  processing in fibroblasts of dystrophin-deficient muscles through matrix metalloproteinases. *Hum Mol Genet*. 2019;28(20):3431-3442. doi:10.1093/HMG/DDZ181
  253. Heydemann A, Ceco E, Lim JE, et al. Latent TGF- $\beta$ -binding protein 4 modifies muscular dystrophy in mice. *J Clin Invest*. 2009;119(12):3703-3712. doi:10.1172/JCI39845
  254. Juban G, Saclier M, Yacoub-Youssef H, et al. AMPK Activation Regulates LTBP4-Dependent TGF- $\beta$ 1 Secretion by Pro-inflammatory Macrophages and Controls Fibrosis in Duchenne Muscular Dystrophy. *Cell Rep*. 2018;25(8):2163-2176.e6. doi:10.1016/J.CELREP.2018.10.077
  255. Grounds MD, Torrisi J. Anti-TNF $\alpha$  (Remicade®) therapy protects dystrophic skeletal muscle from necrosis. *FASEB J*. 2004;18(6):676-682. doi:10.1096/fj.03-1024com
  256. Radley HG, Davies MJ, Grounds MD. Reduced muscle necrosis and long-term benefits in dystrophic mdx mice after cV1q (blockade of TNF) treatment. *Neuromuscul Disord*.

- 2008;18(3):227-238. doi:10.1016/j.nmd.2007.11.002
257. Spencer MJ, Marino MW, Winckler WM. Altered pathological progression of diaphragm and quadriceps muscle in TNF-deficient, dystrophin-deficient mice. *Neuromuscul Disord.* 2000;10(8):612-619. doi:10.1016/S0960-8966(00)00160-7
258. Sacco A, Mourkioti F, Tran R, et al. Short Telomeres and Stem Cell Exhaustion Model Duchenne Muscular Dystrophy in mdx/mTR Mice. *Cell.* 2010;143(7):1059-1071. doi:10.1016/J.CELL.2010.11.039
259. Coppé J-P, Patil CK, Rodier F, et al. Senescence-Associated Secretory Phenotypes Reveal Cell-Nonautonomous Functions of Oncogenic RAS and the p53 Tumor Suppressor. doi:10.1371/journal.pbio.0060301
260. Madaro L, Torcinaro A, de Bardi M, et al. Macrophages fine tune satellite cell fate in dystrophic skeletal muscle of mdx mice. *PLoS Genet.* 2019;15(10). doi:10.1371/journal.pgen.1008408
261. Kuang S, Kuroda K, Le Grand F, Rudnicki MA. Asymmetric Self-Renewal and Commitment of Satellite Stem Cells in Muscle. *Cell.* 2007;129(5):999-1010. doi:10.1016/J.CELL.2007.03.044
262. Chang NC, Chevalier FP, Rudnicki MA. Satellite Cells in Muscular Dystrophy - Lost in Polarity. *Trends Mol Med.* 2016;22(6):479-496. doi:10.1016/j.molmed.2016.04.002
263. Tierney MT, Aydogdu T, Sala D, et al. STAT3 signaling controls satellite cell expansion and skeletal muscle repair. *Nat Med.* 2014;20(10):1182. doi:10.1038/NM.3656
292. Park MD, Silvin A, Ginhoux F, Merad M, Lipschultz J. Macrophages in health and disease. doi:10.1016/j.cell.2022.10.007
301. Babaeijandaghi F, Cheng R, Kajabadi N, et al. Metabolic reprogramming of skeletal muscle by resident macrophages points to CSF1R inhibitors as muscular dystrophy therapeutics. *Sci Transl Med.* 2022;14(651). doi:10.1126/scitranslmed.abg7504
346. Martin AA, Thompson BR, Hahn D, et al. Cardiac Sarcomere Signaling in Health and Disease. *Int J Mol Sci.* 2022;23(24). doi:10.3390/ijms232416223
347. Epelman S, Lavine KJ, Beaudin AE, et al. Embryonic and adult-derived resident cardiac macrophages are maintained through distinct mechanisms at steady state and during inflammation. *Immunity.* 2014;40(1):91-104. doi:10.1016/j.immuni.2013.11.019
348. Lavine KJ, Epelman S, Uchida K, et al. Distinct macrophage lineages contribute to disparate patterns of cardiac recovery and remodeling in the neonatal and adult heart. *Proc Natl Acad Sci U S A.* 2014;111(45):16029-16034. doi:10.1073/pnas.1406508111
349. Martini E, Kunderfranco P, Peano C, et al. Single-Cell Sequencing of Mouse Heart Immune Infiltrate in Pressure Overload-Driven Heart Failure Reveals Extent of Immune Activation. *Circulation.* 2019;140(25):2089-2107. doi:10.1161/CIRCULATIONAHA.119.041694
350. Wong NR, Mohan J, Kopecky BJ, et al. Resident cardiac macrophages mediate adaptive myocardial remodeling. *Immunity.* 2021;54(9):2072-2088.e7. doi:10.1016/j.immuni.2021.07.003
351. Dangain J, Vrbova G. Muscle development in mdx mutant mice. *Muscle Nerve.* 1984;7(9):700-704. doi:10.1002/MUS.880070903
352. COULTON GR, MORGAN JE, PARTRIDGE TA, SLOPER JC. THE mdx MOUSE SKELETAL MUSCLE MYOPATHY: I. A HISTOLOGICAL, MORPHOMETRIC AND BIOCHEMICAL INVESTIGATION. *Neuropathol Appl Neurobiol.* 1988;14(1):53-70. doi:10.1111/J.1365-2990.1988.TB00866.X

353. Pastoret C, Sebillé A. Mdx Mice Show Progressive Weakness and Muscle Deterioration With Age. *J Neurol Sci.* 1995;129(2):97-105. doi:10.1016/0022-510X(94)00276-T
354. Lynch GS, Rafael JA, Hinkle RT, Cole NM, Chamberlain JS, Faulkner JA. Contractile properties of diaphragm muscle segments from old mdx and old transgenic mdx mice. *Am J Physiol - Cell Physiol.* 1997;272(6 41-6). doi:10.1152/ajpcell.1997.272.6.c2063
355. Ishizaki M, Suga T, Kimura E, et al. Mdx respiratory impairment following fibrosis of the diaphragm. *Neuromuscul Disord.* 2008;18(4):342-348. doi:10.1016/j.nmd.2008.02.002
356. Antonczyk A, Krist B, Sajek M, et al. Direct inhibition of IRF-dependent transcriptional regulatory mechanisms associated with disease. *Front Immunol.* 2019;10(MAY):1-23. doi:10.3389/fimmu.2019.01176
357. De Schepper S, Verheijden S, Aguilera-Lizarraga J, et al. Self-Maintaining Gut Macrophages Are Essential for Intestinal Homeostasis. *Cell.* 2018;175(2):400-415.e13. doi:10.1016/j.cell.2018.07.048
358. Schyns J, Bai Q, Ruscitti C, et al. Non-classical tissue monocytes and two functionally distinct populations of interstitial macrophages populate the mouse lung. *Nat Commun.* 2019;10(1). doi:10.1038/s41467-019-11843-0
359. Fonseca MI, Chu SH, Hernandez MX, et al. Cell-specific deletion of C1qa identifies microglia as the dominant source of C1q in mouse brain. *J Neuroinflammation.* 2017;14(1):1-15. doi:10.1186/s12974-017-0814-9
360. Van Hove H, Antunes ARP, De Vlaminck K, Scheyltjens I, Van Ginderachter JA, Movahedi K. Identifying the variables that drive tamoxifen-independent CreERT2 recombination: Implications for microglial fate mapping and gene deletions. *Eur J Immunol.* 2020;50(3):459-463. doi:10.1002/eji.201948162
361. COULIS G, Jaime D, Guerrero-Juarez C, et al. Single-cell and spatial transcriptomics identify a macrophage population associated with skeletal muscle fibrosis. *bioRxiv.* Published online 2023:2023.04.18.537253. <https://www.biorxiv.org/content/10.1101/2023.04.18.537253v1> <https://www.biorxiv.org/content/10.1101/2023.04.18.537253v1.abstract>
362. Liang F, Giordano C, Shang D, Li Q, Petrof BJ. The dual CCR2/CCR5 chemokine receptor antagonist Cenriciviroc reduces macrophage infiltration and disease severity in Duchenne muscular dystrophy (Dmdmdx-4Cv) mice. *PLoS One.* 2018;13(3). doi:10.1371/JOURNAL.PONE.0194421
363. Fu J, Wang D, Mei D, et al. Macrophage mediated biomimetic delivery system for the treatment of lung metastasis of breast cancer. *J Control Release.* 2015;204:11-19. doi:10.1016/j.jconrel.2015.01.039
364. Guo L, Zhang Y, Yang Z, et al. Tunneling nanotubular expressways for ultrafast and accurate m1 macrophage delivery of anticancer drugs to metastatic ovarian carcinoma. *ACS Nano.* 2019;13(2):1078-1096. doi:10.1021/acsnano.8b08872
365. Li S, Feng S, Ding L, et al. Nanomedicine engulfed by macrophages for targeted tumor therapy. *Int J Nanomedicine.* 2016;11:4107-4124. doi:10.2147/IJN.S110146
366. Novak JS, Hogarth MW, Boehler JF, et al. Myoblasts and macrophages are required for therapeutic morpholino antisense oligonucleotide delivery to dystrophic muscle. *Nat Commun.* 2017;8(1):1-13. doi:10.1038/s41467-017-00924-7
367. Yi YS. Folate receptor-targeted diagnostics and therapeutics for inflammatory diseases. *Immune Netw.* 2016;16(6):337-343. doi:10.4110/in.2016.16.6.337

## **Copy right**

Table 1.3 is adapted from reference 181, 182 and 109.

Figure 1.2 is adapted from reference 9.

Supplementary Information (SI) Appendix: Supplementary tables and figures

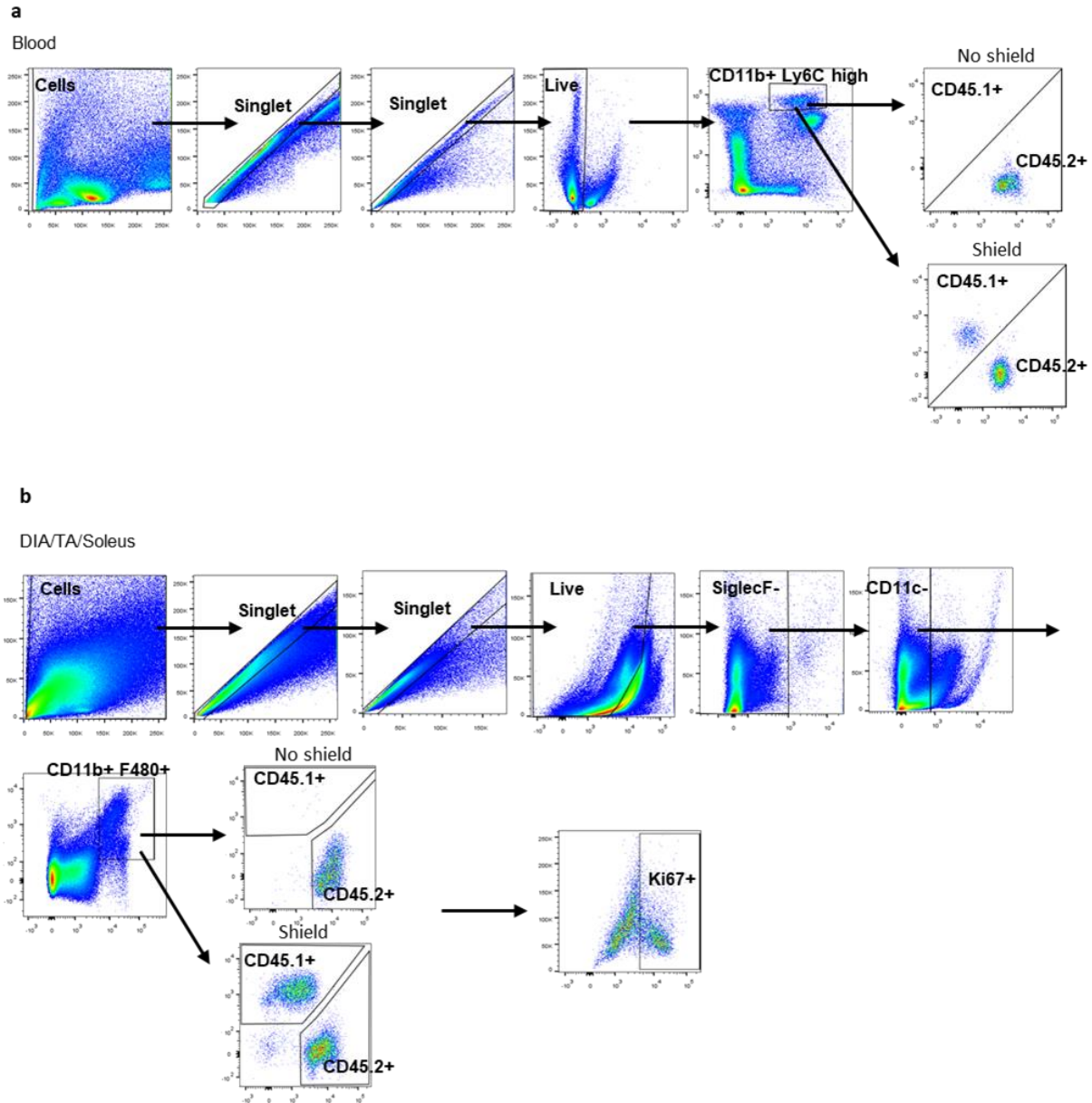


**Figure S2.1. Related to Figure 2.3, Figure2.4 and Figure 2.5. Flow cytometry gating strategies for blood and diaphragm**

a. Blood samples were initially sorted to encompass the entire cell population. Subsequently, two rounds of singlet selections were performed based on parameters involving forward scatter (FSC) and side scatter (SSC) in both height (H) and area (A). Fluorescence Minus One (FMO) controls were employed to establish the boundaries for each gate in all flow cytometry experiments in this CHAPTER. Among the selected

cells, live cells that did not exhibit staining indicating cell death were then filtered based on being positive for CD11b and having a high expression of Ly6C, classifying them as monocytes. The composition of CD45.1 and CD45.2 was subsequently analyzed for these cells.

b. In muscle samples, cell gating was applied after singlet selection and viability assessment, following a similar procedure as with blood samples. Macrophages were identified by gating for cells positive for CD11b and F480, while excluding cells positive for siglecF (eosinophils) and CD11c (dendritic cells). Subsequently, the macrophage population was analyzed to determine the composition of CD45.1 and CD45.2, providing insights into their origin. Additionally, the expression of Ki67 was examined to assess macrophage proliferation.

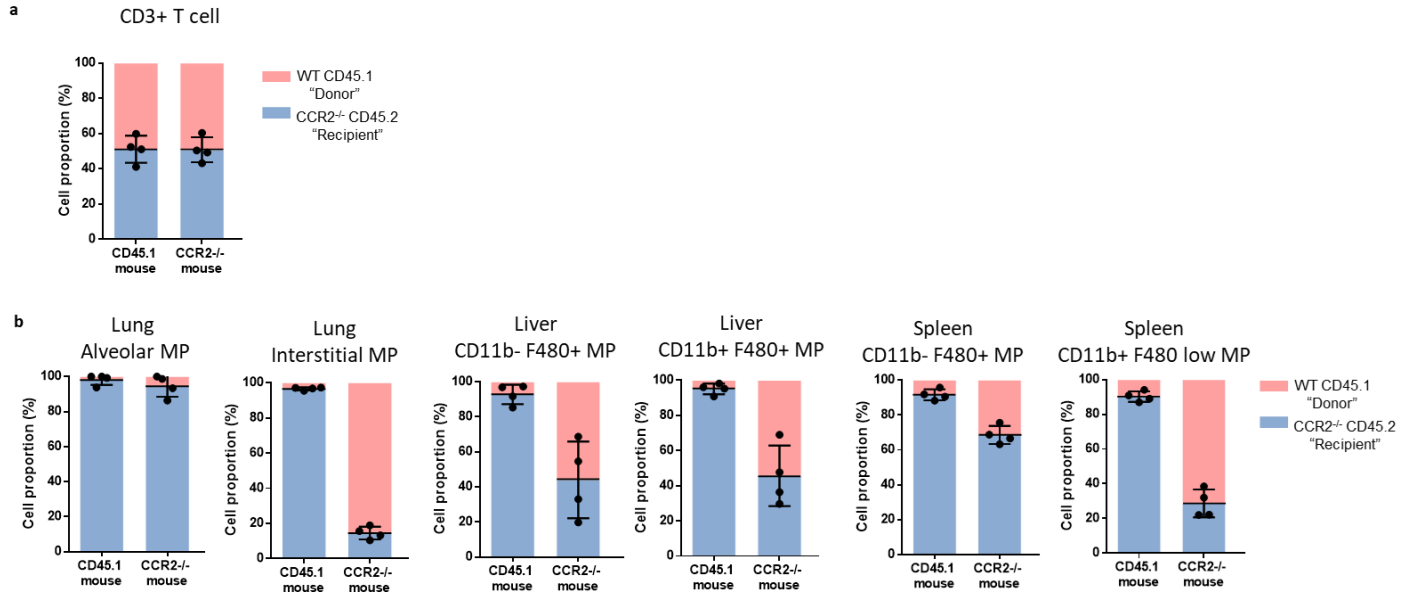


**Figure S3.1 Related to Figure 3.3. Proportions of chimeric blood T cells and origins of macrophages in various tissues**

- a. Relative percentages of CD45.1+ and CD45.2+ CD3+ T cell in the blood after 5 months of parabiosis (n=4 parabolic pairing).
- b. Group mean data are shown for the relative percentages of CD45.1+ and CD45.2+ macrophages in the lung, liver, and spleen in CCR2<sup>-/-</sup> mice after 5 months of parabiosis (n=4 parabolic pairing).

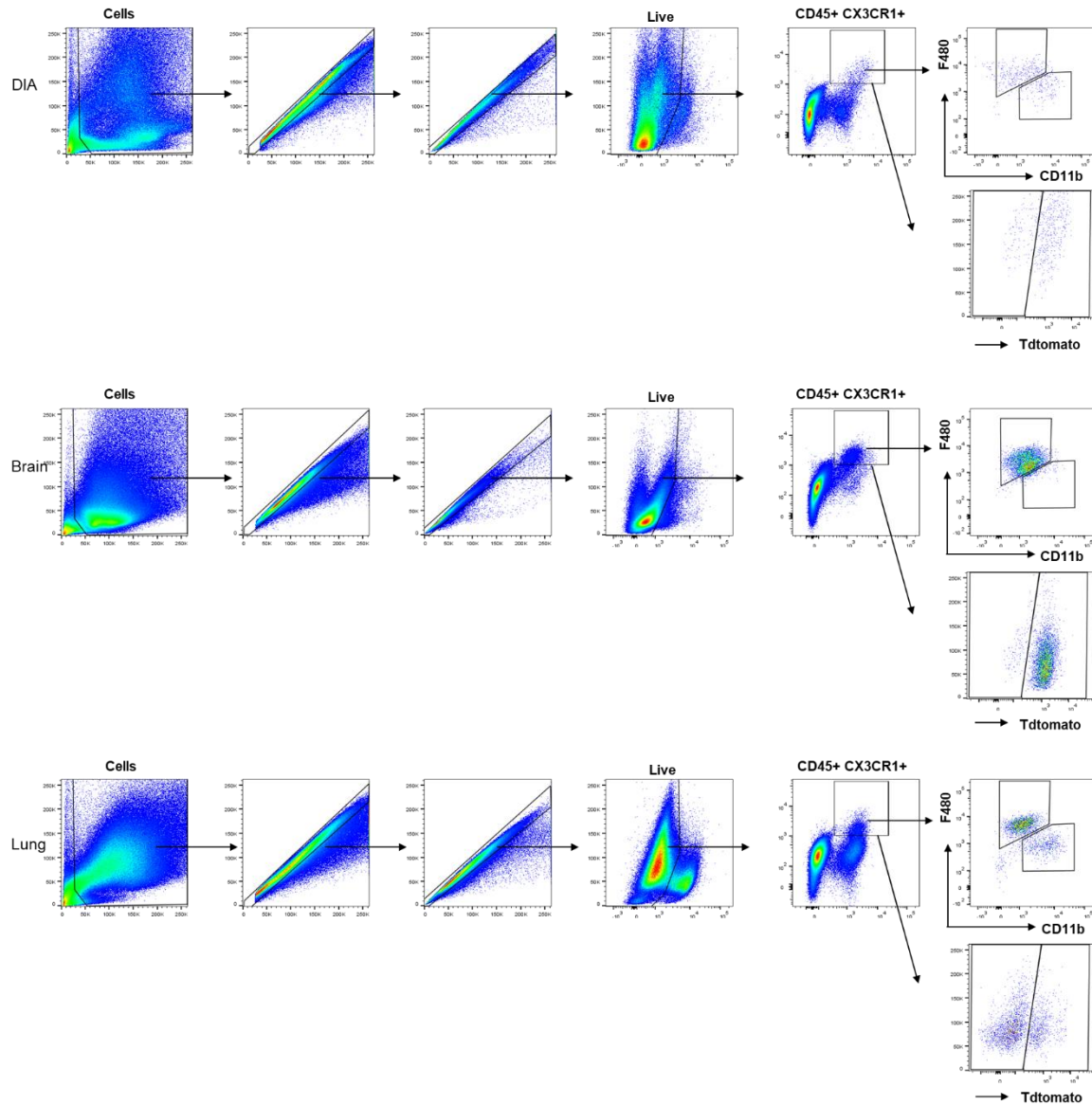


**Figure S3.2 Related to Figure 3.1. Gating strategies for fate mapping experiment harvest at E18.5**

Cell samples isolated from the diaphragm, brain and lung underwent an initial gating to include all cells within the samples. Following this, two rounds of singlet selections were carried out using parameters derived from forward scatter (FSC) and side scatter (SSC) measurements in both height (H) and area (A). Fluorescence Minus One (FMO) controls were employed to establish the boundaries for each gate in all flow cytometry experiments in this CHAPTER. Macrophages were then identified by gating based on CD45 and CX3CR1-YFP expression among live cells. Additionally, the macrophage population was subject to further analysis to assess the expression of F480 and CD11b, alongside the presence of labeling for Tdtomato.

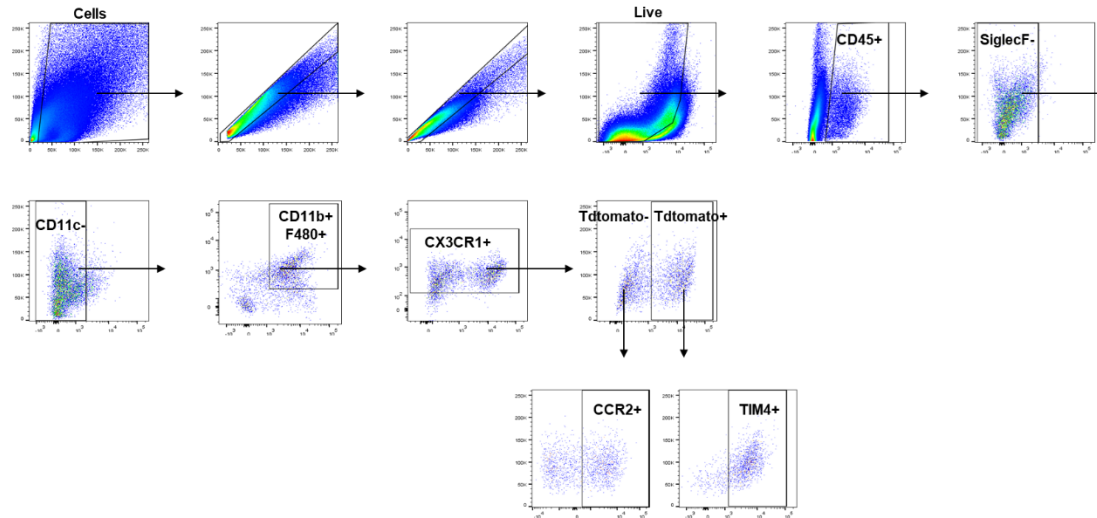
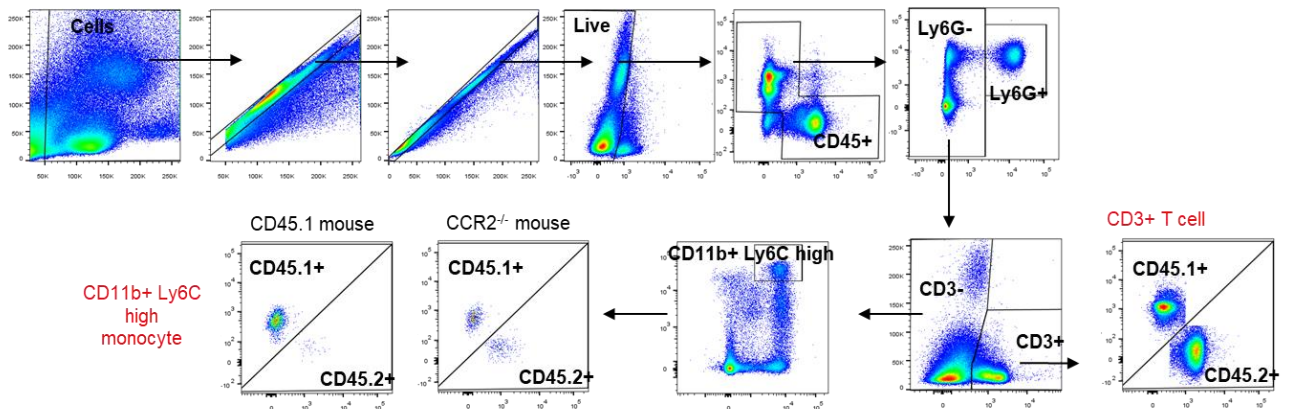


**Figure S3.3 Related to Figure 3.2 and Figure 3.4. Gating strategies for fate mapping experiment harvest at 5 and 9 wks**

Muscle samples underwent a gating process that involved excluding doublet cells in two successive rounds, as well as eliminating non-viable cells. Macrophages were then identified among CD45+ immune cells, with exclusions made for SiglecF+ eosinophils and CD11c+ dendritic cells. The identified macrophage population was defined as CD11b+, F480+, and CX3CR1+. Subsequently, the macrophages were examined for the presence of tamoxifen-labeled Tdtomato expression. Further analysis involved differentiating between CCR2 and TIM4 expression within the subsets of Tdtomato+ and Tdtomato- macrophages.

a Blood



b DIA

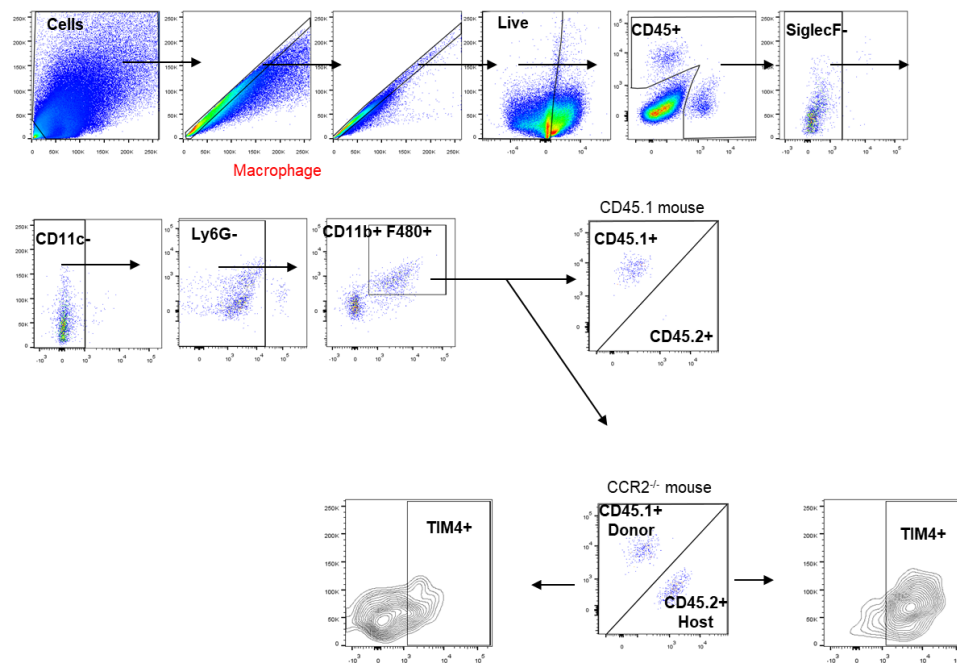


**Figure S3.4 Related to Figure 3.3 and Figure 3.4. Gating strategies for parabiosis**

a. Blood monocytes were analyzed by gating for singlet cells that were viable and fell within the CD45+ population. Neutrophils and T cells were excluded using markers Ly6G and CD3, respectively. Monocytes were defined using CD11b and Ly6C markers. Among these, CD3+ T cell and CD11b+ Ly6C high monocytes were selected for further analysis, specifically to determine the percentage of CD45.1 and CD45.2 within these subsets.

b. In muscle samples, cell gating was carried out after singlet selection and viability evaluation, starting with a gate on CD45 expression. Macrophages were identified by gating for cells that were positive for CD11b and F480, with exclusion criteria for cells positive for siglecF (eosinophils), CD11c (dendritic cells), and Ly6G (neutrophils). Following this, the macrophage population was further analyzed to ascertain the proportion of CD45.1 and CD45.2, thereby shedding light on their origins. Furthermore, the expression of TIM4 in the macrophage population was also examined.

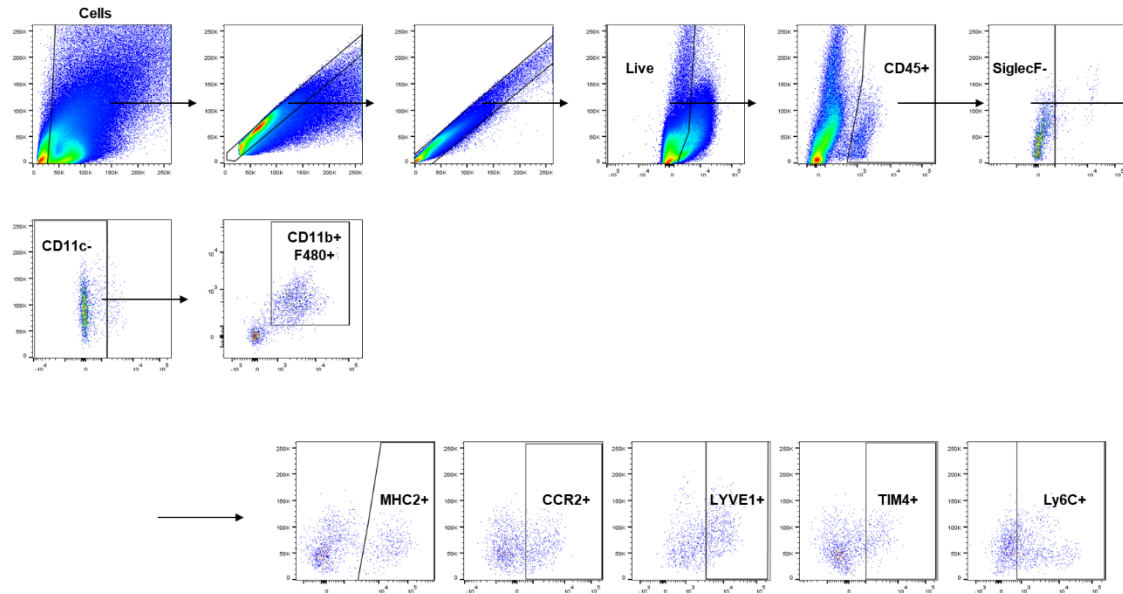


**Figure S3.5 Related to Figure3.5. Gating strategies for WT-CX3CR1-gfp and mdx-CX3CR1-gfp mice at different ages**

Macrophages were identified as singlet cells that were viable, fell within the CD45+ population, and were negative for SiglecF and CD11c while being positive for both CD11b and F480 markers. This subset of macrophages was then subjected to further analysis, specifically evaluating the expression levels of MHC2, CCR2, LYVE1, TIM4, and Ly6C.

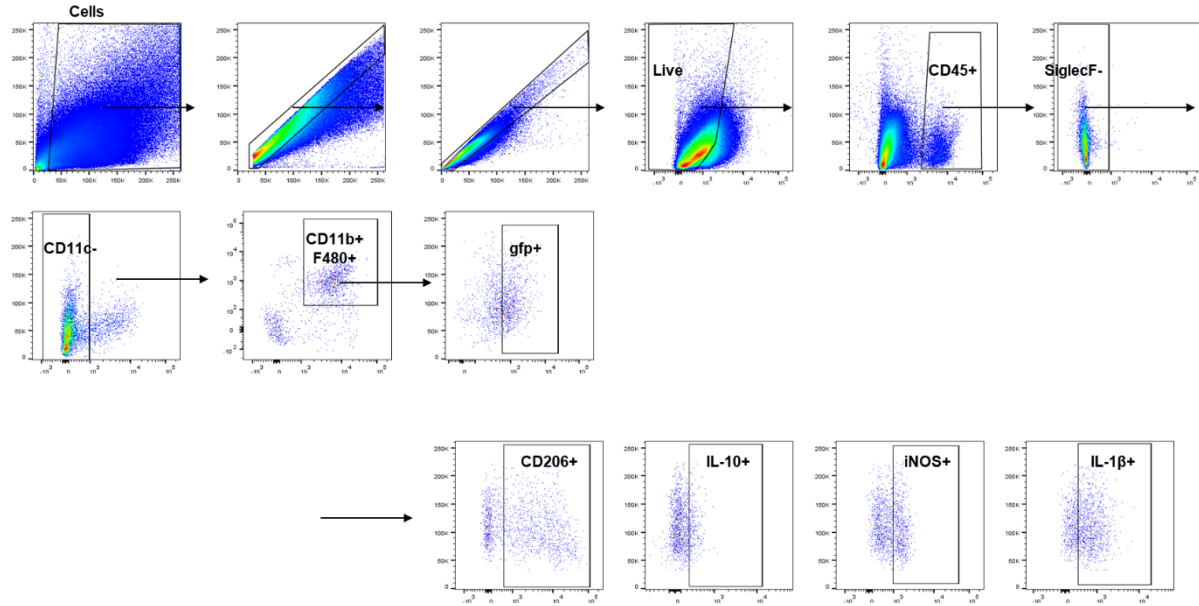


**Figure S3.6. Related to Figure3.6. Gating strategies for chimeric mice transplanted with **gfp+** bone marrows**

Macrophages, as defined in Figure S3.5, underwent analysis based on their GFP expression. Macrophages exhibiting GFP positivity were subsequently assessed for their expression of CD206, IL-10, iNOS, and IL-1 $\beta$ .

**Table S2.1 qPCR primers**

Gene name	F/R	Sequence
HPRT1	F	CGCAGTCCCAGCGTCGTGAT
	R	CGAGCAAGTCTTTCAGTCCTGTCCA
ACTB	F	CGACAACGGCTCCGGCATGT
	R	TCTGGGCCTCGTCACCCACA
MYOD	F	AGAATGGCTACGACACCGCC
	R	GCTGTCTGTGGAGATGCGCT
MYOG(MYF4)	F	GAGGAGCGCGATCTCCGCTA
	R	GTCAGCCGCGAGCAAATGAT
eMyHC	F	GCTCACATATCAGAGTGAGGAGGCA
	R	TCCTCAGCCTGCCTCTTGTAGGA

The primer sequences used for gene amplification by polymerase chain reaction (PCR). Forward (F) and reverse (R) primer sequences are listed for each gene, including housekeeping genes (HPRT1 and ACTB) and muscle-related genes (MYOD, MYOG, eMyHC).

**Table S3.1 Complete DEG list****Up-regulated DEG list**

	baseMean	log2FoldChange	padj
Spp1	3908.469	6.607347	3.59E-06
Pdpn	289.4232	4.321508	0.000102
Met	165.7143	4.292138	0.000109
Cd300lf	278.9194	3.489369	5.32E-13
Vcan	1508.287	3.215134	0.003609
Lhfpl2	408.1864	3.195507	7.90E-12
Fabp5	890.1357	3.161505	2.63E-35
Syng1	171.895	3.147307	0.028642
Il7r	253.5743	3.109778	0.006038
Vegfa	345.927	3.064307	1.74E-08
Tmem119	304.6385	2.925237	0.030843
Olfml3	421.7181	2.823682	1.17E-10
Baspl	649.4023	2.818181	2.25E-28
Mmp14	792.1707	2.75866	0.01088
Ifit2	724.0857	2.728507	0.006497
Tgm2	1842.444	2.700039	1.86E-05
Adam8	1453.145	2.567104	0.000333
Ass1	155.1139	2.55997	3.68E-06
Parvg	309.2195	2.502913	3.14E-10
Fam46c	334.0291	2.481726	4.49E-08
Slfn4	728.5589	2.476307	9.13E-11
Gk	127.6982	2.464906	7.46E-05
Gm5150	128.0011	2.452792	0.000104
Gpr157	112.7466	2.438311	1.45E-06
Ifit1	181.2629	2.412876	0.000313
I830127L07Rik	110.2394	2.405112	0.023196
Uck2	299.4192	2.396064	9.64E-06
Ms4a7	1707.476	2.395191	0.000736
Ms4a4c	926.9568	2.391411	5.48E-16
Havcr2	545.3241	2.369206	1.02E-07
Postn	119.4853	2.309995	0.00065
Rsad2	483.4434	2.217871	0.040141
Rgs1	1406.091	2.199477	0.006338
Cd109	129.5112	2.191023	2.69E-07
Slc9a7	173.4866	2.186829	0.00014
LOC108167440	712.6697	2.183472	3.14E-17
Slfn10-ps	111.4806	2.166532	0.000703
Gm34084	117.8936	2.153388	1.42E-05
B430306N03Rik	135.5315	2.127499	0.016988

Chst11	125.4513	2.108392	0.006163
Lrrc16a	131.1569	2.106033	0.011535
Clec4n	454.0614	2.082718	1.34E-10
Isg15	129.3199	2.05649	0.003746
Ncapg2	335.0241	2.055099	7.25E-10
Ankrd28	181.7602	2.053437	3.19E-07
Gcnt2	295.4656	2.052501	3.24E-05
Sirpb1b	102.7506	2.042148	0.000114
Rai14	245.0297	2.035039	0.000247
Ctsd	13656.61	1.97162	2.95E-22
Lgals3	5246.262	1.96095	1.69E-27
Colla1	293.4888	1.946571	1.45E-11
Galns	237.3913	1.913645	2.69E-08
Ifi205	122.62	1.911773	0.00406
Ly6c2	553.3622	1.905145	2.89E-05
Slc6a8	165.5647	1.876065	0.000396
Hgf	197.695	1.855395	0.000104
Uhrf1bp1	144.0793	1.853382	0.047251
Nt5dc2	318.2509	1.847464	3.09E-06
Sema4d	869.5144	1.837255	3.06E-23
Ptgs2	1122.79	1.821844	0.005895
Fcgr1	2145.534	1.821303	1.78E-19
Glrx	233.688	1.820628	0.000221
Slc27a1	214.3688	1.812127	1.01E-07
Slfn1	471.3028	1.809506	2.19E-06
Galnt6	322.2846	1.808509	6.02E-07
Thbs1	11140.72	1.790328	0.034512
F11r	322.2383	1.789899	0.000224
Ppp1r3b	153.117	1.774976	5.16E-06
Gde1	280.7321	1.765667	1.70E-07
Ctse	663.392	1.759354	0.031597
Abcg1	623.5126	1.74145	5.16E-06
Aprt	411.791	1.739146	2.11E-06
Mmp19	1133.314	1.724809	1.49E-05
Slc39a14	449.8038	1.721128	0.001966
Itgb5	2224.506	1.719194	7.67E-23
Mefv	606.3244	1.717488	6.53E-05
Abhd15	127.1827	1.717473	0.00506
LOC100038947	298.3593	1.697633	2.04E-06
Oas3	411.8539	1.69706	1.69E-06
Gla	534.3785	1.692783	2.35E-05
Irf7	950.0953	1.688031	3.43E-07
Slc15a3	1172.67	1.675117	1.09E-11

Osm	641.1053	1.662561	0.000261
Tgfbr1	1412.804	1.660849	0.006313
Col1a2	362.4199	1.657406	9.38E-07
Hexb	3316.846	1.639856	3.47E-08
Cd276	161.0729	1.638151	0.004833
Ccr5	2019.534	1.637627	1.84E-17
Gtf2h2	112.0609	1.633056	0.001856
Tmem86a	494.1035	1.628614	1.23E-05
Nceh1	928.0962	1.621444	8.90E-14
Mgat5	633.368	1.618478	7.02E-13
Pik3cb	270.6533	1.618172	1.47E-06
Kcna3	125.2497	1.602341	0.000885
Nr4a2	224.1068	1.596247	0.0109
Hilpda	242.504	1.595343	0.04624
Slc37a2	974.7936	1.592142	1.01E-11
Pde7b	160.502	1.587344	0.008405
Cd300c2	1023.984	1.579752	4.89E-08
Dmxl2	620.2051	1.579663	5.41E-09
Pgam1	185.6716	1.579619	0.000221
Cx3cr1	3302.708	1.559027	8.90E-14
Thbs4	167.791	1.558918	9.77E-05
Prdm1	256.9014	1.556479	0.000325
Lst1	443.7461	1.556109	3.54E-09
Fcgr4	488.3659	1.555473	2.54E-05
Pmepa1	231.3179	1.548137	0.000319
Itgav	916.6234	1.546283	9.55E-10
Odc1	441.095	1.545676	0.001253
Acot7	110.1274	1.543168	0.020188
Gpr65	742.7997	1.525948	6.26E-06
Il21r	296.4805	1.524165	1.53E-07
Sirpb1a	152.9598	1.517125	0.040364
Cstb	1061.95	1.515204	3.94E-14
Oasl1	120.7815	1.513064	0.007766
Mnda	356.3205	1.501805	0.000315
Mx1	565.9477	1.498903	0.003726
Col6a3	125.4	1.496515	0.005174
Ms4a14	476.0297	1.491174	0.004421
Tlr13	1653.441	1.488824	4.74E-16
Trem2	930.1611	1.476633	1.18E-05
Igf2r	367.8842	1.476364	2.48E-05
Slc2a1	383.4916	1.469601	0.000182
Gnptab	758.637	1.463983	6.64E-11
Rcbtb2	428.0534	1.461103	0.000426

Plin2	2267.632	1.458186	3.59E-12
Dtx4	406.4593	1.456911	2.01E-05
Ctsl	2326.859	1.444311	3.82E-20
Rtp4	337.9467	1.430642	0.000124
Ggta1	643.3999	1.423115	7.25E-06
Clec4d	692.6566	1.415802	0.00529
Pkm	4318.102	1.412737	0.019713
Enpp1	186.5219	1.412086	0.009534
Cux1	1097.551	1.41135	4.06E-13
Col3a1	651.4377	1.410191	0.005895
Fam129b	1272.553	1.401593	0.000139
Smim3	210.5146	1.392482	0.003845
Zbp1	527.8733	1.392131	2.35E-06
Lmnb1	323.7936	1.390022	0.009692
Helz2	508.7289	1.380081	6.56E-06
Tlr1	529.7455	1.377176	2.17E-06
Rap2a	522.7122	1.368905	4.05E-06
Arhgap27	244.7038	1.354195	0.001499
Fnip2	712.268	1.35182	3.54E-06
Mpeg1	20078.75	1.351279	3.30E-11
Pydc4	360.6062	1.34629	9.10E-05
Nxpe5	410.4776	1.33943	2.82E-08
Mvb12b	303.4323	1.335725	0.000215
Gm5086	129.1696	1.331222	0.036318
Nmi	188.4124	1.330859	0.004825
Coro2a	345.1512	1.314393	1.72E-05
Lpcat2	883.5664	1.311783	1.57E-05
Tmem206	185.6318	1.308753	0.002863
Amdhd2	217.5826	1.284156	0.000716
Cd274	269.8505	1.273383	0.037544
Kenn4	211.9254	1.272007	0.03297
Slamf7	840.4545	1.270948	0.005895
AI504432	484.6628	1.259345	0.000702
Sgk1	809.6667	1.258825	3.59E-06
Clec4e	1043.387	1.256283	0.00538
Cd9	636.8732	1.253656	7.00E-05
Hpgds	623.9805	1.252873	0.021375
Mxd1	547.0024	1.252461	0.007076
Runx3	424.9437	1.252444	0.0004
Frrs1	459.951	1.250565	0.000306
Cpeb2	525.3572	1.249935	2.03E-05
Ifi2712a	739.9373	1.234444	1.58E-07
Vill	216.5134	1.232144	0.004311

Fuca2	571.8349	1.228087	4.69E-06
Epb41l2	1591.439	1.220657	7.76E-09
Rasgef1b	561.4406	1.216486	0.007745
Ero1l	315.2237	1.215202	0.016147
Sh2b2	232.9044	1.209686	0.002362
Arl5c	230.2694	1.201963	0.02259
Abr	924.3256	1.201497	9.47E-07
Glipr1	385.2619	1.199546	0.000107
Dhx58	335.2085	1.193602	0.004507
Rab32	495.7195	1.192175	2.94E-06
Rgs2	1222.891	1.188866	3.45E-06
Sor1l	1079.371	1.187615	0.002306
Specc1	436.3714	1.186982	2.16E-07
Pparg	119.6161	1.183155	0.034938
Fam134b	384.5614	1.180679	0.000341
Fgl2	1345.824	1.180493	0.00028
Haus8	153.8318	1.179429	0.025555
Thyn1	118.2106	1.179204	0.021343
Por	839.8288	1.170082	0.000119
Ccr1	1307.981	1.167487	0.000405
Dock4	367.4668	1.164986	6.22E-05
Ly9	666.0768	1.159667	0.000726
Osbp18	1215.699	1.1585	2.69E-07
Ifi204	1665.679	1.155968	3.92E-07
Cxcr4	1717.769	1.154319	0.0005
Ctss	20657.42	1.152011	5.55E-08
Phf11b	284.039	1.149623	0.01237
Myeov2	196.2751	1.148132	0.009841
Pgk1	722.782	1.146842	0.009879
Il18	154.7919	1.142451	0.032405
Soat1	994.4846	1.142367	2.24E-11
Eif4e	354.5649	1.140661	0.00117
Camk2d	564.8357	1.138193	0.001761
Sik1	702.9056	1.137405	0.013468
Cipc	164.9463	1.136821	0.001938
Cpd	1342.585	1.134037	3.57E-11
Vipas39	297.3841	1.133291	0.002673
Trappc2l	168.217	1.13125	0.030101
Rnh1	1111.473	1.126561	0.000482
Chd7	684.581	1.121258	0.001656
Bcl2a1b	372.2841	1.118285	0.019164
Ifi35	236.3014	1.11807	0.007097
Bin2	777.3529	1.117692	0.000736

Ell2	448.5142	1.117362	0.010986
Slc29a3	1012.174	1.109679	6.40E-06
Prdx6	545.5364	1.107757	0.005929
Ndst1	442.8854	1.107632	0.00122
Cd52	1541.26	1.101412	3.03E-06
LOC108167755	269.9578	1.101377	0.006338
Dck	528.2815	1.099285	0.0024
Tmem192	124.2541	1.096568	0.032921
Heatr1	540.2313	1.095076	0.001687
Fgr	1028.612	1.094909	0.017616
Ifih1	560.9732	1.090884	0.002035
Pld3	948.8834	1.087134	1.74E-08
B4galt1	1155.202	1.085721	1.09E-05
Lonrf3	165.8572	1.085344	0.045491
Emilin1	262.2421	1.081184	0.013715
Hivep3	303.287	1.078578	0.002123
Adssl1	495.8642	1.066516	0.003326
Bst2	495.8561	1.066242	0.000216
Ms4a6d	1625.731	1.062441	5.16E-08
Ube2l6	250.8857	1.062117	0.011322
Abcc3	988.528	1.059062	2.29E-06
Lgmn	10591.08	1.056477	2.75E-07
Slfn8	723.5335	1.052307	0.000524
Zmynd15	153.6566	1.047993	0.012713
Gpr35	688.1125	1.04792	0.023261
Ddx58	542.1749	1.046704	0.005895
Mapkapk3	471.4857	1.043378	0.00041
Ldlrap1	319.0556	1.042794	0.017675
Cox5a	356.1592	1.04254	0.02345
Dock5	377.6152	1.042196	0.046307
Lars2	267474.5	1.040873	0.000234
Arl4c	1378.119	1.040712	4.49E-08
Tor3a	443.454	1.040676	0.028642
Gapdh	423.7113	1.039614	0.001904
Mir6236	39357.41	1.028972	2.88E-05
Smox	439.2814	1.028657	0.021501
Zdhhc21	346.6588	1.027953	0.003623
Itgax	238.8539	1.027855	0.007276
Mdfic	837.1546	1.025401	0.000119
Itga6	1670.51	1.025102	0.000627
Btg1	2430.49	1.024479	2.99E-06
Rufy3	380.5568	1.021115	0.000234
Lpxn	439.6603	1.019906	2.56E-05

Lgals3bp	1742.045	1.019657	0.001165
Dera	138.7174	1.016198	0.027531
Ccdc71l	209.8447	1.013672	0.001495
Cd93	3884.43	1.010452	3.92E-07
Msrbl	627.2399	1.006364	0.013468
Naa25	238.6773	1.006104	0.007468
Cd180	815.1203	1.004159	0.001855
Pyhin1	897.3036	1.001993	0.001154

### Down-regulated DEG list

	baseMean	log2FoldChange	padj
Muc1l	184.8603	-7.37547	1.85E-06
Aldh1a2	169.1396	-5.73848	2.10E-24
Retnla	11132.37	-5.39376	2.10E-15
Cd226	113.7842	-5.34183	1.39E-13
Cd209f	379.7882	-5.25127	0.003095
Dnm1	307.8121	-4.54351	2.30E-07
Hr	115.231	-4.52695	3.67E-16
Gfra2	247.3138	-4.36523	7.76E-28
Mmp9	973.5341	-4.24327	1.39E-11
Fgfr1	1308.626	-4.21284	1.98E-14
Fcna	1270.862	-4.16056	1.45E-12
Lyve1	4092.636	-4.06799	7.67E-17
Gprc5b	163.1189	-3.99073	1.19E-21
Cd163	4208.993	-3.85014	1.48E-12
Mrvl1	285.1385	-3.84829	3.42E-20
Lyz1	2577.6	-3.60826	1.86E-11
Cd209a	219.0915	-3.52921	2.81E-17
Ndnf	161.9863	-3.50953	1.70E-07
Fxyd2	388.8068	-3.47558	4.73E-06
Cd2	203.4498	-3.44876	3.86E-19
Ccl24	623.5767	-3.36162	2.63E-35
Gbp2b	108.8652	-3.23697	1.48E-07
Tmod1	155.7973	-3.16216	1.43E-10
Slc9a3r2	187.6744	-3.11641	1.77E-06
P3h2	119.7663	-3.08629	9.32E-05
Prg4	1462.903	-3.08601	3.08E-05
Mamdc2	430.543	-3.06803	0.000105
Cxcl12	616.088	-3.05552	5.51E-16
Tppp	561.1277	-3.02891	2.10E-12
Cxcl13	168.8237	-2.99964	3.99E-09
Beam	221.7759	-2.95523	2.41E-09

Il6	163.7537	-2.86957	3.77E-06
Myl9	125.9187	-2.85571	2.10E-05
Ednrb	1455.94	-2.8488	3.67E-16
Tns2	101.6259	-2.84595	6.82E-05
Mgl2	3601.923	-2.81522	4.26E-08
Aqp1	669.5304	-2.78785	2.34E-14
Myh11	325.3818	-2.75779	1.48E-10
Dpysl3	332.7675	-2.74688	4.59E-12
Jup	481.1222	-2.73475	1.41E-27
Rcn3	377.6047	-2.72264	1.54E-10
Ltc4s	338.9926	-2.70517	2.36E-15
Adgrf5	417.5101	-2.64196	2.18E-11
Ptprg	105.518	-2.63608	0.003707
Gypc	270.3455	-2.63337	9.13E-11
Serpinb2	173.3638	-2.6092	0.044053
Ptk2	209.492	-2.56847	1.51E-13
Notch3	102.9138	-2.56389	0.000271
Tjp1	121.9808	-2.54597	4.37E-07
Cdr2	186.9134	-2.5443	9.74E-10
Gimap6	129.935	-2.53825	5.12E-08
Egfr	164.9476	-2.53577	1.13E-06
Selp	136.9885	-2.51942	0.000114
Nid2	181.7416	-2.5035	0.00053
Acta2	298.9956	-2.48638	5.86E-09
Mras	121.3431	-2.43566	0.006305
Rras2	104.0598	-2.43217	2.94E-05
Kitl	316.8402	-2.39763	2.39E-13
Ly6c1	117.0971	-2.37601	0.004175
Plekhg5	485.05	-2.37155	2.30E-08
Lpar1	120.0186	-2.366	3.34E-06
Siglech	178.7902	-2.32316	3.40E-05
Jam2	152.4795	-2.3108	7.76E-09
Mill2	100.9478	-2.30435	0.023195
Timp3	248.006	-2.28315	7.54E-07
Tns1	1674.348	-2.28208	8.04E-14
Folr2	2113.441	-2.27407	5.36E-05
Kdr	276.0528	-2.26705	5.40E-06
C1qtnf1	713.8829	-2.265	0.029601
Ptrf	332.0003	-2.25936	3.59E-12
Gprc5c	215.0125	-2.25691	2.94E-05
Ltbpl	122.6458	-2.24482	7.46E-05
Flnb	774.0415	-2.24059	1.91E-16
Cmah	648.9432	-2.23712	1.06E-10

Fam43a	222.6181	-2.18084	2.99E-13
Ltbp4	292.9384	-2.17814	1.49E-12
Selenbp1	266.6599	-2.12422	8.45E-07
Ephx1	511.0835	-2.11652	6.86E-06
Sult1a1	373.7661	-2.1128	5.12E-07
AI467606	363.3242	-2.09823	5.09E-07
Slpi	350.7513	-2.08981	6.97E-06
Serpnb1a	178.9547	-2.08938	3.03E-06
Irf4	413.9938	-2.08241	1.39E-06
Mgll	141.1299	-2.02488	0.000312
Il1rl1	380.4541	-2.02452	1.52E-05
Sema6d	272.9316	-2.02275	6.15E-07
Ptprb	432.9978	-2.01588	2.18E-05
Sdpr	157.9653	-1.9907	0.000183
Mxra7	109.0854	-1.98191	2.70E-05
Pls3	196.8549	-1.97425	4.24E-06
Ehd2	179.0331	-1.97385	0.000387
Palld	133.4408	-1.97186	0.034963
Syne2	565.9845	-1.95774	9.72E-06
Icam2	115.0384	-1.95159	0.004299
Mmrn2	121.483	-1.94591	0.000562
St8sia6	113.1707	-1.9386	3.87E-05
Abca6	165.1122	-1.93756	2.48E-05
Jade2	261.6081	-1.91899	0.001617
Lamb2	148.3044	-1.91441	0.005839
Clstn1	155.2398	-1.8963	2.82E-05
Nfia	135.1793	-1.87773	0.001855
Marveld1	359.8458	-1.87706	1.93E-11
Cbr2	1863.726	-1.87509	9.20E-10
Grap	184.9347	-1.86339	7.96E-10
Myo10	117.3115	-1.85811	0.024444
Cd300lg	275.0923	-1.85623	9.17E-06
Cdh5	393.2749	-1.85224	4.94E-07
Klf2	742.9565	-1.85104	1.29E-11
F5	408.5394	-1.84721	0.000137
Pecam1	383.6582	-1.84477	5.46E-07
Nsmf	281.279	-1.84097	1.28E-05
Igsf9	149.7483	-1.83439	4.73E-05
Otud7b	127.8557	-1.83015	0.003759
Epas1	391.355	-1.81266	1.05E-05
Slc30a4	108.3933	-1.80864	2.08E-05
Cald1	160.8625	-1.80839	0.000174
Bank1	422.6484	-1.80808	0.000254

Rhobtb1	327.8634	-1.80444	1.73E-06
Smpdl3b	212.6311	-1.79701	1.35E-09
Cd81	1687.223	-1.79506	0.006638
Tmem64	130.1248	-1.79355	1.36E-05
Colec12	129.4652	-1.79136	0.002437
Fbln2	163.9117	-1.78178	2.12E-06
Fcgrt	1838.865	-1.77357	0.001379
Alox5	956.4549	-1.76828	8.93E-13
Capn5	108.7562	-1.75036	0.00639
Arhgef10	192.8598	-1.74442	1.43E-05
Cd51	155.8765	-1.74241	0.030267
Cbx6	106.7375	-1.72302	0.005509
Etv1	121.6289	-1.71065	0.000137
Slc14a1	123.9419	-1.70582	0.032922
Rfx2	149.116	-1.67036	0.006034
Tie1	119.8934	-1.66443	0.002076
Dock6	129.1444	-1.66357	0.008754
Cfh	4113.699	-1.65521	3.57E-11
Ablim1	144.8587	-1.65299	0.000958
Igfbp5	215.6867	-1.64588	0.001551
Myh10	180.0161	-1.64055	0.000601
Clec10a	999.3299	-1.63981	2.23E-09
Rasgrp3	512.347	-1.62044	0.000609
Gas6	2982.045	-1.61774	0.033054
Maged1	151.618	-1.61606	0.003618
Heg1	291.9052	-1.61299	2.85E-06
Tpm2	156.7499	-1.60611	0.002362
Qpct	214.2548	-1.60426	6.02E-07
Rgs3	106.3851	-1.59111	0.012405
Aldh7a1	214.8737	-1.59083	0.002473
Podxl	300.0691	-1.58544	0.002484
Ptgs1	595	-1.57526	5.18E-09
Fabp4	593.5907	-1.57071	0.000257
Kank2	165.7801	-1.56271	0.002361
C4b	2036.504	-1.55416	0.038964
Rasgrp2	220.6678	-1.55141	3.04E-05
Rhbdf1	132.4874	-1.54836	0.010228
Flt1	264.7797	-1.54835	0.000381
St3gal5	212.5021	-1.54323	0.010823
Sparcl1	542.8178	-1.54143	0.000291
Uaca	137.8612	-1.54122	0.011566
Kbtbd11	460.4998	-1.52921	3.19E-08
Cend2	261.6211	-1.52664	7.15E-05

Kif23	151.3069	-1.52395	0.010322
Vwf	209.9877	-1.52155	0.026143
Psd3	1471.881	-1.52096	2.16E-13
Chp2	418.803	-1.51973	0.004076
Zfp422	164.8159	-1.50492	0.007011
Lifr	2040.86	-1.47446	4.82E-12
Pla2g16	134.7286	-1.47269	0.001532
Cables1	116.9326	-1.46228	0.002479
Trpv4	210.8669	-1.44901	0.002526
Fam219a	361.4981	-1.43389	1.30E-05
Rhoc	291.0318	-1.43222	0.000221
Aph1b	200.0801	-1.42549	0.001613
F13a1	15644.91	-1.41164	2.96E-29
Zcchc14	179.7704	-1.40854	0.007077
Stard8	1655.833	-1.40699	2.28E-06
Slc13a3	186.3201	-1.39735	4.84E-05
Hspg2	426.4509	-1.38035	0.000241
Zbtb20	606.3293	-1.37948	2.55E-05
Klf9	259.1155	-1.37906	0.003003
Tbc1d4	261.4787	-1.37474	0.042286
Zbtb16	134.0908	-1.37049	0.003733
Igfbp4	1899.36	-1.36694	0.000201
Arhgef12	547.9379	-1.36092	0.000296
Rgs5	399.7366	-1.35975	0.006075
Fer	275.7983	-1.33954	0.007468
Pf4	2673.819	-1.33895	3.13E-06
Ptgir	122.3295	-1.33057	0.02368
Timp2	3811.829	-1.33012	0.025556
Saa3	184.213	-1.32887	0.012184
Hdac10	131.7543	-1.31801	0.010008
Pdlim1	474.8525	-1.31546	3.76E-08
Arhgef3	1002.983	-1.30947	5.36E-05
Slc28a2	511.5807	-1.30172	0.00581
Peg13	269.7377	-1.29849	0.011209
Tmcc2	168.8687	-1.28374	0.002526
Rprd1a	109.2787	-1.28182	0.006362
Slc5a3	116.1677	-1.27691	0.032656
Sorbs3	504.747	-1.27678	0.021018
Fam118a	135.2895	-1.24129	0.027499
Abca9	4523.546	-1.23512	0.000246
Traf5	151.058	-1.23392	0.003725
Hlcs	216.1313	-1.23344	0.000527
Mllt4	407.6512	-1.23272	0.00167

Kifc3	377.3581	-1.23159	0.001499
Pepd	1321.182	-1.2241	4.00E-10
Ecm1	2625.433	-1.22371	6.20E-16
Cav1	429.7749	-1.21493	0.00378
Add3	1332.406	-1.20246	1.06E-06
Eng	564.4118	-1.20158	0.000177
S1pr1	447.7077	-1.19461	0.021563
Foxred2	349.784	-1.18587	1.45E-05
Unc119	196.1026	-1.18261	0.02034
Itsn1	2004.331	-1.17538	1.23E-05
Ttl	126.6901	-1.17415	0.028651
Nhsl2	683.9626	-1.16348	4.90E-07
Slc41a1	155.3378	-1.14996	0.00402
Cd36	6265.23	-1.14988	5.01E-05
Serpinb8	953.6208	-1.14477	2.48E-10
Raph1	829.9247	-1.13941	0.001063
Ms4a8a	222.2039	-1.13826	0.00779
Fgd6	316.2955	-1.13305	1.00E-04
Sptbn1	1430.107	-1.12316	2.01E-05
Susd1	228.1085	-1.1162	0.005388
Map4k2	326.5839	-1.10688	0.003592
Gm13373	139.5595	-1.10065	0.03281
Mepce	267.6858	-1.09828	0.002785
Ttn	234.4312	-1.08976	0.024189
Rnf145	666.8671	-1.08838	0.00013
Il16	614.8687	-1.08788	0.000898
Tfrc	542.5998	-1.08654	0.001578
Trim47	403.4432	-1.0776	5.63E-05
Shtn1	671.7992	-1.06894	0.001071
Ttc3	432.9219	-1.06632	0.003845
Dapk1	667.1027	-1.05858	2.54E-05
Agap3	360.5651	-1.05614	3.38E-05
Rab11fip5	1374.028	-1.05388	2.50E-07
Arsb	434.5315	-1.0534	0.004276
Slco2b1	1789.489	-1.04001	0.000461
Plxnd1	1944.385	-1.03972	2.15E-09
Stxbp6	294.1584	-1.03678	0.031597
Egr1	1650.826	-1.03676	0.000195
Zdhhc14	263.5381	-1.03284	0.021563
Bag5	124.6462	-1.03093	0.035625
Evi5	612.7307	-1.02782	3.43E-06
Col4a2	496.3611	-1.02704	0.002473
Spice1	136.1005	-1.02426	0.029692

Zfp219	269.7427	-1.02213	0.010977
Rrnad1	151.778	-1.02144	0.046689
Epb4111	484.1866	-1.02113	0.002241
Mctp1	422.1943	-1.01875	7.50E-05
Pdlim2	161.1216	-1.00284	0.013153

**Table S3.2 Antibodies resources table**

<b>Antigen</b>	<b>Conjugate</b>	<b>Clone</b>	<b>Cat.#</b>	<b>Company</b>
CCR2	BV711	475301	747964	BD
CCR2	PE-Cy7	SA203G11	150611	Biolegend
CD11b	APC-Cy7	M1/70	101226	Biolegend
CD11c	BUV737	HL3	564986	BD
CD3	Percp-cy5.5	17A2	100217	Biolegend
CD45.1	PE	A20	553776	BD
CD45.2	V500	104	562129	BD
CD45.2	BUV395	104	564616	BD
F4/80	PE- Cy7	BM8	123114	Biolegend
LYVE1	eFluor 570	ALY7	41-0443-82	Invitrogen
Ly6C	APC	HK1.4	128016	Biolegend
Ly6C	FITC	HK1.5	128005	Biolegend
Ly6G	FITC	1A8	127606	Biolegend
MHCII	Percp-cy5.5	M5/114.15.2	107625	Biolegend
SiglecF	PE-CF594	E50-2440	562757	BD
TIM4	BV786	RMT4-54	744631	BD
Ki67	FITC	SolA15	11-5698-82	Invitrogen
BrdU kit	APC		552598	BD